LIÈGE université
Gembloux
Agro-Bio Tech

RNA interference of the E3 ubiquitin ligase RAD18 promotes senescence and reduces tumor growth in pleural mesothelioma

Hélène Brossel

Promoteur : Luc Willems

Année : 2023

COMMUNAUTÉ FRANÇAISE DE BELGIQUE

UNIVERSITÉ DE LIÈGE - GEMBLOUX AGRO-BIO TECH

RNA INTERFERENCE OF THE E3 UBIQUITIN LIGASE RAD18 PROMOTES SENESCENCE AND REDUCES TUMOR GROWTH IN MALIGNANT MESOTHELIOMA

Hélène BROSSEL

Dissertation originale présentée en vue de l'obtention du grade de doctorat en sciences agronomiques et ingénierie biologique.

Promoteur : Luc Willems
Année académique : 2022 – 2023

© Brossel Hélène, Décembre 2022
Toute reproduction du présent document, par quelque procédé que ce soit, ne peut être réalisée qu'avec l'autorisation de l'auteur et de l'autorité académique de l'Université de Liège - Faculté Gembloux Agro-Bio Tech.
Le présent document n'engage que son auteur.

Abstract

Pleural mesothelioma (MPM) is a rare and aggressive cancer of the pleura, mainly induced by asbestos exposure. The standard chemotherapy of MPM consists in a combination of cisplatin (an alkylating agent) and pemetrexed (an antifolate). This treatment induces bulky adducts and decreases the pool of available nucleotides, thus inducing DNA damage leading to the apoptosis of cancer cells. Radiotherapy is another treatment option generating DNA damage through double-strand breaks (DSBs). Moreover, immunotherapy has recently demonstrated efficacy in the sarcomatoid subtype of mesothelioma. Unfortunately, these different treatments remain unsatisfactory and there is an urgent need for new therapeutic strategies.

In the first part of my thesis, DNA damage response is studied in MPM cells treated with gamma-irradiation or chemotherapy regimen. Data show that MPM cells are blocked in S phase (chemotherapy) or G2-M phases (gamma-irradiation) upon genotoxic treatment. The checkpoint inhibitor UCN-01 is able to abrogate this blockage and promotes MPM cells to enter mitosis despite treatment-induced DNA damage, without significant cell death. Furthermore, efficiency of the main DSBs repair mechanisms – namely homologous recombination (HR) and non-homologous end-joining (NHEJ) – is evaluated, since these pathways play a key role in the maintenance of genomic stability upon genotoxic treatments. Data demonstrate differences in repair activities among MPM cell lines and an efficient repair through error-free HR. Thus, MPM treated cells are able to efficiently repair ionizing radiation-induced DNA damage.

The second part of my work presents a therapeutic approach that consists in interfering with DNA damage tolerance (DDT) pathways. Indeed, these pathways are escape routes followed to bypass the unrepaired DNA damage and allow MPM cells to replicate and survive despite the chemotherapy-induced DNA lesions. Results show that interference with especially RAD18, an E3-ubiquitin ligase acting as regulator of PCNA ubiquitination, leads to a significantly lower tumor growth in mice, reduced cell proliferation and higher senescence in presence of the chemotherapy regimen, but no significant induction of cell death. Thus, RAD18 is a potential therapeutic target for MPM treatment in combination with the standard chemotherapy.

This thesis provides a better understanding of the role of DDT mediators in response to chemotherapy, the mechanisms involved in MPM resistance to chemo- as well as radiotherapy and may offer new prospects for novel therapeutic approaches.

Résumé

Le mésothéliome pleural (MPM) est un cancer rare et agressif de la plèvre, principalement induit par l'exposition à l'amiante. La chimiothérapie standard du MPM consiste en la combinaison de cisplatine (un agent alkylant) et de pemetrexed (un antifolate). Ce traitement a pour but d'induire des adduits à l'ADN et de diminuer la réserve de nucléotides disponibles, induisant ainsi des dommages à l'ADN menant à l'apoptose des cellules cancéreuses. La radiothérapie est une autre option de traitement menant à des dommages à l'ADN en créant des cassures double brin (DSBs). De plus, l'immunothérapie a récemment démontré son efficacité dans le sous-type sarcomatoïde du mésothéliome. Malheureusement, ces différents traitements restent insatisfaisants et il est urgent de développer de nouvelles stratégies thérapeutiques.

Dans la première partie de cette thèse, la réponse aux dommages à l'ADN est étudiée dans les cellules de MPM traitées par radiation gamma ou par traitement chimiothérapeutique. Les données montrent que les cellules de MPM sont bloquées en phase S (chimiothérapie) ou en phases G2-M (gamma-irradiation) en présence de traitement génotoxique. L'inhibiteur de checkpoint UCN-01 est capable d'abroger ce blocage et induit l'entrée en mitose des cellules de MPM malgré la présence des dommages à l'ADN induits par le traitement, sans mort cellulaire significative. Par ailleurs, l'efficience des mécanismes principaux de réparation des dommages à l'ADN – à savoir la recombinaison homologue (HR) et la jonction d'extrémité non-homologue (NHEJ) – est évaluée, étant donné que ces voies jouent un rôle clé dans la maintenance de la stabilité génomique en présence de traitements génotoxiques. Les données démontrent des différences dans les activités de réparation parmi les lignées cellulaires de MPM et une réparation efficace de la voie HR. Ainsi, les cellules de MPM traitées sont capables de réparer de manière efficace les dommages à l'ADN induits par les radiations gamma.

La seconde partie de mon travail présente une approche thérapeutique consistant en l'interférence avec les voies de tolérance aux dommages à l'ADN (DDT). En effet, il s'agit de voies échappatoires empruntées afin de contourner les dommages à l'ADN non réparés. Ces voies permettent aux cellules de MPM de se répliquer et de survivre malgré les lésions à l'ADN induites par la chimiothérapie. Les résultats montrent que l'interférence avec RAD18, une E3-ubiquitin ligase agissant comme régulateur de l'ubiquitination de PCNA, mène significativement à une diminution de la croissance tumorale en souris, une diminution de la prolifération cellulaire et une augmentation de la sénescence en présence du traitement chimiothérapeutique, mais pas d'induction significative de la mort cellulaire. Ainsi, RAD18 est une cible thérapeutique potentielle dans le traitement du MPM en combinaison avec la chimiothérapie standard du mésothéliome.

Cette thèse apporte une meilleure compréhension du rôle des médiateurs de DDT en réponse à la chimiothérapie, les mécanismes impliqués dans la résistance du MPM face

à la chimio- et à la radiothérapie et pourrait offrir de nouvelles perspectives pour de nouvelles approches thérapeutiques.

Acknowledgment

Je tiens à exprimer ma gratitude à l'ensemble des personnes qui ont été présentes lors de mes années d'études supérieures – 5 années en sciences pharmaceutiques à l'UCL suivies de 4 années de thèse en sciences agronomiques et ingénierie biologique à l'ULiège. Le passage d'une université à l'autre a été très enrichissant pour moi, de même que pour le changement de sujet d'étude de recherche.

Je souhaite sincèrement remercier :

- Mon promoteur Luc Willems, pour m'avoir permis de travailler au sein de son laboratoire sur un sujet qui me tient à cœur. Merci également pour son encadrement et ses encouragements lors de mon passage au FRIA et dans le courant de ma thèse. J'ai pu ainsi travailler et me développer aux côtés d'une super équipe ! Je sors grandie de cette expérience.

- Mes collègues de laboratoire : d'abord, un merci général à tous les membres de notre équipe pour votre côté humain, notre entre-aide et cette belle entente que nous avons développé entre nous. On forme une belle équipe et merci pour ces super soirées que nous avons passées ensemble, tant à l'intérieur qu'en dehors des murs de l'université. Je peux dire que les gembloutois savent faire la fête ! J'ai hâte de fêter ma fin de thèse avec vous ! ☺ J'espère vraiment garder contact avec vous par la suite.

- Un énorme merci à Alexis pour ton aide aux souris, pour les stats et la bio-informatique – pour ne citer qu'une partie. Les discussions enrichissantes que nous avons eues m'ont permises d'éclaircir nombre de points ! Tu es toujours disponible pour aider, débrouillard et tu as beaucoup de mérite. L'équipe dans laquelle tu travailleras au cours de ta carrière aura beaucoup de chance de t'avoir avec eux.

- Mélanie, merci d'avoir amené un vent de fraicheur au labo avec tes blagounettes, merci pour ton aide précieuse aux souris et ton soutien quand ça n'allait pas, tu as toujours eu les mots justes ! Tu es une de mes plus belles rencontres gembloutoises ☺

- Clotilde, merci pour ton soutien qui m'aura été essentiel, ton réconfort et tes conseils lors des moments difficiles de ma thèse, où la motivation n'y était plus. Merci pour ta bienveillance. Je te souhaite le meilleur et que tu t'épanouisses dans ta carrière professionnelle. Tu es une très belle personne et tu mérites vraiment le meilleur !

- Mégane, tu es la première avec qui j'ai créé un lien d'amitié en plus de celui de collègue au labo. Merci pour ton aide précieuse dans les manips et en informatique, on a finalement presque commencé notre aventure au labo ensemble. On a partagé beaucoup de choses toutes les deux durant tout ce temps, merci pour tout !

Mégane et Clotilde, c'est vraiment dommage que nous n'ayons pas pu partir toutes les trois en Australie pour l'IMIG 2020, mais la conférence sur le mésothéliome à Nantes a rattrapé le coup ! J'en garde de très bons souvenirs.

- Aurélie, merci d'avoir toujours été disponible pour les autres, pour ta gentillesse, ton aide aux souris, à l'irradiation des cellules et pour ton expertise en biomol !

- Thomas Joris, merci pour les supers soirées qu'on a passées avec le reste de l'équipe ! Je regrette qu'on ne se soit pas vus plus souvent durant nos thèses parce que tu es vraiment au top, gentil, déterminé et courageux !

- Jean-Rock, merci pour ton aide aux manips, commandes, et aux souris. Merci également pour ton soutien au labo et l'organisation aux événements du laboratoire – toujours prêt à faire la fête ! Beaucoup de bonheur avec ta petite Louna golden retriever.

- Thomas Jouant, Xavier et Louise, pour les soirées au sein et en dehors du labo ; bienvenue à tous les 3 dans l'équipe en tant que doctorants et courage pour la réalisation de votre thèse !

- Merci également aux post-docs de notre laboratoire pour m'avoir transmis leurs connaissances dans leur domaine : Malik et notre bio-informaticien Majeed ; bienvenue à Mohthash dans notre équipe !

- Vikas, qui m'a encadrée au début de ma thèse, et avec qui je garde contacte même s'il ne fait plus partie de notre équipe. Tu m'as appris sur la culture indienne, sur la vie et son sens, tu as fait en sorte de m'apprêter à être autonome pour la suite de ma thèse. Tu m'as fait grandir, merci pour ta bienveillance.

- Hélène Gazon, qui ne travaille également plus au laboratoire d'épigénétique mais qui était le pilier de notre équipe lorsqu'elle était encore présente. Merci pour ton aide dans les manips de biomol et de m'avoir appris les marches à suivre dans la structure du GIGA et du labo. Tu es très pédagogue et tu as le cœur sur la main. Merci d'avoir été là dans les moments de doutes, tant personnels que professionnels.

- Bernard, ancien doctorant du labo dont j'ai continué le sujet. Merci pour ton aide dans les données et ta disponibilité pour répondre à mes questions sur la suite du sujet.

- Mes chers parents pour m'avoir appris à toujours donner le meilleur de moi-même, pour m'avoir transmis leur amour des langues et leurs valeurs d'autodiscipline et de rigueur, et pour leur soutien continu lors de mes années d'études. Merci également pour la relecture de ma thèse. Je peux voir que vous êtes fiers de moi.

- Steve, qui m'a soutenue quotidiennement lors de ma thèse, qui a été un support considérable lors du passage du FRIA, et qui me rend fière d'avoir réalisé mes études. Merci pour ton écoute quotidienne, ton investissement et pour tout ce que tu fais dans notre vie personnelle.

- Laurent, mon frère préféré, et ma belle-sœur, Stefania ; les copains : Maureen, Nadège, Simon, Eline, Tristan, Nico, Pepe, Kopitz, Maxou, Olux ; mes amis de secondaires : Vicky, Lisou, Cla, Jo, Coco, Lolo, Aurore et Dylan ; Boris et Flo ; Raph ; pour votre soutien inconditionnel et toutes ces activités qu'on a réalisées lors de m'a thèse et qui m'ont permis de décompresser.

- Ma marraine, Arielle, et mon grand-père, Florent, pour m'avoir toujours encouragée dans mes études et la réalisation de ma thèse.

- Les plateformes de vecteurs viraux (Manu, François et Alex), d'imagerie et de cytométrie en flux (Sandra, Rafaat, Céline, Alex et Gaëtan) et d'immunohistochimie (Chantal, Fabienne, Tiffany et Hülya) du GIGA pour leur aide précieuse dans les manips et leur temps. Merci également à Audrey pour la gestion de la culture cellulaire ainsi que son soutien et son écoute attentive.

- L’équipe de la pharmacie de Mangombroux : Valérie, Arlette, Marine et Joanne, pour m’avoir tant appris sur le métier de pharmacien et sur moi-même. Vous avez de très belles valeurs. Merci également d’avoir continué de prendre de mes nouvelles après mon stage en ce qui concerne mes projets personnels et professionnels. J’espère que vous pourrez plus tard proposer des produits dans lesquels j’aurais contribué ☺

- Et enfin Laure Bindels, ma promotrice lors de mes recherches sur le microbiote intestinal dans le cadre de mon mémoire à l’UCL (MNut, LDRI), pour m’avoir formée avec beaucoup de rigueur et donné le goût de la recherche scientifique.

Table of contents

List of figures

List of tables

List of abbreviations

°C	Degree Celsius
•NO	Nitric oxide
•NO2	Nitrogen dioxide
•ONOO	Peroxinitrite
^{18}F-FDG PET-Scan	Fluorodeoxyglucose positron emission tomography
53BP1	p53-binding protein 1
8-oxoG	Eight-oxoguanine
9-1-1	RAD9-HUS1-RAD1
A	Adenine
Alt-EJ	Alternative end joining
AMP	Adenosine monophosphate
ANOVA	Analysis of variance
APAF1	Apoptotic protease activating factor 1
APC	Antigen-presenting cell
APE1	AP endonuclease 1
APTX	Aprataxin
ATCC	American Type Culture Collection
ATM	Ataxia-telangiectasia mutated
ATR	Ataxia telangiectasia and Rad3-related protein
ATRIP	ATR interacting protein
BAP1	BRCA1-associated protein-1
BCA	Bicinchoninic acid
BCL-2	B-cell lymphoma-2
BER	Base excision repair
BH3	BCL-2 homology domain 3

BID	BH3-interacting death domain
BLM	Bloom syndrome RecQ like helicase
BMM	Biphasic malignant mesothelioma
bp	Base pair
BRCA1	Breast cancer type 1 susceptibility protein
BRCA2	Breast cancer type 2 susceptibility protein
BSA	Bovine serum albumin
CDC25C	Cell division cycle 25 C
CDK	Cyclin-dependent kinase
CDKI	CDK inhibitor
CDKN2A	Cyclin dependent kinase inhibitor 2 A
cDNA	Complementary DNA
CEA	Carcinoembryonic antigen
CFP	Cyan fluorescent protein
cGAS/STING	cGMP-AMP synthase/stimulator of interferon genes
CHK1	Checkpoint kinase 1
CHK2	Checkpoint kinase 2
c-NHEJ	Classical-NHEJ
CP	Cisplatin 10μM + pemetrexed 10μM
Ct	Cycle threshold
CT	Computed tomography
CtIP	C-terminal binding protein interacting protein
CTL	Control
CTLA-4	Cytotoxic T-lymphocyte-associated protein 4
DAB	3, 3'-diaminobenzidine
DAPI	4’,6-diamidino-2-phenylindole
DCs	Dendritic cells
dATP	Deoxyadenosine triphosphate

dCTP	Deoxycytidine triphosphate
DDT	DNA damage tolerance
DHFR	Dihydrofolate reductase
dHJs	Double Holliday junctions
DISC	Death inducing signaling complex
D-loop	Displacement loop
DMEM	Dulbecco's modified Eagle medium
DMSO	Dimethylsulfoxide
DNA	Deoxyribonucleic acid
DNA2	DNA replication helicase/nuclease 2
DNA-PKcs	DNA-dependent protein kinase catalytic subunit
dNTP	Deoxyribonucleotide triphosphate
DSB	Double-strand break
DSBR	Double-strand break repair
dsDNA	Double-strand DNA
DUB	Deubiquitinase
EDTA	Ethylenediaminetetraacetic acid
EMA	European Medicines Agency
EMM	Epithelioid malignant mesothelioma
ERCC1	Excision repair cross-complementation group 1
ETAA1	Ewing's tumor-associated antigen 1
EXO1	Exonuclease 1
FA	Fanconi anemia
FACS	Fluorescence activated cell sorting
FADD	FAS-associated death domain
FAK	Focal adhesion kinase
FBS	Fetal bovine serum
FC	Fold change

FDA	Food and Drug Administration
Fe	Iron
FEN1	Flap endonuclease 1
FGF	Fibroblast growth factor
FR	Fork reversal
FSC	Forward scatter
FSC-A	Forward scatter area
FSC-H	Forward scatter height
G	Guanine
G0 phase	Gap 0 phase
G1 phase	Gap 1 phase
G2 phase	Gap 2 phase
GARFT	Glycinamide ribonucleotide formyltransferase
GFP	Green fluorescent protein
GG-NER	Global genome NER
GMP	Guanosine monophosphate
γH2AX	Histone variant H2AX phosphorylated at the serine 139
GIGA	Groupe interdisciplinaire de génoprotéomique appliquée
GSH	Glutathione
GxABT	Gembloux Agro-Bio Tech
Gy	Gray
H	Hydrogen
H2AX	Histone variant H2AX
H_2O	Water
H_2O_2	Hydrogen peroxide
hHLTF	Human HLTF
HIRAN	HIP116-Rad5p-N-terminal
HLTF	Helicase-like transcription factor

HMGB-1	High-mobility group box 1 protein
HR	Homologous recombination
HRP	Horseradish peroxidase
IAP	Inhibitor of apoptosis
IARC	International Agency for Research on Cancer
IHC	Immunohistochemistry
IMRT	Intensity-modulated radiotherapy
IFN-γ	Interferon gamma
iNOS	Inducible nitric oxide synthase
Lig1	DNA ligase 1
Lig3	DNA ligase 3
Lig4	DNA ligase 4
LOH	Loss of heterozygosity
M	Mitosis
MCL-1	Myeloid cell leukemia 1
MDC1	Mediator of DNA damage checkpoint protein 1
MDM2	Mouse double minute 2 homolog
MDSCs	Myeloid-derived suppressor cells
MGMT	O^6-methylguanine-DNA methyltransferase
MHC	Major histocompatibility complex
MM	Malignant mesothelioma
MMEJ	Microhomology-mediated end joining
MMR	Mismatch repair
MMS2	Methyl methanesulfonate sensitive 2
MOI	Multiplicity of infection
MOMP	Mitochondrial outer membrane permeabilization
MPM	Pleural mesothelioma
MRN	MRE11-RAD50-NBS1

MSH	MutS homologs
MT	Metallothionein
mTOR	Mammalian target of rapamycin
MUS81	Methyl methanesulfonate and ultraviolet-sensitive clone 81
NADPH	Nicotinamide adenine dinucleotide phosphate
NER	Nucleotide excision repair
NF2	Neurofibromin 2
NF-κB	Nuclear factor-kappa-light-chain-enhancer of activated B cells
NHEJ	Non-homologous end-joining
NK cells	Natural killer cells
NOX	NADPH oxidase
NSG mouse	NOD scid gamma mouse
nt	Nucleotide
NT	Non-target
O_2	Oxygen
$O_2^{\bullet -}$	Superoxide anion radical
OH^-	Hydroxide
$OH^\bullet$	Hydroxyl radical
PARP-1	Poly (ADP-ribose) polymerase 1
PBS	Phosphate-buffered saline
PCNA	Proliferating cell nuclear antigen
PD-1	Programmed cell death protein 1
PDGF	Platelet-derived growth factor
PD-L1	PD-ligand 1
PD-L2	PD-ligand 2
PFA	Paraformaldehyde
PI	Propidium iodide

PIKK	Phosphatidylinositol 3-kinase-related kinase
PNKP	Polynucleotide kinase 3'-phosphatase
Pol	Polymerase
pRB	Retinoblastoma protein
PTIP	Pax transactivation domain-interacting protein
PUMA	p53 upregulated modulator of apoptosis
qPCR	Quantitative polymerase chain reaction
RF	Replication fork
RFP	Red fluorescence protein
RIF1	RAP-interacting factor 1
RNS	Reactive nitrogen species
ROS	Reactive oxygen species
RPA	Replication protein A
rpm	Revolutions per minute
S phase	Synthesis phase
SASP	Senescence-associated secretory phenotype
SD	Standard deviation
SDSA	Synthesis-dependent strand annealing
SEM	Standard error of the mean
Ser	Serine
SHPRH	SNF2 histone linker PHD RING helicase
shRNA	Short hairpin RNA
SMAC	Second mitochondria-derived activator of caspase
SMARCAL1	SWI/SNF-related matrix-associated actin-dependent regulator of chromatin subfamily A-like protein 1
SMM	Sarcomatoid malignant mesothelioma
SNF2	Sucrose non-fermentable 2
SOD	Superoxide dismutase

SSA	Single-strand annealing
SSB	Single-strand break
SSC	Side scatter
ssDNA	Single-stranded DNA
SUMO	Small ubiquitin-like modifier
SV40	Simian virus 40
TAMs	Tumor-associated macrophages
tBID	Truncated BID
TBS	Tris-buffered saline
TBST	TBS supplemented with 0.1% Tween 20
TCGA	The cancer genome atlas program
TC-NER	Transcription couped repair
TCR	T-cell receptor
TDP1	Tyrosyl-DNA phosphodiesterase 1
TFIIH	Transcription factor II H
TGF-β	Transforming growth factor beta
TILs	Tumor-infiltrating lymphocytes
TLS	Translesion synthesis
TMN	Tumor mutational bruden
TNF-α	Tumor necrosis factor-α
TNM	Tumor – node – metastasis
TOP1	Topoisomerase 1
TOP3	Topoisomerase 3
TOPBP1	DNA topoisomerase 2-binding protein 1
TP53	Tumor protein 53
TRAIL	TNF-related apoptosis-inducing ligand
TRAILR	TRAIL receptor
Treg cells	Regulatory T cells

Tris	Tris(hydroxymethyl)aminomethane
TS	Thymidylate synthase
TS	Template switching
U	Units
UBC13	Ubiquitin conjugating 13
UBZ	Ubiquitin-binding zinc finger
VEGF	Vascular endothelial growth factor
WHO	World Health Organization
WRN	Werner syndrome RecQ like helicase
WT-1	Wilm’s tumor-1
XIAP	X-linked inhibitor of apoptosis protein
XLF	XRCC4-like factor
XPF	Xeroderma protein F
XPG	Xeroderma protein G
XRCC1	X-ray repair cross-complementing protein 1
XRCC4	X-ray repair cross-complementing protein 4
ZRANB3	Zinc finger ran-binding domain-containing protein 3

1

Introduction

1. Malignant mesothelioma

1.1. Malignant mesothelioma

Malignant mesothelioma (MM) is a rare and aggressive cancer of mesothelial cells that is mainly induced by asbestos exposure (Chew and Toyokuni 2015). MM has been recognized as an occupational disease in 1982 in Belgium (EUROGIP 2006). This cancer shows a poor prognosis since it presents a median overall survival of 12 months after diagnosis. The rate of survival at 5 years is less than 5% (Mutti et al. 2018).

Mesothelial cells compose the serous membrane of various cavities of the body - the pleura, the peritoneum, the pericardium and the tunica vaginalis. All these tissues come from the mesoderm during the embryonic development (Chu, van Zandwijk, and Rasko 2019). Among them, pleural mesothelioma (MPM) is the most frequent neoplasm; it represents 80 to 90% of the cases. Peritoneal (10-20%), pericardial (<1%) and testicular (<1%) mesothelioma are rarer cases **(Figure 1)** (Wadowski and De Rienzo 2020)(Broeckx and Pauwels 2018)(Eren and Akar 2002)(Greimelmaier et al. 2020).

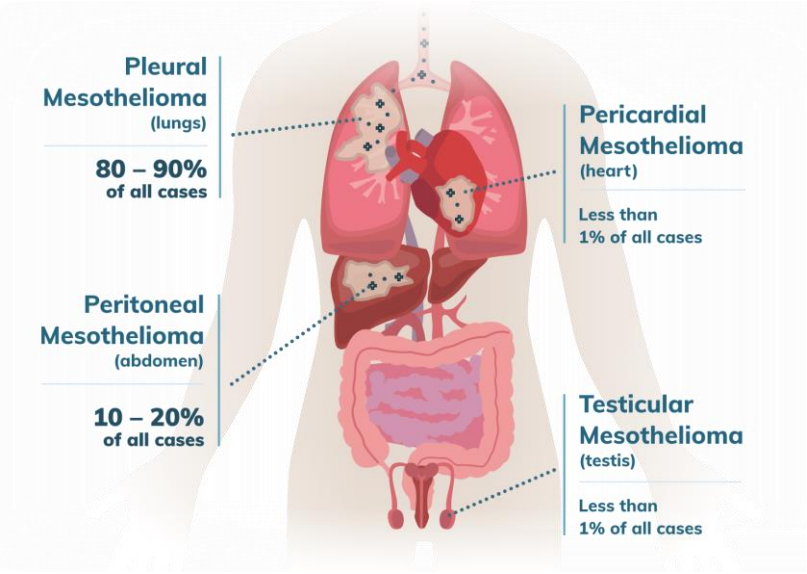

Figure 1. Types of mesotheliomas. Mesothelial cells are found in different locations in the body: the pleura, the peritoneum, the pericardium and the tunica vaginalis. Pleural mesothelioma represents 80 to 90% of the cases, which is the most common one compared to the other forms of MM (Chu, van Zandwijk, and Rasko 2019)(Molinar n.d.)

1.2. The pleura

The pleura is composed of two different layers of serous membrane overlaying the lungs. The outer one is called the parietal pleura and is attached to the chest wall, the diaphragm and the mediastinum, while the inner one, called the visceral pleura, covers the lungs **(Figure 2)** (Ingelfinger, Feller-Kopman, and Light 2018). Each sheet is composed of a single layer of mesothelial cells disposed on the basal lamina with an underlying connective tissue that contains the nerves, blood and lymphatic vessels (Donaldson et al. 2010). Mesothelial cells show an elongated shape with a size of approximatively 25µm and possess an apical pole containing microvilli and a basal pole (Mutsaers 2004).

Between the two layers stand a negative pressure and the pleural space (20µm) which contains the pleural fluid. This liquid is obtained through blood transudation and has a continuous turnover: it constantly runs from the pulmonary capillaries due to hydraulic pressure and is reabsorbed by the stomata that stand on the parietal pleura (Yalcin, Choong, and Eizenberg 2013)(Finley and Rusch 2011). It exerts a lubricant effect which facilitates slipping movements by reducing friction between both membranes while breathing. It also has an immunological role given the presence of resident pleural macrophages and, to a lesser extent, lymphocytes. During inflammation, immunological cells and proteins leak through the mesothelial layer. This disturbs the integrity of the membrane and leads to fluid accumulation called pleural effusions (Donaldson et al. 2010).

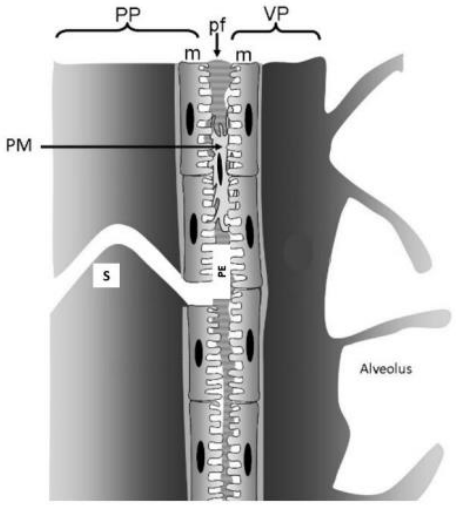

Figure 2. Histological structure of the pleura. The pleura is made up of mesothelial cells (m) forming two layers. The visceral pleura (VP) and the parietal pleura (PP) delimit the pleural cavity (PE) containing pleural macrophages (PM) and the pleural fluid (pf) that is continuously renewed and reabsorbed by the stomata (S). Both layers are composed of a single layer of mesothelial cells disposed on the basal lamina with an underlying connective tissue that comprises the nerves, blood and lymphatic vessels (Donaldson et al. 2010).

1.3. Histological subtypes of MM

There are three different histological subtypes of MM: epithelioid, sarcomatoid and biphasic. The latter represents a combination of epithelioid and sarcomatoid, with variable proportions of these two subtypes **(Figure 3)** (Rachael, Elliott, and Jones 2020). Defining the histological subtype is useful for diagnosis as it shows prognosis importance **(Figure 4)** (Galateau Salle et al. 2018).

The epithelioid subtype, characterized by polygonal, oval or cuboidal cells, is the more frequent one with 50-60% of the cases, and has the best prognosis with 12 to 27 months of survival. The sarcomatoid subtype (10% of cases), with spindle cells, is the most aggressive one and shows 7 to 18 months of survival, and biphasic (30-40% of cases) stands between the 2 subtypes with 8 to 21 months of survival (Yap et al. 2017)(Bonelli et al. 2017)(Husain et al. 2013).

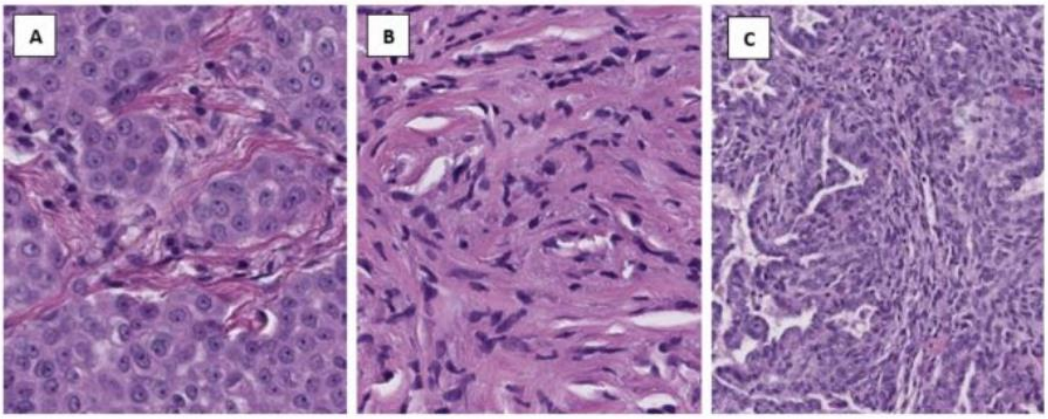

Figure 3. Mesothelioma histological subtypes. (A) The epithelioid subtype is composed of polygonal, oval or cuboidal cells. **(B)** The sarcomatoid subtype is characterized by spindle cells. **(C)** The biphasic subtype consists of a mix of the morphology of the epithelioid and the sarcomatoid subtypes (Rachael, Elliott, and Jones 2020).

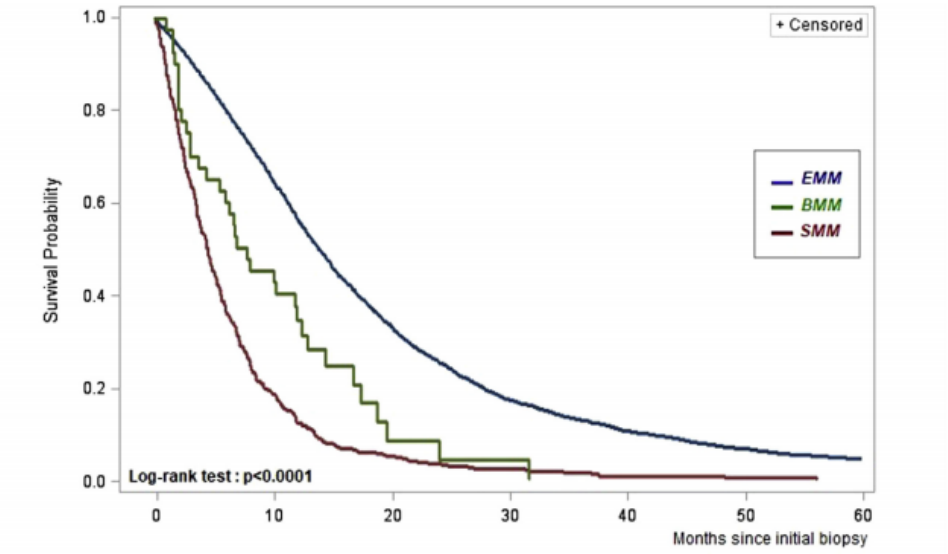

	N	Median	1 yr-survival [CI95%]	2 yrs-survival [CI95%]	5 yrs-survival [CI95%]
EMM	5219	14 mos	55% [53%; 57%]	24% [23%; 26%]	4% [3%; 5%]
BMM	42	8 mos	38% [23%; 53%]	8% [0%; 19%]	0%
SMM	465	4 mos	12% [9%; 15%]	3% [1%; 5%]	0%

Figure 4. Overall median survival curves comparing the different mesothelioma histological subtypes. The epithelioid subtype shows better prognosis than the sarcomatoid subtype. Prognosis of the biphasic subtype stands between the epithelioid and the sacromatoid ones. Overall, MPM is an aggressive cancer with a rate of survival at 5 years after diagnosis of less than 5%. Epithelioid (EMM, in blue), sarcomatoid (SMM, in red) and biphasic (BMM, in green) histological subtypes of MPM (Galateau Salle et al. 2018).

1.4. Epidemiology

Since MPM is strongly linked with asbestos exposure, its worldwide distribution is heterogeneous and depends on its use **(Figure 5)**. Since 1950, asbestos started to be massively used and has been leading to an increase of MM's incidence (H. Yang, Testa, and Carbone 2008)(Prazakova et al. 2014)(O. D. Røe and Stella 2015). Because of professional exposure, it usually affects more men than women (F. Brims 2021)(Ejegi-Memeh et al. 2021). Indeed, in 2020, 21,560 men and 9,310 women were listed, with a total of 30,870 new cases in the world. 43.3% of those were scored in Europe, with 363 in Belgium (GCO-WHO 2020). USA, England and Australia were countries with the biggest number of cases in early 2000, due to the extensive use of asbestos during the first half of the 20th century (Prazakova et al. 2014)(Stayner, Welch, and Lemen 2013).

Since MPM has a long latency period, different peaks of the incidence of MPM can be approximately predicted for each country. In Europe, the peak happened in 2020, while it was 20 years earlier in the United States of America (Van Meerbeeck et al. 2011). Nowadays, China, India, Russia, Brazil and other developing countries are still producing asbestos and therefore will get a higher and delayed peak (Stayner, Welch, and Lemen 2013).

Currently, estimates show that 125 million people are professionally exposed to asbestos, and that between 100,000 and 140,000 cancer deaths are related to asbestos per year. These numbers might be underestimated since there is a lack of data in developing countries (Ramazzini 2010)(Park et al. 2011)(Delgermaa et al. 2011). As long as asbestos is not completely banned and safely removed, the worldwide incidence of MPM might increase considering its massive ongoing use in developing countries (Vainio et al. 2016)(Cavone et al. 2019).

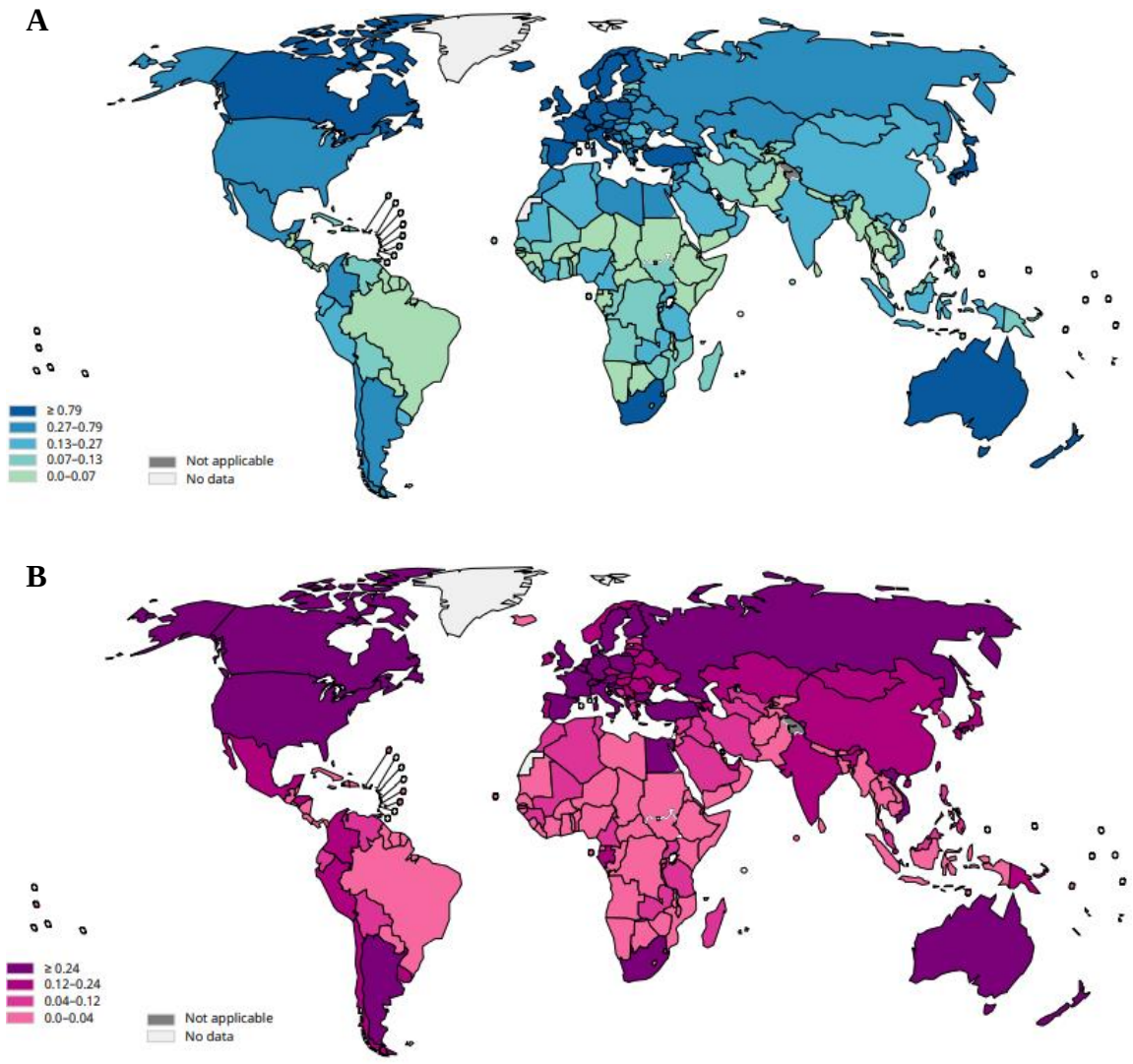

Figure 5. Worldwide map illustrating the repartition of mesothelioma cases in 2020. **(A)** Incidence rate of MPM cases in men per 100,000. **(B)** Incidence rate of MPM cases in women per 100,000 (Globocan 2020).

1.5. Etiologies

As mentioned previously, asbestos exposure is the main etiological factor of MM. Nonetheless, other factors can be responsible for the emergence of MM, such as another mineral fiber, known as erionite, the simian virus 40 (SV40), carbon nanotubes, genetic predispositions and radiations (Attanoos et al. 2018).

1.5.1. Asbestos

This fibrous silicate mineral is extracted from mines notably in Canada, India, Russia and Australia (Frank and Joshi 2014). At first glance, asbestos is quite an attractive material because it is low-priced and has excellent physicochemical characteristics. Indeed, it is stable, flexible, strong, fire resistant and it has thermal, electric and acoustic insulation properties. All these interesting features led to an extensive use in the textile industries and in the construction sector, notably to build roads, for insulation works (buildings, houses, boats), in cement, gaskets and brake pads production (EUROGIP 2006)(H. Yang, Testa, and Carbone 2008)(O. D. Røe and Stella 2015).

Table 1. Physical and chemical properties of asbestos fibers. (IARC 2018)

Common Name	CAS No.	Synonyms	Non-Asbestos Mineral Analogue	Idealized Chemical Formula	Colour	Decomposition Temperature (°C)	Other Properties
Asbestos	1332-21-4*	Unspecified		Unspecified			
Serpentine group of minerals							
Chrysotile	12001-29-5*	Serpentine asbestos; white asbestos	Lizardite, antigorite	$[Mg_3Si_2O_5(OH)_4]_n$	White, grey, green, yellowish	600–850	Curled sheet silicate, hollow central core; fibre bundle lengths = several mm to more than 10 cm; fibres more flexible than amphiboles; net positive surface charge; forms a stable suspension in water; fibres degrade in dilute acids
Amphibole group of minerals							
Crocidolite	12001-28-4*	Blue asbestos	Riebeckite	$[NaFe^{2+}_3Fe^{3+}_2Si_8O_{22}(OH)_2]_n$	Lavender, blue green	400–900	Double chain silicate; shorter, thinner fibres than other amphiboles, but not as thin as chrysotile; fibre flexibility: fair to good; spinnability: fair; resistance to acids: good; less heat resistance than other asbestos fibres; usually contains organic impurities, including low levels of PAHs; negative surface charge in water
Amosite	12172-73-5*	Brown asbestos	Grunerite	$[(Mg,Fe^{2+})_7Si_8O_{22}(OH)_2]_n$	Brown, grey, greenish	600–900	Double chain silicate; long, straight, coarse fibres; fibre flexibility: somewhat; resistance to acids: somewhat; occurs with more iron than magnesium; negative surface charge in water
Anthophyllite	77536-66-4*	Ferroanthophyllite; azbolen asbestos	Anthophyllite	$[(Mg, Fe^{2+})_7Si_8O_{22}(OH)_2]_n$	Grey, white, brown-grey, green	NR	Double chain silicate; short, very brittle fibres; resistance to acids: very; relatively rare; occasionally occurs as contaminant in talc deposits; negative surface charge in water
Actinolite	77536-67-5*	Unspecified	Actinolite	$[Ca_2(Mg, Fe^{2+})_5Si_8O_{22}(OH)_2]_n$	Green	NR	Double chain silicate; brittle fibres; resistance to acids: none; occurs in asbestiform and non-asbestiform habit; iron-substituted derivative of tremolite; common contaminant in amosite deposits; negative surface charge in water
Tremolite	77536-68-6*	Silicic acid; calcium magnesium salt (8:4)	Tremolite	$[Ca_2Mg_5Si_8O_{22}(OH)_2]_n$	White to pale green	950–1040	Double chain silicate; brittle fibres; acid resistant; occurs in asbestiform and non-asbestiform habit; common contaminant in chrystotile and talc deposits; negative surface charge in water

* identified as asbestos by CAS Registry
NR, not reported
From ATSDR (2001), USGS (2001), HSE (2005), NTP (2005)

Based on their structure and chemical composition, asbestos fibers are classified into two different categories: the amphiboles (long and straight fibers) and the serpentines (short and curly fibers) **(Table 1)**. The serpentines contain only the chrysotile fibers, which represent the most commercialized type of asbestos worldwide. The amphiboles comprise the actinolite, amosite, anthophyllite, tremolite and crocidolite fibers **(Figure 6)** (Barlow et al. 2017)(Mott 2012). These are considered more carcinogenic than the serpentines, because of their longer size and their higher iron content that can catalyze reactive oxygen species (ROS) production (Gibbs and Berry 2008)(Toyokuni 2014)(Toyokuni 2002). Moreover, the amphibole fibers persist longer in the lung compared to the serpentine ones (Pacella et al. 2021). This explains why only the use of amphiboles was first banned in Europe, followed in the end by the banishment of all kinds of asbestos fibers in 2005 (EUROGIP 2006).

Despite these slight differences between the amphiboles and the serpentines, the World Health Organization (WHO) and the International Agency for Research on Cancer (IARC) classified all forms of asbestos in Group 1, which means that there is sufficient evidence to conclude that they are human carcinogens. Any contact with asbestos is considered as a potential risk to develop MPM since there is no limited dose defined to promote MPM (IARC 2018).

Furthermore, asbestos can induce other pathologies than MM, such as pleural effusions, pleural thickening and plaques, asbestosis – which consists in interstitial pulmonary fibrosis – and lung cancer (O. D. Røe and Stella 2015). All these asbestos-related diseases leave us facing a burden that we have been experiencing for the last decades, and that we will have to continue to face as long as we don't completely ban its use.

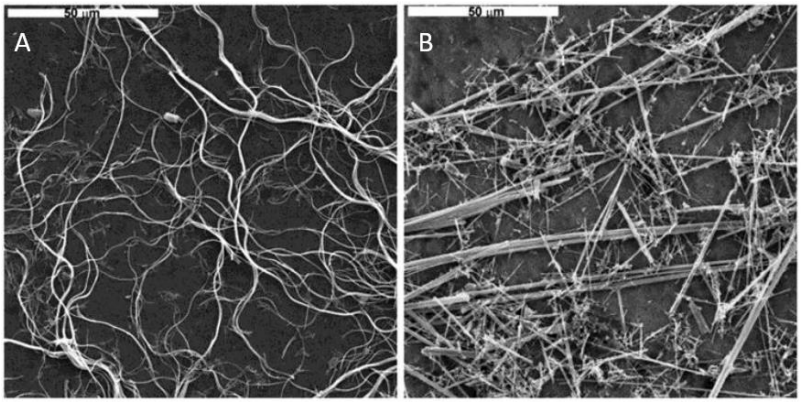

Figure 6. Electron microscopy of asbestos fibers. Asbestos is a fibrous silicate mineral classified into two different categories: the serpentines and the amphiboles. **(A)** Serpentines are the mostly used form of asbestos and consist in the chrysotile fibers which are small and curly shaped. **(B)** Crocidolite fibers are part of the amphiboles category. They have a needle-like shape. Because of their higher iron content and their longer size, they are potentially more carcinogenic. Despite these differences, all forms of asbestos are considered carcinogens to humans (Barlow et al. 2017).

1.5.2. Erionite

Erionite is a type of aluminosilicate mineral with fibrous network that is responsible for MM's occurrence upon environmental exposure. Indeed, erionite fibers have physical characteristics similar to asbestos. It is part of the zeolites family and is found in volcanic tuff – a rock made of volcanic ashes and debris that compact by the effect of groundwater. Deposits of erionite are found in Cappadocia (Turkey), in Sierra Nevada (USA) and in North Italy (Attanoos et al. 2018).

The discovery of a high rate of patients with MPM in villages in Cappadocia enable researchers to highlight the link between erionite exposure and MM's incidence (Baris et al. 1978)(Michele Carbone and Yang 2012). The carcinogenic activity of this fiber was confirmed by inhalation or intrapleural injection in rats that all developed MPM (Wagner et al. 1990). Erionite is classified as a group 1 carcinogen by the IARC and is in fact much more carcinogenic than asbestos (Michele Carbone et al. 2012)(IARC 2018).

1.5.3. Carbon nanotubes

Nanotechnologies show interesting industrial applications but raise questions about health and environment security. Since carbon nanotubes share structural similarities with asbestos fibers, there is a suspicious toxic effect of this product (Donaldson et al. 2010). Indeed, their carcinogenic potential has been demonstrated in rodents (Poland et al. 2008). Thus, manufactures of nanotubes should ensure against lung exposure since it would conduct a health risk if inhaled (Suzui et al. 2016)(Miozzi et al. 2016).

1.5.4. Genetic predispositions

As some families show a higher number of MPM cases, questions about MM's genetic predispositions were raised. Although MPM tumor development is characterized by low mutation rate compared to other cancers, major structural chromosomal rearrangements drive oncogenesis. Tumor suppressor genes were found to be recurrently mutated and significantly linked with MM's incidence, with an autosomal dominant inherence: *breast cancer type 1 susceptibility protein (BRCA1)-associated protein–1 (BAP1), neurofibromin 2 (NF2), cyclin dependent kinase inhibitor 2 A (CDKN2A)* and *tumor protein 53 (TP53)* (H. Yang, Testa, and Carbone 2008)(Roushdy-Hammady et al. 2001)(Bueno et al. 2016). As a matter of fact, a mice model having *BAP1*, *NF2* and *CDKN2AB* simultaneously inactivated in mesothelial cells showed that *BAP1* deletion alone doesn't induce MM. Indeed, once it is combined with *CDKN2AB* and *NF2* deletions, MPM development was drastically accelerated (Badhai et al. 2020). Furthermore, the inherence of MPM has been shown to be strongly associated with BAP1 germline mutation (Cheung and Testa 2017).

BAP1 is a tumor suppressor gene coding for a deubiquitinase (DUB), an enzyme responsible for the removal of ubiquitin on its substrates. BAP1 can be subjected to post-translational modifications, such as phosphorylation or ubiquitination, and is thereby tightly regulating cell ubiquitin signaling (Masclef et al. 2021). This DUB plays essential roles in the regulation of multiple cellular processes, including gene expression, DNA replication, DNA damage repair, cell cycle progression and cell differentiation (Masclef et al. 2021)(Murali, Wiesner, and Scolyer 2013). *BAP1*

mutation is known to be a tumor predisposition, notably for uveal melanoma and MM, therefore defining the "BAP1 cancer syndrome" (Michele Carbone et al. 2020)(Dowell and Patel 2016)(Michele Carbone et al. 2013). Both germline (1 to 7%, hereditary MM) and somatic (between 20 and 64%, sporadic MM) mutations of *BAP1* can occur in MM, with point mutations, copy number loss and rearrangements. *BAP1* mutation leads to prolonged overall survival since diagnosis. However, *BAP1* genomic aberration doesn't modulate responses to treatments in MPM (Dudnik et al. 2021)(Cigognetti et al. 2015)(Dudnik, Reinhorn, and Holtzman 2021).

NF2 encodes merlin, a protein that activates the Hippo pathway and inhibits the mammalian target of rapamycin (mTOR) pathway, involved in contact-dependent inhibition of cell proliferation (López-Lago et al. 2009)(Su et al. 2017). Merlin is known to inhibit cyclin D1 expression, Rac/Pak and focal adhesion kinase (FAK) signaling pathways. Thus, loss of merlin promotes cell cycle progression, cell invasion and migration (H. Yang, Testa, and Carbone 2008)(Hylebos et al. 2016)(W. Li et al. 2010).

CDKN2A encodes $p16^{INK4a}$ and $p14^{ARF}$ *via* alternative open reading frames. $p16^{INK4a}$ is a cyclin-dependent kinase (CDK) inhibitor (CDKI) that blocks the cyclin D - CDK4/6 complexes, thereby preventing the phosphorylation of the retinoblastoma protein (pRb). Non-phosphorylated pRb forms a repressive complex with E2F that binds to the promoter regions of E2F target genes and inhibits the transcription of genes required for the G1-S phases transition, thereby preventing the cell cycle progression. Another protein encoded by this tumor repressor gene is $p14^{ARF}$ which inactivates the E3 ubiquitin ligase mouse double minute 2 homolog (MDM2) that is responsible for p53 proteasomal degradation and inhibition of its transcriptional activity. Thus, homozygous deletions of *CDKN2A* impair both pRb and p53 regulations (H. Yang, Testa, and Carbone 2008)(Hylebos et al. 2016)(Fischer and Müller 2017).

TP53 is less mutated in MPM compared to the other genes mentioned (H. Yang, Testa, and Carbone 2008). This gene encodes the p53 transcription factor involved in the regulation of the cell cycle, apoptosis and senescence. Indeed, under stress conditions, notably DNA damage, p53 is activated and can lead to the arrest of the cell cycle through the activation of p21 in order to enable the repair of the damage. However, under sustained cellular stress along with unresolved DNA damage, p53 drives senescence or the intrinsic apoptosis pathway (Hylebos et al. 2016)(Niazi, Purohit, and Niazi 2018)(Chipuk et al. 2004).

1.5.5. Simian virus 40

Between 1954 and 1961, the production of Salk's poliomyelitis vaccine required primary rhesus monkey kidney cells. Unfortunately, these cells were contaminated in an endemic way with the SV40, leading to millions of people infected as it can be transmitted horizontally (Cutrone et al. 2005)(Michele Carbone, Gazdar, and Butel 2020). Indeed, this DNA virus can cause overexpression of cellular proliferation receptors in contaminated cells and thus shows potential oncogenic activity (B. W. Robinson, Musk, and Lake 2005)(Bocchetta et al. 2008).

There is no notable proof of a link between SV40 infection and MPM incidence. Indeed, epidemiological studies don't point out any significant association between these two outcomes since a low prevalence of SV40 was found in MPM patients

(Michele Carbone, Gazdar, and Butel 2020)(Manfredi et al. 2005). However, an *in vivo* experiment on hamsters shows that intracardiac, intrapleural and intraperitoneal injection of SV40 significantly lead to MPM development (Cicala, Pompetti, and Carbone 1993). *In vitro* experiments also show that SV40 is able to infect and transform human mesothelial cells. Moreover, DNA sequences similar to the SV40 were found in MPM biopsies, suggesting the integration of SV40's genome (M Carbone et al. 1994). Hence, the correlation between SV40 infection and MM's incidence stays controversial (Attanoos et al. 2018)(B. M. Robinson 2012)(Jaurand and Fleury-feith 2005).

1.5.6. Radiations

It has been demonstrated that people who have undergone abdominal or thoracic radiotherapy for cancer treatment are significantly more likely to develop MM. Moreover, people with occupational exposure of radiations also have a higher risk of MM. Furthermore, "Thorotrast", the radioactive contrast agent containing thorium dioxide and previously used for medical imaging procedure, possesses oncogenic activity (O. D. Røe and Stella 2015)(Attanoos et al. 2018)(J. E. Goodman, Nascarella, and Valberg 2009).

1.6. Tumorigenesis

Since MPM has a long latency period, tumorigenesis of this cancer is a process that takes years to set up and is still nowadays not fully understood. Oncogenesis results from chronic and unresolved inflammation **(Figure 7)** (Yap et al. 2017).

Inhaled asbestos fibers migrate to the lungs, reach the pleural cavity by the negative pressure that stands there, and are retained in the parietal pleura (Donaldson et al. 2010)(Toyokuni 2014). Fibers smaller than 5µm are drained out of the pleural fluid to the lymphatic system through the stomates (Schinwald et al. 2012). Bigger fibers remain persistent and induce irritation along with direct inflammation through mechanical contact toward mesothelial cells that produce ROS and reactive nitrogen species (RNS) (B. W. Robinson, Musk, and Lake 2005)(Shukla et al. 2003)(Ozben 2007). Moreover, ferrous ions located on the surface of asbestos fiber catalyze ROS production through the Fenton reaction, along with oxidation of Fe^{2+} to Fe^{3+}. Hypoxic conditions resulting from sustained cell proliferation and oxygen deficiency within the tumor generate RNS as well as peroxynitrite *via* the respiratory chain (Toyokuni 2014)(Toyokuni 2002)(Lu´ıs, Brito, and Pojo 2020). Fibers also promote DNA damage and mutations through interference with chromosomal segregation during mitosis (Bibby et al. 2016).

Within this inflammatory state, asbestos-exposed mesothelial cells secrete cytokines, notably the high-mobility group box 1 protein (HMGB-1) (Qi et al. 2013). This protein drives the tumor necrosis factor (TNF)-α/nuclear factor-kappa B (NF-κB) pathway, which promotes the transcription of genes involved in cell proliferation and apoptosis prevention, leading to survival of mesothelial cells (H. Yang, Testa, and Carbone 2008)(Zolondick et al. 2021)(Naugler and Karin 2008).

Inflammatory chemokines are also released and recruit immune cells, such as neutrophils and monocytes, and lead to pleural effusions in the pleural cavity. Fibers that are over 15µm are persistent and undergo frustrated phagocytosis by the

macrophages. Under these circumstances, macrophages recruited in the pleural fluid keep trying to phagocyte the fibers even though they are not able to perform their task properly. This results in the accumulation of ROS *via* the nicotinamide adenine dinucleotide phosphate (NADPH) oxidase (NOX) of macrophages and the release of the phagosome's content into the extracellular medium, which further increases the oxidative burden (Chew and Toyokuni 2015)(Donaldson et al. 2010)(Hamaidia et al. 2016).

Furthermore, tumor microenvironment of MPM is highly immunosuppressive, which is a negative prognostic factor. Indeed, transformation of mesothelial to mesothelioma cells attracts myeloid-derived suppressor cells (MDSCs) and regulatory T (Treg) cells. These cells allow transforming cells to escape from immune surveillance, thereby enable tumor cells to proliferate and survive (Yap et al. 2017).

Subsequently, mesothelial cells release growth factors that promote tumor growth, among them platelet-derived growth factor (PDGF), fibroblast growth factor (FGF), transforming growth factor beta (TGF-β) and vascular endothelial growth factor (VEGF) (Bibby et al. 2016)(Izzi et al. 2012). The latter also drives the neo-angiogenesis that is crucial for cancer progression – since it enables oxygen and nutrients supply and waste products removal – and metastatic spread (Nishida et al. 2006).

Altogether, unresolved and chronical inflammation as well as persistent oxidative stress lead, slowly but surely, to the onset of MPM (Yap et al. 2017)(Izzi et al. 2012).

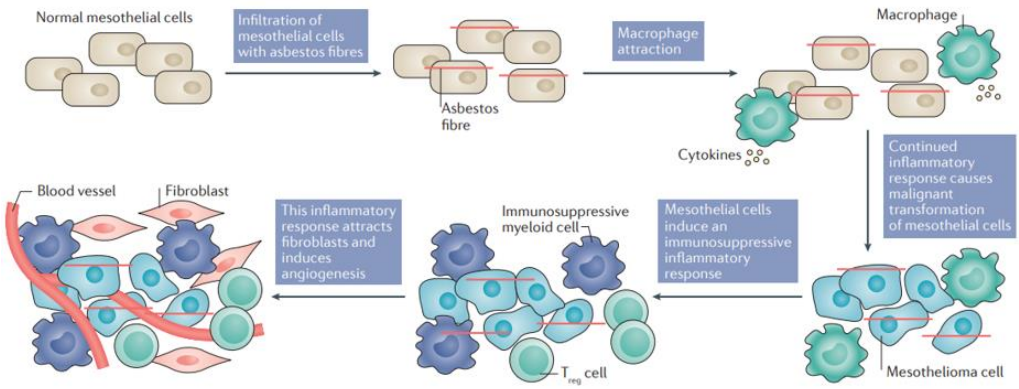

Figure 7. Oncogenesis of MPM. Mesothelial cells are in contact with inhaled asbestos fibers and release inflammatory cytokines. Macrophages are recruited and undergo frustrated phagocytosis, causing continued inflammatory response. Oncogenic transformation of mesothelial to mesothelioma cells attracts immune-suppressing cells, including myeloid-derived suppressor cells (MDSCs) and regulatory T (Treg) cells, enabling the transforming cells to escape from immune surveillance. Tumor growth and progression is sustained by the secretion of growth factors (VEGF, FGF) that lead to angiogenesis and fibrosis (Yap et al. 2017).

1.7. Tumor microenvironment

Tumor microenvironment of MPM is quite heterogeneous and complex. Cellular composition consists in endothelial, stromal and immune cells, including tumor-infiltrating lymphocytes (TILs), tumor-associated macrophages (TAMs), MDSCs, granulocytes and natural killer (NK) cells. This configuration varies among individuals and differs according to the histological subtype. Indeed, the epithelioid subtype displays notably a greater proportion of dendritic cells (DCs), B and T-cells, whereas non-epithelioid subtypes exhibit a larger proportion of TAMs, Treg cells and MDSCs (Napoli et al. 2021)(de Perrot et al. 2020)(Chu, van Zandwijk, and Rasko 2019)(Ramamonjisoa and Ackerstaff 2017). Moreover, tumor microenvironment shows spatial heterogeneity with a continuum between « hot » and « cold » profiles, which contain respectively high and low lymphocyte infiltration **(Figure 8)** (Brossel et al. 2021)(Minnema-Luiting et al. 2018).

Furthermore, T-cells might get their function impaired following co-inhibitors signaling or sustained stimulation of the T-cell receptor (TCR); this state is called exhaustion. Exhausted T-cells are characterized by the upregulation of notably 2 co-inhibitory receptors, cytotoxic T-lymphocyte-associated protein 4 (CTLA-4) and programmed cell death protein 1 (PD-1), and the loss of effector functions, including cytokine production, cell proliferation and cytotoxic activity (Brossel et al. 2021)(Wherry 2011)(Pauken and Wherry 2015)(Petitprez et al. 2020). Finally, tumor microenvironment is also characterized by hypoxia, which is closely associated with metabolism modifications and angiogenesis. Thus, hypoxia promotes tumor progression as well as metastatic potential and leads to poor prognosis (Yue Li, Zhao, and Li 2021).

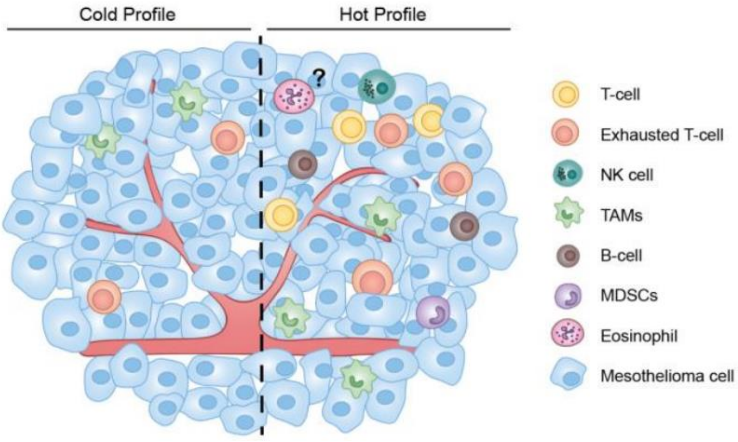

Figure 8. Tumor microenvironment heterogeneity in MPM. This heterogeneity is characterized by the presence of endothelial, stromal and immune cells, including tumor-infiltrating lymphocytes (TILs), tumor-associated macrophages (TAMs), MDSCs, granulocytes and natural killer (NK) cells. Moreover, spatial heterogeneity is observed, with a continuum between "hot" and "cold" profiles, resulting respectively in high and low lymphocyte infiltration (Brossel et al. 2021).

1.8. Diagnosis

MPM has a long latency period, as it generally takes between 10 and 40 years to develop after asbestos exposure (H. H. Sun, Vaynblat, and Pass 2017). Symptoms are usually non-specific, insidious and with a late onset. Thus, MPM is generally diagnosed at an advanced stage. The clinical features include persistent dry cough, thoracic pain, fatigue, weight loss, constipation, night sweats and pleural effusions. Typically, tumor invasion of the chest wall and the excessive accumulation of fluid in the pleural cavity make breathing difficult and lead to dyspnea. Drainage of the fluids can relieve the patient (Delourme et al. 2013)(Van Thiel, Gaafar, and Van Meerbeeck 2011). Less common symptoms resulting from complications due to local invasion consist of hemoptysis, dysphagia, hoarseness, cardiac tamponade, superior vena cava obstruction and Horner's syndrome (Van Meerbeeck et al. 2011)(Dowell and Patel 2016).

MPM diagnosis starts with patient's anamnesis of occupational history with emphasis on asbestos exposure and consists in imaging as well as histological studies. Since medical exams show low sensitivity and specificity for MM, more than one method of analysis should be performed (F. Brims 2021)(Popat et al. 2022).

On the one hand, there are imagery-based techniques that help to define and follow the stage of the cancer through the tumor-node-metastasis (TNM) classification (Bonomi et al. 2017)(Groot et al. 2018). These techniques include chest radiography (X-ray) and computed tomography (CT)-scan which show great variability of images depending on the stage of the disease. These methods give us information about the localization of the pleural effusions and the presence of any thickening of the pleura, which is usually unilateral **(Figure 9)** (Naveed Z. Alam & Raja M. Flores 2020). Additionally, although not routinely used, tumor extend can be detectable with magnetic resonance imaging (Rachael, Elliott, and Jones 2020)(Strange et al. 2021). Candidates for surgical resection can undergo fluorodeoxyglucose positron emission tomography (^{18}F-FDG PET-Scan) in order to exclude any extra thoracic spread. Other more invasive techniques such as mediastinoscopy, laparoscopy and endobronchial ultrasound can be performed on these patients (Dowell and Patel 2016)(Bonomi et al. 2017).

On the other hand, thoracoscopy followed by immunohistochemistry (IHC) studies on biopsies should be performed using several biomarkers in order to confirm the diagnosis of MPM (Delourme et al. 2013). This method helps to define the histological subtype of the tissue sample and to discriminate MPM from adenocarcinoma (Bianco et al. 2018). To this end, the combination of two mesothelioma-associated markers (such as calretinin, Wilm's tumor-1 (WT-1), cytokeratin 5/6) as well as two adenocarcinoma-associated markers (namely carcinoembryonic antigen (CEA), Ber-EP4, MOC-31) should be used (Morgan et al. 1999). The sarcomatoid subtype should be confirmed with cytokeratin staining (Popat et al. 2022). Moreover, loss of BAP1 staining (more frequent in the epithelioid subtype) and/or detection of homozygous deletion of *CDKN2A* (more frequent in the sarcomatoid subtype) can help in MPM diagnosis. MTAP staining can substitute molecular analysis of *CDKN2A* (with 96% specificity and

78% sensitivity) since *MTAP* is located near *CDKN2A* (Cigognetti et al. 2015)(Popat et al. 2022)(Sinn, Mosleh, and Hoda 2021).

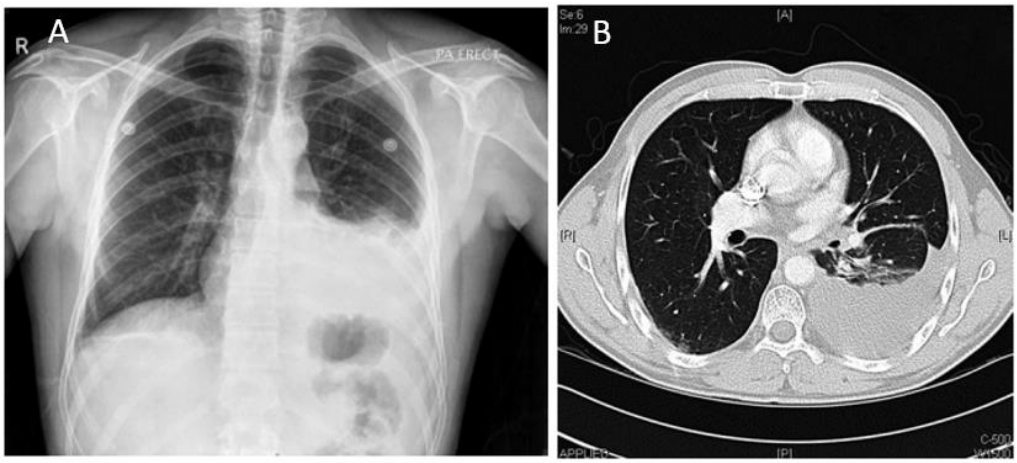

Figure 9. Imaging of MPM. (A) Chest X-ray of early MPM with unilateral pleural effusions. Progressive cases may exhibit pleural thickening and nodularity. **(B)** CT-scan of early MPM – simple pleural effusion (Naveed Z. Alam & Raja M. Flores 2020).

1.9. Staging

Establishing the staging and the prognosis of MPM is important as it allows better stratification of patients into risk groups for therapeutic management. Moreover, it helps to identify candidates that can be enrolled in clinical trials (Bonomi et al. 2017).

The international TNM staging system is currently the recommended cancer classification. It is established on the extend and propagation of the tumor and considers the primitive tumor size (T), the lymph node metastasis (N) and the distant metastasis (M) **(Table 2)** (Brierley, Gospodarowicz, and Christian 2016)(Popat et al. 2022)(Groot et al. 2018).

Nonetheless, this classification is considered difficult to apply and sometimes unsuitable for MPM staging since MPM diagnosis relies on imaging data and this system is based on surgical data (Delourme et al. 2013). Other parameters are proposed to establish a prognosis score, including the histological subtypes (epithelioid versus non-epithelioid), weight loss, low albumin and hemoglobin blood levels, the detection of a hyperleukocytosis, anemia and thrombocytosis (Delourme et al. 2013)(F. J. H. Brims et al. 2016)(Edwards et al. 1999).

Table 2. 8th edition of the UICC (Union for International Cancer Control) TNM classification of MPM. There are 4 categories characterized by the extend of the primitive tumor, lymph node metastasis and distant metastasis. (Brierley, Gospodarowicz, and Christian 2016).

T	Tx	Primary tumor cannot be assessed
	T0	No evidence of primary tumor
	T1	Tumor involves the ipsilateral parietal or visceral pleura only, with or without involvement of visceral, mediastinal, or diaphragmatic pleura
	T2	Tumor involves the ipsilateral pleura (parietal or visceral pleura), with at least one of the following: • Invasion of diaphragmatic muscle • Invasion of lung parenchyma
	T3	Tumor involves ipsilateral pleura (parietal or visceral pleura), with at least one of the following: • Invasion of endothoracic fascia • Invasion into mediastinal fat • Solitary focus of tumor invading soft tissues of the chest wall • Non-transmural involvement of the pericardium
	T4	Tumor involves ipsilateral pleura (parietal or visceral pleura), with at least one of the following: • Chest wall, with or without associated rib destruction (diffuse or multifocal) • Peritoneum (via direct transdiaphragmatic extension) • Contralateral pleura • Mediastinal organs (esophagus, trachea, heart, great vessels) • Vertebra, neuroforamen, spinal cord • Internal surface of the pericardium (transmural invasion with or without pericardial effusion)
N	NX	Regional lymph nodes cannot be assessed
	N0	No regional lymph node metastasis
	N1	Metastases to ipsilateral intrathoracic lymph nodes (includes ipsilateral bronchopulmonary, hilar, subcarinal, paratracheal, aortopulmonary, paraesophageal, peridiaphragmatic, pericardial fat pad, intercostal, and internal mammary nodes)
	N2	Metastases to contralateral intrathoracic lymph nodes. Metastases to ipsilateral or contralateral supraclavicular lymph nodes
M	M0	No distant metastasis
	M1	Distant metastasis MPM

Stage	T	N	M
IA	T1	N0	M0
IB	T2, T3	N0	M0
II	T1, T2	N1	M0
IIIA	T3	N1	M0
IIIB	T1,T2,T3 T4	N2 any N	M0 M0
IV	Any T	Any N	M1

1.10. Treatments

MPM is a highly aggressive disease with no curable treatment available yet. MPM management requires a multimodal approach combining different therapies among which surgery, chemotherapy, radiotherapy and immunotherapy. Since MPM is generally diagnosed at an advanced stage and is associated with poor prognosis, palliative care is commonly intended. The health care strategy will depend on the staging, histological subtype, performance status and comorbidities of the patient. Treatments extend median overall survival by only a few months; therefore, it is necessary to find new therapeutic strategies (Janes, Alrifai, and Fennell 2021)(G. L. Ceresoli and Bombardieri 2019).

1.10.1. Surgery

Few patients are eligible for surgery, since this procedure can only by performed in early stages of the disease. Different methods can be implemented.

Extrapleural pneumonectomy is a curative and aggressive approach with a high post-surgery morbidity level. This technique consists in the resection of the pleura (both visceral and parietal), the lung, the diaphragm and the pericardium. The median overall survival obtained with this method reaches 18 months (Janes, Alrifai, and Fennell 2021)(Tsao et al. 2009)(Davidson, Firat, and Michael 2018).

Pleurectomy/decortication is a palliative approach that consists in the surgical removal of the macroscopic malignancies. Thus, this procedure includes both the excision of the parietal pleura and the decortication of the visceral pleura. These resections can also be accompanied with ablation of the diaphragm and the pericardium if the malignancies are extended (G. L. Ceresoli and Bombardieri 2019)(Mossman et al. 2013)(Rice et al. 2011).

Furthermore, drainage of pleural effusions and talc insufflation in the pleural space is called pleurodesis. Talc is used as a sclerosing agent that causes adhesion of the two sheets of the pleura, therefore relieving dyspnea in patients and preventing recurrent pleural effusions in the pleural space (Mossman et al. 2013)(Novello et al. 2016)(Mercer, Hassan, and Rahman 2018).

1.10.2. Chemotherapy

Chemotherapy consists in the administration of a chemical substance in order to interfere with cell proliferation or to induce apoptosis of cancer cells (DeVita and Chu 2008). This treatment is provided with a palliative intent for MPM patients that are ineligible for surgery and harbor a good performance status. The first-line standard chemotherapy of unresectable MM, approved by the FDA, is composed of a combination of cisplatin and pemetrexed (G. L. Ceresoli and Bombardieri 2019)(Vogelzang et al. 2003)(Cantini et al. 2020)(Scherpereel et al. 2020).

Cisplatin is a platinum-based drug that induces bulky adducts on the DNA, after being bioactivated through aquation reactions. This aquation process is directly related to chloride ion concentration. Indeed, because of low chlorine concentration in the intracellular medium, the two chlorines of the cisplatin structure are being replaced by two molecules of water, resulting in a dicationic aqua complex. This electrophile complex is highly reactive with the nucleophilic sites of DNA, especially the N^7 of

guanines **(Figure 10)**. Thus, cisplatin is an alkylating agent covalently binding to DNA, creating mostly intrastrand-crosslinks compared to interstrand-crosslinks, with generally binding of two adjacent guanines or one adenine and one guanine (1,2-GG > 1,2-AG). This results in a distortion of the double DNA helix, as cisplatin adducts are rigid while the rest of the chain remains flexible. DNA deformation and covalent bonds block DNA transcription as well as the DNA replication machinery in S phase of the cell cycle (Dasari and Bernard Tchounwou 2014)(Ghosh 2019)(Siddik 2003).

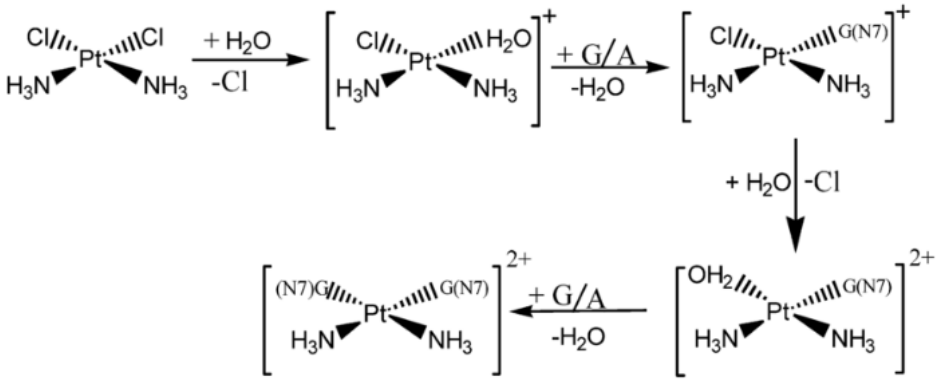

Figure 10. Cisplatin bioactivation through aquation process. Cisplatin undergoes aqua activation in order to create covalent bounds to DNA *via* electrophilic-nucleophilic interactions. Intrastrand-crosslinks with two adjacent guanines or one adenine and one guanine are the most frequent genotoxic insults obtained. Resulting DNA distortion leads to DNA replication and transcription arrest at the damage site (Sarmah and Roy 2013).

Carboplatin, another platinum-based compound, demonstrates clinically similar efficacy and tolerance in MPM patients compared to cisplatin, when combined with pemetrexed. Therefore, carboplatin can substitute cisplatin regimen in case of medical contraindications (Giovanni Luca Ceresoli et al. 2006)(Santoro et al. 2008)(G. L. Ceresoli et al. 2008).

Pemetrexed is an antifolate agent as it is an analogue of folic acid **(Figure 11)**. It acts as a competitive inhibitor of key enzymes involved in the *de novo* synthesis of deoxyribonucleotide triphosphates (dNTPs): the thymidylate synthase (TS), the dihydrofolate reductase (DHFR) and the glycinamide ribonucleotide formyltransferase (GARFT) (Rollins and Lindley 2005)(Chamizo et al. 2015). The interference of the purines and pyrimidines metabolism leads to nucleotides depletion in the cell. Therefore, this antimetabolite inhibits cell replication, DNA synthesis and repair **(Figure 12)** (Adjei 2004). Moreover, since its mechanism of action generally impacts folate metabolism, pemetrexed medication is strongly associated with hematological toxicity, notably megaloblastic anemia. In order to reduce this harmful effect, the standard regimen requires supplementation of vitamin B12 and folic acid (Van Thiel, Gaafar, and Van Meerbeeck 2011)(T. Y. Yang et al. 2013).

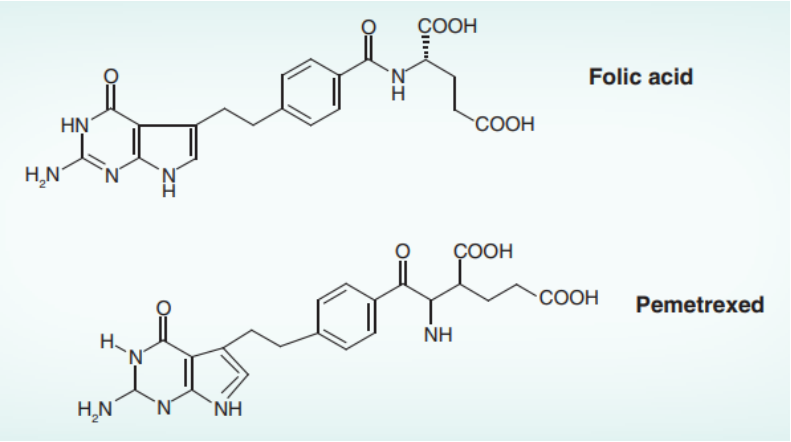

Figure 11. Chemical structure of pemetrexed. Comparison of the molecular structure of pemetrexed with folic acid (Mircea, Aurelia, and Bratu 2014).

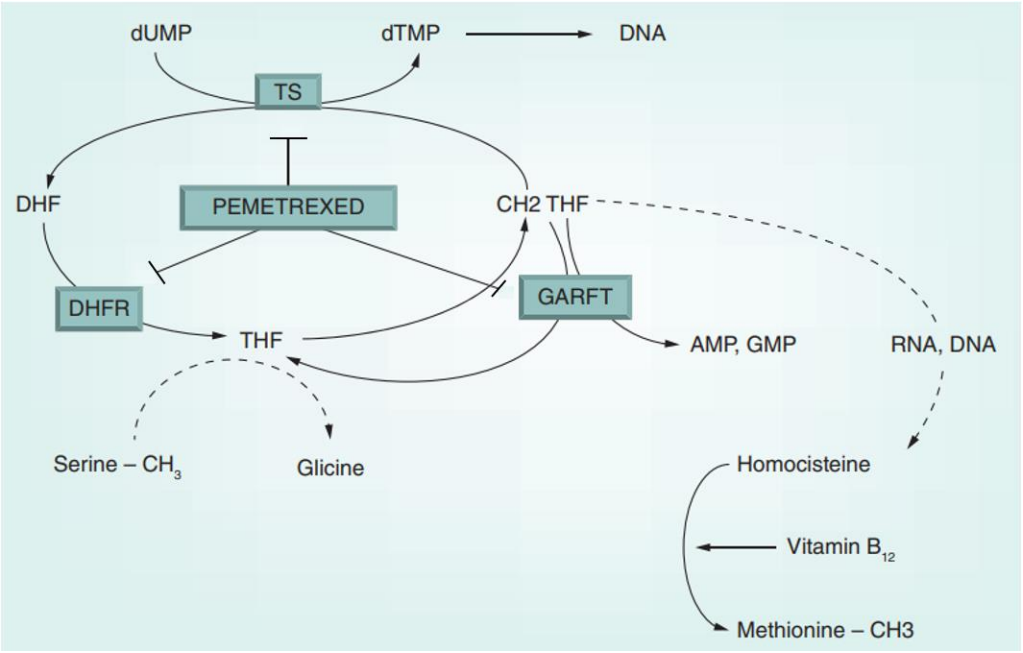

Figure 12. Mechanism of action and targets of pemetrexed through folate metabolism. Pemetrexed inhibits key enzymes of the *de novo* synthesis of deoxyribonucleotides triphosphates (dNTPs): thymidylate synthase (TS), dihydrofolate reductase (DHFR) and glycinamide ribonucleotide formyltransferase (GARFT); therefore, this antifolate agent interferes with DNA synthesis, cell replication and DNA repair (Mircea, Aurelia, and Bratu 2014).

The combination of cisplatin and pemetrexed shows significant survival benefit compared to cisplatin alone. Indeed, cisplatin + pemetrexed reaches median overall survival of 12.1 months (versus 9.3 months for cisplatin alone) and progression-free survival of 5.7 months (while cisplatin alone attains 3.9 months). The quality of life of MPM is also significantly improved with this combination (Vogelzang et al. 2003).

As angiogenesis is a key step for tumor growth and metastatic spread, anti-angiogenic agents have been also tested in the context of MM. Bevacizumab, a monoclonal antibody against VEGF, demonstrated therapeutic potential in combination with cisplatin and pemetrexed. Indeed, the addition of bevacizumab significantly increased the median overall survival from 16.1 to 18.8 months and progression-free survival from 7.3 to 9.2 months (Zalcman et al. 2016).

Mechanisms of resistance to the first-line standard chemotherapy of MPM include several pathways **(Figure 13)** (Siddik 2003)(S. H. Chen and Chang 2019)(Galluzzi et al. 2012). Chemoresistant cells can emerge from a decrease of the intracellular concentration through inhibition of uptake and/or an increase in efflux, as well as an increase of intracellular inactivation through scavengers, such as metallothionein (MT) or glutathione (GSH). Other ways leading to chemoresistance are overexpression of targeted enzymes of pemetrexed and increased DNA damage repair (Brossel et al. 2021)(Gottesman, Fojo, and Bates 2002)(Holzer, Manorek, and Howell 2006)(Brozovic, Ambriović-Ristov, and Osmak 2010).

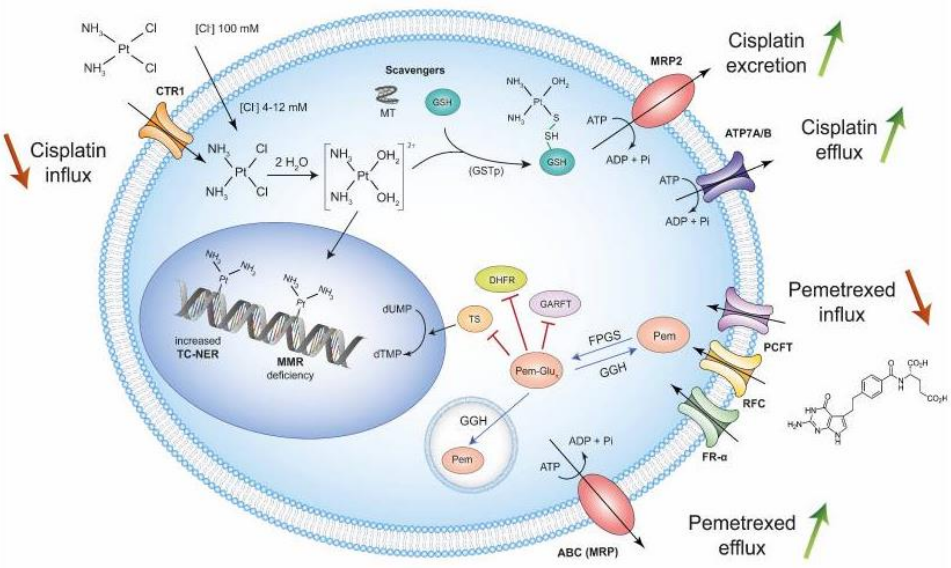

Figure 13. Mechanisms of resistance of cisplatin and pemetrexed. Selection of chemoresistant MPM cells can emerge upon decrease of influx and/or increase in efflux, inactivation through scavengers, overexpression of the targets and DNA damage repair (Brossel et al. 2021).

Since the first-line standard chemotherapy can induce resistance or relapse, a second-line therapy can be proposed to MPM patients. Several second-line treatments have been investigated alone or in combination with cisplatin and pemetrexed. Among them, one can mention vinorelbine (which is part of the vinca alkaloid family and inhibits the polymerization of microtubules, hence stops cell division); gemcitabine (which is an antimetabolite, analog to deoxycytidine, thus inhibits DNA synthesis); doxorubicin (which belongs to the anthracyclines class of drugs and is an intercalating agent as well as an inhibitor of the topoisomerase II, therefore favoring double-strand break (DSB) formation) (Abdel-Rahman and Kelany 2015)(Zauderer et al. 2014)(Baas 2002)(Klotz et al. 2019)(Toyokawa et al. 2014). However, no regimen has been approved as standard yet as all the molecules tested only show moderate efficacy compared to cisplatin + pemetrexed (Byrne et al. 2020)(Muers et al. 2008)(Petrelli et al. 2018).

1.10.3. Radiotherapy

Radiotherapy consists in the irradiation of cancer cells with ionizing radiation in order to prevent cell proliferation (G. L. Ceresoli and Bombardieri 2019). This method should be used only in a multimodal intent within MPM treatment.

Prophylactic drain site radiotherapy limits the seeding of tumors and tract metastasis. Its potential benefit remains controversial; therefore, it is not recommended in clinical practice (Scherpereel et al. 2020).

Palliative radiotherapy is used in order to relieve the pain and to improve the patient's quality of life (Luna et al. 2021).

Post-operative radiotherapy (after extrapleural pneumonectomy or pleurectomy with or without decortication) should only be considered within the context of clinical trials and/or included in both national and international surgical registries (Scherpereel et al. 2020)(Flores et al. 2006).

Intensity-modulated radiotherapy (IMRT) improves dose precision and distribution. This technique is combined with chemotherapy and/or surgery (Perrot et al. 2017).

1.10.4. Immunotherapy

As mentioned previously, transforming mesothelial cells set up an immunosuppressive inflammatory response in order to escape from immune surveillance. The aim of the immunotherapy is either to activate the immune system of the host or to overcome the immunosuppressive systems within the tumor microenvironment, in order to kill the cancer cells (Calabrò, Rossi, and Maio 2018).

In MM, immune checkpoint inhibitors include anti-CTLA-4 (ipilimumab) and anti-PD-1/PD-ligand 1 (PD-L1) (pembrolizumab, nivolumab) monoclonal antibodies, impairing the immunosuppressive response (B. Li, Chan, and Chen 2019)(de Gooijer et al. 2020).

CTLA-4 is a T-cell receptor that binds to the co-stimulatory receptors CD80 (B7-1) and CD86 (B7-2) on the antigen-presenting cell (APC), hence inducing a decrease of the lymphocyte response and limiting its cytotoxicity toward tumor cells. Besides, CTLA-4 prevents the interaction of B7-1/B7-2 with CD28, its competitive receptor that triggers T-cell activation and proliferation when TCR also binds to antigen and the major histocompatibility complex (MHC) **(Figure 14 A)**. Thus, blocking the interaction

between B7-1/B7-2 and CTLA-4 with an anti-CTLA-4 antibody allows T-cells to be active and to eliminate cancer cells (Rowshanravan, Halliday, and Sansom 2018)(Postow, Callahan, and Wolchok 2015).

PD-1 is another immunologic checkpoint that promotes negative regulation of T-cell activity. Interaction between PD-1 and its ligands, PD-L1 and PD-L2, is required to suppress T-cell effector function. In fact, PD-1 engagement attenuates the stimulatory signaling obtained from binding of TCR to peptide-MHC complex. Moreover, sustained antigen exposure upregulates PD-1's expression. Other immune cells also express PD-1: B-cells, NK cells, DCs, monocytes and macrophages. Since tumor cells express PD-L1, the PD-1 pathway is activated and results in immune suppression in the tumor microenvironment **(Figure 14 B)**. Thereby, PD-1/PD-L1 blockade can restore T-cell processes and functions, such as proliferation, survival, glucose uptake, cytokine production and cytotoxic activity (Brossel et al. 2021)(Šmahel 2017)(Postow, Callahan, and Wolchok 2015).

The combination of anti-CTLA-4 (ipilimumab) and anti-PD-1 (nivolumab) has been compared to the standard chemotherapy as front-line treatment in MPM unresectable patients. Immunotherapy displays a notable benefit, particularly in the non-epithelioid subtype, as it provides an overall survival of 18.1 months, with a 3-year survival rate of 23%, while chemotherapy reaches 14.1 months and a 15% survival rate (Baas et al. 2021). Additionally, antibodies targeting CTLA-4 or PD-1 prevent CD8+ T-cells exhaustion as they block the co-inhibitory receptors, thereby maintaining potent effector functions (Blum et al. 2019)(Alcala et al. 2019). Overall, the association of ipilimumab and nivolumab appears to be an effective therapeutic strategy, as it has been approved by the Food and Drug Administration (FDA) and the European Medicines Agency (EMA) as a new first line treatment for unresectable MPM (Metro et al. 2021).

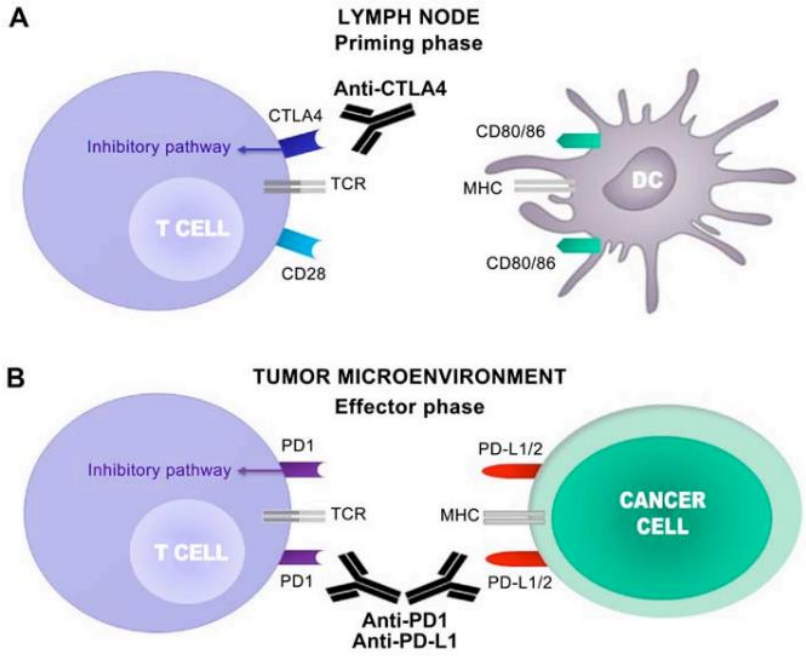

Figure 14. T-cell regulation at different stages through CTLA-4 and PD-1. (A) T-cell activation requires co-stimulatory interactions of TCR with peptide-MHC complex as well as CD28 with CD80/CD86. If CTLA-4 binds to CD80/CD86, an inhibitory signal suppresses ongoing T-cell activation. **(B)** PD-L1 and PD-L2 are expressed by cancer cells. PD-1 engagement with its ligand attenuates the stimulatory signaling obtained from the binding of TCR to peptide-MHC complex and leads to negative regulation of T-cell activity. Antibodies against CTLA-4/PD-(L)1 can restore T-cell effector function (Stucci et al. 2017).

2. DNA damage in MPM and their management

2.1. DNA damage in MPM

Genomic instability is a common aspect of malignancies. Cancer frequently results from mutations of tumor suppressor genes or oncogenes. Genome integrity is supervised by different mechanisms, such as DNA damage checkpoints, DNA repair pathways and cell cycle checkpoints. Any deficiency of these processes often results in genomic instability and drives cells to malignant transformation (Yao and Dai 2014).

Though MPM is characterized by a low mutation rate compared to other cancers, many sources cause DNA damage in MPM cells (Brossel et al. 2021). Indeed, asbestos fibers directly interfere with the mitotic spindle and lead to major structural chromosomal rearrangements driving oncogenesis (E. Dopp et al. 1995)(Jensen et al. 1996)(Ault et al. 1995)(Somers et al. 1991). Also, ROS and RNS are generated through asbestos fibers and the frustrated phagocytosis undergone by macrophages. Resulting sustained inflammation further increases the oxidative burden (Shukla et al. 2003)(Hamaidia et al. 2016).

ROS are highly reactive compounds that are formed from oxygen (O_2) and include superoxide anion radical ($O_2^{\bullet-}$), hydrogen peroxide (H_2O_2) and hydroxyl radical ($OH^{\bullet}$). Production of ROS occurs in low amount under normal physiological conditions. High amount of ROS within the cell leads to oxidative stress and its deleterious effects (Pizzino et al. 2017). The NOX is a membrane-bound enzyme complex belonging to the class I enzymes, which catalyzes oxidoreduction reactions. It harbors different isoforms and performs redox reactions through electronic transfer. The superoxide anion radical is produced from oxygen by the NOX ($NADPH + 2\ O_2 \rightarrow NADP^+ + H^+ + 2\ O_2^{\bullet-}$) (Magnani and Mattevi 2019)(Kalyanaraman 2013). The superoxide dismutase (SOD), another class I enzyme, catalyzes the dismutation of superoxide anion radical into oxygen and hydrogen peroxide ($2\ O_2^{\bullet-} + 2\ H^+ \rightarrow O_2 + H_2O_2$) (Kalyanaraman 2013)(Griess et al. 2017). Furthermore, the hydroxyl radical, an extremely oxidative component, is produced from hydrogen peroxidase in the presence of iron through the Fenton reaction ($Fe^{2+}_{(aq)} + H_2O_2 + e^- \rightarrow Fe^{3+}_{(aq)} + OH^-_{(aq)} + OH^{\bullet}$) (Jiang et al. 2012)(Governa et al. 1999).

RNS, in turn, are produced by the inducible nitric oxide synthase (iNOS) and include nitric oxide ($^{\bullet}NO$) and nitrogen dioxide ($^{\bullet}NO2$). The combination of nitric oxide and superoxide anion radical leads to the generation of peroxinitrite ($^{\bullet}ONOO$), which is a particularly unstable compound **(Figure 15)** (Kalyanaraman 2013)(Sugiura and Ichinose 2011)(Förstermann and Sessa 2012).

Detoxification of these reactive oxygen and nitrogen species can be undergone by a few mechanisms. On the one hand, polyphenols, flavonoids as well as vitamin A, C and E are free radical scavengers. These molecules are able to supply free electrons to radicals, in order to neutralize them, and are thereafter regenerated (Valko et al. 2006)(Milisav, Ribarič, and Poljsak 2018)(Z. Liu et al. 2018). On the other hand, antioxidant enzymes are able to detoxify the reactive species. The SOD is considered as one of them since the hydrogen peroxidase produced is less reactive than other ROS and can be detoxified by the catalase, another antioxidant enzyme, in oxygen and water (2

$H_2O_2 \rightarrow 2\ H_2O + O_2$) (Y. Wang et al. 2018)(Fattman, Schaefer, and Oury 2003). A further detoxification enzyme is the glutathione peroxidase which catalyzes the reduction of peroxide hydrogen to water ($2GSH + H_2O_2 \rightarrow GS–SG + 2H_2O$) (Kalyanaraman 2013). Moreover, clearance of damaged molecules and DNA repair mechanisms can restore the normal physiological conditions of the cell (Rajapakse et al. 2020)(Kaarniranta et al. 2020)(Homma and Fujii 2020).

ROS and RNS are unstable components that impair multiple components of cells. Indeed, their oxidizing power drives the degradation of lipids *via* lipid peroxidation and protein deterioration which leads to methionine sulfoxide, dityrosine and 3-nitrotyrosine formation along with reticulation and fragmentation of polypeptide chains (D. Wu and Yotnda 2011)(Hogg and Kalyanaraman 1999)(Baraibar, Ladouce, and Friguet 2013). Moreover, these reactive species induce mutagenic oxidative lesions, such as oxidation of the DNA, which frequently results in eight-oxoguanines (8-oxoG), as well as DNA bases nitration and deamination (Ba et al. 2014)(Thanan et al. 2014)(Dedon and Tannenbaum 2004). During DNA replication, 8-oxoG leads to mismatch pairing where this lesion is paired with adenine, followed by substitution of guanine to thymine and cytosine to adenine (Thanan et al. 2014)(David, O'Shea, and Kundu 2007). Besides oxidation of guanines, ROS also alter phosphodiester bonds of the DNA backbone which leads to DSB upon DNA replication (Berquist and Wilson 2012).

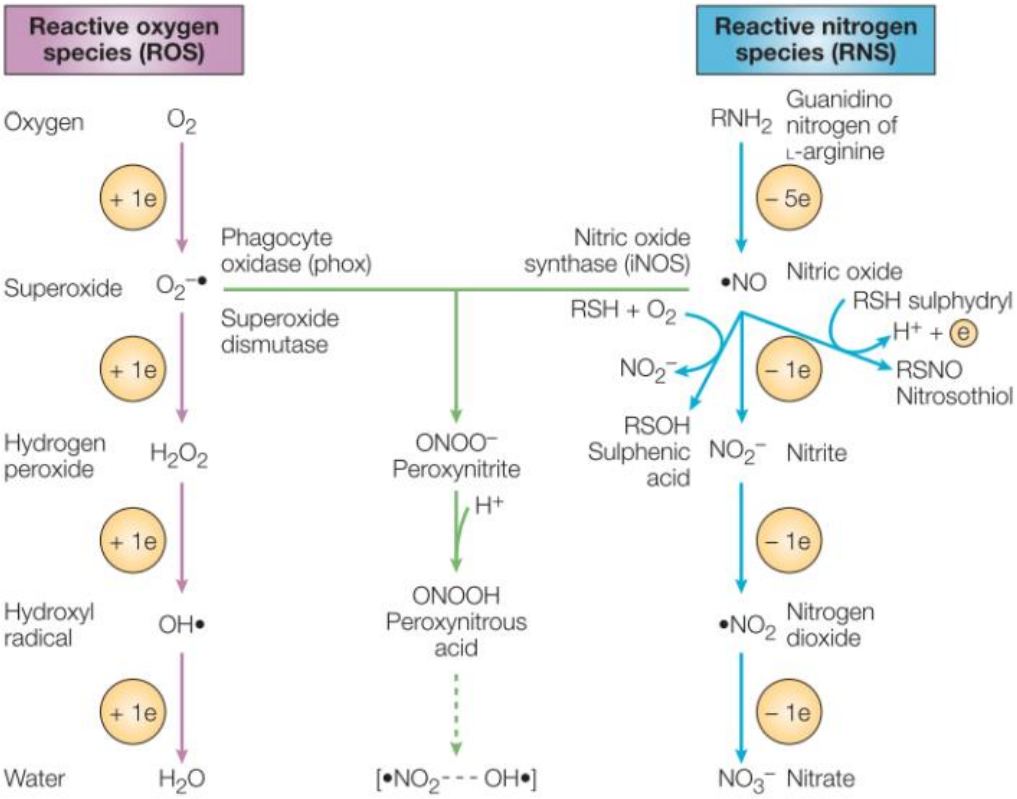

Figure 15. ROS and RNS production and metabolic pathways. Reactive oxygen species (ROS) comprise superoxide anion, hydrogen peroxide and hydroxyl radical. They are generated *via* the NOX. Reactive nitrogen species (RNS) are produced by the inducible nitric oxide synthase (iNOS) and include nitric oxide and nitrogen dioxide. Superoxide anion and nitric oxide assembling leads to the formation of peroxynitrite, a particularly reactive compound (Fang 2004).

Moreover, DNA lesions are also generated by the standard chemotherapy treatment. Indeed, cisplatin creates bulky adducts blocking DNA replication while pemetrexed inhibits DNA synthesis by reducing the pool of nucleotides available for DNA replication (Dasari and Bernard Tchounwou 2014)(Adjei 2004). The combination of these two drugs also ensures a high frequency of fork collapse that leads to single-strand breaks (SSBs) converted into DSBs upon DNA replication, along with genome instability (Brossel et al. 2021)(Toumpanakis and Theocharis 2011).

Furthermore, radiotherapy also causes genotoxic insults. Ionizing radiation-induced DNA damage includes the following: free radicals that lead to damaged bases, abasic sites (also called apurinic/apyrimidinic sites, AP sites), SSBs and DSBs (Santivasi and Xia 2014)(Sutherland et al. 2000).

DNA damage obtained from all these effects promotes oncogenic transformation of mesothelial cells. Nonetheless, those genotoxic insults can be managed by the cells through different mechanisms.

2.2. DNA damage response

2.2.1. ATM – ATR pathways

The maintenance of genome integrity is essential for cell survival. Remaining DNA damage being potentially mutagenic, it is necessary to ensure their detection and repair, which is managed by the DNA damage response (Jackson and Bartek 2009).

When DNA damage occurs, the DNA damage response provides detection of the lesion and transmission of signal through a protein cascade using sensors, transducers and effectors. Among sensors, upstream kinases named ataxia-telangiectasia mutated (ATM), ataxia telangiectasia and Rad3-related protein (ATR) and DNA-dependent protein kinase catalytic subunit (DNA-PKcs) are members of the phosphatidylinositol 3-kinase-related kinase (PIKK) family. The functions of these proteins are of utmost importance as they promote and regulate DNA damage repair, they ensure cell cycle checkpoints activation and initiate signaling to apoptosis (Blackford and Jackson 2017)(Fedak, Adler, and Abegglen 2022)(Lovejoy and Cortez 2009). ATM and ATR show an extensive crosstalk as they both phosphorylate hundreds of substrates. ATM is mainly activated by DSB while ATR responds to a wide range of DNA damage, including single-stranded DNA (ssDNA) and lesions that interfere with DNA replication (Weber and Ryan 2015). DNA-PKcs primarily promotes non-homologous end-joining (NHEJ), which is part of the DSB repair pathways (Reynolds et al. 2012). Accordingly, DNA damage response can lead to cell cycle arrest, DNA repair, apoptosis or senescence (Roos and Kaina 2013)(Ciccia and Elledge 2010).

In response to DSB, the MRE11-RAD50-NBS1 (MRN) complex is rapidly recruited to the site of DNA damage and promotes ATM kinase activity by transducing signal through phosphorylation of several substrates, including ATM itself, checkpoint kinase 2 (CHK2), BRCA1, p53-binding protein 1 (53BP1), p53, histone H2AX and mediator of DNA damage checkpoint protein 1 (MDC1) **(Figure 16)** (Tatfi, Hermine, and Suarez 2019)**.** CHK2, BRCA1, 53BP1 and p53 play a role in DNA repair, cell cycle arrest through checkpoint activation and apoptosis while ɣH2AX (H2AX phosphorylated at the serine 139) recruits proteins for DNA repair and promotes chromatin remodeling. MDC1 binds to ɣH2AX as well as the MRN complex and promotes additional recruitment of ATM promoting further ɣH2AX formation, leading to a positive feedback loop which amplifies the signal (Roos and Kaina 2013)(J. Smith et al. 2010)(Maréchal and Zou 2013).

While ATM plays a role in DSB response, ATR is activated in a broader spectrum of DNA lesions **(Figure 17)**. ATR forms a complex at the damaged site with ATR interacting protein (ATRIP) which regulates its localization and signaling (Brown and Baltimore 2003). ATRIP binds to ssDNA coated with replication protein A (RPA), which could arise from stalled replication fork or resection of DNA end through homologous recombination (HR), one of DSB repair pathways. Indeed, RPA is a

heterotrimeric complex (RPA1, RPA2, RPA3) coating ssDNA in order to protect replication fork from degradation thereby maintaining its stability. RPA also drives ATRIP-dependent ATR recruitment and activation at the damaged site (Maréchal and Zou 2013)(Caldwell and Spies 2020)(Bezine, Vignard, and Mirey 2014). Checkpoint kinase 1 (CHK1) is a key substrate of ATR phosphorylation, which causes autophosphorylation to achieve full activation (H. L. Smith et al. 2020). Recruitment of activating proteins, including Ewing's tumor-associated antigen 1 (ETAA1) and DNA topoisomerase 2-binding protein 1 (TOPBP1), further triggers ATR. ETAA1 is recruited to ssDNA through interaction with RPA whereas TOPBP1 is recruited by the MRN complex and the RAD9-HUS1-RAD1 (9-1-1) clamp (Bass et al. 2016)(Mordes et al. 2008)(Delacroix et al. 2007).

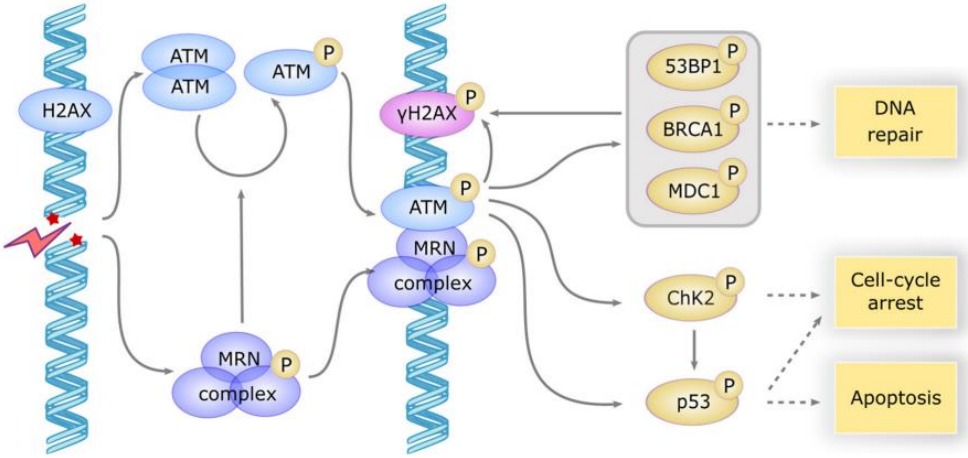

Figure 16. ATM activation and signaling in response to DSB. The MRN complex is rapidly recruited at the DSB site and induces activation of ATM, which phosphorylates a large subset of downstream proteins, such as H2AX which recruits repair proteins, MDC1, 53BP1 and BRCA1 involved in DNA repair, CHK2 taking part in cell cycle arrest and p53 promoting cell cycle arrest as well or apoptosis (Tatfi, Hermine, and Suarez 2019).

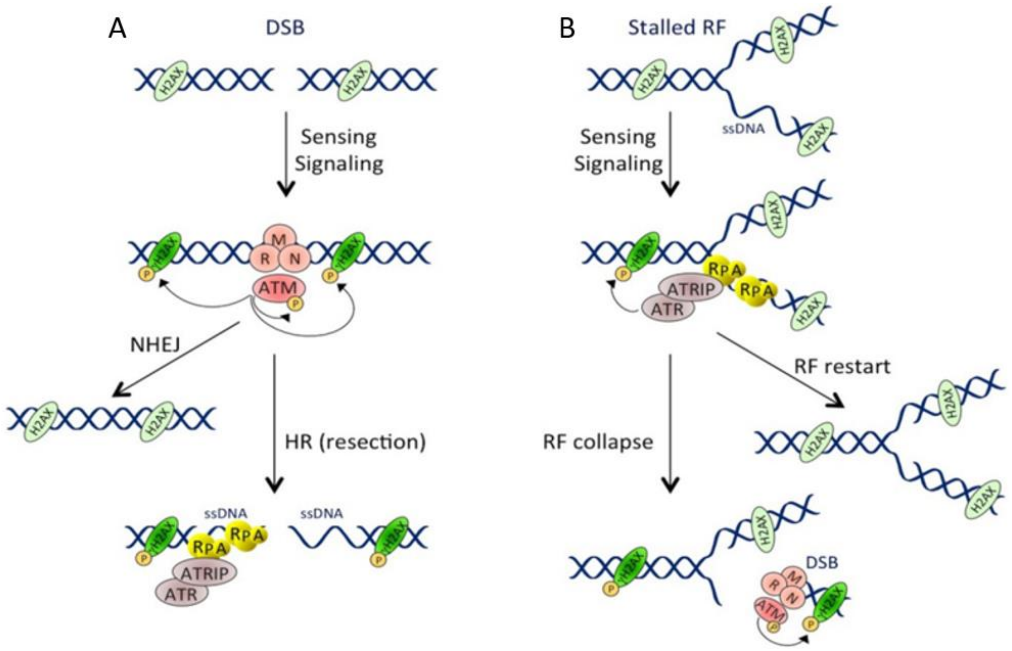

Figure 17. ATM and ATR pathways in response to DNA damage. (A) ATM pathway upon DSB. DSB induces MRN-dependent ATM recruitment which leads to phosphorylation of notably ATM itself and H2AX standing near the damaged site. DSB repair occurs through either non-homologous end joining (NHEJ) or homologous recombination (HR). Repair of DSB through HR requires resection of the extremities of the lesion, which leads to ssDNA stretches that are coated by replication protein A (RPA). This structure is recognized by ATRIP, which recruits and activates ATR. **(B)** ATR pathway upon replication stress. When the DNA polymerase faces a damage upon replication, the replication fork (RF) stalls. Recruited RPA coats ssDNA in order to maintain fork stability and drives ATRIP-dependent ATR recruitment and activation, which leads notably to phosphorylation of H2AX. Provided stress is transient, RF restarts, whereas it collapses in the event of prolonged stress. In this case, RF breakdown forms DSB and activates ATM pathway as well as another and stronger wave of H2AX phosphorylation (Bezine, Vignard, and Mirey 2014).

2.2.2. Checkpoints activation and cell cycle arrest

The cell cycle consists of 4 distinct and successive phases, including G1 – S (DNA duplication) – G2 – M (mitosis), and in order to conduct cell division. Checkpoints are involved in each phase to ensure that everything is accurately achieved before entering the next phase. When DNA damage occurs, ATM – ATR pathways promote checkpoints activation and cell cycle arrest through CHK2 and CHK1, respectively, thus allowing time for DNA damage repair. Cell cycle arrest is indeed maintained until the DNA integrity is restored (Goodarzi, Block, and Lees-Miller 2003).

The DNA damage response pathway followed depends on the cell cycle phase in which DNA damage occurs **(Figure 18)**. G1 checkpoint is managed by the ATM –

CHK2 signaling which induces downstream p53 phosphorylation and CDK inhibitor p21 transcription (Sullivan et al. 2018). Through inhibition of cyclin E/CDK2 complex, p21 prevents pRB phosphorylation as well as subsequent S phase entering (H. L. Smith et al. 2020)(Goodarzi, Block, and Lees-Miller 2003).

Intra-S as well as G2-M checkpoints are predominantly mediated by the ATR – CHK1 cascade through inactivating phosphorylation of cell division cycle 25 C (CDC25C) phosphatase. Phosphorylated CDC25C is thereby incapable of triggering the cyclin B/CDK1 complex which is required for mitotic progression (Brown and Baltimore 2003)(H. L. Smith et al. 2020)(Dart et al. 2004).

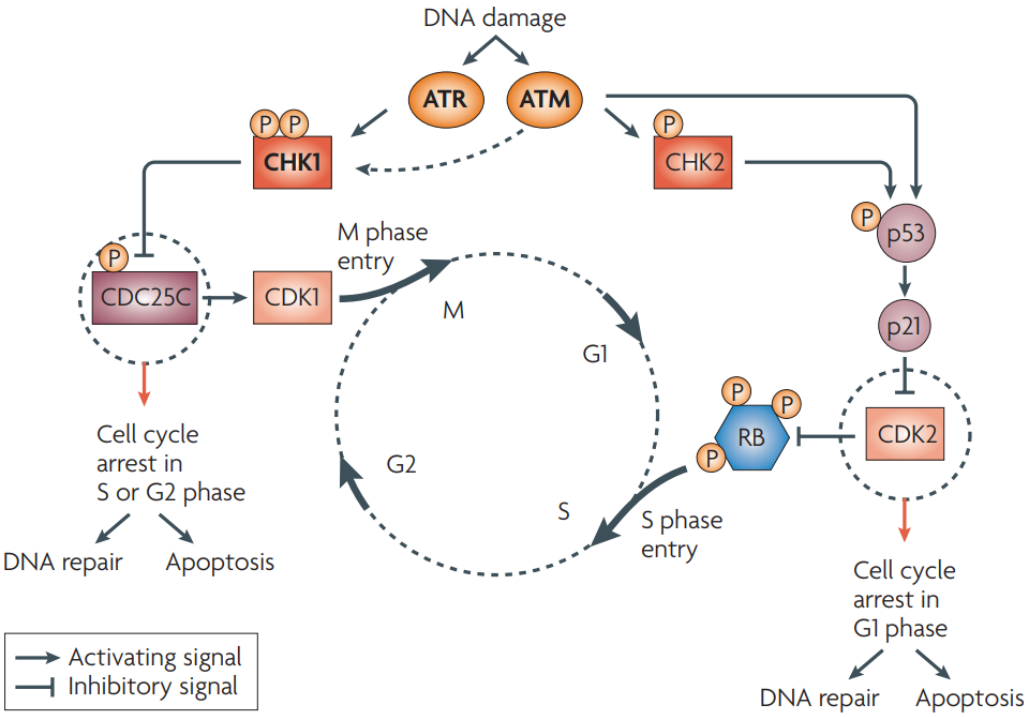

Figure 18. Checkpoints activation and cell cycle arrest through ATM-ATR pathways. The DNA damage response pathway followed depends on the cell cycle phase in which DNA damage occurs. G1 checkpoint involves ATM – CHK2 signaling. Phosphorylation of CHK2 by ATM leads to p53-dependent accumulation of p21. By inhibiting the cyclin E/CDK2, p21 prevents pRB phosphorylation and subsequent S phase entering. Intra-S and G2-M checkpoints are mainly regulated by ATR and its checkpoint kinase CHK1. Once activated, ATR and CHK1 promote the inhibitory phosphorylation of CDC25C that is thereby unable to trigger the cyclin B/CDK1 complex, which is essential for mitotic entry (Lapenna and Giordano 2009).

Depending on the extent of DNA damage, cell cycle arrest can either lead to apoptosis, senescence or DNA repair. Indeed, p53 phosphorylation subsequently drives transcription of genes and activation of proteins involved in these processes (Bezine, Vignard, and Mirey 2014)(Lapenna and Giordano 2009).

2.2.3. Apoptosis

If DNA lesions are too significant and cannot be fixed, apoptosis is a way of protection against oncogenesis. Apoptosis is a programmed cell death process that removes defective cells as well as ensuring no spillage of their contents into the extracellular environment. Indeed, apoptotic cells undergo DNA fragmentation by endonucleases and trigger disposal of proteins. This leads to apoptotic bodies formation that enclose cell contents and can be phagocytized by immune cells such as macrophages (Ichim and Tait 2016)(Elmore 2007)(X. Xu, Lai, and Hua 2019).

There are mainly two different pathways that drive apoptosis, each requiring specific triggering pro-apoptotic signals to launch a widespread cascade of cysteine-aspartic proteases, called caspases. Indeed, the cascade of caspases can either be initiated by another cell at the cell surface (the extrinsic pathway), or by the cell itself at its mitochondria (the intrinsic pathway) **(Figure 19)** (Roos and Kaina 2013)(D'Arcy 2019).

The intrinsic pathway is engaged by a range of stimuli, basically DNA damage, cellular stress and ATM-induced p53 activation, and triggers mitochondrial outer membrane permeabilization (MOMP), thus releasing cytochrome c from the mitochondrial intermembrane space. Afterwards, cytochrome c, apoptotic protease activating factor 1 (APAF1) and pro-caspase-9 interact together to form the apoptosome, which activates caspase-9. Activated caspase-9 triggers, in turn, caspases-3 and 7, and leads to apoptosis (Bock and Tait 2020)(Kiraz et al. 2016)(Goldar et al. 2015). Moreover, second mitochondria-derived activator of caspase (SMAC) is also released during MOMP and promotes caspase activation through neutralization of members of inhibitor of apoptosis (IAP) family proteins (Adrain, Creagh, and Martin 2001). Besides, B-cell lymphoma-2 (BCL-2) family proteins orchestrate apoptosis through high regulation of MOMP. Indeed, some of those proteins are pro-apoptotic, such as BAX and BAK, while others are anti-apoptotic, such as BCL-2, BCL-X_L and myeloid cell leukemia 1 (MCL1), which counteract MOMP induction (Youle and Strasser 2008)(Kalkavan and Green 2018). Additionally, BCL-2 homology domain 3 (BH3)-only proteins, a subfamily of BCL-2 proteins involving p53 upregulated modulator of apoptosis (PUMA), BH3-interacting death domain (BID) and BIM, transmit diverse apoptotic signals to activate BAX and BAK, and therefore promote MOMP (Shamas-Din et al. 2011).

Furthermore, the extrinsic pathway is initiated upon ligand binding to death receptors, which include TNF and TNF-related apoptosis-inducing ligand (TRAIL) binding to TRAIL receptor (TRAILR) as well as FASL binding to FAS. These receptors are located at the plasma membrane and require dimerization mediated by the adaptor FAS-associated death domain (FADD) protein to recruit and activate initiator caspases-8 and 10 through death inducing signaling complex (DISC) formation which further promotes activation of caspases-3 and 7 (Elmore 2007)(Kiraz et al. 2016)(Dickens et al. 2012).

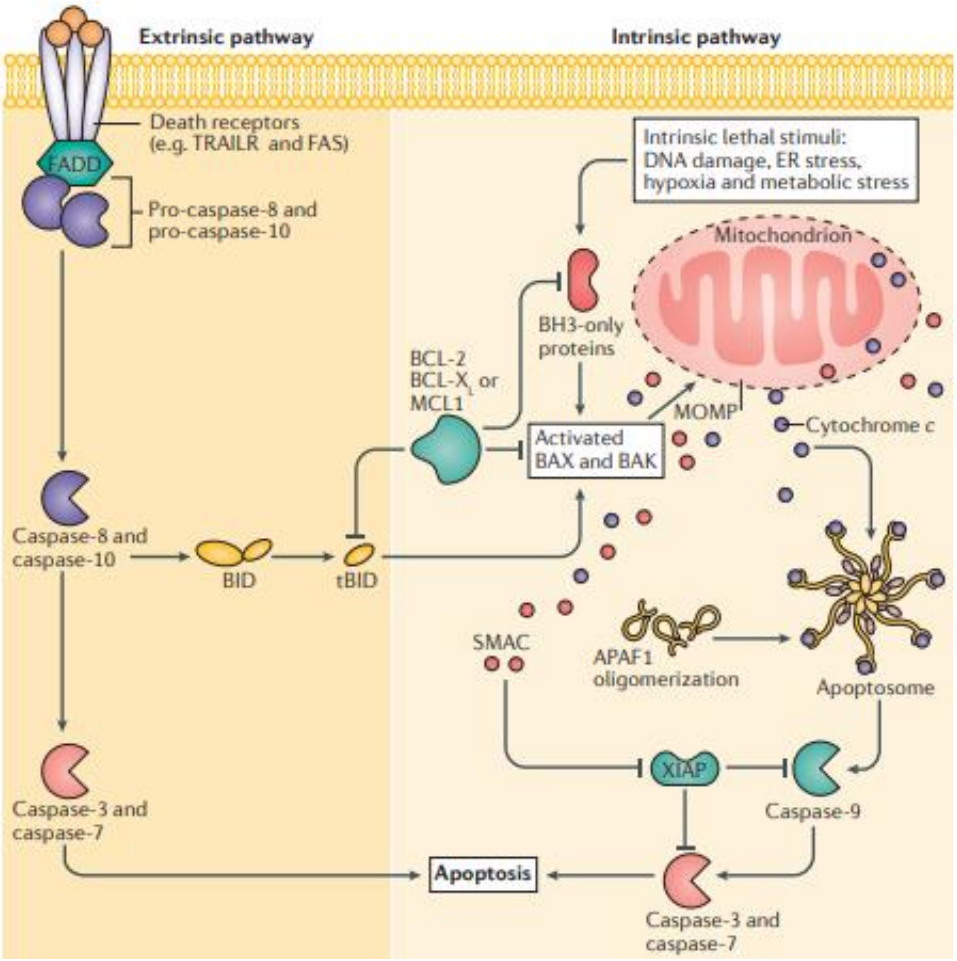

Figure 19. Extrinsic and intrinsic pathways of apoptosis. Several cell stresses engage the intrinsic pathway. BCL-2 homology domain 3 (BH3)-only proteins activate BAX and BAK which trigger mitochondrial outer membrane permeabilization (MOMP). Anti-apoptotic BCL-2 family proteins interfere with this signaling. Following MOMP, second mitochondria-derived activator of caspases (SMAC) and cytochrome c are released from the mitochondria to the cytosol. Cytochrome c, apoptotic protease activating factor 1 (APAF1) and pro-caspase-9 form the apoptosome, which induces caspase-9 activation. In turn, caspase-9 proteolytically activates caspases-3 and 7 and leads to apoptosis. SMAC also facilitates apoptosis by blocking the caspase inhibitor X-linked inhibitor of apoptosis protein (XIAP). The extrinsic pathway is mediated by death receptors, such as TNF-related apoptosis-inducing ligand receptor (TRAILR) and FAS. The adaptor FAS-associated death domain (FADD) protein recruits and activates caspases-8 and 10 which further promote activation of caspases-3 and 7. Moreover, crosstalk between the extrinsic and intrinsic apoptotic pathways is possible since caspase-8 is able to cleave the pro-apoptotic BH3-interacting death domain (BID). Activated and truncated BID (tBID) thereafter activates BAX and BAK, which further leads to MOMP (Ichim and Tait 2016).

Despite the two distinct routes, crosstalk between the intrinsic and extrinsic pathways can occur. Indeed, caspase-8 cleavage of pro-apoptotic BH3-only protein BID generates an active and truncated form of BID (tBID), which thereafter activates BAX as well as BAK, and ultimately triggers MOMP. Besides, caspase-3 and 7 are activated in both pathways and lead to apoptotic cell death (Esposti 2002)(Schug et al. 2011).

2.2.4. Senescence

Senescence is another possible outcome of DNA damage-induced cell cycle arrest, with DNA lesions resulting from chemotherapy, ionizing radiation, oxidative and genotoxic stress. Moreover, progressive telomere shortening, mitochondrial dysfunction, inflammation and oncogenic activation are other causes that can drive this process. Cellular senescence limits tumor growth by preventing proliferation of potentially dysfunctional, damaged or transformed cells (Calcinotto et al. 2019)(Collado, Blasco, and Serrano 2007)(Shmulevich and Krizhanovsky 2021).

Senescence is a permanent state of cell cycle arrest that shows remaining metabolic activity with phenotypic, physiological and gene expression changes. Of note, senescence is different from quiescence. Indeed, senescence occurs in G1 or G2 phases and persistent stress prevents cell cycle restart while quiescence happens in G0 phase and growth factors, mitogenic signals or resolution of transient stress resume cell growth (Marescal and Cheeseman 2020)(Campisi 2013). Although senescence is considered irreversible, the sequential inactivation of tumor suppressor genes can resume cell cycle progression (Beauséjour et al. 2003).

Senescent cells are characterized by an enlarged and flat morphology as well as increased lysosomal β-galactosidase activity. This enzyme catalyzes the hydrolysis of terminal β-galactose residues of β-galactosides with maximal activity at pH 4 – 4.5 in normal conditions whereas its potency is detectable at pH 6 in senescent cells. However, the role of lysosomal β-galactosidase in senescence remains unknown (B. Y. Lee et al. 2006)(Huang et al. 2022).

Senescent cells also demonstrate significant changes in their secretome called senescence-associated secretory phenotype (SASP), which shows autocrine and paracrine effects thereby affecting nearby non-senescent cells. Its composition varies depending on the cell type, the environment and the persistence of the senescence, and basically includes proinflammatory cytokines, growth modulators, angiogenic factors and proteases (Kumari and Jat 2021)(Ou et al. 2021)(Chambers et al. 2021). Moreover, prolonged activation of p53/p21 and $p16^{INK4a}$/pRB tumor suppressor pathways plays a central role in regulating senescence **(Figure 20)**. Indeed, persistent engagement of DNA damage response leads to constitutive activation of p53 which triggers CDKI, such as $p16^{INK4a}$ and p21 that act as negative regulators of cell cycle progression, thereby promoting senescence. Furthermore, these pathways induce broad changes in proliferative gene expression as p53 and pRB are key transcriptional regulators. As already mentioned, inhibition of pRB phosphorylation mediates subsequent binding with E2F in order to form a complex which prevents transcriptional activity of E2F target genes and, ultimately, leads to cell cycle arrest (Shmulevich and Krizhanovsky 2021)(Kumari and Jat 2021)(Herranz and Gil 2018).

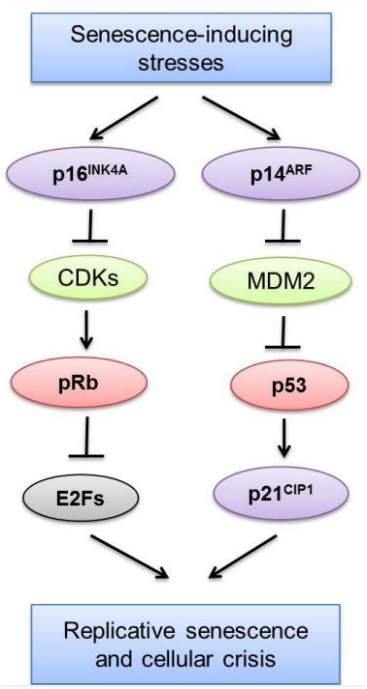

Figure 20. Senescence regulation through p53/p21 and p16^{INK4a}/pRB pathways. Senescence-inducing stresses lead to activation of p53, p16^{INK4a} and p14^{ARF}. P53 triggers the CDKI p21^{WAF} while p14^{ARF} manages the prolonged activity of p53 through inhibition of MDM2. Besides, p16^{INK4a} interferes with CDKs and promotes complex formation of pRB-E2F, thus preventing transcription of E2F target genes. Adapted from (Choi and Lee 2015).

2.3. DNA damage repair pathways

DNA damage generated by the chemotherapy regimen and the fibers-dependent oxidative and inflammatory environment initiate the DNA damage response pathways and, subsequently, DNA damage repair. As an extensive variety of DNA damage can occur, a broad range of repair mechanisms is available in damaged cells, such as mismatch repair (MMR), base excision repair (BER), nucleotide excision repair (NER), and DSB repair pathways. Moreover, the repair pathway followed depends on the lesion. Indeed, regarding DNA damage in MPM cells, 8-oxoG are processed by 8-oxoguanine glycosylase and BER while cisplatin-induced crosslinks are mostly repaired by NER. Cisplatin adducts can lead to DSBs upon DNA replication. Moreover, gamma irradiation also induces DSB which can mainly be repaired by NHEJ or HR, depending on the phase of the cell cycle (Toumpanakis and Theocharis 2011)(Hoeijmakers 2001)(Fuso Nerini et al. 2020)(Basu and Krishnamurthy 2010). Here is a review of the different DNA repair mechanisms.

2.3.1. Direct lesion reversal, MMR, BER, SSBR, NER and FA pathways

Direct repair of a DNA lesion, such as DNA methylation, doesn't require any excision nor de novo DNA synthesis as it can be undergone by a single protein able to directly reverse the damage. For instance, O^6-methylguanine-DNA methyltransferase (MGMT) is able to transfer the methyl group of O^6-methylguanine to a cysteine which acts as an acceptor site. Thus, MGMT plays an important role in protecting against genotoxic effect of alkylators (Pegg 2000)(Yi and He 2013).

MMR pathway consists in the detection and removal of inadequate base pairing (Stojic, Brun, and Jiricny 2004)(G. M. Li 2015). Indeed, mismatches are recognized by MutS homologs (MSH) 2 and 6 proteins, which form the MutSα complex, while strand discrimination is mediated by MutL. Exonuclease 1 (EXO1) then performs excision. DNA synthesis is subsequently conducted through polymerase (Pol) δ/ε, followed by ligation using DNA ligase 1 (Lig1) (D. Liu, Keijzers, and Rasmussen 2017)(Jiricny 2013).

BER corrects indirect SSBs as well as non-helix distorting base lesion that can emerge from oxidative stress, base alkylation, methylation, deamination or hydroxylation (Berquist and Wilson 2012)(T. H. Lee and Kang 2019). BER can follow two different subpathways – a long and a short patch. In both cases, DNA glycosylase detects and releases the damaged base through N-glycosylic bond, thus leaving an AP site. AP endonuclease 1 (APE1) or a glycosylase with endonuclease activity recognizes the AP site, creates a nick at this point and excises it. Then, the pathway can follow the short or the long patch, depending on the number of nucleotide(s) to repair. Indeed, the short patch involves a repair tract of a single nucleotide using Pol β, DNA ligase 3 (Lig3) and X-ray repair cross-complementing protein 1 (XRCC1), the latter acting as a scaffold protein. Alternatively, engagement of the long patch is applied for a repair tract of at least two nucleotides. This pathway requires proliferating cell nuclear antigen (PCNA), flap endonuclease 1 (FEN1) as well as Pol δ/ ε for DNA synthesis, and Lig1 for ligation (Meas, Wyrick, and Smerdon 2019)(J. S. Sung and Demple 2006)(Krokan and Bjørås 2013)(S. Zhao, Tadesse, and Kidane 2021)(Demin et al. 2021).

Moreover, direct SSBs can be processed through SSB repair pathway, which shares similarities with BER but starts differently. The nick sensor poly (ADP-ribose) polymerase 1 (PARP-1) recognizes SSB and recruits the scaffold protein XRCC1. The 3'-phosphates and 5-AMP groups located on the broken ends are then either processed by polynucleotide kinase 3'-phosphatase (PNKP) or aprataxin (APTX), respectively. Subsequent gap-filling and ligation steps meet the ones of BER pathway (Tiwari and Wilson 2019)(Takahashi et al. 2007). Furthermore, incomplete processing of DNA supercoiling by topoisomerase 1 (TOP1) during DNA replication and transcription leads to SSB. This specific type of DNA damage is taken over by the two key proteins involved in SSB repair, namely PARP-1 and XRCC1, which engage PNKP and process the TOP1-DNA intermediates through tyrosyl-DNA phosphodiesterase 1 (TDP1) (Tiwari and Wilson 2019)(Mei et al. 2020).

NER fixes helix distorting DNA lesions, such as cisplatin bulky adducts. There are two subpathways that ultimately merge into a common path. They differ in their manner of recognizing DNA damage, but they share the same process. One is applied for the

entire genome including the non-transcribed regions and is called global genome NER (GG-NER), while the other one, named transcription couped repair (TC-NER), is only followed when bulky adducts occur in a transcribed DNA strand of active genes, thus causing RNA polymerase stalling. In either situation, the transcription factor II H (TFIIH) complex is recruited on the lesions, helicases open the DNA double helix and cut out a short stretch of DNA containing the lesion, leaving ssDNA subsequently coated with RPA. Xeroderma protein F (XPF)/excision repair cross-complementation group 1 (ERCC1) heterodimer is subsequently recruited and makes a 5' incision. Then, xeroderma protein G (XPG) removes a 22-30 nucleotide-long strand on the 3' end of the damaged strand. Gap-filling is finally performed by Pol δ, translesion synthesis (TLS) Pol κ or Pol ε using the non-damaged DNA strand as a template. Sealing is thereafter processed either by Lig1 or Lig3 (Duan et al. 2020)(Spivak 2015)(Marteijn et al. 2014).

Interstrand crosslinks occurring apart from S phase are processed by NER, while the ones generated during DNA replication are fixed through the Fanconi anemia (FA) pathway (W. Liu et al. 2020). In this case, the interstrand crosslink is surrounded by two converging replication forks, thus forming an X shaped DNA structure recognized by FANCM and FAAP24, which recruit the other components of the FA core complex (Ciccia et al. 2007). This complex is composed of multiple subcomplexes acting together to lead to the activation of FA pathway through the mono-ubiquitination of both FANCD2 and FANCI, respectively on lysine-561 (K-561) and K-523, by the E2-ubiquitin conjugase UBE2T/E3-ubiquitin ligase FANCL complex (W. Liu et al. 2020). Furthermore, ATR-CHK1 mediate pathway regulation through phosphorylation of several members of the FA machinery, notably the FANCD2-FANCI complex (Clauson, Schärer, and Niedernhofer 2013). Once FA pathway activated, several repair pathways are sequentially followed in order to repair the interstrand crosslink. First, mono-ubiquitinated FANCD2-FANCI complex promotes the recruitment of ERCC1/XPF endonuclease at the stalled replication fork to unhook the interstrand crosslink on one parental DNA strand (Faridounnia, Folkers, and Boelens 2018). Then, TLS polymerases, such as REV1 followed by Pol ζ, engage the bypass of the remnant crosslink (Budzowska et al. 2015). Subsequently, NER mediates the removal of the remaining crosslink on the parental DNA strand. Finally, the remaining DSB is preferentially repaired through HR or single-strand annealing (SSA), which are both explained in the next section (Benitez et al. 2019)(Palovcak et al. 2018).

2.3.2. Double-strand break repair

Although DNA DSBs are part of endogenous processes, these genotoxic insults are extremely deleterious types of DNA lesions as they can cause deletions, loss of heterozygosity and chromosome rearrangements, which can potentially lead to cell death or oncogenesis.

There are several ways to repair DSBs, where each method depends on the DNA end resection and the phase of the cell cycle. Indeed, the 5'-3' DNA end resection, also called 5'-3' degradation, plays a key role in the decision-making process of the repair pathway choice as it initiates HR, SSA or alternative end-joining (Alt-EJ) whilst it simultaneously limits NHEJ **(Figure 21)** (Ceccaldi, Rondinelli, and D'Andrea

2016)(Symington and Gautier 2011). This procedure first consists in the resection of short stretches – about 20 nucleotides – from the 5' ends of the notch by MRE11 (of the MRN complex) and C-terminal binding protein interacting protein (CtIP) in order to form 3' single-stranded tails (Lamarche, Orazio, and Weitzman 2010). These small sections of ssDNA are then available to line up accurately with matching sequences in Alt-EJ pathway. In a second step, BRCA1 along with a bunch of helicases and exonucleases (Bloom syndrome RecQ like helicase (BLM), DNA replication helicase/nuclease 2 (DNA2), Werner syndrome RecQ like helicase (WRN), CtIP and EXO1) extend the original resection to perform longer stretches of ssDNA, required for HR and SSA (Ceccaldi, Rondinelli, and D'Andrea 2016). Furthermore, the stage of the cell cycle undertaken during the DSB will also influence the choice of the DNA repair procedure employed. Indeed, DNA resection along with HR, SSA and Alt-EJ are homology-dependent processes that take place in S and G2 phases since those methods need a sister chromatid template to perform the repair (Symington and Gautier 2011). In contrast, NHEJ can operate at any phase of the cell cycle but predominantly proceeds in the G1 phase. Moreover, 53BP1 and BRCA1 are opponents playing a significant role in the regulation of this complex interplay of repair mechanisms. DSBs occurring in G1 phase specifically promote ATM-dependent 53BP1 phosphorylation which further inhibits BRCA1 and mediates RAP-interacting factor 1 (RIF1) and Pax transactivation domain-interacting protein (PTIP) translocation at the lesion site. Therefore, 53BP1 protects DNA broken ends from resection by preventing CtIP from reaching DNA ends and favors NHEJ repair. However, in response to DSBs during S-G2 phases, ATM phosphorylates CtIP as well as BRCA1 which prevents 53BP1 activation and RIF1 translocation to DSBs, hence antagonizing 53BP1-management of NHEJ repair, promoting DNA resection, and leading to HR engagement (Daley and Sung 2014)(Y. Xu and Xu 2020)(Bunting et al. 2010).

DSBs are principally repaired *via* HR or NHEJ. Classical-NHEJ (c-NHEJ) is a fast process occurring in G0/G1 phases that engages the tethering of the DNA broken ends **(Figure 21)** (Jeggo and Löbrich 2007). To do so, the Ku70/Ku80 heterodimer clamp recognizes, protects and maintains both ends of the DSB. Each heterodimer recruits DNA-PKcs in order to form the DNA-PK complex which stabilizes the DNA end synapsis. Hence, short complementary DNA regions are able to hybridize. The protein Artemis is then mobilized and processes the DNA discontinuities through its exonuclease activity. Thus, Artemis removes in a 5'-3' direction the overhangs that don't hybridize. Therefore, permanent loss of genetic information related to this region of the genome induces deletion mutation (Rodgers and Mcvey 2016). Sequence gaps are then filled by DNA polymerase λ or μ. Subsequently, X-ray repair cross-complementing protein 4 (XRCC4) and XRCC4-like factor (XLF) (also called Cernunnos) are recruited and promote ligation of the DNA ends by DNA ligase 4 (Lig4) which catalyzes covalent phosphodiester bonds (Davis and Chen 2013)(Menon and Povirk 2017)(H. H. Y. Chang et al. 2017)(Brandsma and Gent 2012). Besides, NHEJ is also involved in the DSBs occurring during V(D)J recombination of immunoglobulins and TCRs. Indeed, these DSBs arise from rearrangements of the gene segments in order to create a highly diverse repertoire of unique antigen binding sites during the early

stages of B and T-cell maturation of the adaptive immune system (Cooper and Alder 2006)(Chi, Li, and Qiu 2020)(Frit et al. 2014).

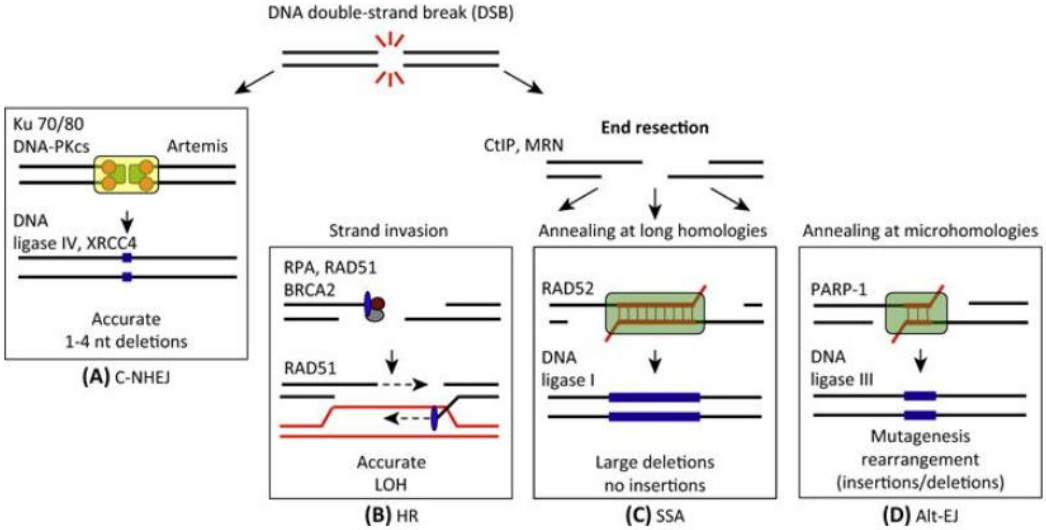

Figure 21. DNA double-strand break repair pathways. DNA end resection is a key process in defining the DSB repair pathway choice. Its restriction occurring in G0/G1 cell cycle phases leads to classical NHEJ (c-NHEJ), which is considered globally accurate despite potential deletions. In contrast, end resection procedure is promoted in S-G2 phases during which resection-dependent pathways such as HR, SSA and Alt-EJ compete for the DSB repair. Varying fidelity and different genetic outcomes, such as loss of heterozygosity (LOH), nucleotide (nt) deletions or insertions, result from these repair mechanisms. HR is defined as extremely accurate while SSA and Alt-EJ are characterized as highly mutagenic processes using respectively long and microhomologies (Ceccaldi, Rondinelli, and D'Andrea 2016).

Of note, Alt-EJ, also known as microhomology-mediated end joining (MMEJ), is a slow and error-prone repair pathway that is engaged in the absence of Ku as a back-up procedure when HR or c-NHEJ fail **(Figure 21)**. Initiation of this process requires DNA end resection and relies on microhomologies annealing next to the broken DNA ends (H. H. Y. Chang et al. 2017). Importantly, Alt-EJ is completely dependent on PARP-1 that recognizes DNA discontinuities, initially recruits the MRN complex as well as CtIP for DNA end resection and competes with Ku to bind to DNA ends (M. Wang et al. 2006)(Huichen Wang et al. 2003). Moreover, PARP-1 triggers DNA end processing and ligation by DNA polymerase θ and the XRCC1/Lig3 complex (Kent et al. 2015)(Audebert, Salles, and Calsou 2004). This back-up process is considered highly mutagenic as it induces deletions, chromosomal translocations and mutagenic rearrangements, thereby driving genome instability (Rodgers and Mcvey 2016)(Frit et al. 2014)(Sfeir and Symington 2015).

HR pathway is a critical mechanism for stalled replication forks recovery as well as DNA DSBs repair (Arnaudeau, Lundin, and Helleday 2001). This procedure is considered error-free and conservative since it requires an undamaged DNA template –

such as the sister chromatid – entailing sufficient sequence identity with the damaged strand to conduct the repair, thereby occurring in S-G2 cell cycle phases (Johnson and Jasin 2000).

Following ATR – CHK1 signaling, HR repair process is initiated through recognition and nucleolytic excision of the DSB by the MRN-CtIP complex (H. L. Smith et al. 2020). BRCA1 interacts with CtIP to switch the balance of DNA repair from error-prone NHEJ to error-free HR. 5'-3' resection of the DNA ends generates ssDNA protrusions promptly coated with RPA **(Figure 22)** (Y. Xu and Xu 2020)(Sartori et al. 2007). The recombinant mediator breast cancer type 2 susceptibility protein (BRCA2) thereafter facilitates the displacement of RPA from ssDNA ends to enable the DNA recombinase RAD51 to subsequently form nucleoprotein filaments on ssDNA sites (Zhang 2013). This is notably mediated with the help of RAD52 which promotes annealing of complementary ssDNA and enhances RAD51 recombinase activity (Nogueira et al. 2019). The RAD51-ssDNA filaments promote strand invasion on homologous sequences of the sister chromatid (Mazin and Kowalczykowski 2016)(P. Sung et al. 2004). Hence, a displacement loop (D-loop) structure is obtained and then extended at the 3' end by DNA synthesis after removal of RAD51 on the invading strand by DNA translocase RAD54 (Crickard et al. 2020). At this point, two different mechanisms can take over the process: double-strand break repair (DSBR) and synthesis-dependent strand annealing (SDSA) (Filippo, Sung, and Klein 2008).

In DSBR, D-loop extension is followed by capturing the second 3' overhang by the sister chromatid, gap-filling through DNA synthesis at the 3' end of the invading strand and ligation, thereby resulting in the annealing of the ssDNA forming a four-way DNA intermediates called double Holliday junctions (dHJs). These dHJs can undergo resolution by restriction endonucleases called resolvases, cutting only one DNA strand, thus potentially generating either crossover or non-crossover products, depending on the combination of the cleavage orientations. Indeed, cutting on the crossing strand and on the non-crossing strand of dHJs leads to crossover while cutting on both crossing strand results in non-crossover (Mehta and Haber 2014)(Wright, Shah, and Heyer 2018)(J. Li et al. 2019). Therefore, genomic instability could arise from resolution of the dHJs by resolvases since HR engaged between two homologous sequences or chromosomes can potentially engage respectively loss of heterozygosity or chromosomal rearrangements through crossover recombinants. Alternatively, reassignment of each strand of the dHJ to its original complementary strand by helicase BLM and topoisomerase TOP3α leads to dHJs dissolution, thereby preventing any exchange of genetic material as it always results in non-crossover products (Bachrati and Hickson 2009)(L. Wu et al. 2000)(P. Sung and Klein 2006).

In contrast, SDSA mediates unwinding of the D-loop through strand displacement and annealing of complementary ssDNA between broken ends. DNA synthesis and ligation ensue final step of the repair, hence dHJs ultimately resolve through branch migration. Repair products obtained by this process are exclusively non-crossover (Mehta and Haber 2014)(Wright, Shah, and Heyer 2018)(J. Li et al. 2019).

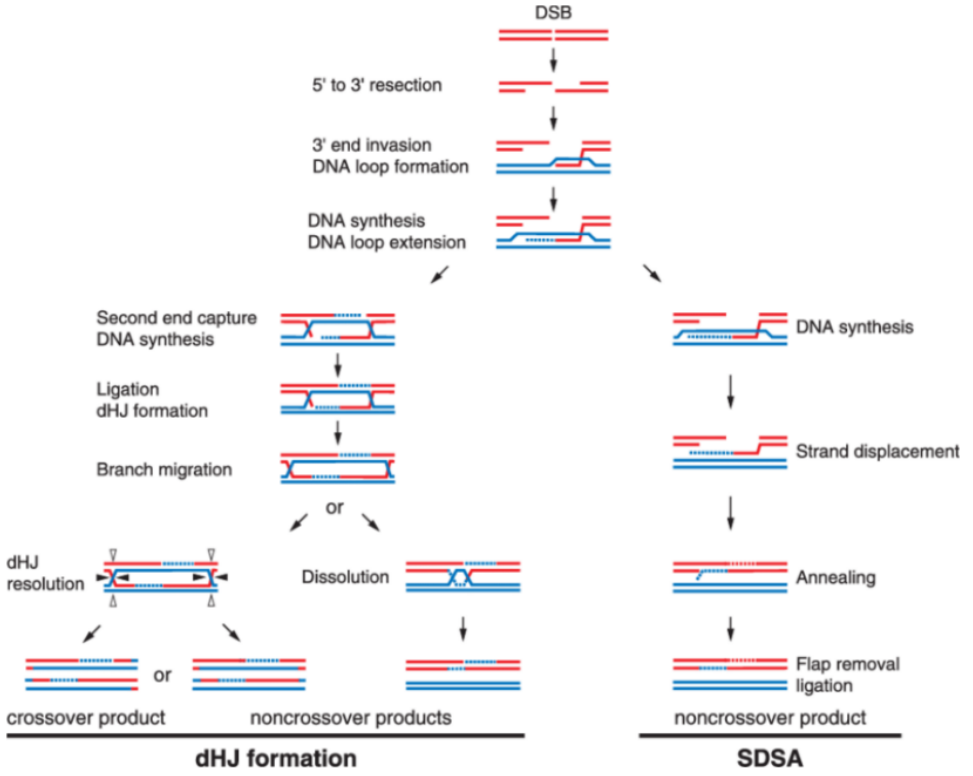

Figure 22. DNA double-strand break repair by homologous recombination-mediated pathways. These mechanisms include double-strand break repair (DSBR) and synthesis-dependent strand annealing (SDSA). In both pathways, DNA resection initiates the repair and provides single-stranded DNA (ssDNA) tails. The 3' end of ssDNA overhangs invades a homologous sequence of the intact sister chromatid in order to use it as a template for DNA synthesis of the invading strand. In DSBR, formation of four-way DNA intermediates called double Holliday junctions (dHJs) occurs through capture of second DSB end, and DNA synthesis gap-filling followed by ligation. dHJs can undergo resolution by specific endonucleases called resolvases, thus potentially generating either crossover or non-crossover products, depending on the combination of the cleavage orientations (asymmetric - a black arrow at one HJ and a white one at the other HJ - or symmetric – black arrows at both HJs -, respectively). Alternatively, reassignment of each strand of the dHJ to its original complementary strand leads to dHJ dissolution, thereby always resulting in non-crossover products. By contrast, SDSA is mediated through strand displacement, annealing of the ssDNA followed by DNA synthesis and ligation. Repair products obtained by this process are exclusively non-crossover (Maloisel, Fabre, and Gangloff 2008).

Unlike HR, SSA is a RAD51 and strand invasion-independent process that mediates the repair of DSB surrounded by long repeated sequences **(Figure 21)** (Rodgers and Mcvey 2016). Upon DNA resection, RAD52 binds to single-strand tails and promotes annealing of exposed complementary homologies which are further processed by ERCC1-XPF endonuclease complex (Rossi et al. 2021). Then, DNA synthesis and ligation take place. Ultimately, genomic sequences between homologous regions are lost, which results in a large deletion and genetic information loss. SSA is therefore characterized as extremely mutagenic (Ceccaldi, Rondinelli, and D'Andrea 2016)(H. H. Y. Chang et al. 2017)(Al-minawi, Saleh-gohari, and Helleday 2008)(Bhargava, Onyango, and Stark 2016).

This complex interplay of repair mechanisms preserves genomic integrity and enables MPM tumor cells to survive despite occurrence of DNA damage. Unrepaired DNA lesions can further be processed by the DNA damage tolerance (DDT) pathways (Brossel et al. 2021).

2.4. DNA damage tolerance pathways

Provided DNA damage cannot be repaired and apoptosis is not mediated, DDT pathways can take over. The DDT process has been well described in yeast *Saccharomyces cerevisiae* but remains not fully understood in humans. These pathways act as escape routes followed to resume the stalled replication fork and prevent apoptosis, thus maintaining cell cycle progression and cell viability. Therefore, DDT provides cell tolerance regarding DNA damage during replication and promotes cell survival despite potential genome instability (Liptay, Barbosa, and Rottenberg 2020)(Gargi and Chen 2013).

Different subpathways can operate for DDT processing of DNA damage and restart of the stalled replication fork. These mechanisms are tightly regulated by PCNA **(Figure 23)**. This homotrimeric ring-shaped structure encircles double-stranded DNA and manages the processivity of DNA polymerase δ within the leading strand during DNA replication. Moreover, this sliding clamp acts as a scaffold to recruit proteins involved in several processes, including DNA replication, DNA damage repair – such as in NER – and DDT (Essers et al. 2005)(Boehm, Gildenberg, and Washington 2016). Post-translational modifications of PCNA determine the choice of the DDT pathway followed by the cell. Indeed, along with ATM-dependent BRCA1 and BAP1 phosphorylation in DDR signaling, mono-ubiquitination of PCNA on K-164 by the E2-ubiquitin conjugase RAD6/E3-ubiquitin ligase RAD18 complex mediates the TLS pathway **(Figure 23, A)** (Gargi and Chen 2013)(Fan et al. 2020)(Hedglin and Benkovic 2015)(Ripley, Gildenberg, and Washington 2020). Thus, mono-ubiquitinated PCNA recruits specialized low-fidelity polymerases, called TLS polymerases, at the stalled replication fork. These TLS polymerases belong to the Y-family (Pol η, ι, κ, and REV1) as well as to the B-family (Pol ζ). They all share the same general structural organization and ensure that DNA replication resumes without any discontinuity. Indeed, they promote bypass of the lesion through incorporation of a nucleotide opposite the DNA damage – as they lack proofreading activity and their catalytic site is wider and more flexible than replicative polymerases –, thus tolerating a broad range of damaged

template bases. However, each TLS polymerase is characterized by its intrinsic features and possesses its own specific catalytic activities. Indeed, lesion bypass can result in an accurate or mutagenic outcome considering the TLS polymerase engaged (Kannouche and Lehmann 2004)(Lehmann et al. 2007)(Vaisman et al. 2017)(Tomczyk et al. 2016)(M. F. Goodman and Woodgate 2013). For instance, cisplatin bulky adducts are mainly processed by the Pol η, REV1 and Pol ζ. Pol η and REV1 are able to appropriately insert deoxycytidine triphosphate (dCTP) opposite cisplatin-GG intrastrand adducts, although Pol η might misincorporate due to its high error rate. After operation of Y-family TLS polymerases, Pol ζ is engaged to further extend the newly synthesized DNA strand beyond the damaged site despite distortion of the double DNA helix resulting from the lesion bypass. Interestingly, Pol ζ can result in an error-free or error-prone process depending on which TLS polymerase, respectively Pol η or Pol κ, operates first. Once typical DNA structure is reached following Pol ζ intervention, high-fidelity replicative polymerase is then recruited to proceed DNA replication (Muniandy et al. 2010)(Shachar et al. 2009)(W. Yang and Gao 2018)(Knobel and Marti 2011).

Therefore, TLS doesn't result in DNA damage removal and is thus potentially mutagenic depending on the TLS polymerase recruited and its related error rate. Overall, damage bypass by TLS is intrinsically considered error-prone but healthier than incomplete replication as it plays an important role in cellular survival (Vaisman et al. 2017)(Rocha et al. 2018).

Furthermore, mono-ubiquitination of PCNA can be extended into a K-63-linked poly-ubiquitin chain by the methyl methanesulfonate sensitive 2 (MMS2)/ubiquitin conjugating 13 (UBC13) (E2) – helicase-like transcription factor (HLTF)/SNF2 histone linker PHD RING helicase (SHPRH) (E3) complex. Poly-ubiquitinated PCNA promotes template switching (TS) pathways which include HR **(Figure 23, B)** and fork reversal (FR) **(Figure 23, C)** (Leung et al. 2019)(Eddins et al. 2006). Like TLS, these pathways also mediate processing and restart of the stalled replication fork. As they both rely on the intact sister chromatid to conduct DNA replication of the damaged strand, these two processes are considered error-free, thereby preventing fork collapse and maintaining genome integrity (Ripley, Gildenberg, and Washington 2020)(Branzei and Szakal 2016). HR repair has been previously described. FR consists in the remodeling of the stalled fork followed by its resolution and restart. FR requires ATR/ATRIP signaling and is initiated by ssDNA protected by RPA. Then, DNA recombinase RAD51 displaces RPA in a BRCA2-dependent manner (Zellweger et al. 2015). Several helicases of the sucrose non-fermentable 2 (SNF2) family subsequently drive the reversal of the stalled fork through their ATP-dependent mechanical remodeling of chromatin structure, thus forming a 4-way junction structure, also called chicken foot structure. Such helicases with double-stranded DNA (dsDNA) translocase activity include SWI/SNF-related matrix-associated actin-dependent regulator of chromatin subfamily A-like protein 1 (SMARCAL1), zinc finger ran-binding domain-containing protein 3 (ZRANB3) and HLTF, through its HIP116, Rad5p, N-terminal (HIRAN) domain (Dhont, Mascaux, and Belayew 2016)(Ryan and Owen-hughes 2011)(Chavez, Greer, and Eichman 2018). Ultimately, fork resolution is either processed by HR or branch migration. Restart of the fork leading to DNA replication resuming is mediated

by DNA2/WRN upon HR or PARP-1/RECQ1 upon branch migration (Liptay, Barbosa, and Rottenberg 2020)(Quinet and Lemac 2017). On an alternative mechanism, endonuclease methyl methanesulfonate and ultraviolet-sensitive clone 81 (MUS81) processes non-resolved fork by inducing DSB which is afterward processed by HR (Liptay, Barbosa, and Rottenberg 2020)(Neelsen and Lopes 2015).

Besides ubiquitination, PCNA can undergo post-translational modification on K-164 by small ubiquitin-like modifier (SUMO) which also plays a role in the regulation of the DDT pathways (Bergink and Jentsch 2009)(Moldovan, Pfander, and Jentsch 2007). Studies on yeast *Saccharomyces cerevisiae* showed that the SUMOylated PCNA recruits DNA helicase Srs2 which disrupts RAD51 nucleoprotein filaments thereby preventing unscheduled HR and promoting TLS pathway. Thus, SUMO and ubiquitin together control DDT pathway choice for the processing of DNA damage at the stalled replication fork during S phase (Papouli et al. 2005)(Gali et al. 2012)(Pfander et al. 2005)(Krejci et al. 2003)(Seong et al. 2009).

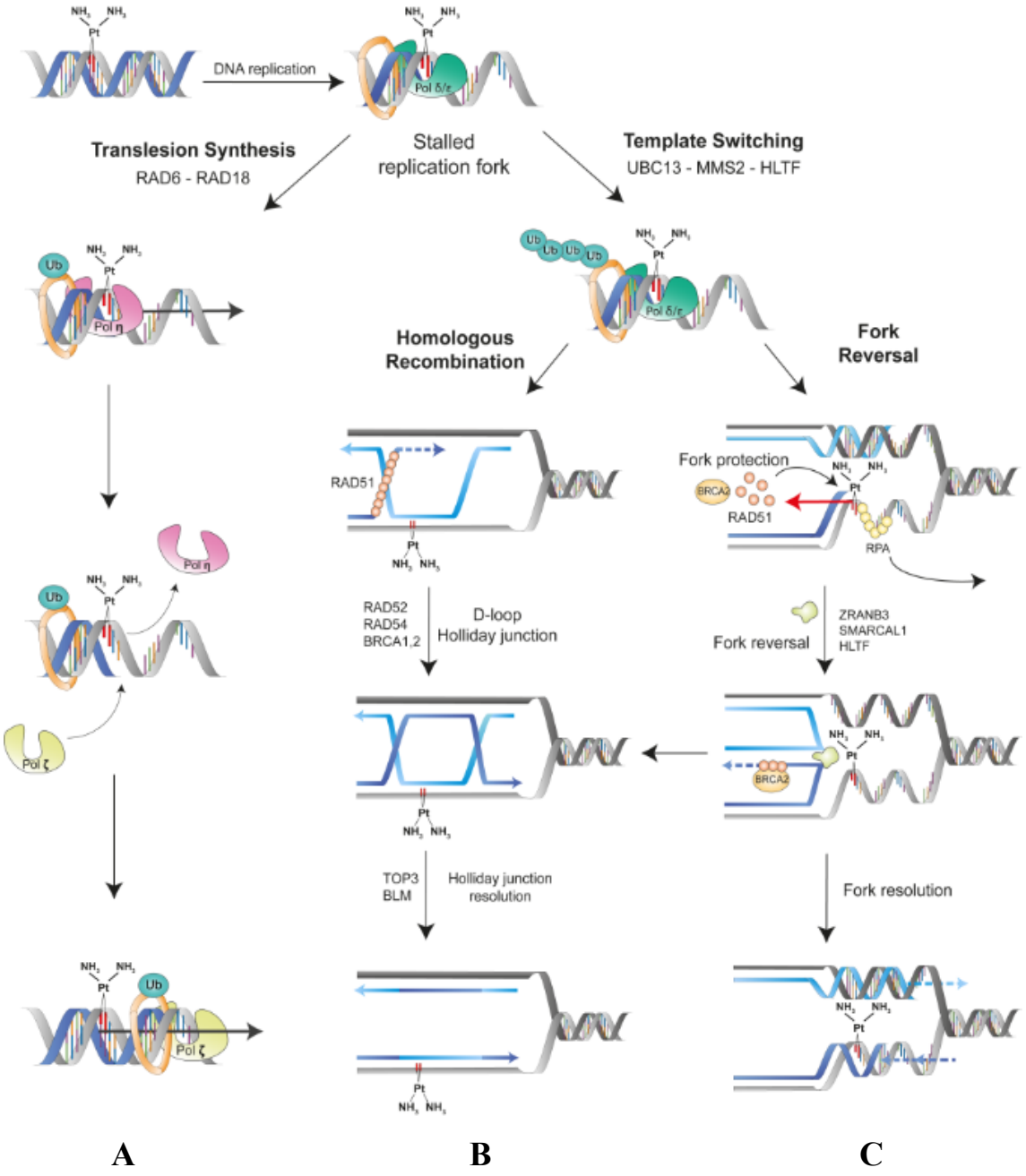

Figure 23. DNA damage tolerance pathways. Unrepaired cisplatin adducts stall the replication fork during S phase and promote activation of the DDT pathways. **(A)** Mono-ubiquitinated PCNA by the RAD6-RAD18 complex mediates the translesion synthesis pathway. Polη incorporates a nucleotide opposite to the cisplatin adduct while Pol ζ is

subsequently engaged to further extend the newly synthesized strand despite distortion of the double helix, thereby bypassing the DNA lesion. Poly-ubiquitinated PCNA by the UBC13-MMS2-HLTF complex engages the template switching pathways which include **(B)** homologous recombination and **(C)** fork reversal. In HR, RAD51 mediates strand invasion while RAD52 promotes annealing of complementary ssDNA. Then, RAD54 promotes D-loop and Holliday junction formation which are afterward resolved by helicase BLM and topoisomerase TOP3. In FR, RAD51 displaces RPA of the ssDNA with the help of BRCA2. Helicases SMARCAL1, ZRANB3 or HLTF subsequently process the remodeling of the stalled fork to obtain a 4-way junction structure that can be resolved by HR or branch migration (Brossel et al. 2021).

2

Aims of the thesis

Pleural mesothelioma (MPM) is a poor prognosis and rare type of cancer that develops from the mesothelial cells of the pleura and is mainly due to asbestos exposure. The first-line chemotherapy of MPM consists in the combination of cisplatin (an alkylating agent) and pemetrexed (an antifolate). This treatment induces DNA damage and decreases the pool of available nucleotides, thus leading to apoptosis. Radiotherapy is another treatment option that induces DNA damage in order to prevent the proliferation of cancer cells. Unfortunately, these current treatments show unsatisfactory response, therefore MPM remains an untreatable disease. Hence, there is an urgent need to develop new therapeutic strategies.

In order to improve the efficiencies of these treatments, studies of (i) DNA damage response and repair as well as (ii) DNA damage tolerance pathways might give us a more comprehensive view of the mechanisms involved and potentially give rise to new therapeutic approaches in MPM treatments.

In the first part of this thesis, we study the process of DNA damage response and characterize DNA damage repair mechanisms occurring in MPM cells in the context of genotoxic insults.

To that end, the goals of this first part consist in:

- Evaluating the consequences of gamma irradiation and chemotherapy regimen on the cell cycle progression

- Determining the impact of checkpoint inhibition on cell cycle progression upon chemotherapy and gamma irradiation

- Quantifying the efficiencies of the two main double-strand break (DSB) repair pathways: non-homologous end-joining (NHEJ) and homologous recombination (HR)

In the second part of this thesis, we investigate the DNA damage tolerance (DDT) pathways in MPM cells upon chemotherapy.

To do so, we aim at:

- Understanding and characterizing the fine-tuned regulation of the DDT mechanisms in MPM cells

- Investigating new potential therapeutic targets by interfering with the DDT pathways

- Determining the impact of DDT pathway interference on tumor growth in mice, with or without chemotherapy regimen

3

Material and methods

1. Cell culture

Human mesothelioma cell lines, namely ZL34 (CVCL_5906, sarcomatoid), M14K (CVCL_8102, epithelioid), M38K (CVCL_8108, biphasic) and NCI-H28 (referred to as H28, CVCL_1555, sarcomatoid) and human non-malignant mesothelial cells Met5A (CVCL_3749) were obtained from the American Type Culture Collection (ATCC, USA). All cell lines were cultivated in Dulbecco's modified Eagle medium (DMEM, Lonza) supplemented with 10% heat-inactivated fetal bovine serum (FBS, Gibco) and 1% antibiotics, namely penicillin (10.000 units (U)/mL) and streptomycin (10.000 U/mL) (Penicillin-streptomycin solution, VWR) (referred to as complete DMEM). All cell lines were cultivated under controlled and standard conditions at 37°C in a humidified atmosphere with 5% CO_2. Cell washes were operated with phosphate-buffered saline (PBS, VWR) and centrifugations (Megafuge 40R, Thermo Scientific) were performed at 1200 revolutions per minute (rpm) for 5 minutes at room temperature.

2. Generation of stable transduced cell lines displaying RAD18 and HLTF depletion

ZL34 and M14K cells depleted for human RAD18 and HLTF expression were generated using lentiviral short hairpin RNA (shRNA) particles. All references and sequences are gathered in **Table 4** (see appendix 1). Viral particles expressing shRNAs were operated to target RAD18 (n=2) or HLTF (n=2) independently, while two scrambles – one for each target, namely ScrR and ScrH – were used as controls. RAD18 shRNA lentiviral plasmids were purchased at Merck and allow the expression of puromycin resistance gene. Control shRNA was anti-luciferase shRNA (ScrR) while a positive lentiviral plasmid expressing red fluorescence protein (RFP) was used to confirm efficient transduction of lentiviral particles. Both of these control plasmids also exhibit puromycin resistance. Lentiviral plasmids for human HLTF (hHLTF) shRNA were obtained from Vector Builder and allow neomycin resistance gene expression. Control shRNAs both express green fluorescent protein (GFP) as well as neomycin resistance gene and consist of shRNA non-target (NT) (ScrH) and another plasmid for ensuring efficient transduction of lentiviral particles.

Lentiviral vectors were produced by GIGA Viral vectors platform. Briefly, Lenti-X™ 293T Cell Lines (Part #632180, Clontech) were co-transfected with shRNA plasmids, psPAX2 (Part #12260, Addgene) and pVSV-G plasmids (Emi, Friedmann, and Yee 1991). Viral supernatants were collected 48 - 96 hours post-transfection and filtered (0.45 µm). ZL34 and M14K cells were incubated for 72 hours with a combination of RAD18 and HLTF lentiviral particles (comprising either shRNA 1, 2 or the related scramble). The overall multiplicity of infection (MOI) applied was 30, consisting of a MOI of 15 regarding RAD18 and 15 as well concerning HLTF. The double scramble, named ScrR ScrH, was the experimental control condition. Subsequently, media containing the viral particles were washed and all transduced cells were then subjected for 2 weeks to both puromycin (ant-pr-1, Invivogen) and neomycin (ant-gn-1,

Invivogen) selection at 1 µg/mL and 1 mg/mL, respectively. Thereafter, cells were frozen in FBS 90% – dimethylsulfoxide (DMSO) 10% ($1x10^6$ cells/aliquot) for further experiments.

3. RTqPCR

Cultured cells ($2x10^5$ cells in 6-well plates, Greiner Bio-One) were harvested in a dry cell pallet. Total RNA was extracted using NucleoSpin® RNA Plus kit (Macherey-Nagel) which consists of samples lyse and a series of centrifugations on spin columns in order to remove DNA and isolate as well as purify RNA. This step was followed by RNA quantification with NanoDrop™ 1000 UV-visible spectrophotometer (v3.8.1, Thermo Scientific). 1µg of RNA per condition was engaged in reverse transcription to synthetize complementary DNA (cDNA) using random hexamer mix of the Fast Gene® Scriptase II cDNA Synthesis kit (NIPPON Genetics EUROPE) on the C1000 Touch Thermal Cycler (Bio-Rad). Amplification of the cDNA obtained was performed by quantitative polymerase chain reaction (qPCR) using Takyon SYBR master mix (Takyon One-Step Kit Converter, Eurogentec) containing primers for RAD18, HLTF and GAPDH used as housekeeping gene **(Table 3)**. Amplification reactions were processed by the Light Cycler®480 (Roche Diagnostics) with a denaturation step at 95°C for 5 minutes followed by 45 cycles involving 15 seconds at 95°C, 20 seconds at 60°C and 40 seconds at 72°C. The process ends with the acquisition of melting curves which requires 1 minute at 65°C followed by a consistent increase of the temperature until 97°C. The Light Cycler®480 SW 1.5.1. software (Roche Life Science) provides amplification outputs to calculate the relative fold gene expression using the $2^{-\Delta\Delta Ct}$ method.

Table 3. Sequences of primers of genes analyzed in qPCR.

Gene	Forward primer	Reverse primer
RAD18	5'-CAG-CTG-TTT-ATC-ACG-CGA-AG-3'	5'-TTA-AAT-CAC-GAT-CAG-AGA-GCA-AA-3'
HLTF	5'-GTTCAAAGATTAATGCGCT-3'	5'-AAAGACAGGAATGTTGTAAACTGAGA-3'
GAPDH	5'-GCACCGTCAAGGCTGAGAAC-3'	5'-TGGTGAAGACGCCAGTGGA-3'

4. Western blot

Proteins were extracted with lysis RIPA buffer and quantified using Pierce™ bicinchoninic acid (BCA) Protein Assay kit (Thermo Fisher Scientific). This is based on the reduction of cupric (Cu2+) to cuprous (Cu+) ions by proteins in alkaline environment. The chromogenic reagent BCA allows colorimetric detection of Cu+ by forming a purple complex displaying maximal optical absorption at 562 nm, with absorbance being proportional to protein concentration. Spectrophotometric dosage was performed with ImageQuant™ LAS 400 (GE Healthcare Life Sciences). Bovine serum albumin (BSA) provided with the kit was used as calibration standard for total protein

quantification of samples. 50µg of proteins per condition were heated at 95°C for 5 minutes and subsequently loaded on running gels for migration at 120 volts. Then, proteins were transferred onto a nitrocellulose membrane (Whatman Protran BA85, GE Healthcare Life Sciences) for an hour at 100 volts. Protein revelation was afterwards obtained through Ponceau S (Sigma) staining to ensure effective protein transfer. Membranes were subsequently cut according to the weight of proteins of interest in order to separate them for following incubations. Each part was washed three times in tris(hydroxymethyl)aminomethane (Tris)-buffered saline (TBS, VWR) supplemented with 0.1% Tween 20 (Sigma) (TBST) and then incubated in blocking buffer, consisting of TBST – BSA 5% (VWR), for an hour. Proteins were thereafter individually labeled with primary antibodies – RAD18 rabbit dilution 1:1000 (#9040, Cell Signaling); HLTF rabbit dilution 1:1000 (HPA015284, Merck); Tubulin mouse dilution 1:5000 (T9026, Merck) – through overnight incubation at 4°C in the blocking solution. Tubulin was used as housekeeping gene in all western blot assays. The next day, membranes were washed with TBST and incubated for an hour at room temperature with polyclonal secondary antibodies coupled with the horseradish peroxidase (HRP) – goat anti-rabbit dilution 1:2500 (ab205718, Abcam); goat anti-mouse dilution 1:1000 (ab205719, Abcam) – in blocking solution. Membranes were again washed with TBST and chemiluminescent HRP substrate (Pierce ECL Western Blotting Substrate, Thermo Fisher Scientific), containing luminol, was added onto the membrane directly before acquisition of pictures provided by a cooled CCD camera (ImageQuant LAS 4000 mini, GE Healthcare Life Sciences).

5. Chemotherapy treatment

10mM stocks of pemetrexed disodium heptahydrate (Merck) and cisplatin (VWR) in NaCl 0.9% were prepared and stored at -20°C for maximum a month.

6. Gamma irradiation treatment

Gammacell 40 Exactor (MDS Nordion) operated gamma irradiation of mesothelioma and mesothelial cells with a dose rate of 1,28Gy per minute. Range of doses applied to cells was from 1 to maximum 10Gy. The medium was replaced before ionizing treatment.

7. Cell cycle analysis

Mesothelioma and mesothelial cells were plated in 6-well plates ($2x10^5$ cells/well) and treated with chemotherapy (cisplatin 10µM + pemetrexed 10µM), gamma irradiation (10Gy) and/or checkpoint 1 inhibitor UCN-01 (7-hydroxystaurosporine 50nM, Sigma). 24 hours later, both floating and adherent cells were harvested, washed in PBS – FBS 10% and fixed with 70% chilled ethanol. After overnight incubation at -20°C, cells were washed twice with PBS – FBS 10% in order to completely remove ethanol. Cells were then resuspended and underwent RNAse treatment (RNAse A (Merck) 50µg/ml – 0.1%

Tween 20 – PBS) for 30 minutes at 37°C. Then, propidium iodide (PI) staining (PI (Sigma) 20µg/ml in PBS) of cells was performed at room temperature in the dark for 10 minutes before flow cytometry analysis (CytoFLEX, Beckman Coulter Life Technologies). Gating method was based on forward scatter (FSC) and side scatter (SSC). Cell doublets were excluded through the FSC-H (height) versus FSC-A (aera) gating strategy. PI staining was detected *via* the PI 585 channel and 10.000 events were counted per condition. Distribution graphs were analyzed using CytExpert software (version 2.4, Beckman Coulter Life Technologies) through quantification of cells in each cell cycle phase. Indeed, cell cycle profiles represented the number of cells (x-axis) depending on DNA content (y-axis), which was obtained from PI staining, and thereby related to the cell cycle phase. The shape of the profiles defined the different cell cycle phases. For instance, untreated cells showed, from left to right, a G1 peak phase (which is related to a 2n DNA content) and a single peak at G2-M phases (4n DNA content). The S phase stood between these two peaks and was characterized by a lower cell count and DNA content comprising between 2 and 4n. SubG1 stood ahead of the G1 phase and included apoptotic cells while cells beyond the G2-M phases were polyploid as they contained more than two genome copies. Thus, cell cycle analysis could be used to highlight apoptosis through the Sub-G1 cell population.

8. Apoptosis assay

As apoptosis is strongly associated with exposure of phosphatidylserine on the outer plasma membrane, and late apoptosis shows loss of plasma and nuclear membranes integrity, Annexin V – PI double staining turns out to be an interesting method to detect and quantify apoptotic cells. Mesothelioma cells were plated ($2x10^5$ cells/well) in 6-well plates and were submitted to cisplatin (10µM) and pemetrexed (10µM) for 48 hours. Floating and adherent cells were harvested, washed in PBS and resuspended in Annexin V buffer (BD Pharmingen, BD Biosciences) previously diluted 10 times in sterile distilled water. Following addition of 3µl of Annexin V-FITC conjugated (Immunotools) and 5µl of PI (1µg/ml), cells were incubated for 15 minutes in the dark at room temperature. Flow cytometry acquisition (FACS Canto II, BD Biosciences) was obtained through FITC as well as PI 680 channels and a 10.000 cell count. Analysis was performed with the FlowJo™ v10 software (BD Biosciences). Quadrant partitioning was achieved to distinguish positive from negative Annexin V and PI cells independently, with cells exhibiting Annexin V+/PI- being considered as early and Annexin V+/PI+ as late apoptotic cells. Results are indicated in percentages of cells positive for both early and late apoptosis.

9. Mitotic trap assay

This assay was conducted in order to quantify cells initiating mitosis upon several treatments.

Mesothelioma and mesothelial cells were plated ($2x10^5$ cells/well) in 6-well plates and submitted the next day to gamma irradiation (10Gy) or the combination chemotherapy of cisplatin (10µM) and pemetrexed (10µM) and/or checkpoint 1 inhibitor UCN-01 (50nM). Two hours later, the spindle inhibitor paclitaxel (1µM, Taxol®, Cell Signaling) was added in required conditions and incubated overnight for 16 hours at 37°C. Then, cells were harvested by trypsinisation, washed in PBS – FBS 10% and fixed with 70% ethanol at -20°C. After overnight incubation, cells were washed with PBS – FBS 10% and labeled in a two-hour incubation with primary rabbit IgG antibody targeting phosphorylated serine 10 of histone H3 diluted at 1:1600 (#3377, Cell Signaling). Subsequently, cells were washed and stained for an hour in the dark at room temperature with secondary anti-rabbit IgG antibody Alexa Fluor 488 diluted at 1:1000 (A-11008, Invitrogen). Cells were washed again in PBS – FBS 10% and submitted to RNAse treatment as well as PI staining as already explained in the cell cycle assay protocol. Fluorescence activated cell sorting (FACS) acquisition was also performed with CytoFLEX as previously described through cell cycle profiles in addition to FITC channel for Phospho-Histone H3 (Ser10) – Alexa Fluor 488 labeling. Thereafter, FACS analyses were conducted using CytExpert software with simultaneous evaluation of cell cycle profiles and phospho-histone H3 (Ser10) labeling, thereby obtaining quantification of cell cycle distribution of phases and cell entering mitosis indicated by the number of phosphorylated histone H3(Ser10) positive cells.

10. Efficiencies of double-strand breaks repair pathways: HR – NHEJ

Quantification of DSBs repair efficiencies was performed using fluorescent reporter constructs specifically designed to determine repair through HR and NHEJ. This system has been developed by Seluanov's team (Seluanov, Mao, and Gorbunova 2010) and all plasmids were kindly provided by Vera Gorbunova (University of Rochester, USA). This assay is based on plasmids that contain the GFP gene with recognition sites for a rare-cutting endonuclease, called I-SceI, in order to induce DSB.

Both HR and NHEJ constructs are originally GFP negative and efficient repair of the DSB through the pathway in question restores functional GFP expression.

The NHEJ reporter plasmid (GFP-Pem1-Ad2) exhibits the GFP gene including a 3 kb intron from the Pem1 gene which contains an adenoviral exon (Ad2) flanked by inverted nonpalindromic I-SceI recognition sequences. Thus, endonuclease cleavage removes Ad2 and generates incompatible DNA ends that can subsequently be repaired through NHEJ pathway, thus restoring GFP gene expression. Of note, a wide range of NHEJ events are able to manage the DSB repair as occurrence of deletions and insertions in the intron don't affect the repair efficiency.

The HR reporter plasmid (GFP-Pem1) contains in its first intron a 22 bp deletion ensuring no repair through NHEJ and displaying inverted I-SceI restriction sites whose digestion produces incompatible ends. This HR construct further includes a second copy of the GFP-Pem1 first intron and exon which lacks promoter and the first ATG codon.

Thus, following DSB induction by I-SceI digestion, HR gene conversion exclusively re-establishes functional GFP expression.

Reporter plasmids were digested overnight at 37°C with I-SceI endonuclease (New England Biolabs) and then linearized plasmids were purified with the QIAquick gel extraction kit (QIAGEN). Mesothelioma and mesothelial cells seeded in 6-well plates ($2x10^5$ cells/well) were independently co-transfected with rather HR, NHEJ plasmids (2µg) or the pEGFP-Pem1 control plasmid (without Ad2) and the pECFP-C1 plasmid (0.5µg) as internal control for transfection efficiency using the Neon electroporation system (Thermo Fisher Scientific). Two hours after transfection, cells were submitted to 10Gy gamma irradiation. Two days later, cells were harvested through trypsinization, washed in PBS and fixed for 10 minutes with paraformaldehyde (PFA, Merck) 4% in PBS. Cells were subsequently washed in PBS and data acquisition was performed by flow cytometry using the FACS Canto II and the BD FACSDiva™ software (BD Biosciences). The ratios between the number of GFP (488nm) and cyan fluorescent protein (CFP) (405nm) positive cells counted provided quantitative measurement of HR and NHEJ repair efficiencies.

11. Beta-galactosidase assay

This assay was performed with the Senescence β-Galactosidase Staining Kit (#9860, Cell Signaling). ZL34 RAD18/HLTF knocked down cells were seeded in a 24-well plate (20,000 cells/well). The next day, cells were treated or not with cisplatin (10µM) and pemetrexed (10µM). Two days later, fixative and staining 10x solutions were heated at 37°C for an hour and diluted 10 times. X-Gal powder was solubilized in DMSO at a concentration of 20mg/ml and added (50µl/ml) to the β-Galactosidase staining solution containing the solutions A, B (both 10µl/ml) as well as the previously diluted staining solution (930µl/ml). Subsequently, pH of the β-Galactosidase staining solution was adjusted to 6. Indeed, lower and higher pHs would respectively lead to false positive and negative results. Cells were washed in PBS and incubated 15 minutes with the fixative solution. Cells were washed again twice, the β-Galactosidase staining solution was added and the plate was sealed with Parafilm® M (Bemis, Fisher Scientific) in order to prevent evaporation and pH changes. The plate was then kept in a dry incubator at 37°C without CO_2 for 24 hours. Thereafter, ten pictures per condition were randomly taken at 200x magnification on the Olympus CKX41 microscope (Olympus Corporation). In each picture, blue (senescent) and colorless (non-senescent) cells were counted. Quantification of senescent cells was obtained for each condition by dividing the sum of all counted blue cells of a same condition by all – both blue and colorless – cells.

12. Confocal microscopy: ɣH2AX staining

ZL34 cells were seeded ($5x10^4$ cells) on coverslips (Fisher Scientific) placed on the flat bottom of a 24-well plate (Greiner Bio-One) and treated the next day with either 10Gy of gamma irradiation or cisplatin (10µM) and pemetrexed (10µM). Two hours

after treatment, cells were first washed in PBS and fixed with PFA 4% for 15 minutes in the dark at room temperature. At this point and between each following steps, three washes of Triton X-100 (0.1%) in PBS were required. Cells were then incubated with glycine (50mM, VWR) in PBS for 10 minutes and permeabilized with Triton X-100 (0.5%) in PBS for 10 minutes at room temperature. Cells were thereafter incubated in blocking agent consisting of BSA (1%) – Tween 20 (0.1%) – PBS for an hour at room temperature. Primary rabbit IgG antibody targeting γH2AX (Ser139) (#9718, Cell Signaling) was diluted at 1:400 in the blocking solution and left overnight at 4°C for cell staining. An isotype control rabbit IgG antibody was used in parallel as a negative control to evaluate non-specific binding of the primary antibody. Subsequently, secondary anti-rabbit IgG antibody Alexa Fluor 488 (A-11008, Invitrogen) was added to the blocking solution at a dilution of 1:1000 and incubated with cells for an hour in the dark at room temperature. Afterwards, three washes with PBS were performed followed by 4′,6-diamidino-2-phenylindole (DAPI) staining (Biolegend) for 10 minutes in the dark. Following another washing step of PBS, coverslips were mounted on slides with ProLong™ Glass Antifade Mountant (ThermoFisher) and scanned using confocal microscopy (Zeiss LSM880 AiryScan Elyra S1, Carl Zeiss) with 63x objective. Images were computed with the Imaris software (Oxford Instruments).

13. Mice experiments

Ethical Committee approved animal welfare, experimental models and conditions related to this study through ethical protocol #2366. Mice experiments were performed in the central animal facility of Université de Liège (approval number LA1610002) in accordance with sanitary requirements. All animals used for the experiments were 8-week-old NSG mice (n=8/group) kept in ventilated cages. Mice were provided by the central animal facility of Université de Liège (approval number LA2610359) and were randomized into groups and cages in order to minimize weight, sex, and tumor growth differences among the conditions. Experiments implying non-treated and chemotherapy treated mice were both processed in parallel in the same room, but mice receiving chemotherapy treatments were separated from the non-treated ones. ZL34 cells transduced with lentivectors expressing shRNA targeting RAD18 and/or HLTF were washed twice, resuspended, and kept on ice in a 50% v/v solution composed of FBS free DMEM and Matrigel® (Basement Membrane Matrix, Corning). For each injection, 200µl containing $1x10^6$ cells were inoculated subcutaneously through 25-gauge needle into both flanks of mice. Tumor volume was measured three times a week with a digital caliper and the ellipsoid formula (L*(l*l)/2). Once average tumor volume reached 500mm^3, mice in the treatment group were administrated cisplatin (1µg/g) and pemetrexed (60µg/g) intraperitoneal injections once to twice a week with an interval of 3 to 4 days between each injection. Mice conditions were checked every day throughout a scoring table comprising ethical endpoints such as signs of pain, limits of weight loss, tumor size and animal welfare. Once any limit reached, immediate euthanasia of the mouse in question was required with a 200µl intraperitoneal injection of pentobarbital. Mouse death was then confirmed through decapitation. Both tumors were thereafter

carefully collected and measured with the digital caliper. To allow further analysis, tumors were subsequently cut in half: one half was fixed overnight in PFA 4% then put in 70% ethanol, while the other half was frozen in liquid nitrogen and afterwards kept at -80°C.

14. Immunohistochemistry of tumor mice

Cross-sections, staining and scanning of slices were carried out by GIGA Immunohistochemistry platform. Tumor mice previously fixed in PFA4% and kept in ethanol 70% were embedded in paraffin and then sectioned into slices for subsequent staining. Heat-induced antigen retrieval was performed with ethylenediaminetetraacetic acid (EDTA) using a pressure cooker. After a washing step with water, endogenous peroxidases were blocked with hydrogen peroxide for 20 minutes in order to eliminate background noise. Afterwards, three PBS washed were performed and non-specific sites were blocked for 10 minutes in Protein Block Serum-free (X0909, Agilent Technologies). Primary rabbit monoclonal antibody targeting Ki67 (790-4286, Roche) diluted twice in the antibody diluent Dako Real (EnVision+, S202230-2, Agilent Technologies) was then incubated for an hour at room temperature. Once washed three times with PBS, secondary antibody anti-rabbit peroxidase conjugated (EnVision+, K400311-2, Agilent Technologies) was incubated for 30 minutes and again washed three times in PBS. Negative control consists in secondary anti-rabbit antibody staining only. Then, hydrogen peroxide and the chromogen 3, 3'-diaminobenzidine (DAB) were added for 10 minutes for revelation. Furthermore, after two washes with water, counterstaining with hematoxylin and eosin was carried out with successive baths listed in **Table 4**. Isopropanol was used to removal all traces of water on the slice. Slides were subsequently scanned in visible light with the NDP NanoZoomer Digital Pathology (Hamamatsu) and images were thereafter analyzed with QuPath software (Bankhead P. et al, University of Edinburgh). Detection of positive cells was performed with a manual threshold applied to all images.

Table 4. Steps for hematoxylin-eosin staining.

Steps	Products	Time
1	Water wash	30sec
2	Hematoxylin	2min
3	Water wash	30sec
4	Isopropanol 100%	30sec
5	Isopropanol 100%	30sec
6	Isopropanol 100%	30sec
7	Xylene	30sec
8	Xylene	1min
9	Xylene	Exit

15. Bioinformatics analysis

Mutational and clinical data from mesothelioma patients were extracted from the cancer genome atlas program (TCGA) MESO (n=82) (NCI Genomic Data Commons portal) using GDCquery. Mutational analysis was performed using R with « maftools » package (version 2.12.0). Eighty-three DDR and DDT genes (see list in appendix 2) were selected based on their activity in DNA damage response, repair and tolerance pathways. An analysis of their mutational pattern was carried out.

In order to investigate differential gene expression, microarray data collected from GSE2549 were grouped into two groups: MPM tumor specimens (n=40) and normal pleura specimens (n=5). Samples were quantile normalized in order to have identical value distribution and log transformation was subsequently applied to data. « Limma » package (version: 3.26.8) was used to fit the model and get the differential gene expression between MPM and normal pleura. Significance level cutoff was set to log fold change (FC)>2 and adjusted p-value<0.05. Volcano plot was created using « ggplot2 » R package (version: 3.3.6). Selected DDR and DDT genes were annotated on the graph.

16. Statistical analysis

Statistical analyses were performed using the GraphPad Prism 8 version 8.4.3 and R Studio version 4.2.0 softwares – the latter was operated with the packages « ggplot2 » version 3.3.6 and « tidyverse » version 1.3.2. Normality of distribution was determined by the Shapiro-Wilk test while homogeneity of variances was evaluated through the Fisher F-test. Considering these two parameters as valid assumptions, one-way analysis of variance (ANOVA) followed by Tukey's multiple comparisons test were performed in order to compare means of more than two conditions in the context of only one independent variable. In case of two independent variables, two-way ANOVA was conducted followed by Dunnett's multiple comparisons test when means of conditions were compared to the control one while Tukey's post-test was performed when all means were compared between them. If only two populations were compared, Student's t-test was used, and if multiple comparisons had to be carried out, the Holm-Sidak correction was implemented. In the case of non-Gaussian distribution, medians of more than two groups were calculated through nonparametric Kruskal-Wallis test followed by Dunn's multiple comparisons test, while medians of two conditions were assessed by the Mann-Whitney test. Linear regression obtained through mice experiments were analyzed with R Studio. Tumor growth modelization was conducted using the « nlme » (version 3.1-157), « lme4 » (version 1.1-29) and « emmeans » packages (version 1.7.4-1). Linear mixed regression was performed with the following equation: lmer (volume ~condition + time + condition:time + sex + sex:condition + (time|ID)), thus considering that the slope and the intercept may vary from one mouse to another and allowing that the slope also varies over time. Linear regression slopes of the different conditions were compared through two-way ANOVA followed by Holm post-test. Data

of β-galactosidase assay were analyzed through a binomial model with multiple comparisons followed by Tukey's post-test *via* R Studio using the « glm2 » (version 1.2.1) and « emmeans » (version 1.7.4-1) packages. Data are expressed as means ± standard deviation (SD), except in non-parametric tests where medians were indicated, and for mice experiment where standard error of the mean (SEM) was designated, with populations varying over time. Statistical significance is indicated by $p<0.05$ (*), $p<0.01$ (**) and $p<0.001$ (***).

4

Results

1. DNA damage response and repair in pleural mesothelioma

DNA damage response is of paramount importance for the maintenance of genomic stability. Studying the DNA damage signaling upon several genotoxic MPM treatments, such as ionizing radiation and chemotherapy, would give us a better view of the ability of MPM cells to detect and further promote the repair of therapy-induced DNA damage.

1.1. γH2AX foci highlight double-strand breaks in DNA of MPM cells upon gamma irradiation and chemotherapy

Activation of the DNA damage response pathways due to genotoxic treatment was brought out through γH2AX staining of ZL34 sarcomatoid MPM cell line. Indeed, γH2AX foci arise near the damaged site from ATM phosphorylation following its recruitment by the MRN complex upon DNA DSB in order to further enable DNA repair. These foci are detectable in confocal microscopy through fluorescent cell imaging following γH2AX staining **(Figure 24, B)**. Visualization and quantification of the number of γH2AX foci per cell as well as foci fluorescence intensity were performed on ZL34 MPM cells submitted to 10Gy gamma irradiation or chemotherapy (10µM cisplatin combined with 10µM pemetrexed) **(Figure 24, A, C and D)**. As phosphorylation on serine 139 of H2AX is a phenomenon that happens rapidly and early in the process of DNA damage response, cells were fixed two hours post-treatment, thus demonstrating by fluorescence microscopy their γH2AX status at that time. Therefore, the number of foci is related to the number of DSBs occurring in cells while the fluorescence intensity shows the amount of γH2AX rising in response to DSB at the same location.

Results show that both genotoxic treatments at the dosage form used lead to a significant higher number of γH2AX foci compared to non-treated cells, together with a significant difference between the two treatments. Indeed, non-treated cells show a median of 3.17 foci per cell, a minimum number of foci of 0.00 and a maximum of 11.33, while cells treated with the chemotherapy exhibit a median of 48.67 foci per cell, a minimum of 15.00 and a maximum of 117.7 foci. As compared to the latter, cells treated with 10Gy of gamma irradiation show a significant higher number of γH2AX foci with a median of 113.70 foci per cell, a minimum of 34.33 and a maximum of 263.00 foci.

Furthermore, regarding the fluorescence intensity of γH2AX foci, both treatments are significantly different from each other and from the non-treated cells, with a median of fluorescence of 6,440 for non-treated cells, 7,414 for chemotherapy-treated cells and 11,435 for gamma irradiated cells. Moreover, all three conditions show a similar minimum fluorescence intensity with 3,637 for non-treated cells, 3,336 for chemotherapy-treated cells and 3,469 for gamma irradiated cells, whereas maximum intensity of fluorescence reaches 11,617 for non-treated cells, 21,198 for chemotherapy-treated cells and 30,179 for gamma irradiated cells. Of note, non-treated cells exhibit the basal level of γH2AX foci number and intensity in absence of genotoxic treatment and can be considered as the reflection of endogenous DNA DSBs.

Hence, DNA damage response pathways are activated in ZL34 treated cells in response to DSBs, as DSBs significantly occur upon gamma irradiation and chemotherapy, compared to non-treated cells, with a significantly higher activation in gamma irradiated cells compared to chemotherapy-treated cells.

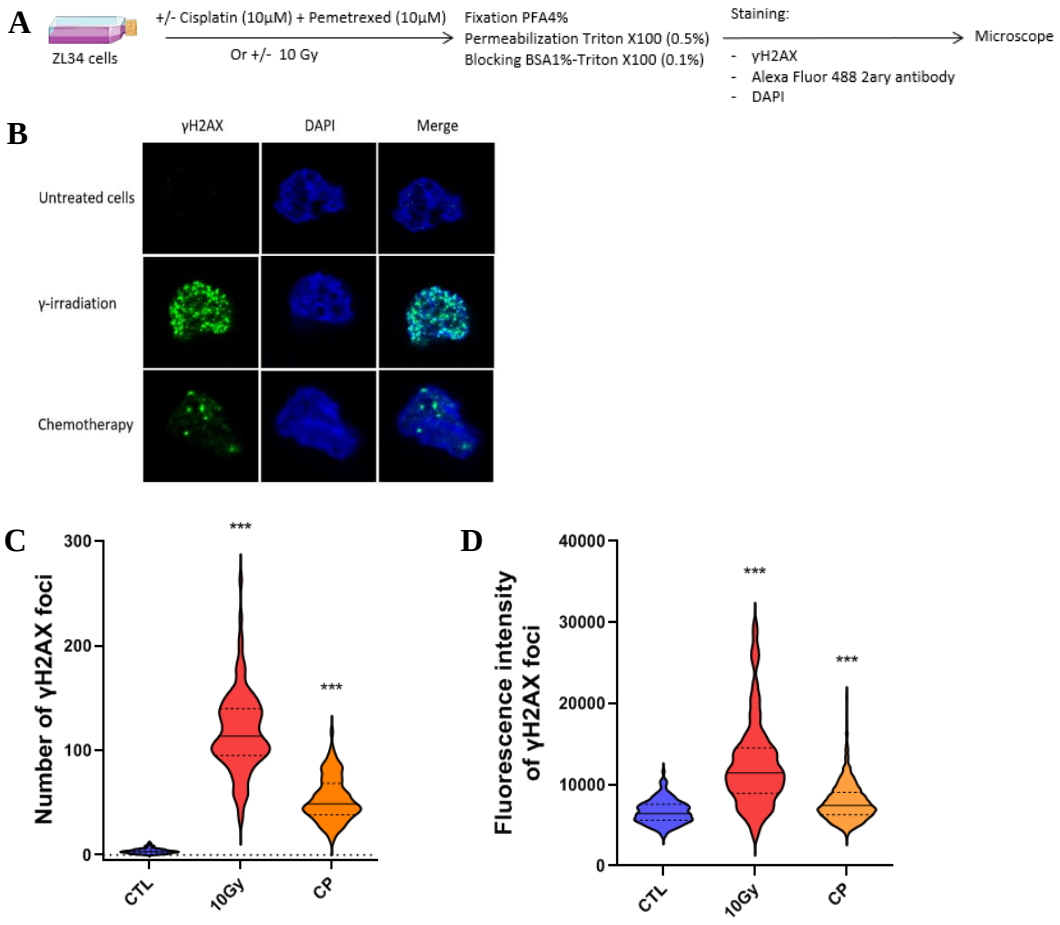

Figure 24. γH2AX staining of MPM cells upon gamma irradiation and chemotherapy treatments. (A) Experimental model. ZL34 sarcomatoid MPM cells were treated with 10Gy or chemotherapy (cisplatin 10µM + pemetrexed 10µM). Two hours later, cells were fixed with PFA 4% and permeabilized with Triton X100 (0.5%). Then, cells were incubated an hour with a blocking solution of BSA (1%) – Triton X100 (0.1%) followed by overnight incubation with γH2AX primary antibody, an hour with Alexa Fluor 488 secondary antibody and DAPI staining. **(B)** Images of γH2AX foci (Alexa Fluor 488 + DAPI staining) of non-treated, gamma irradiated or chemotherapy-treated ZL34 cells obtained by confocal fluorescence microscopy. Violin plots showing the quantification of γH2AX foci **(C)** and their fluorescence intensity **(D)** in ZL34 cells in the absence of treatment or two hours after treatment with 10Gy gamma irradiation or chemotherapy of cisplatin 10µM combined with pemetrexed 10µM. Analysis were achieved through Imaris software with 100 cells per condition, in 3 independent experiments. Statistical analysis of both number and fluorescence intensity of γH2AX foci were performed with non-parametric Kruskal-Wallis test followed by Dunn's multiple comparisons between all conditions.

1.2. Gamma irradiation mediates G2-M phases blockage of MPM and mesothelial cells

To study DNA damage repair mechanisms, genotoxic insults management by MPM cells was investigated. Cell cycle analysis of ZL34 sarcomatoid MPM cells upon increasing ionizing radiation, from 0 to 10Gy, was first considered in order to demonstrate the impact of this genotoxic treatment on cell cycle profiles. 24 hours after gamma irradiation treatment, cells were fixed and permeabilized with 70% ethanol followed by RNAse treatment and PI staining **(Figure 25, A)**. Flow cytometry analysis was then conducted to quantify the number of cells in each phase of the cell cycle according to the different doses of gamma irradiation used. This quantification was determined by the DNA content of each counted cell, which is reflected by its PI fluorescence. Cell cycle profile of untreated cells shows, from left to right, a peak at G1 phase (which is associated with a 2n DNA content) and a single peak at G2-M phases (4n DNA content). Between these two peaks stands the S phase which shows a cell count of a lesser extent and exhibits between 2 and 4n DNA content. The subG1 part of the cell cycle includes apoptotic cells and stands before the G1 phase while polyploid cells are located beyond the G2-M phases.

This experiment indicates that gamma irradiation treatment induces cell cycle arrest in G2-M phases of ZL34 cells, with a dose-dependent effect as the G2-M peak increases along with the administrated dose – from 22.38% at 1Gy to 78.70% at 10Gy –, whereas the G1 peak conjointly decreases with the dose – as it goes from 60.80% at 1Gy to 18.35% at 10Gy **(Figure 25, B)**. Thus, three repetitions of ZL34 cell cycle analysis show an average percentage of 78.15% of cells blocked in G2-M phases at 10Gy of ionizing radiation, which is the highest blockage obtained within the different doses tested. Moreover, gamma irradiation does not induce any significant apoptosis nor polyploidy, in neither dose used. Cell cycle analysis with the same parameters was then achieved on several cell lines of MPM (ZL34, M14K, M38K and H28) as well as Met5A mesothelial cell line **(Figure 25, A and C)**. Results obtained from these various cell lines with mesothelial cells and different MPM histological subtypes also show a dose-dependent blockage in G2-M phases upon gamma irradiation. Indeed, there is no significant difference between 1Gy treated and corresponding untreated cells regarding the number of cells in G2-M phases. At 3Gy of irradiation treatment, the average percentage of cells in G2-M phases is significantly higher in ZL34 (with 40.62%), M14K (with 41.75%) and M38K (with 39.91%) cells compared to respective non-treated cells. When treated with 5Gy, all cell lines tested except H28 exhibit a G2-M phases blockade as their number of cells in these cell cycle phases is significantly higher in comparison to non-treated conditions with an average percentage of 57.64% for ZL34, 45.30% for M14K, 53.21% for M38K and 41.00% for Met5A cells. Finally, at 10Gy of gamma irradiation, all cell lines studied display a significant increase of cells in G2-M phases compared to corresponding non-treated cells – with 78.15% (ZL34 cells), 67.85% (M14K cells), 71.46% (M38K cells), 37.77% (H28 cells) and 48.97% (Met5A cells), thus demonstrating a cell cycle blockade following the S phase where DNA is replicated. Of note, MPM and mesothelial cells exhibit about the same average percentage of cells in G2-M phases in absence of gamma irradiation treatment, ranging

from 14.81% (H28 cells) to 28.90% (ZL34 cells), with 21.46% for Met5A mesothelial cells.

Thus, this experiment reveals that MPM and mesothelial cells exhibit a G2-M phases blockade in response to gamma irradiation in a dose-dependent manner, with 10Gy being the dose that demonstrates the higher percentage of cells in G2-M phases in all cell lines studied. Therefore, following experiments were conducted only with 10Gy regarding gamma irradiation treatment.

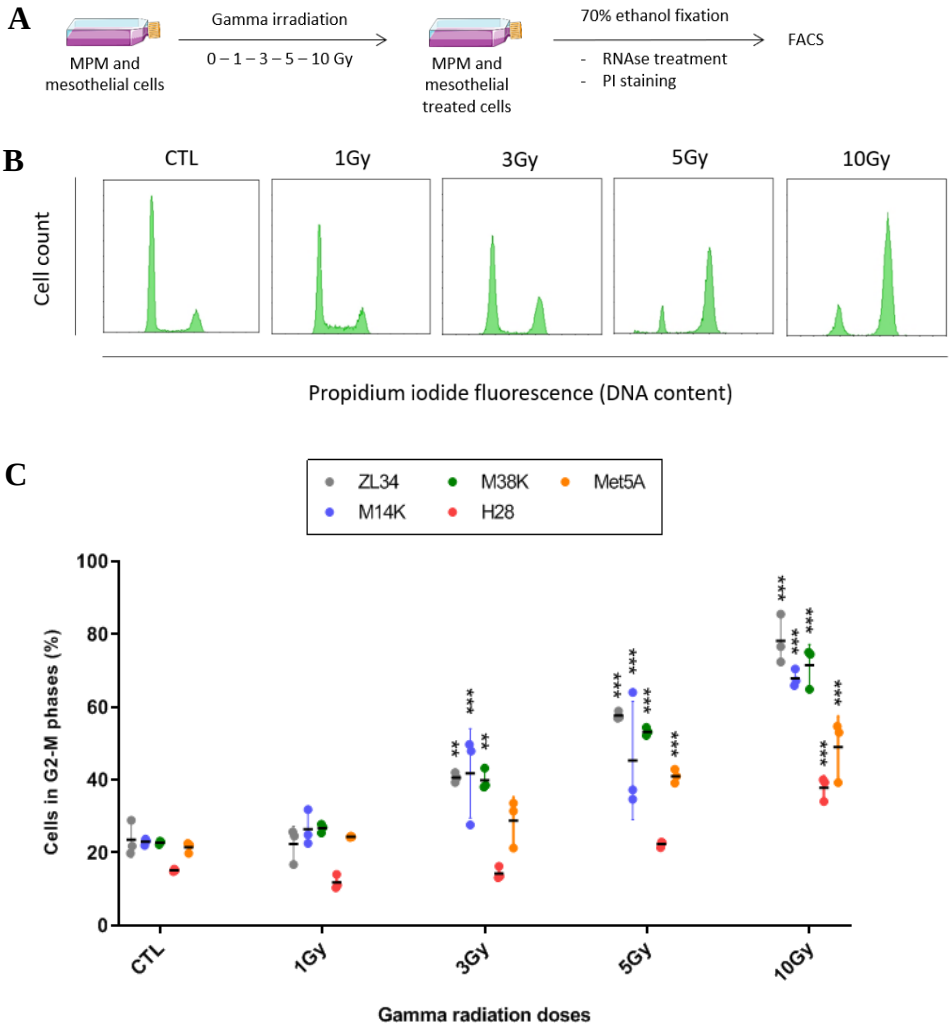

Figure 25. MPM and mesothelial cells' treatment with increasing doses of gamma irradiation. (A) Experimental model. MPM (ZL34, M14K, M38K and H28) and mesothelial (Met5A) cells were submitted to increasing ionizing radiation (0 – 1 – 3 – 5 – 10Gy). 24 hours later, cells were fixed and permeabilized overnight with 70% ethanol at -20°C, then treated with RNAse, stained with PI and analyzed in flow cytometry. **(B)** Study of ZL34 MPM cell cycle submitted to increasing doses of ionizing radiation (0 – 1 – 3 – 5 – 10Gy). Cell cycle profiles showing the number of cells at each phase. Y-axis shows the number of cells while x-axis represents the DNA content, which is defined by PI fluorescence. **(C)** Raw data from Bernard Staumont. Quantification (%) of MPM (ZL34, M14K, M38K and H28) and mesothelial (Met5A) cells in G2-M phases upon increasing doses of gamma irradiation (0 – 1 – 3 – 5 – 10Gy). Results are indicated as means ± SD of 3 independent experiments. Statistical analysis was performed with two-way ANOVA followed by Dunnett's multiple comparisons to non-treated cells.

1.3. Checkpoint kinase 1 inhibitor promotes the release of MPM cells blocked in their cell cycle upon gamma irradiation or chemotherapy

The G2-M phase arrest observed in MPM and mesothelial cells treated with gamma irradiation might be prevented using a checkpoint kinase inhibitor. To verify this hypothesis, an inhibitor of the CHK1, called UCN-01, was administered to MPM and mesothelial cells with or without 10Gy of gamma irradiation. Cell cycle profiles were analyzed in flow cytometry as previously described **(Figure 26, A)**.

For each cell line, cells treated only with UCN-01 exhibit a cell cycle profile similar to the respective non-treated cells **(Figure 26, B and C)**. Indeed, the average percentage of cells in G2-M phases ranges from 17.463% (H28 cells) to 29.267% (M14K cells) in control cells while it varies from 12.40% (H28 cells) to 23.91% (M14K cells) in UCN-01 treated cells. As considered previously, cells submitted to an ionizing treatment of 10Gy show a significant increase of cells in G2-M phases – indicating cell cycle arrest in these phases – with an average percentage ranging from 40.59% (H28 cells) to 86.32% (ZL34 cells), which therefore can vary by a factor of two according to the cell line. Although treatment with 10Gy leads to G2-M phases arrest, the addition of UCN-01 prevents gamma irradiation-induced phase blockade, thus restoring a normal cell cycle profile. Indeed, when treated with UCN-01 and 10Gy gamma radiation, the average percentage of cells in G2-M phases reaches 24.32% in ZL34 cells, 35.31% in M14K cells, 22.81% in M38K cells, 20.91% in H28 cells and 27.66% in Met5A mesothelial cells, thereby not leading to any significant difference with their respective non-treated cell line. Furthermore, this phenomenon happens without any significant increase of apoptotic nor polyploid cells.

Altogether, these results indicate that CHK1 inhibitor UCN-01 is able to release MPM and mesothelial cells from their G2-M phases blockade induced by the gamma irradiation and is thereby promoting them to pursue their progression in the cell cycle despite DNA damage.

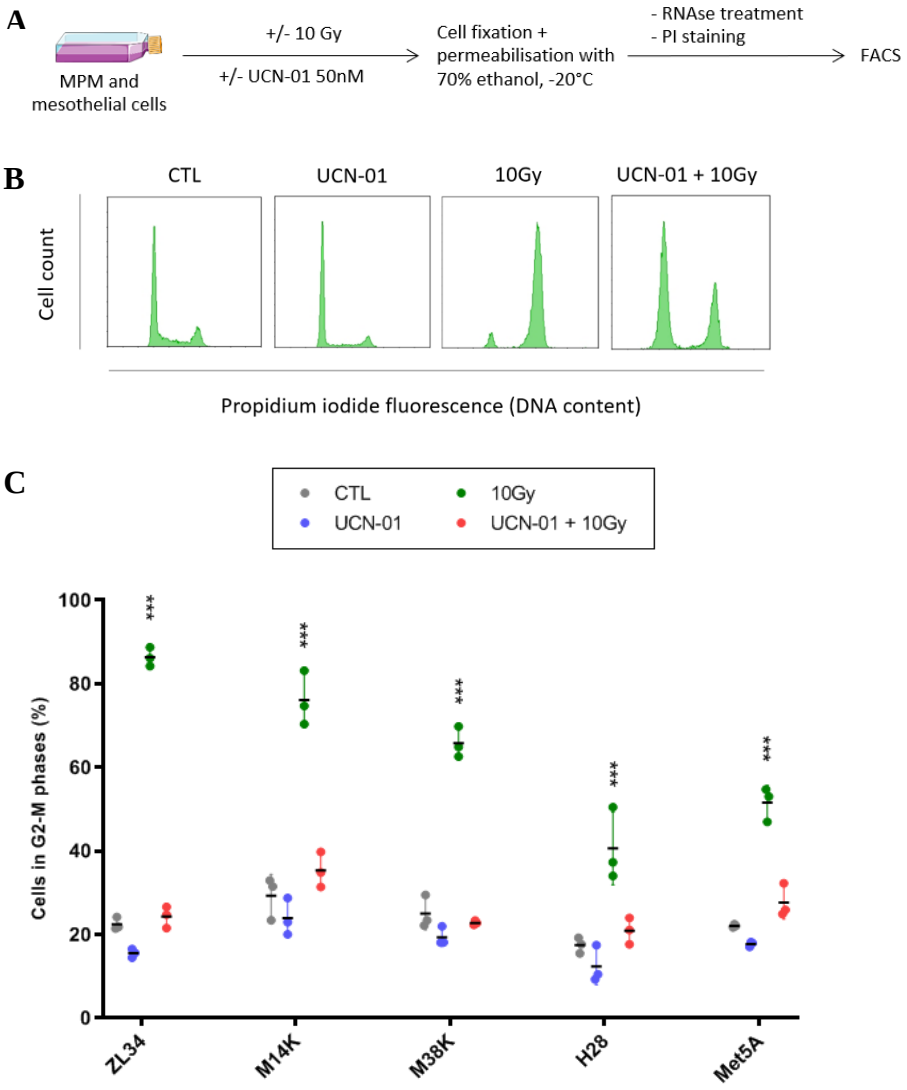

Figure 26. Gamma irradiation and UCN-01 treatments of MPM and mesothelial cells. **(A)** Experimental model. ZL34 sarcomatoid MPM cells were treated or not with 10Gy gamma irradiation and/or CHK1 inhibitor UCN-01 (50nM). 24 hours post-treatment, cells were fixed and permeabilized overnight with 70% ethanol at -20°C, then treated with RNAse, stained with PI and analyzed in flow cytometry. **(B)** Cell cycle profiles of MPM (ZL34, M14K, M38K and H28) and mesothelial (Met5A) cells, with or without checkpoint kinase 1 inhibitor UCN-01 and/or 10Gy gamma irradiation treatment. **(C)** *Raw data from Bernard Staumont.* Quantification (%) of cells in G2-M phases, with y-axis showing the number of cells while x-axis represents the quantity of DNA defined as detected PI fluorescence. Results are indicated as means ± SD of 3 independent experiments. Statistical significance was determined by two-way ANOVA followed by Dunnett's multiple comparisons with non-treated control cells.

In order to confirm that UCN-01 mediates MPM cells release from gamma irradiation-induced G2-M cell cycle phases arrest, an experiment called mitotic trap assay was performed. This analysis consists in the blockage and the quantification of cells entering mitosis, during mitotic spindle formation. To do so, cells were treated with gamma irradiation and/or CHK1 inhibitor UCN-01 and/or an anti-microtubule agent which inhibits the mitotic spindle, called paclitaxel (Taxol) **(Figure 27, A)**. Concomitantly with cell cycle study, phospho-histone H3(Ser10) staining was also achieved to quantify cells initiating mitosis **(Figure 27, B)**. Mitotic index obtained for each condition is characterized by the amount of positive phospho-histone H3(Ser10) cells.

Data indicate that gamma irradiated cells show only few positive phospho-histone H3(Ser10) cells – with an average percentage less than 1% in all MPM cell lines and reaching 3.11% in Met5A mesothelial cell line – even though they are blocked in G2-M phases **(Figure 27, C)**. These mitotic indexes are generally lower than the untreated control cells which vary from 1.73% (H28 cells) to 4.08% (M14K cells), except Met5A cell line which stands with 2.74%. However, paclitaxel administered alone significantly increases the mitotic indexes of all cell lines compared to related control cells, thus blocking cells in mitosis. Indeed, the average percentage of positive phospho-histone H3(Ser10) cells in presence of only Taxol® ranges from 15.35% (H28 cells) to 57.43% (ZL34 cells). UCN-01 treatment associated with 10Gy irradiation gives rise to mitotic indexes comparable to the ones of related control cells. Moreover, gamma irradiation combined with paclitaxel leads to low mitotic indexes – similar to the ones in presence of 10Gy of ionizing radiation only – while the addition of UCN-01 to both treatments together leads to a significant increase of the mitotic indexes in all cell lines except H28, compared to the non-treated related cells – the significant average percentages varying from 12.00% (Met5A cells) to 32.68% (ZL34 cells), while H28 exhibits only 6.15%. Of note, the condition with Taxol treatment alone shows an amount of positive phospho-histone H3(Ser10) cells which is about twice as high as compared to the one combining the three treatments.

Therefore, these results validate that CHK1 inhibitor releases cells from ionizing radiation-induced G2-M cell cycle phases blockade, and further initiates their access to mitosis despite DNA damage generated from gamma irradiation.

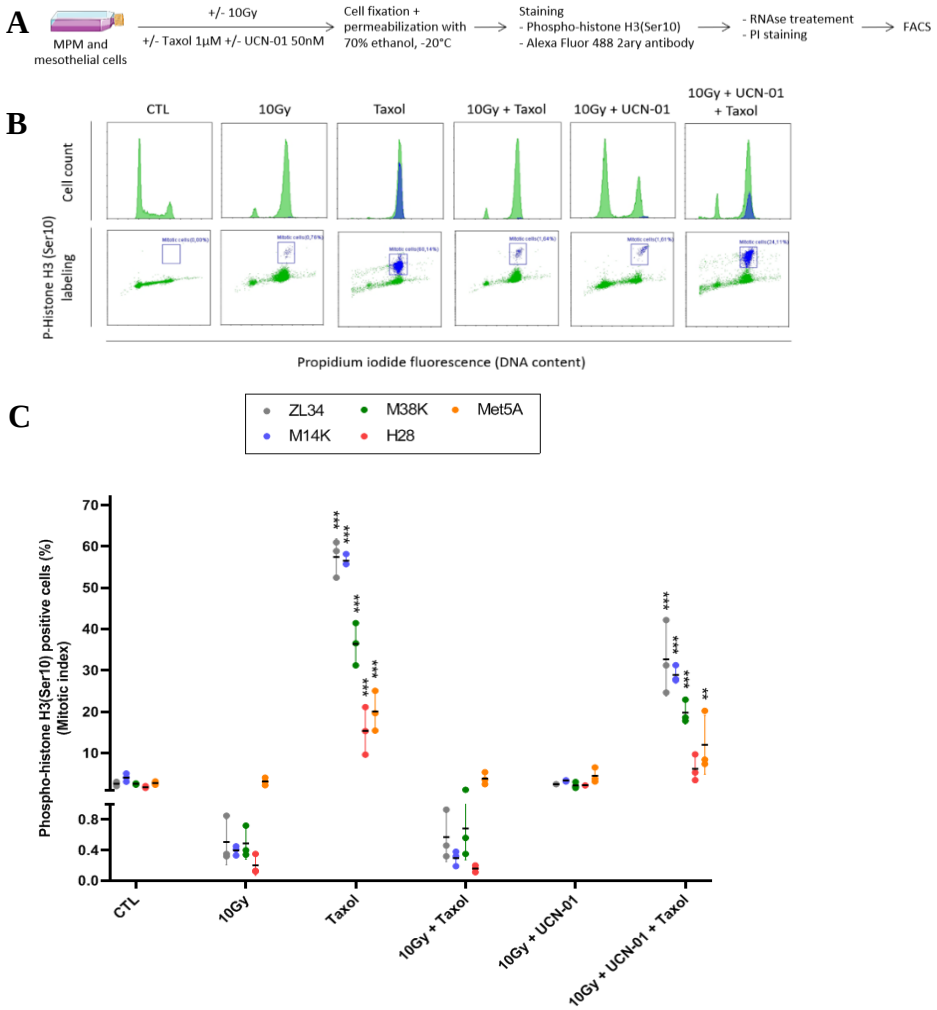

Figure 27. Mitotic trap assay of MPM and mesothelial cells upon gamma irradiation. **(A)** Experimental model. 2 hours after 10Gy gamma irradiation and/or UCN-01 (50nM), MPM and mesothelial cells were incubated or not with paclitaxel (Taxol®, 1µM) for 16 hours. Cells were fixed as well as permeabilized overnight with 70% ethanol at -20°C and then stained with rabbit phospho-histone H3(Ser10) primary antibody followed by anti-rabbit Alexa Fluor 488 secondary antibody. RNAse treatment and PI staining were further performed. Both assays were analyzed in flow cytometry. **(B)** Cell cycle profiles and phospho-histone H3(Ser10) staining of ZL34 cells. Y-axis shows the quantification of stained cells while x-axis represents DNA quantification from PI staining. **(C)** *Raw data from Bernard Staumont.* Mitotic trap assay of MPM (ZL34, M14K, M38K and H28) and mesothelial (Met5A) cells. Quantification (%) of phospho-histone H3(Ser10) positive cells (y-axis) according to each condition (x-axis). Results are presented as means ± SD from 3 independent experiments. Statistical significance was evaluated with two-way ANOVA followed by Dunnett's multiple comparisons to non-treated cells.

A mitotic trap assay was also performed with the standard chemotherapy of MM, cisplatin and pemetrexed. Indeed, evaluating the impact of a different genotoxic treatment than gamma irradiation on the cell cycle progression upon checkpoint and mitotic spindle inhibitors would be of interest. ZL34 and M14K MPM cells were submitted to cisplatin and pemetrexed treatment, with or without CHK1 inhibitor UCN-01 and/or mitotic spindle inhibitor Taxol®. Cells were subsequently stained and analyzed in the same way as previously described in figure 26 **(Figure 28, A)**.

Data show that chemotherapy regimen leads to a S phase arrest in ZL34 and M14K cells **(Figure 28, B)** with few positive phospho-histone H3(Ser10) cells for this condition – with average percentages of 0.19% in ZL34 cells and 0.24% in M14K cells **(Figure 28, C)**. These mitotic indexes are not significantly different from the ones of non-treated control cells and also similar to the ones obtained in the context of 10Gy treatment (0.51% for ZL34 cells and 0.40 for M14K cells; **Figure 27, C**). The combination of Taxol®, cisplatin and pemetrexed generates slightly higher mitotic indexes, reaching average percentages of 5.84% in ZL34 cells and 6.05% in M14K cells. These are not significantly different from the ones of untreated cells – the latter demonstrating mitotic indexes of 2.09% for ZL34 cells and 2.74% for M14K cells –, but a bit higher than the ones collected in the case of Taxol® combined with 10Gy gamma irradiation (with 0.57% in ZL34 cells and 0.30% in M14K cells; **Figure 27, C**). Moreover, the association of UCN-01 and the chemotherapy agents induces low mitotic indexes, similar to the ones obtained in the presence of the chemotherapy alone – with 0.38% in ZL34 cells and 0.22% in M14K cells. Furthermore, Taxol® combined with the chemotherapy and CHK1 inhibitor leads to average mitotic indexes of 5.21% for ZL34 and 5.5% for M14K cells, which are similar to the ones of the untreated cells and the condition combining chemotherapy and Taxol®. Taxol® alone exhibits significant higher mitotic indexes in both studied cell lines with 41.54% in ZL34 and 64.13% in M14K cells.

Thus, the combination of chemotherapy, UCN-01 and Taxol® stalls the mitosis process of MPM cells, but in a lesser manner (with average percentages of 5.21% in ZL34 cells and 5.5% in M14K cells) compared to the mitotic trap assay performed with gamma irradiation (with 32.68% and 28.91%, respectively). Overall, inhibition of cell cycle checkpoint kinase 1 in the context of chemotherapy regimen promotes the entry of some cells in mitosis – to a lesser extent than in the context of gamma irradiation as genotoxic treatment, and at a slightly higher level than non-treated cells –, thus progressing through the cell cycle despite DNA damage.

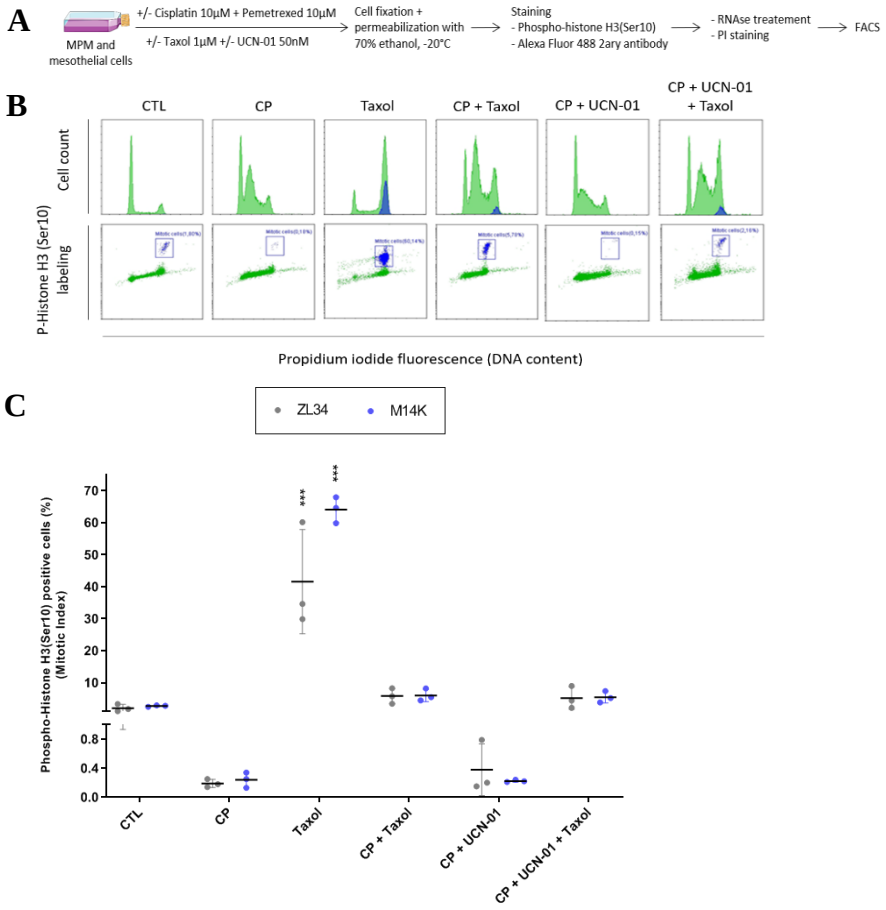

Figure 28. Mitotic trap assay of MPM cells upon chemotherapy regimen.
(A) Experimental model. ZL34 sarcomatoid and M14K epithelioid MPM cells were treated or not with cisplatin (10µM) and pemetrexed (10µM) for 24 hours, with or without UCN-01 (50nM) and/or Taxol® (1µM) for 16 hours. Cells were then fixed and permeabilized overnight with 70% ethanol -20°C, subsequently stained with rabbit phospho-histone H3(Ser10) primary antibody and further with anti-rabbit Alexa Fluor 488 secondary antibody. RNAse treatment and PI staining of the cells were then performed followed by flow cytometry analysis. **(B)** Study of cell cycle profiles and phospho-histone H3(Ser10) staining of ZL34 cells. Y-axis shows the quantification of stained cells whereas x-axis represents the quantity of DNA defined by the fluorescence of PI staining. **(C)** Mitotic trap assay of ZL34 and M14K MPM cells, quantifying cells entering mitosis upon chemotherapy treatment (cisplatin 10µM + pemetrexed 10µM), CHK1 inhibitor UCN-01 (50nM) and/or mitotic spindle inhibitor Taxol® (1µM). Quantification (%) of positive phospho-histone H3(Ser10) MPM cells – meaning that they are entering mitosis – stands in y-axis, while the different treatment conditions are reflected in x-axis. Results are expressed as means ± SD from 3 independent experiments. Statistical significance was assessed with two-way ANOVA followed by Dunnett's multiple comparisons to non-treated cells.

1.4. HR and NHEJ pathways are efficient in repairing double-strand breaks upon gamma irradiation in MPM cells

DSB are the most genotoxic insults resulting from DNA damaging agents. In order to evaluate the ability of MPM cells to repair this type of DNA lesion, the efficiency of the two main DSB repair pathways, HR and NHEJ, were evaluated on several MPM and mesothelial cell lines upon gamma irradiation. Indeed, efficient repair of those DNA damage results in maintaining genomic stability, while inefficient repair induces mutagenesis and leads to genomic instability.

To do so, two fluorescent reporter constructs were used as labels of each DSB repair mechanism – namely HR and NHEJ **(Figure 29, A)**. Both plasmids express GFP gene containing I-SceI restriction sites. This rare-cutting endonuclease thus generates DSB within the GFP gene through digestion, therefore linearizing the plasmids. Both constructs are originally GFP negative. Following transfection, efficient repair of the DSB by the HR or NHEJ machinery, respective to the reporter plasmid used, restores GFP gene expression. Hence, the green fluorescence arising is further detected and quantified *via* flow cytometry. HR and NHEJ plasmids were independently co-transfected with another plasmid expressing CFP as an internal control for transfection efficiency **(Figure 29, B)**.

Data indicate that gamma irradiation does not significantly impact HR nor NHEJ repair efficiencies in all MPM and mesothelial cell lines. Furthermore, graphs highlight a great variation in basal activity level of the two DSB repair pathways between the different cell lines studied. Indeed, the NHEJ efficiency average percentage of non-treated cells reaches 63.36% in ZL34 cells, 14.83% in M14K cells, 24.56% in M38K cells and 16.16% in H28 cells. For its part, basal levels of HR in non-treated cells also exhibit a slight fluctuation with 17.53% in ZL34 cells, 13.73% in M14K cells, 11.86% in M38K cells and 7.1% in H28 cells. Regarding non-treated Met5A mesothelial cells, their level of both NHEJ and HR efficiencies appear equivalent to MPM cells as they respectively attain 35.83% and 6.13%. Moreover, NHEJ seems to be a DSB repair pathway more often chosen compared to HR, both in the absence and in the presence of gamma irradiation treatment.

Therefore, HR and NHEJ are globally activated in MPM and mesothelial cells in the absence of genotoxic treatment, with usually a predominance in NHEJ repair activity, and gamma irradiation does not significantly impact the efficiency of these repair processes.

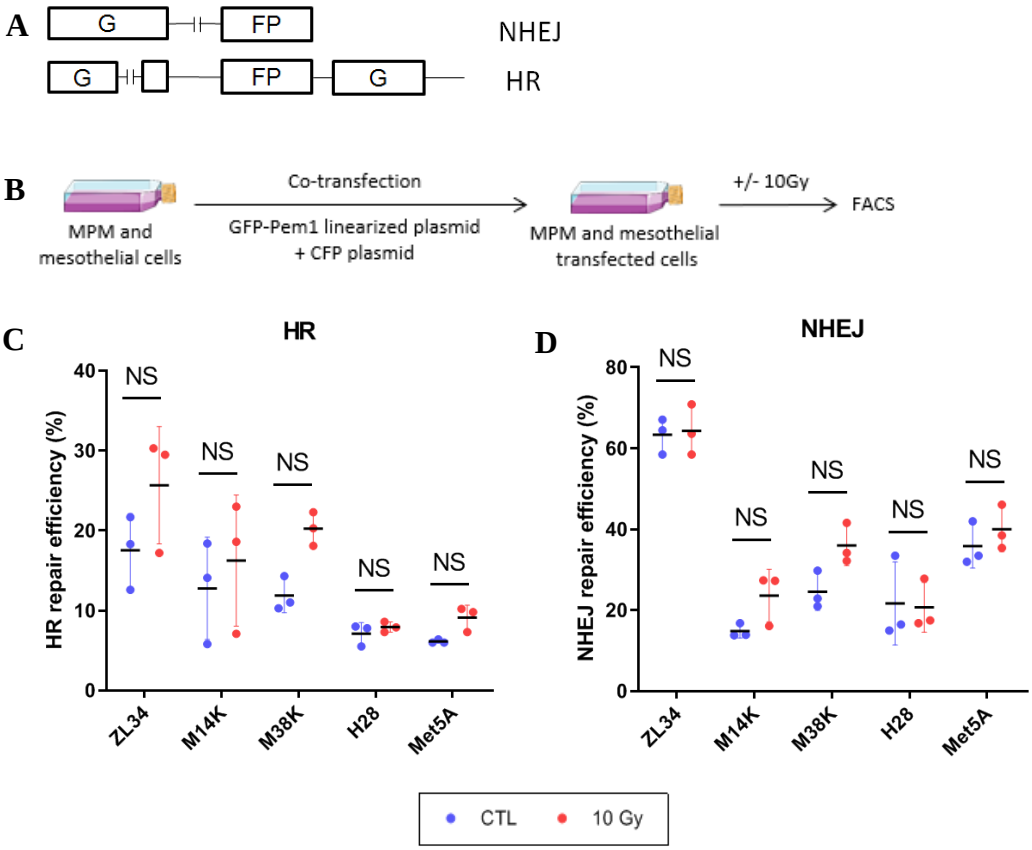

Figure 29. Efficiency evaluation of double-strand breaks repair through homologous recombination (HR) and non-homologous end-joining (NHEJ) in MPM and mesothelial cells upon gamma irradiation. (A) Fluorescent reporter plasmids modeling. These plasmids are originally GFP negative and enable efficiency quantification of DSB repair through HR and NHEJ. **(B)** Experimental model. HR and NHEJ fluorescent reporter plasmids both underwent overnight digestion with I-SceI to induce DSB. MPM and mesothelial cells were co-transfected with either HR or NHEJ linearized plasmids and an internal control plasmid expressing CFP. Cells were treated or not with 10Gy gamma irradiation and analyzed in flow cytometry where GFP and CFP fluorescence were measured. Quantification (%) of HR **(C)** and NHEJ **(D)** efficiencies in MPM (ZL34, M14K, M38K and H28) and mesothelial (Met5A) cells with or without 10Gy gamma irradiation treatment. Raw data from Bernard Staumont. Results are shown as means ± SD from 3 independent experiments. Multiple Student's t-tests with the Holm-Sidak correction were performed as statistical analysis.

2. DNA damage tolerance pathways in pleural mesothelioma

2.1. BAP1 and TP53 are the most frequently mutated DDR and DDT genes in MPM

Bioinformatic analysis was performed in order to investigate genetic mutations regarding DDR and DDT genes in MPM patients. TCGA MESO database tables 82 MPM patients with clinical data displaying records of genomic sequences. 83 genes related to DNA damage response, DDR and DDT were selected with regard to their mention in the context of this thesis **(Appendix 2)** and investigated in the MPM sample of the TCGA database. An oncoplot was generated where each column represents one patient while each row represents one studied gene **(Figure 30)**.

Data reveal that, among the genes investigated, *BAP1* and TP53 are the most frequently mutated genes with respectively 28% and 16% of mutation in MPM patients. *BAP1* is mostly mutated *via* a deletion occuring from a frame shift while *TP53* is generally mutated through missense mutation. Of note, there is no patient displaying these two mutations at the same time. Besides these two genes, *ATR*, *ETAA1* and *RAD50* all exhibit 2% of mutation among the patients of the TCGA MPM sample. *ATR* and *RAD50* both demonstrate missense mutation while *ETAA1* manifests frame shift deletion. Furthermore, *MSH6*, *POLE*, *POLN*, *PRKDC*, *RAD18*, *RIF1* and *ZRANB3* show 1% of missense mutation, *MDC1* and *RAD51* with 1% of nonsense mutation and *REV3L* with 1% of frame shift insertion.

Overall, few DDR and DDT genes are mutated in MPM, with *BAP1* and *TP53* being the most frequently ones. Others concern very few MPM patients with genes involved in DNA damage response, MMR, TLS, FR, HR and NHEJ.

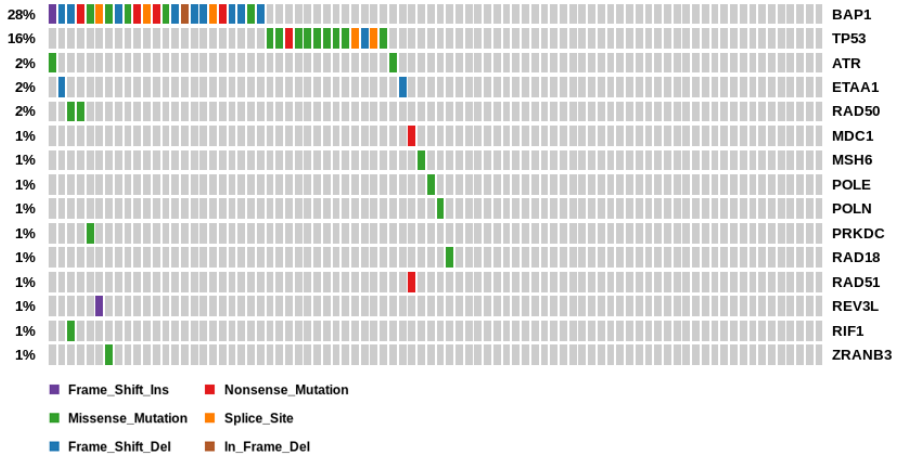

Figure 30. Few DDR and DDT genes are mutated in MPM. Oncoplot generated from TCGA database where 82 MPM patients were considered for mutational quantification (%) regarding DDR and DDT genes listed in Appendix 2. Each column represents one patient while each row represents one studied gene. The type of mutation is noticed through a color coding.

2.2. Tumor growth of ZL34 cells exhibiting RAD18 interference is significantly lower upon chemotherapy

Investigation of the DDT pathways would provide a more comprehensive understanding of the tolerance mechanisms regarding DNA damage in MM. To do so, RNA interference was performed on two ubiquitin ligases playing a crucial role in the regulation of DDT pathways, namely RAD18 and HLTF, as these two proteins direct the pathway choice in an upstream manner upon PCNA ubiquitination. Moreover, these two major regulators of the DDT pathways are not frequently mutated **(Figure 30)** and not transcriptionally modified **(Appendix 3, Figure 37)**. Thus, investigating the impact of RAD18 and/or HLTF interference in MPM cells could be worthwhile.

Among the various cell lines studied in the first part of this thesis, ZL34 sarcomatoid cells are the ones exhibiting the most efficient HR and NHEJ repair. Moreover, ZL34 cells are particularly resistant to therapies and are thus hard to treat. Considering these features, further experiments were performed only on those cells.

Thereby, ZL34 cells were transduced with lentivectors expressing shRNA designed to target independently RAD18 and HLTF **(Figure 31, A and B)**. Scramble shRNAs were used as control, with double scramble being the experimental control condition **(Appendix 1, Table 5)**.

Cell lines exhibiting the greatest inhibition(s), namely ScrR ScrH (control cells), R1 ScrH (displaying RAD18 interference), ScrR H2 (demonstrating HLTF interference) and R1 H1 (exhibiting both RAD18 and HLTF interference) were further analyzed in a mouse model. Thus, the cell lines were injected in both flanks of NSG mice and then subsequently treated or not with the standard chemotherapy – consisting of repeated intraperitoneal injections of cisplatin (1µg/g of body weight mouse) and pemetrexed (60µg/g of body weight mouse) – and the tumor volume was followed over time **(Figure 31, C)**. Tumor growth of non-treated mice does not show any significant difference between all conditions and tumor volume kept increasing over time, without any plateau observed **(Figure 31, D and E)**. Thus, interference of the DDT pathways in ZL34 cells does not impact tumor growth in the absence of genotoxic treatment. However, mice treated with cisplatin and pemetrexed exhibit a significant lower tumor growth over time in ZL34 cells presenting RNA interference of RAD18 only compared to the double scramble control cells **(Figure 31, F and G)**. Besides knocked down for RAD18 compared to control cells, there is no significant difference of tumor growth regarding all other conditions.

Therefore, the complex interplay of DDT pathways in the context of exogenous DNA lesions is elegantly illustrated through this experiment as RAD18 alone – hence, TLS pathway – seems essential for tumor growth upon chemotherapy-induced DNA damage, unlike HLTF inhibition alone as well as the double interference of RAD18 and HTLF which do not demonstrate any influence regarding tumor growth in mice.

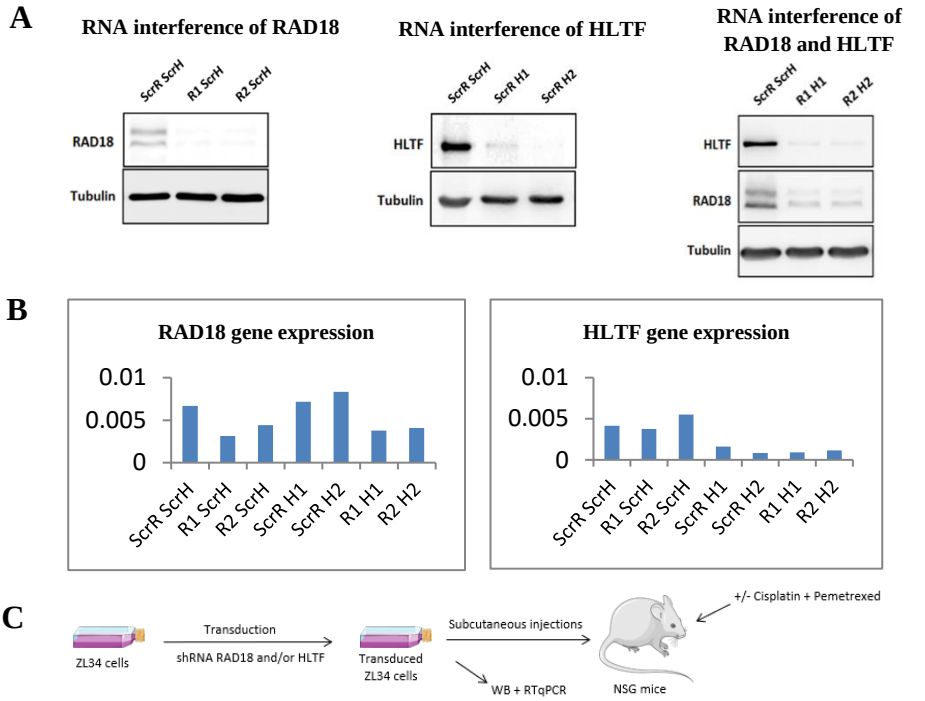
A
RNA interference of RAD18
ScrR ScrH
R1 ScrH
R2 ScrH
RAD18
Tubulin
RNA interference of HLTF
ScrR ScrH
ScrR H1
ScrR H2
HLTF
Tubulin
RNA interference of RAD18 and HLTF
ScrR ScrH
R1 H1
R2 H2
HLTF
RAD18
Tubulin
B
RAD18 gene expression
0.01
0.005
0
ScrR ScrH
R1 ScrH
R2 ScrH
ScrR H1
ScrR H2
R1 H1
R2 H2
HLTF gene expression
0.01
0.005
0
ScrR ScrH
R1 ScrH
R2 ScrH
ScrR H1
ScrR H2
R1 H1
R2 H2
C
ZL34 cells
Transduction
shRNA RAD18 and/or HLTF
Transduced ZL34 cells
Subcutaneous injections
WB + RTqPCR
NSG mice
+/- Cisplatin + Pemetrexed
D
Tumor volume over time without chemotherapy
Tumor volume (mm³)
Time (Days)
Scramble
HLTF
RAD18
RAD18 + HLTF
E
Linear regression of the mice experiment not involving chemotherapy
Tumor volume (mm³)
Time (Days)
NS
F
Tumor volume over time with chemotherapy
C+P
C+P
C+P
C+P
Tumor volume (mm³)
Time (Days)
G
Linear regression of the mice experiment involving chemotherapy
Tumor volume (mm³)
Time (Days)
*

Figure 31. RNA interference of RAD18 and/or HLTF in ZL34 MPM cells and mice experiment involving subcutaneous injection of those cells. (A) ShRNAs targeting RNA of RAD18 (n=2) and HLTF (n=2) were cloned independently into a lentiviral vector. Scramble shRNAs were used as controls – one for each target. Thus, ZL34 MPM cells were transduced with RAD18 and/or HLTF lentivectors (shRNA #1 RAD18 = R1, shRNA #2 RAD18 = R2, shRNA #1 HLTF = H1 and shRNA #2 HLTF = H2) as well as scramble shRNAs (scramble RAD18 = ScrR and scramble HLTF = ScrH) according to the distinct conditions, the double scramble being the experimental control condition. Expression of RAD18 and HLTF was analyzed by immunoblot with tubulin as loading control, and **(B)** RTqPCR with GAPDH as housekeeping gene. **(C)** Experimental model. ZL34 transduced cells (ScrR ScrH, R1 ScrH, ScrR H2 and R1 H1) were injected subcutaneously into both flanks of NSG mice (n=8/group) submitted or not to repeated cisplatin (1µg/g) and pemetrexed (60µg/g) intraperitoneal injections. Tumor growth was followed over time. **(D)** Tumor volume (mm^3) measured over time in the absence of chemotherapy regimen, from first measurement. **(E)** Statistical analysis related to the mice experiment in absence of chemotherapy. Two-way ANOVA followed by Holm post-test were performed. Results are indicated as means ± SEM. **(F)** Tumor volume (mm^3) measured over time in presence of chemotherapy regimen, from first injection of cisplatin and pemetrexed in mice. Each mouse was treated independently, once the mean of both of its tumors reached $500mm^3$. Arrows show chemotherapy injections administered to mice over time. **(G**) Statistical analysis related to the mice experiment in presence of chemotherapy. Two-way ANOVA followed by Holm post-test were performed. Results are indicated as means ± SEM, with variation of the number of mice over time.

2.3. RAD18 interference tends to decrease cell proliferation of ZL34 cells in mice upon chemotherapy

At the end of the experiment involving chemotherapy treatments of mice, tumors were harvested, fixed and sectioned into slices. Staining was performed in order to investigate how RAD18 interference promotes a statistically significant lower tumor growth of ZL34 cells in mice treated with chemotherapy regimen compared to non-treated ones. Cell proliferation was studied through Ki67 staining in double scramble (ScrR ScrH, named scramble) control and RAD18 knocked down (R1 ScrH, named RAD18) conditions. Histological sections were labeled with Ki67 antibody as well as the chromogen DAB, and counterstained with hematoxylin and eosin **(Figure 32, B)**. Stained slices were scanned in visible light to allow quantification of Ki67 positive cells.

Results show that there is no significant difference regarding the number of Ki67 positive cells between the scramble and the cells presenting an interference for RAD18 **(Figure 32, D)**. Indeed, scramble tumors harbor a mean of Ki67 positive cells of 27.29% with a minimum of 17.07% and a maximum of 39.01%, while RAD18 knocked down tumors show a mean of 19.43%, a minimum of 13.54% and a maximum of 26.52%. Although there is no significant impact of RAD18 knock down on the number of Ki67 positive cells, RAD18 interference tends to decrease the proliferation of ZL34 cells in tumors of mice.

Of note, histological sections demonstrate a great heterogeneity regarding structural aspects of the cancerous tissue **(Figure 32, A)** and distribution of Ki67 positive cells **(Figure 32, B and C)**. Indeed, the chosen slices nicely reflect the unevenness of Ki67 positive cells concentration and the variability of morphological characteristics of the tumors. Moreover, heat maps highlight clusters of positive Ki67 cells which are present in both conditions **(Figure 32, D)**.

Overall, tumors obtained through subcutaneous injection of ZL34 transduced cells exhibit variable morphology and Ki67 positive cells distribution and RAD18 interference tends to decrease cell proliferation within the tumor.

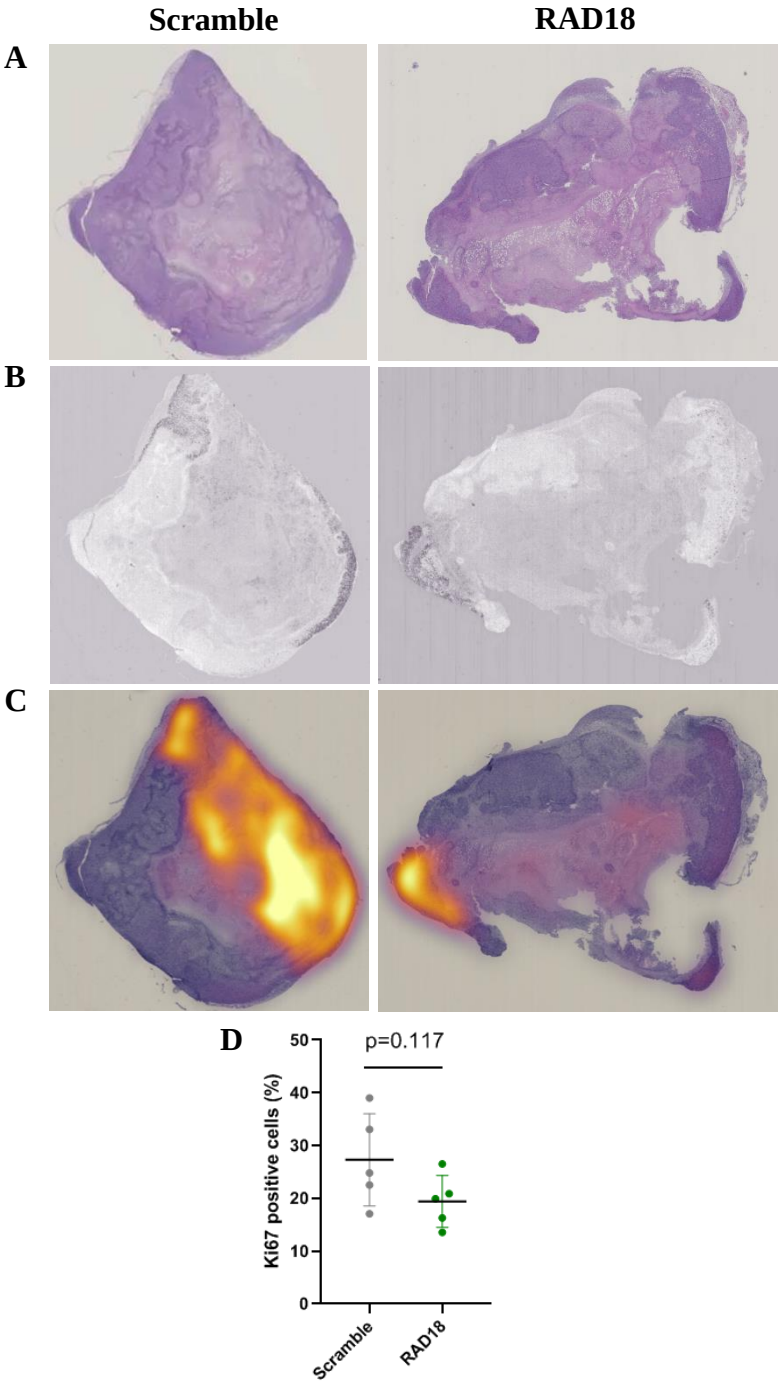
Scramble
RAD18
A
B
C
D
p=0.117
Ki67 positive cells (%)
50
40
30
20
10
0
Scramble
RAD18

Figure 32. Ki67 staining of tumors from mice injected with ZL34 MPM cells exhibiting RAD18 interference or scramble control cells. Histological sections of mice tumors stained with hematoxylin and eosin dyeing **(A)**, DAB staining of Ki67 **(B)** and heat map of Ki67 staining through DAB **(C)** in mice tumors having arisen from subcutaneous injection of ZL34 MPM cells with RAD18 RNA interference or the double scramble, upon chemotherapy. **(D)** Quantification (%) of Ki67 positive cells in histological sections of mice tumors obtained following subcutaneous injection of ZL34 MPM cells presenting RNA interference of RAD18 or the double scramble. Mice were treated with chemotherapy once the mean of the size of both tumors attained 500mm³. Analyzed tumors come from mice having received variable numbers of chemotherapy injections – from 2 to 4. Statistical significance was evaluated by Student's t-test.

2.4. RAD18 interference promotes senescence in ZL34 cells upon chemotherapy

Besides cell proliferation through quantification of Ki67 positive cells, it would be interesting to evaluate the senescence status of ZL34 cells exhibiting RAD18 and/or HLTF interference. Demonstration of senescence-associated β-galactosidase was performed on ZL34 transduced cells incubated in the presence or absence of cisplatin and pemetrexed for 48 hours. Cells were fixed, permeabilized and then incubated with X-Gal, namely β-galactosidase's substrate. Afterwards, staining of β-galactosidase and detection of its activity were performed at pH 6, which is a characteristic of senescent cells. Quantification of positive cells – colored in blue – was then achieved **(Figure 33, B)**.

Data indicate that chemotherapy treatment leads to a significant increase of senescence-associated β-galactosidase in all conditions compared to non-treated cells **(Figure 33, A)**. Indeed, all non-treated conditions exhibit similar average percentage of senescence-associated β-galactosidase with a basal activity reaching 0.52% for the scramble, 0.83% for RAD18, 0.74% for HLTF and 0.66% for RAD18 + HLTF knock down cells. The combination of cisplatin and pemetrexed, by contrast, induces significantly higher average percentages compared to their related control cells. Interestingly, cells displaying RAD18 interference demonstrate significant higher senescence-associated β-galactosidase upon chemotherapy with an average percentage attaining 7.00%, compared to the other treated conditions which similarly and respectively show 2.03% for the scramble, 1.97% for HLTF and 2.00% for RAD18 + HLTF knock down cells.

Therefore, on the one hand, treatment for 48 hours with the combination of cisplatin and pemetrexed induces senescence-associated β-galactosidase in ZL34 MPM cells, and on the other hand, interference of RAD18 in those cells demonstrates a significant increase in senescence-associated β-galactosidase in presence of the standard chemotherapy regimen.

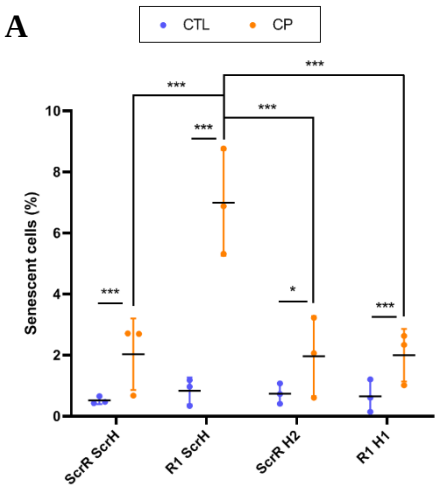

B

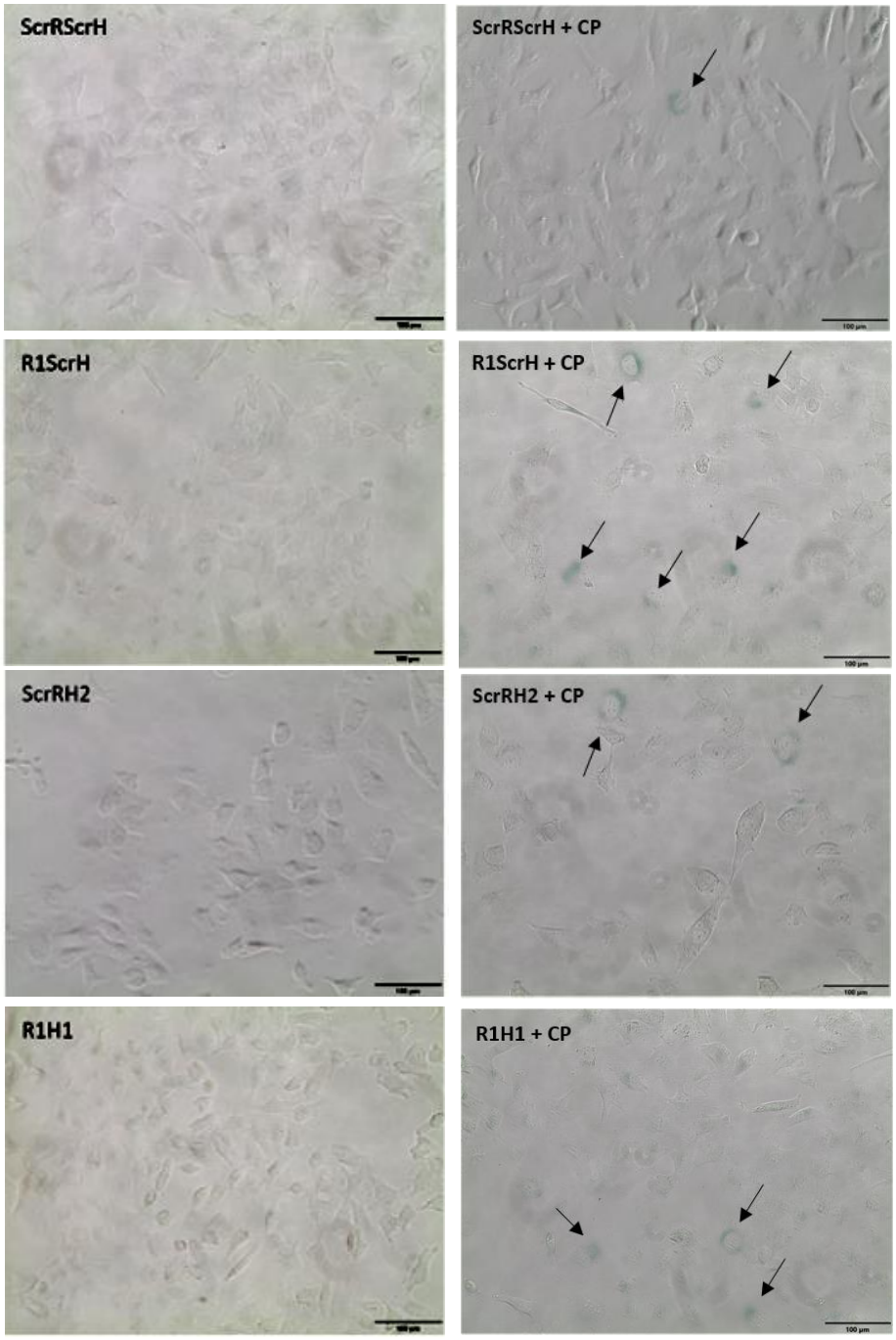
ScrRScrH
ScrRScrH + CP
R1ScrH
R1ScrH + CP
ScrRH2
ScrRH2 + CP
R1H1
R1H1 + CP

Figure 33. β-galactosidase assay on ZL34 cells with RAD18 and/or HLTF interference. **(A)** Quantification (%) of positive ZL34 transduced cells counted visually under the microscope comparing all conditions between them. Data are the sum of 10 different pictures and expressed as mean ± SD, in 3 independent experiments. Statistical analysis consists in a binomial model with multiple comparisons followed by Tukey's post-test. **(B)** Images of RAD18 and/or HLTF interfered ZL34 cells following β-galactosidase staining and treated or non-treated with cisplatin (10µM) and pemetrexed (10µM) for 48 hours. Cells appearing in blue are positive for senescence-associated β-galactosidase.

2.5. Chemotherapy induces S phase arrest and DNA fragmentation in ZL34 cells independently of RAD18 and/or HLTF interference

Given the results obtained in mice experiments, it would also be of interest to study the cell cycle of MPM transduced cells to get an overview of the impact of RAD18 and/or HLTF interference on the cell cycle progression. Moreover, susceptibility to chemotherapy-induced apoptosis would also be interesting to investigate – especially in RAD18 knocked down cells which show a significant lower tumor growth in mice upon chemotherapy.

To do so, ZL34 cells transduced with lentivectors expressing RAD18 and/or HLTF shRNAs were incubated for 48 hours in presence or absence of cisplatin (10µM) and pemetrexed (10µM). Fixation and permeabilization with 70% ethanol followed by RNAse treatment and PI staining were performed. Cells were analyzed in flow cytometry **(Figure 34, A)**. Cell cycle profiles were collected, and cells of each condition were quantified in all phases of the cell cycle **(Figure 34, B)**.

Data reveal that the chemotherapy composed of cisplatin and pemetrexed significantly increases the number of cells in S phase in all conditions studied compared to respective non-treated cells **(Figure 34, C)**. Moreover, when comparing only treated cells between them, there is no significant impact of RAD18 and/or HLTF interference on the number of cells in S phase compared to the scramble. Thus, chemotherapy induces a cell cycle arrest during S phase whether DDT pathways were inhibited or not. Indeed, non-treated conditions exhibit means of cells in S phase going from 13.96% (scramble) to 21.03% (RAD18 + HLTF interference) while the treated ones attain means similar between them with 51.63% for the scramble, 65.13% for RAD18, 58.06% for HLTF and 62.46% for RAD18 + HLTF knock down cells.

Furthermore, the SubG1 part of cell cycle exhibits cells having undergone a loss of DNA following DNA fragmentation, thus displaying reduced DNA content following permeabilization and indicating apoptosis. The number of cells in SubG1 is significantly higher upon chemotherapy with means of 2.83% for the scramble, 3.00% for RAD18, 2.57% for HLTF and 2.67% for RAD18 + HLTF knock down cells, compared to non-treated cells, which demonstrate means from 0.17% (RAD18 interference) to 0.40% (HLTF interference) **(Figure 34, D)**. However, comparison between SubG1 cells of treated conditions only does not reveal any significant difference, which means that RAD18 and/or HLTF interference does not impact apoptosis upon chemotherapy. Besides, there is no significant polyploidy observed in treated in cells, whether interferences of RAD18 and/or HLTF were involved or not (data not shown).

Thus, the chemotherapy regimen of 48 hours leads to a significant S phase blockade with no impact of RAD18 and/or HLTF interference on the cell cycle arrest observed, as well as a significant apoptosis, without regard to RAD18 and/or HLTF interference.

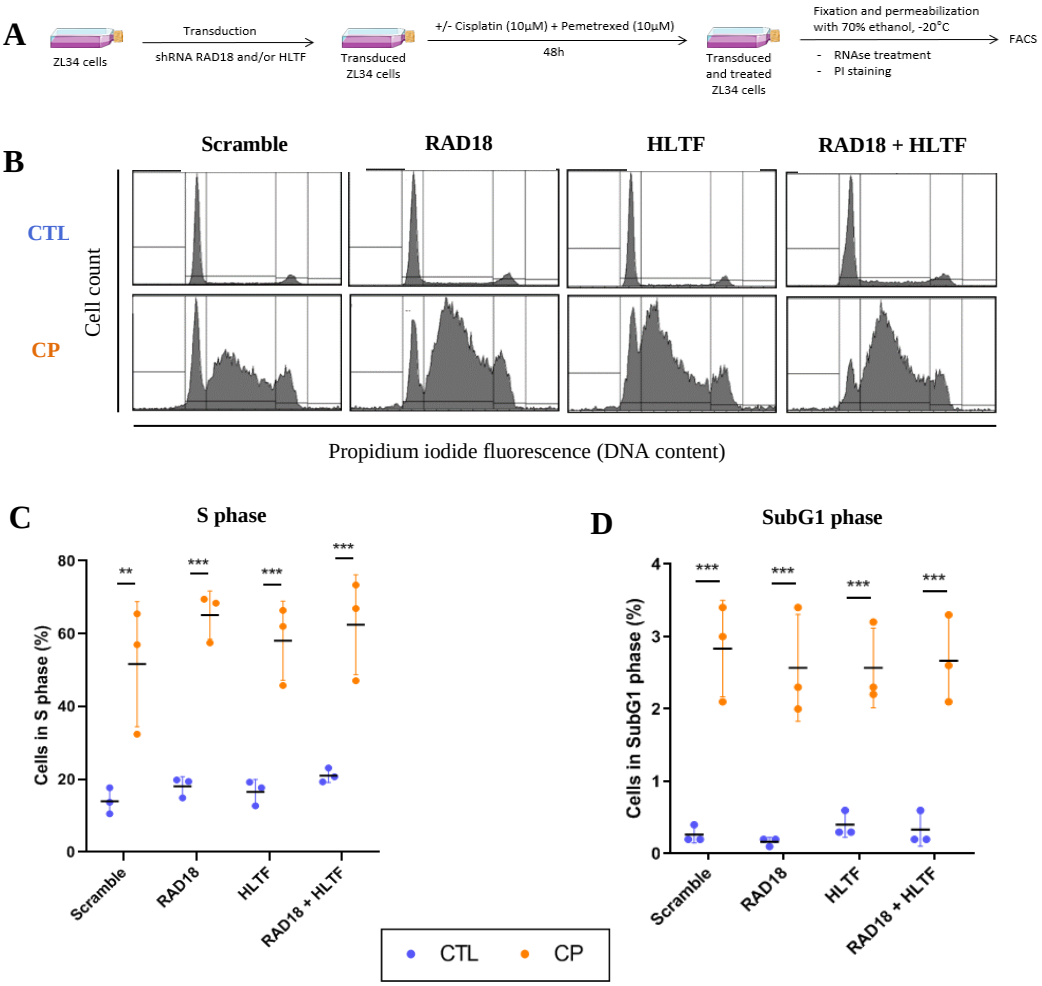

Figure 34. Cell cycle analysis of RAD18 and/or HLTF knocked down ZL34 cells. **(A)** Experimental model. ZL34 MPM cells were transduced with lentivectors expressing shRNAs against RNA of RAD18 and/or HLTF, with scramble shRNAs (ScrR and ScrH) as controls. Transduced cells were treated or not with cisplatin (10µM) and pemetrexed (10µM) for 48 hours. Cell cycle profiles and their quantification were evaluated upon cell permeabilization with ethanol, PI staining and flow cytometry. **(B)** Cell cycle profiles of ZL34 transduced cells incubated or not with cisplatin (10µM) and pemetrexed (10µM) for 48 hours. **(C)** Quantification (%) of RAD18 and/or HLTF knocked down ZL34 cells in S phase of the cell cycle, comparing all conditions between them. **(D)** Quantification (%) of RAD18 and/or HLTF knocked down ZL34 cells in SubG1 phase of the cell cycle, comparing all conditions between them. Data are collected from 3 independent experiments and expressed as means ± SD. Two-way ANOVA with Tukey's post-test where means of all conditions were compared between them.

2.6. HLTF and RAD18 + HLTF interferences significantly decrease phosphatidyl serine exposure upon chemotherapy

Apart from cell cycle analysis, cell apoptosis assay was performed to deeply analyze chemotherapy-induced apoptosis in the RAD18 and/or HLTF knock down conditions.

ZL34 cells that were transduced with lentivectors expressing RAD18 and/or HLTF shRNAs were kept for 48 hours with or without the chemotherapy, labeled with Annexin V – FITC and PI, and subsequently analyzed by flow cytometry **(Figure 35, A)**. Quadrant partitioning was achieved to distinguish positive from negative Annexin V and PI cells independently, with cells exhibiting Annexin V+/PI- being considered as early and Annexin V+/PI+ as late apoptotic cells **(Figure 35, B)**.

Results show that early and late apoptosis taken together are significantly higher upon chemotherapy **(Figure 35, C)**. Indeed, the mean of total Annexin V positive cells reaches 26.00% in the scramble, 18.23% in RAD18 and 14.83% in HLTF knock down cells. In contrast, the condition displaying RAD18 + HLTF interference does not exhibit any significant difference with the scramble in presence of chemotherapy. Indeed, the double knocked-down cells show a mean of Annexin V positive cells of 13.73% when treated with the chemotherapy. Of note, a greater variance can be denoted regarding results of non-treated RAD18 + HLTF knock down cells compared to the other non-treated conditions. Moreover, non-treated cells exhibit various means of Annexin V positive cells, going from 2.63% (RAD18 interference) to 6.73% (RAD18 + HLTF interference). Furthermore, comparison of apoptosis between only treated cells reveals that HLTF and RAD18 + HLTF knock down cells are significantly lower compared to the scramble **(Figure 35, D)**. By contrast, RAD18 does not show any significant difference of Annexin V positive cells with the scramble in presence of chemotherapy.

Thus, there is significantly less apoptosis in HLTF and RAD18 + HLTF knock down cells treated with the chemotherapy compared to the treated scramble. Therefore, the significant decrease of apoptosis observed suggests a link with HLTF knock down, where HLTF interference seems to promote cell survival.

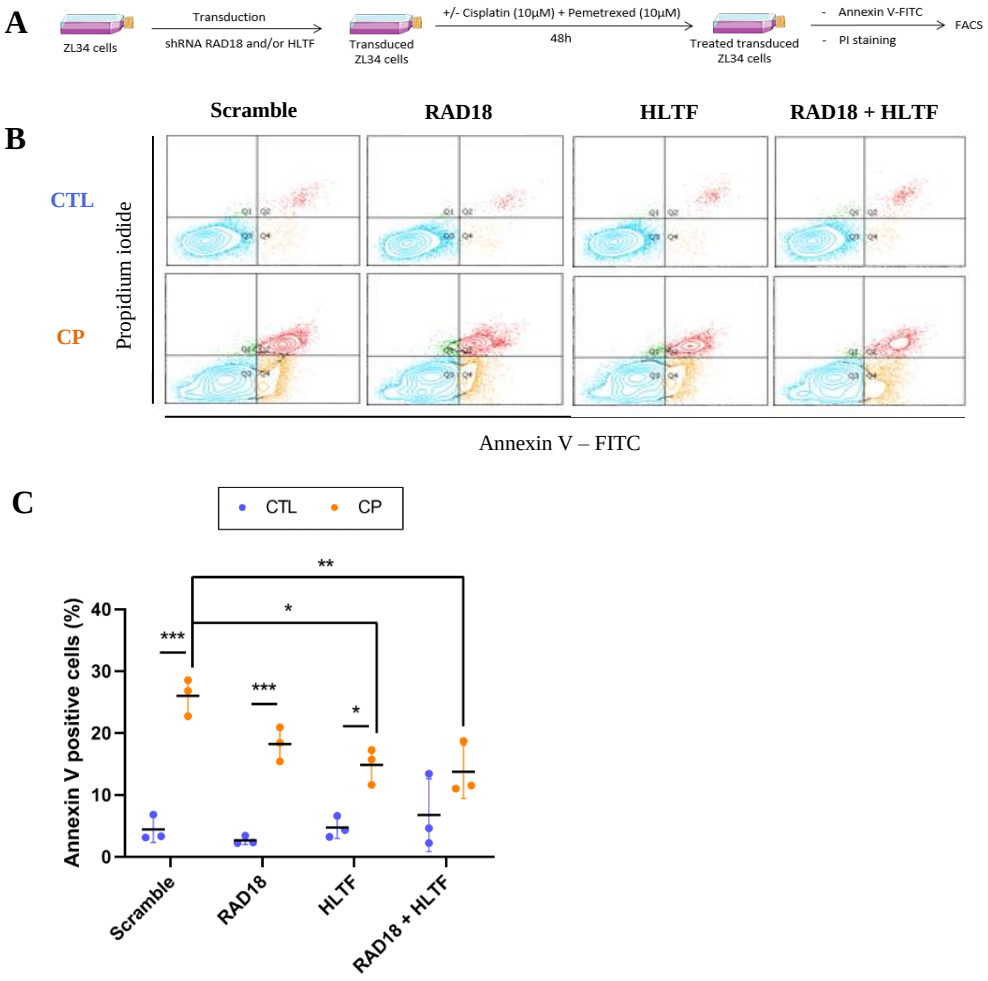

Figure 35. Apoptosis assay of RAD18 and/or HLTF knocked down ZL34 cells. **(A)** Experimental model. ZL34 MPM cells were transduced with lentivectors expressing shRNAs against RNA of RAD18 and/or HLTF, with scramble shRNAs (ScrR and ScrH) as controls. Transduced cells were treated or not with cisplatin (10µM) and pemetrexed (10µM) for 48 hours. Cells were collected, labeled with Annexin V-FITC and PI, and analyzed in flow cytometry. **(B)** Plots of Annexin V – PI staining. Quadrant 1 represents necrotic cells which are Annexin V-/PI+ cells, quadrant 2 highlights late apoptotic cells with Annexin V+/PI+ cells, quadrant 3 reflects non-apoptotic cells which are Annexin V-/PI- cells and quadrant 4 shows early apoptotic cells with Annexin V+/PI- cells. **(C)** Quantification (%) of Annexin V positive cells of RAD18 and/or HLTF knocked down ZL34 cells comparing all conditions between them. Data are collected from 3 independent experiments and expressed as means ± SD. Statistical significance was evaluated using two-way ANOVA with Tukey's post-test where means of all conditions were compared between them.

5

Discussion

1. Two approaches related to DNA damage management in MPM therapy

MPM is a rare and aggressive cancer that is strongly linked with asbestos exposure. Indeed, asbestos fibers were shown to physically interfere with the mitotic spindle, thus causing chromosomal damage (Elke Dopp and Schiffmann 1998). Chronic inflammation resulting notably from the biopersistance of fibers and the generation of ROS as well as RNS favor the oncogenesis of MPM (Urso et al. 2019). Moreover, the standard chemotherapy regimen of MPM aims at inducing bulky adducts and at reducing the pool of nucleotides available for DNA synthesis (Dasari and Bernard Tchounwou 2014)(Rollins and Lindley 2005). Therefore, MPM is strongly linked with a context of genotoxicity through DNA damage.

DNA damage response is essential for genomic integrity. This process consists of the detection of the DNA lesion, cell cycle control and the appropriate repair of the damage. DNA damage response and repair play a key role in carcinogenesis and tumor progression (Marta Betti et al. 2017). Indeed, defect in these pathways drives mutagenesis as DNA damage remains unrepaired. In contrast, efficient processes of damage sensing and repair can lead to resistance to genotoxic treatments as therapy-induced DNA lesions are efficiently taken over, thus leading to cell survival with genomic stability. However, these mechanisms are likely to give rise to mis-repaired lesions or incapable of repairing DNA lesions. Replication of damaged DNA leads to high frequency of fork collapse and genomic instability. In this case, DDT pathways can take over to enable tolerance of the DNA damage, thus allowing the bypass of the lesion and the resumption of DNA synthesis despite the presence of the remaining lesion, thereby promoting survival and preventing genome instability (Gargi and Chen 2013).

Given the importance of taking into account DNA damage management in the context of MM, this thesis aims at studying and getting a deeper understanding of (i) DNA damage response to gamma irradiation or chemotherapy and checkpoint inhibition, as well as evaluating the mechanisms of DSBs repair in the context of ionizing radiation, and (ii) DDT pathways and their regulation upon chemotherapy in MM. These two approaches provide a better understanding of the resistance to chemo- as well as radiotherapy, and highlight potential therapeutic targets.

2. The importance of mutational status in MPM therapy

Despite major structural chromosomal rearrangements driving tumorigenesis, MPM is characterized by a low mutation rate, compared to other cancer types (Brossel et al. 2021). Indeed, TCGA data reveal that MPM exhibit 0.726 somatic mutations per megabase **(Figure 36)** while lung cancer and melanoma stand with around 10 somatic mutations per megabase (Bueno et al. 2016)(Hmeljak et al. 2018)(Alexandrov et al. 2013).

BAP1, *CDK2NA* and *NF2* are the three most frequently mutated genes in MPM (Sekido 2013)(Fred et al. 2016). In this study, the oncoplot generated from TCGA database showed that *BAP1* and *TP53* are the most frequently mutated genes in MM, while other DDR and DDT genes are very poorly mutated. All these mutated tumor suppressor genes are part of functions regarding checkpoint control, cell cycle regulation, cellular proliferation and DNA repair. Among other altered genes in MM, *CDKN2B*, *LATS2* and *LATS1* were shown to display recurrent copy loss that was correlated with loss of expression of these genes. Moreover, gene fusions and splice alterations were reported to be frequent mechanisms involved in *BAP1*, *NF2* and *SETD2* inactivation in the context of MPM (Bueno et al. 2016)(Murakami et al. 2011). Of note, simultaneous dysregulations of several pathways can ensue from the loss a single tumor suppressor gene. For instance, the loss of merlin activity results in cell proliferation through the Hippo, mTOR and FAK signaling pathways (Cakiroglu and Senturk 2020).

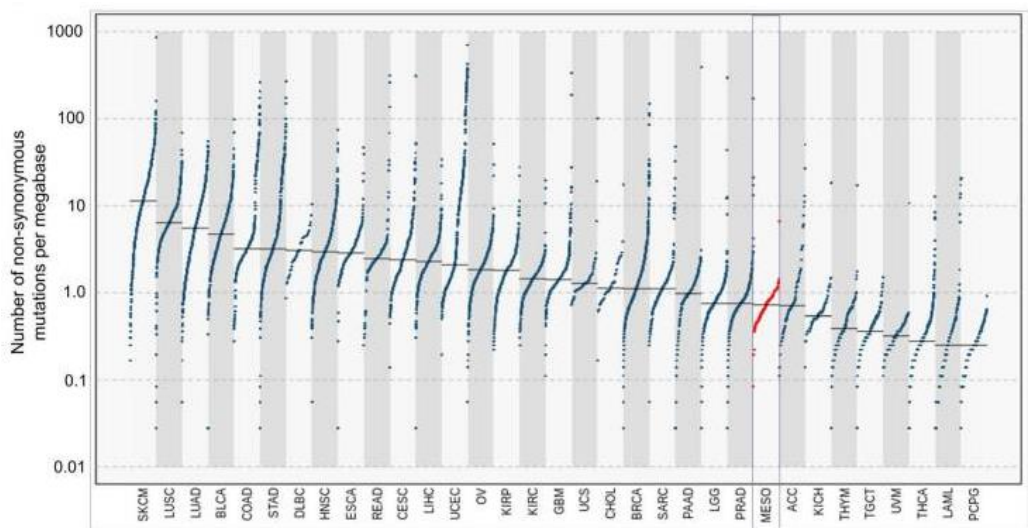

Figure 36. MPM exhibits a low tumor mutational burden compared to other cancers. X-axis represents the different types of cancer studied while y-axis shows the number of genomic non-synonymous mutations per megabase in exons (Brossel et al. 2021).

Furthermore, *TP53* mutation was shown to be linked with lower overall survival and never be related to the epithelioid histological subtype, thus demonstrating the aggressiveness of *TP53*-mutant MPM cells (Bueno et al. 2016).

Thus, screening for common alterations of genes and pathways is essential in order to get a better understanding of MPM resistance to therapies and a global view of repair defects and upregulations in MM. It would be of interest to investigate which molecular processes cancer cells rely on for DNA damage repair and tolerance. Moreover, further research on gene polymorphisms and altered gene expression could give rise to useful biomarkers, highlight new potential therapeutic targets, predict treatment outcome and optimize treatment decisions. Further investigations are needed in the context of this study.

3. Targeting DNA damage response and repair in MPM therapy

Efficient and overexpression of mechanisms of DNA damage response and repair promote resistance to anti-cancer treatments. Indeed, DNA damaging agents aiming at inducing DNA damage to dividing cells, such as chemo- and radiotherapies, are less effective in case of efficient DNA damage response and repair. Thus, DNA remains intact and genomic stability is maintained (Toumpanakis and Theocharis 2011)(Giglia-mari, Zotter, and Vermeulen 2011). In the case of MM, overexpression of *CHK1* as well as genes involved in DNA repair mechanisms, notably DSB repair, participate in genotoxic treatment resistance (Fred et al. 2016)(D. O. Røe et al. 2010). In contrast, in the context of defects in DNA damage repair, mutagenesis is driven and gives rise to oncogenesis (Carusillo and Mussolino 2020). Hence, healthy mesothelial cell deficient in repair mechanisms and exposed to asbestos fibers are less armed to defend themselves and face the high amount of DNA damage generated in the context of MPM (Toumpanakis and Theocharis 2011)(Marta Betti et al. 2017)(Sekido 2013). In these circumstances, cancer cells increase their reliance on and become addictive to other DNA repair pathways to survive and proliferate (Nickoloff et al. 2017). Hence, targeting these rescue pathways appears to be an attractive strategy to prevent DNA damage repair and overcome cancer cell proliferation through the ultimate induction of apoptosis (Shaheen et al. 2011). Demonstration of this paradigm can be described through the principle of synthetic lethality where mutation in simultaneously two different genes leads to cell death, whereas mutation of either gene alone leads to cell viability (Nijman 2011). This concept is greatly illustrated through PARP inhibitors. Indeed, ovarian, breast and prostate cancer cells show deficiency in HR repair, thereby expressing addiction to the BER pathway. Thus, when ssDNA breaks occur, BER can efficiently repair the damage through PARP. In the context of PARP inhibitor treatment, BER cannot efficiently process the lesion, and leads to unrepaired ssDNA that can potentially be converted to DSB. Cells with efficient HR pathway are able to repair the damage and promote cell survival while cells lacking BRCA, being thus HR-deficient cells, initiate apoptosis (H. Li et al. 2020)(Hall and Benafif 2015). The reverse concept could be applied within the framework of MM. Indeed, BER pathway was shown to be altered in some MPM cell lines (Toumpanakis and Theocharis 2011)(M Betti et al. 2020)(Erčulj et al. 2012)(Chernikova, Game, and Brown 2012). Thus, targeting HR in this context would be relevant. Furthermore, the synthetic lethality principle has been applied on addiction to target cell cycle checkpoints. Indeed, as p53 conducts G1-S cell cycle checkpoint, gamma-irradiated MPM cells exhibiting p53 loss become addictive to G2-M checkpoint (Origanti et al. 2012)(Leijen, Beijnen, and Schellens 2010)(Mukhopadhyay, Senderowicz, and Ferbeyre 2005)(Gabrielli, Brooks, and Pavey 2012)(Bridges et al. 2016). Thus, it would be of interest to exploit G2-M checkpoint inhibition in the context of MPM cell lines demonstrating p53 loss in order to investigate the treatment outcome in presence of gamma-irradiation. Besides, conducting the same experiment in the context of chemotherapy could also produce relevant results.

The response of MPM and mesothelial cells to DNA damage was evaluated upon chemo- and radiotherapy, as well as checkpoint inhibition. DNA damage response consists in the sensing and the signaling of the DNA damage to promote the repair of the detected lesions (Goldstein and Kastan 2015). Gamma-irradiation induces a large panel of DNA lesions, including base modifications (80%) such as 8-oxoG resulting from ROS and oxidative stress, and damage on the sugar phosphate backbone (20%) involving SSBs and DSBs, the latter being the most cytotoxic one (Roos and Kaina 2013). With regard to chemotherapy, cisplatin bulky adducts promote fork replication stalling which can further lead to DSBs. As cisplatin adducts require NER as mechanism of repair, NER-deficient MPM cells are hypersensitive to cisplatin treatment (M Betti et al. 2020)(Dunkern, Fritz, and Kaina 2001). Among the MPM cell lines and the mesothelial cell line studied in this thesis, DNA damage response was shown to be activated through γH2AX foci detection upon chemo- and radio-therapy **(Figure 24, C and D)**. Indeed, H2AX is rapidly phosphorylated in response to activation of the MRN complex and ATM following DSB detection. Thus, chromatin in this form allows enough space for DNA damage repair (Roos and Kaina 2013). Beside γH2AX foci, activation of the DNA damage response was highlighted though cell cycle arrest in S phase upon chemotherapy **(Figure 28, B)**, and in G2-M phase upon radiotherapy **(Figure 25, C)**. Thus, MPM cells rely on G1-S phases checkpoint when treated with chemotherapy, while they rely on G2-M phases checkpoint when treated with gamma-irradiation. MPM cells thereby count on a checkpoint or another depending on the DNA damaging agent in question. This phenomenon was observed in normal and tumor cell lines, including in the context of MPM (Vivo et al. 2003)(Ma et al. 2012)(Gogineni et al. 2011)(H. Zhao et al. 2001)(Zanellato et al. 2011)(Salaroglio et al. 2022). Cell cycle arrests are triggered to give time for DNA repair and prevent mitosis with unrepaired DNA lesions (Awlik and Eyomarsi 2004). The dose-dependent G2-M phases blockage upon irradiation was also observed in other cell types (H. Zhao et al. 2001)(Naderi, Hunton, and Wang 2002). Among actors of the DNA damage response, ATR – CHK1 pathway is the one mediating G2-M cell cycle checkpoint upon DNA damage (Lapenna and Giordano 2009). Thus, in the context of gamma-irradiation, MPM cells rely on the G2-M checkpoint to arrest cell cycle progression in case of presence of DNA damage. Therefore, inhibiting CHK1 in irradiated cells would be a strategy to prevent G2-M checkpoint, drive DNA damaged cells through premature mitosis and subsequently, promote the apoptosis of those cells through mitotic catastrophe (Suzuki, Yamamori, and Bo 2017)(On et al. 2011). Indeed, inhibitors of G2-M checkpoint, including UCN-01, promote chemo- and radiotherapy sensibility in several cellular types (Playle et al. 2002)(Mack et al. 2004)(Bunch and Eastman 1996). Inhibition of WEE1, a kinase involved in G2-M checkpoint, also sensitizes MPM cells to cisplatin treatment, irrespective of p53 mutational status (Indovina et al. 2014).

In this study, mitotic trap assay performed on four MPM cell lines showed that G2-M arrest was abrogated by UCN-01 and that cells were driven through cell cycle and forced to go through mitosis despite DNA lesions, however with no significant induction of apoptosis **(Figure 27, C)**. Therefore, characterizing p53 status in our studied cell would be of interest as it could be wild type, thus making them less sensitive to checkpoint

inhibition. Moreover, it could be worthwhile and relevant to characterize the cells that are able to enter mitosis without G2-M cell cycle checkpoint. Another idea could be to sort those cells and subsequently keep them in culture under genotoxic treatment and CHK1 inhibition, to evaluate their mutation status and analyze cell apoptosis.

DNA damage repair mechanisms, and more specifically DSB repair pathways, demonstrate a potential key role in MPM cells that are able to prematurely enter mitosis upon genotoxic treatment. Indeed, the performance of these repair processes is crucial for the mutagenic status of these cells. Moreover, cells that are deficient in HR and NHEJ pathways are more sensitive to gamma-irradiation, with NHEJ being the dominant process of repair as it plays an important role during all the cell cycle phases, while HR contributes to DSB repair particularly in late S-G2 phases (Rothkamm et al. 2003). In addition, HR and NHEJ were both shown to be activated in response to gamma-irradiation in the context of glioblastoma (Bee et al. 2013). Results in this study show that in three out of four MPM cell lines, HR efficiency stands higher than mesothelial cells **(Figure 29, C)**, which could mean that those MPM cells rely on HR. Indeed, some key genes involved in HR, such as *RAD50*, *RAD54L* and *BRCA2*, were shown to be overexpressed in some MPM cell lines (Toumpanakis and Theocharis 2011). Regarding NHEJ, there is only the ZL34 cell line that demonstrates a higher efficiency compared to mesothelial cells **(Figure 29, D)**. In both HR and NHEJ, there is no impact of gamma-irradiation on the performance of repair. In all cell lines studied, NHEJ seems to globally exhibit a higher level of efficiency activity compared to HR. Overall, results show that the level of repair efficiency depends strongly on the cell line studied. Indeed, studies on pancreas cancer cells demonstrated that NHEJ pathway was predominantly followed to repair DSB upon cell irradiation, while HR was significantly increased in breast cancer cells compared to normal mammary epithelial cells (Ying-hua Li et al. 2012)(Mao et al. 2009). Other evaluations of repair pathways, such as BER and NER, should be made to get a better understanding of the underlying and intricate regulations of DNA damage management in MPM under genotoxic treatment.

Immunotherapy has been demonstrating substantial interest in the context of cancer treatment. Combining DDR inhibitors with immunotherapy appears to be an attractive treatment strategy (T. Chen et al. 2022)(Vikas et al. 2020). Importantly, the DDR inhibitor targeting a certain DDR pathway leads to a specific cellular response as well as variable immunomodulatory effects, depending on the nature of the DNA damage generated (Mouw and D'Andrea 2018). Indeed, DNA repair deficiency leads to an increase of DNA damage, thereby promoting the generation of tumor specific neoantigens which drive a T-cell-mediated anti-tumor immune response (Mouw and D'Andrea 2018)(Mouw et al. 2018). In addition, DNA lesions arising from DNA damaging agents and/or DDR inhibition drive the secretion of anti-tumor and proinflammatory cytokine, namely type 1 interferons, through the cyclic guanosine monophosphate (GMP)-AMP synthase (cGAS)/stimulator of interferon genes (STING) pathway (Won and Bakhoum 2020). Indeed, this DNA sensing pathway is triggered through cytosolic DNA fragments generated by PARP inhibition-induced unrepaired DNA damage (Pantelidou et al. 2020). However, DNA damage, interferon gamma (IFN-γ), PARP inhibitors as well as RAD51 inhibitors were shown to upregulate PD-

L1 expression, thereby suggesting that DDR inhibitors could enhance the response of immune checkpoint inhibitors (Garcia-diaz et al. 2017)(Peyraud and Italiano 2020)(Sato et al. 2017)(Mimura et al. 2018)(Gu et al. 2022). Several ongoing clinical trials are investigating the outcome of DDR inhibition-based combination strategies. PARP inhibitors already showed great success in HR-deficient ovarian, breast and pancreatic cancers (Peyraud and Italiano 2020). Other DDR inhibitors – such as the ones targeting ATM, ATR, CHK1, DNA-PK, APE1 and WEE1 – are evaluated in clinical trials (Cleary et al. 2020)(T. Chen et al. 2022). Early results show that even if most DDR inhibitors are well tolerated during the initial phase of the trials, adverse effects – such as neutropenia – are likely to occur, thus requiring a decrease of the dose to limit drug toxicity. Furthermore, the accumulation of DNA damage presumably promotes potential carcinogenic mutations driving emergence of other cancers (T. Chen et al. 2022). Further research is needed to moderate these effects. The combination of DDR inhibitors with immune checkpoint inhibitors should also be tested in the context of MM.

4. Targeting DNA damage tolerance pathways in MPM therapy

DDT pathways are escape routes followed by the cells in order to resume the stalled replication fork in occurrence of unrepaired DNA damage upon DNA replication. Indeed, the prolonged stalling of replication forks can result in the formation of further deleterious damage – notably DSBs that could lead to gross DNA rearrangements. Thus, DDT mechanisms protect against the collapse of arrested replication forks and prevents cell death (Roos and Kaina 2013).

RAD18 and HLTF are proteins that tightly regulate DDT pathways through PCNA ubiquitination. Mono-ubiquitination of PCNA mediated through the RAD6-RAD18 complex leads to TLS pathway involving TLS polymerases that are able to bypass DNA damage. Thus, TLS pathway contributes to genetic instability, mutagenesis and cisplatin resistance.

Among these specialized TLS polymerases, Pol η is strongly associated with the management of bulky adducts, notably cisplatin-GG cross-links (P. Saha et al. 2020)(Alt et al. 2007). Indeed, Pol η efficiently and accurately inserts dCTP opposite the 3'dG of cisplatin-GG, while 5'dG bypass is generally less efficient and results in dATP mispairing, because of the rigidity of platinum cross-links (Alt et al. 2007)(Ummat et al. 2012). Moreover, in the context of ovarian cancer, the expression of Pol η was shown to be upregulated along with cell survival upon cisplatin treatment, whereas downregulation of Pol η appears to enhance cisplatin-induced apoptosis (Kumar et al. 2015). Furthermore, Pol η happens to be essential for overcoming cisplatin-induced S phase arrest (Albertella et al. 2005). Of note, p53 favors the induction of Pol η by increasing its transcription upon ultraviolet-irradiation, thereby promoting cell survival (Lerner et al. 2018). Thus, mounting evidence suggests that Pol η inhibition could sensitize cancer cells to chemotherapy, restrain drug-induced mutagenesis and prevent development of secondary tumors (Leung et al. 2019)(P. Saha et al. 2020). Beside Pol η, Pol ζ was also shown to play an important role in cisplatin adducts bypass through TLS. Indeed, this polymerase is able to extend the DNA primer set by Pol η despite double helix distortion resulting from the cisplatin-induced intrastrand adduct (Shachar et al. 2009)(Y. Lee, Gregory, and Yang 2014). Moreover, cells lacking Pol ζ or only its catalytic subunit, namely REV3L, are more sensitive to cisplatin treatment compared to the ones expressing it (Zander and Bemark 2004)(F. Wu et al. 2004). Furthermore, expression of Pol ζ was shown to be up regulated in cervical cancer compared to normal cervical tissues, and appears to be linked with poor prognosis (Shi, Li et al. 2013)(L. Yang et al. 2015). The same observation occurred in glioma were Pol ζ status predicts chemotherapy resistance, tumor recurrence as well as cell invasion (J. Yang et al. 2021)(Huibo Wang et al. 2009). In addition to Pol η and ζ, REV1 is another TLS polymerase that also plays a role in the bypass of cisplatin bulky adducts (Hicks et al. 2010). Therefore, targeting TLS polymerases seems to be an attractive strategy to prevent mutagenicity as well as genome instability, get higher overall survival in MPM patients and overcome cisplatin resistance.

RAD18 is an E3-ubiquitin ligase that centrally governs DDT pathways regulation. This protein is highly expressed in melanoma, glioma and esophageal squamous cell cancer compared to normal tissues and cells. Upregulated expression of RAD18 was shown to be associated with poor prognosis and worse overall survival (Zou et al. 2018)(B. Wu et al. 2019)(J. Sun et al. 2022). In addition, patients with locally advanced rectal cancer with low RAD18 expression got a better response to neoadjuvant chemo- and radiotherapy compared to those with high RAD18 expression (Yan and Chen 2019). Moreover, by downregulating p53 expression, RAD18 promotes resistance to radiotherapy, tumor progression and represses apoptosis of glioma cells (B. Wu et al. 2019)(Hunt, Barker, and Chen 1987). Knock down of RAD18 upon radiotherapy and/or 5-fluorouracil in glioblastoma and rectal cancer cells led to a significant decrease of cell proliferation and viability, promotion of apoptosis and suppression of migration as well as invasion (Yan and Chen 2019). Furthermore, RAD18 was shown to promote apoptosis through induction of caspase-9 and caspase-3 (Yan and Chen 2019). Beside its activity in TLS, RAD18 also contributes to DSBs repair. Indeed, RAD18 is recruited to DSB site to propagate signaling for DNA repair during G1 phase by interaction with ubiquitinated chromatin proteins through its ubiquitin-binding zinc finger (UBZ) domain. In this context, the RAD6B-RAD18 complex catalyzes mono- and poly-ubiquitination of histone H2A to facilitate RAD9 recruitment at the DSB (Mustofa et al. 2021)(Inagaki et al. 2011). Moreover, fibroblasts that are depleted in RAD18 demonstrate an accumulation of ssDNA that are managed during G2-M checkpoint to avoid mitosis entry with persistent DNA damage (Y. Yang et al. 2017).

In this study, ZL34 cells exhibiting RAD18 interference were shown to induce a significant lower tumor growth in mice upon chemotherapy **(Figure 31, F and G)**. Several analyses were performed in order to explain this observation. IHC of RAD18 knock down tumor mice that were treated with the chemotherapy showed that cell proliferation – observed through Ki67 staining – tends to be lower compared to the control tumor cells **(Figure 32, D)**. In addition, while chemotherapy treatment leads to a significant increase of senescence-associated β-galactosidase compared to non-treated cells, cells displaying interference of RAD18 demonstrate an even higher significance regarding quantification of senescence compared to the control, HLTF and RAD18 + HLTF interferences **(Figure 33, A)**. These findings go along with the observations obtained in the mice experiment as these two assays demonstrate a reduced cell proliferation in RAD18 knock down cells in presence of the chemotherapy. Moreover, cell cycle analysis revealed an S phase arrest in all conditions due to the chemotherapy **(Figure 34, C)**. Although this analysis showed a significant increase in SubG1 cells in all treated conditions, it did not highlight any significant SubG1 quantification in treated RAD18 knock down cells compared to the other treated cell lines **(Figure 34, D)**. Furthermore, apoptosis assay showed that there was a significant increase of apoptotic cells in all conditions except in cells exhibiting RAD18 + HLTF interference, and that there was significantly less apoptosis in cells with HLTF and RAD18 + HLTF interferences in presence of chemotherapy compared to the control **(Figure 35, C)**.

Thus, RAD18 interference is not associated with a greater apoptosis upon chemotherapy, but the fact that conditions exhibiting HLTF interferences show significantly less apoptosis could induce a clear distinction with RAD18 interference regarding tumor growth in mice. When approaching from another angle, it would be only HLTF presence that leads to lower tumor growth in mice and as much apoptosis as the control condition upon chemotherapy. Furthermore, cisplatin treatment promotes senescence and drives TLS through an increase of Pol η expression, thus treated cells stop proliferating and accumulate DNA damage which drives genomic instability. RAD18 interference disables TLS pathway and leads to less cell proliferation along with a higher senescence. Of note, concomitant interference of RAD18 + HLTF surprisingly does not lead to apoptosis of cells upon chemotherapy, as both DDT pathways are disabled in a context of DNA damage induction. Indeed, it would be expected that unrepaired DNA damage could not be processed by DDT pathways and kept accumulating until induction of apoptosis, notably through p53 activity. Thus, repair mechanisms could otherwise be very efficient or other pathways might play a role in taking over the management of tolerance processes. Further experiments are therefore required to investigate more deeply DDT pathways in MPM to explain the mechanisms behind the results of the mice experiment.

Furthermore, RAD18 inhibitors should be tested in combination with immune checkpoint inhibitors, such as ipilimumab and nivolumab, in order to study the impact of DDT inhibition – and more specifically, TLS inhibition – in the context of MM. Indeed, RAD18 inhibition could significantly influence the tumor microenvironment, and by extension, could also impact the immunotherapy response. It could thereby either lead to the same, a better or worse immunotherapy efficacy, compared to immunotherapy alone. This outcome would greatly influence the potential further approval of RAD18 inhibitors in MM therapy. Further investigation of the genetic and cellular features driving synergic or antagonistic effect of RAD18 inhibition on immune checkpoint inhibitors would be needed to get a better understanding of the underlying mechanisms.

Cisplatin, a platinum-based alkylating agent, and pemetrexed, an antifolate, are part of the standard chemotherapy of MM. Cisplatin has been shown to induce S-phase arrest in MPM cells as well as in other cancer cells (Zanellato et al. 2011)(Salaroglio et al. 2022)(S. Saha et al. 2022). In ovarian cancer cells, cisplatin seems to faster induce a transient S phase arrest since it is obtained after only 12 hours of treatment, compared to our studied cell lines which demonstrated S phase blockade after 48 hours of treatment. Thus, it is important to consider timing of treatment respectively to the cell type studied. Moreover, a durable G2-M phases arrest was observed in ovarian cancer cells following 12 to 18 hours of treatment and finally a G1 phase arrest after treatment of 18 hours (He et al. 2013).

Senescence is a state of growth arrest. Treatment with chemotherapeutic drugs or ionizing radiation can lead to therapy-induced senescence in tumor cells (Gorgoulis et al. 2019)(Mikuła-Pietrasik et al. 2020). Senescent cells show specific characteristics of their own, such as resistance to apoptotic stimuli, increased activation of senescence-associated-β-galactosidase, altered metabolism, persistent DNA damage and secretion

of the SASP which is enriched in proinflammatory factors including chemokines, cytokines and growth factors (B. Y. Lee et al. 2006)(Prasanna et al. 2021)(Mongiardi et al. 2021). Senescence-associated-β-galactosidase activity is usually used as a biomarker for senescent state. In this thesis, MPM cells treated with cisplatin showed higher senescence-associated-β-galactosidase activity compared to non-treated cells. Moreover, among treated cells, the ones exhibiting only RAD18 interference led to an even higher increase of senescence observed. Persistent activation of the DNA damage response was shown to promote the induction of senescence (Piskorz and Cechowska-Pasko 2022). Cellular senescence could be considered as a potent strategy to overcome cancer progression. However, several issues remain within the generation and persistence of therapy-induced senescent cells. Indeed, the SASP shows detrimental aspects and pro-tumorigenic effects as it promotes the protection of tumor cells from immune clearance and provides growth factors, thus stimulating angiogenesis, cancer cell proliferation, migration and invasion. Moreover, senescent cancer cells are able to restore the progression of their cell cycle, thus leading to aggressive recurrence and treatment resistance (B. Wang, Kohli, and Demaria 2020)(Saleh et al. 2020). Importantly, the immunosuppressive effect of the SASP would be responsible for the worse survival observed when senescent cells are present in the tumor microenvironment (Eggert et al. 2016). Gamma-irradiation leads to an increase of senescence-associated-β-galactosidase, p16, p21 and SASP induction in several cancer, notably in neuroblastoma, breast and colon carcinoma cell lines (B. D. Chang et al. 1999)(Jones et al. 2005)(Demaria et al. 2017). Interestingly, accelerated senescence appears to be p53 dependent in the context of ionizing radiation. Indeed, p53-deficient breast cancer cells are unable to undergo cell cycle arrest for an extended period of time, and ultimately result in apoptotic cell death. In contrast, cells expressing wild type p53 allow accelerated senescence through proliferative recovery (Jones et al. 2005). However, glioblastoma cells exhibiting p53 mutation are able to recover from ionizing radiation and resume proliferation (Quick and Gewirtz 2006). Thus, the radiotherapy outcome in p53-mutant cancer cells seems to be dependent on the cancer type or other factors such as potential additional mutations altering survival pathways. Further investigations are needed in this research field to characterize the variables involved in the response to radiotherapy to optimize treatment options in patients. Beside ionizing radiation, chemotherapies, and among which notably cisplatin, were shown to induce senescence in both cancer and nonmalignant cells, thereby promoting respectively cancer relapse and tumorigenesis through the SASP (B. Wang, Kohli, and Demaria 2020)(Roberson et al. 2005). Furthermore, the chronic inflammation induced by the SASP also gives rise to therapy side effects such as fatigue, appetite loss, cardiovascular morbidity and decline in physical functions (Mantovani et al. 2008)(Cupit-Link et al. 2017)(Bhakta et al. 2016). Moreover, senescent cells additionally contribute to age-related disease and dysfunctions observed in cancer patients. These side effects remain consistent for months after the end of the treatment, thus suggesting that senescent cells persist and can’t be properly cleared by the immune cells (Sanoff et al. 2014).

5. Conclusion

In conclusion, this thesis demonstrates that (i) ionizing radiation-induced G2-M arrest was abrogated by checkpoint 1 inhibitor which drove cells through premature mitosis despite DNA lesions and that (ii) RAD18 interference led to lower tumor growth through senescence-associated-β-galactosidase activity and apoptosis. Further investigations are needed to get a better understanding of DNA damage response, repair and tolerance. Overall, effective combination therapies seem to be more relevant to overcome MPM resistance than the use of one single agent. Thereby, it is required to study the impact of RAD18 inhibition on the tumor microenvironment, and by extension, on the efficacy of immunotherapy. A further improved comprehension of intrinsic resistance to chemo- and radiotherapy may open perspectives for new therapeutic strategies to overcome MPM.

6

List of scientific publications

Publications in scientific journals as first co-authors:

- Abdala, A. *et al.* (2019) 'BLV : lessons on vaccine development', *Retrovirology*, **16**(26), 1–6. doi: 10.1186/s12977-019-0488-8.

- Brossel, H. *et al* (2021) 'Activation of DNA Damage Tolerance Pathways May Improve Immunotherapy of Mesothelioma', *Cancers*, **13**(13), 3211. doi: 10.3390/cancers13133211.

Oral and poster communications:

- Poster presentation at GIGA-Cancer seminar: « Tolerance to DNA damage in malignant pleural mesothelioma » (18/10/19)

- Oral presentation at the *2èmes journées francophones sur le mésothéliome* in Nantes: « Régulation des voies de tolérance aux dommages à l'ADN par la E3 ubiquitine ligase RAD18: Mécanismes et perspectives thérapeutiques dans le cadre du mésothéliome pleural malin» (28/11/19 - 29/11/19)

- Poster presentation at the *2èmes journées francophones sur le mésothéliome* in Nantes: « Régulation des voies de tolérance aux dommages à l'ADN par la E3 ubiquitine ligase RAD18: Mécanismes et perspectives thérapeutiques dans le cadre du mésothéliome pleural malin » (28/11/19 - 29/11/19)

- Poster presentation at GIGA-Cancer seminar: « Role of the DNA damage tolerance pathways in malignant pleural mesothelioma » (14/12/21)

7

Bibliography

Abcam. 2022a. “Cisplatin.” https://www.abcam.com/cisplatin-antineoplastic-agent-ab141398.html (November 29, 2022).

Abcam. 2022b. “Paclitaxel.” https://www.abcam.com/taxol-f-benzyl-paclitaxel-analog-ab143553.html (November 29, 2022).

Abdel-Rahman, Omar, and Mohamed Kelany. 2015. “Systemic Therapy Options for Malignant Pleural Mesothelioma beyond Firstline Therapy: A Systematic Review.” *Expert Review of Respiratory Medicine* 9(5): 533–49.

Adjei, Alex A. 2004. “Pharmacology and Mechanism of Action of Pemetrexed.” *Clinical Lung Cancer* 5(SUPPL. 2): S51–55. http://dx.doi.org/10.3816/CLC.2004.s.003.

Adrain, C., E. M. Creagh, and S. J. Martin. 2001. “Apoptosis-Associated Release of Smac/DIABLO from Mitochondria Requires Active Caspases and Is Blocked by Bcl-2.” *EMBO Journal* 20(23): 6627–36.

Al-minawi, Ali Z, Nasrollah Saleh-gohari, and Thomas Helleday. 2008. “The ERCC1 / XPF Endonuclease Is Required for Efficient Single-Strand Annealing and Gene Conversion in Mammalian Cells.” 36(1): 1–9.

Albertella, Mark R, Catherine M Green, Alan R Lehmann, and Mark J O Connor. 2005. “A Role for Polymerase H in the Cellular Tolerance to Cisplatin-Induced Damage.” *Cancer Research* 65(21): 9799–9807.

Alcala, Nicolas et al. 2019. “Redefining Malignant Pleural Mesothelioma Types as a Continuum Uncovers Immune-Vascular Interactions.” *EBioMedicine* 48: 191–202.

Alexandrov, L. B. et al. 2013. “Signatures of Mutational Processes in Human Cancer.” *Nature* 500(7463): 415–21.

Alt, Aaron et al. 2007. “Bypass of DNA Lesions Generated.” *Science* 318(5852): 967–71.

Arnaudeau, Catherine, Cecilia Lundin, and Thomas Helleday. 2001. “DNA Double-Strand Breaks Associated with Replication Forks Are Predominantly Repaired by Homologous Recombination Involving an Exchange Mechanism in Mammalian Cells.” *Journal of Molecular Biology* 307(5): 1235–45.

Attanoos, Richard L et al. 2018. “Malignant Mesothelioma and Its Non-Asbestos Causes.” 142(6): 753–60.

Audebert, Marc, Bernard Salles, and Patrick Calsou. 2004. “Involvement of Poly(ADP-Ribose) Polymerase-1 and XRCC1/DNA Ligase III in an Alternative Route for DNA Double-Strand Breaks Rejoining.” *Journal of Biological Chemistry* 279(53): 55117–26.

Ault, J G et al. 1995. “Behavior of Crocidolite Asbestos during Mitosis in Living Vertebrate Lung Epithelial Cells.” *Cancer Research* 55(4): 792–98.

Awlik, T Imothy M P, and K Handan K Eyomarsi. 2004. “ROLE OF CELL CYCLE IN MEDIATING SENSITIVITY TO RADIOTHERAPY.” *Int J Radiat Oncol Biol Phys* 59(4): 928–42.

Ba, Xueqing et al. 2014. “The Role of 8-Oxoguanine DNA Glycosylase-1 in

Inflammation." *International Journal of Molecular Sciences* 15(9): 16975–97.
Baas, Paul. 2002. "Chemotherapy for Malignant Mesothelioma: From Doxorubicin to Vinorelbine." *Seminars in Oncology* 29(1): 62–69.
Baas, Paul et al. 2021. "First-Line Nivolumab plus Ipilimumab in Unresectable Malignant Pleural Mesothelioma (CheckMate 743): A Multicentre, Randomised, Open-Label, Phase 3 Trial." *The Lancet* 397(10272): 375–86.
Bachrati, Csana´ d Z., and Ian D Hickson. 2009. "Dissolution of Double Holliday Junctions by the Concerted Action of BLM and Topoisomerase IIIa." (2): 91–102.
Badhai, Jitendra et al. 2020. "Combined Deletion of Bap1, Nf2, and Cdkn2ab Causes Rapid Onset of Malignant Mesothelioma in Mice." *Journal of Experimental Medicine* 217(6).
Baraibar, Martin A., Romain Ladouce, and Bertrand Friguet. 2013. "Proteomic Quantification and Identification of Carbonylated Proteins upon Oxidative Stress and during Cellular Aging." *Journal of Proteomics* 92: 63–70. http://dx.doi.org/10.1016/j.jprot.2013.05.008.
Baris, Y. I. et al. 1978. "An Outbreak of Pleural Mesothelioma and Chronic Fibrosing Pleurisy in the Village of Karain/Urgup in Anatolia." *Thorax* 33(2): 181–92.
Barlow, Christy A., Jennifer Sahmel, Dennis J. Paustenbach, and John L. Henshaw. 2017. "History of Knowledge and Evolution of Occupational Health and Regulatory Aspects of Asbestos Exposure Science: 1900–1975." *Critical Reviews in Toxicology* 47(4): 286–316. http://dx.doi.org/10.1080/10408444.2016.1258391.
Bass, Thomas E. et al. 2016. "ETAA1 Acts at Stalled Replication Forks to Maintain Genome Integrity." *Nature Cell Biology* 18(11): 1185–95.
Basu, Alakananda, and Soumya Krishnamurthy. 2010. "Cellular Responses to Cisplatin-Induced DNA Damage." *Journal of Nucleic Acids* 2010.
Beauséjour, Christian M. et al. 2003. "Reversal of Human Cellular Senescence: Roles of the P53 and P16 Pathways." *EMBO Journal* 22(16): 4212–22.
Bee, Leonardo et al. 2013. "The Efficiency of Homologous Recombination and Non-Homologous End Joining Systems in Repairing Double- Strand Breaks during Cell Cycle Progression." *PLoS ONE* 8(7).
Benitez, Anaid et al. 2019. "FANCA Promotes DNA Double Strand Break Repair by Catalyzing Single-Strand Annealing and Strand Exchange." 71(4): 621–28.
Bergink, Steven, and Stefan Jentsch. 2009. "Principles of Ubiquitin and SUMO Modifications in DNA Repair." *Nature* 458(March): 461–67.
Berquist, Brian R., and David M. Wilson. 2012. "Pathways for Repairing and Tolerating the Spectrum of Oxidative DNA Lesions." *Cancer Letters* 327(1–2): 61–72. http://dx.doi.org/10.1016/j.canlet.2012.02.001.
Betti, M et al. 2020. "XRCC1 and ERCC1 Variants Modify Malignant Mesothelioma Risk : A Case – Control Study." *Mutation Research - Fundamental and Molecular Mechanisms of Mutagenesis* 708(1–2): 11–20. http://dx.doi.org/10.1016/j.mrfmmm.2011.01.001.

Betti, Marta et al. 2017. “Germline Mutations in DNA Repair Genes Predispose Asbestos-Exposed Patients to Malignant Pleural Mesothelioma.” *Cancer Letters* (July): 1–8. http://dx.doi.org/10.1016/j.canlet.2017.06.028.

Bezine, Elisabeth, Julien Vignard, and Gladys Mirey. 2014. “The Cytolethal Distending Toxin Effects on Mammalian Cells: A DNA Damage Perspective.” *Cells* 3(2): 592–615.

Bhakta, Nickhill et al. 2016. “Cumulative Burden of Cardiovascular Morbidity in Paediatric, Adolescent, and Young Adult Survivors of Hodgkin’s Lymphoma: An Analysis from the St Jude Lifetime Cohort Study.” *The Lancet Oncology* 17(9): 1325–34. http://dx.doi.org/10.1016/S1470-2045(16)30215-7.

Bhargava, Ragini, David O Onyango, and Jeremy M Stark. 2016. “Regulation of Single-Strand Annealing and Its Role in Genome Maintenance.” *Trends in Genetics* xx: 1–10. http://dx.doi.org/10.1016/j.tig.2016.06.007.

Bianco, Andrea et al. 2018. “Clinical Diagnosis of Malignant Pleural Mesothelioma.” *Journal of Thoracic Disease* 10(7): S253–61.

Bibby, Anna C. et al. 2016. “Malignant Pleural Mesothelioma: An Update on Investigation, Diagnosis and Treatment.” *European Respiratory Review* 25(142): 472–86. http://dx.doi.org/10.1183/16000617.0063-2016.

Blackford, Andrew N., and Stephen P. Jackson. 2017. “ATM, ATR, and DNA-PK: The Trinity at the Heart of the DNA Damage Response.” *Molecular Cell* 66(6): 801–17. http://dx.doi.org/10.1016/j.molcel.2017.05.015.

Blum, Yuna et al. 2019. “Dissecting Heterogeneity in Malignant Pleural Mesothelioma through Histo-Molecular Gradients for Clinical Applications.” *Nature Communications* 10(1): 1–12. http://dx.doi.org/10.1038/s41467-019-09307-6.

Bocchetta, Maurizio et al. 2008. “The SV40 Large T Antigen-P53 Complexes Bind and Activate the Insulin-like Growth Factor-I Promoter Stimulating Cell Growth.” *Cancer Research* 68(4): 1022–29.

Bock, Florian J., and Stephen W.G. Tait. 2020. “Mitochondria as Multifaceted Regulators of Cell Death.” *Nature Reviews Molecular Cell Biology* 21(2): 85–100. http://dx.doi.org/10.1038/s41580-019-0173-8.

Boehm, E M, M S Gildenberg, and M T Washington. 2016. 39 DNA Replication Across Taxa *The Many Roles of PCNA in Eukaryotic DNA Replication*. 1st ed. Elsevier Inc. http://dx.doi.org/10.1016/bs.enz.2016.03.003.

Bonelli, Mara A., Claudia Fumarola, Silvia La Monica, and Roberta Alfieri. 2017. “New Therapeutic Strategies for Malignant Pleural Mesothelioma.” *Biochemical Pharmacology* 123: 8–18. http://dx.doi.org/10.1016/j.bcp.2016.07.012.

Bonomi, Maria et al. 2017. “Clinical Staging of Malignant Pleural Mesothelioma: Current Perspectives.” *Lung Cancer: Targets and Therapy* 8: 127–39.

Brandsma, Inger, and Dik C. Gent. 2012. “Pathway Choice in DNA Double Strand Break Repair: Observations of a Balancing Act.” *Genome Integrity* 3: 1–10.

Branzei, Dana, and Barnabas Szakal. 2016. “DNA Damage Tolerance by Recombination : Molecular Pathways And.” *DNA Repair*.

http://dx.doi.org/10.1016/j.dnarep.2016.05.008.

Bridges, Kathleen A et al. 2016. “Defective Human Tumor Cells.” *Oncotarget* 7(44): 71660–72.

Brierley, James D, Mary K Gospodarowicz, and Wittekind Christian. 2016. “Pleural Mesothelioma.” In *TNM Classification of Malignant Tumours*, , 113–14.

Brims, Fraser. 2021. “Epidemiology and Clinical Aspects of Malignant Pleural Mesothelioma.” *Cancers* 13(16): 1–15.

Brims, Fraser J.H. et al. 2016. “A Novel Clinical Prediction Model for Prognosis in Malignant Pleural Mesothelioma Using Decision Tree Analysis.” *Journal of Thoracic Oncology* 11(4): 573–82. http://dx.doi.org/10.1016/j.jtho.2015.12.108.

Broeckx, Glenn, and Patrick Pauwels. 2018. “Malignant Peritoneal Mesothelioma: A Review.” *Translational Lung Cancer Research* 7(5): 537–42.

Brossel, Hélène et al. 2021. “Activation of Dna Damage Tolerance Pathways May Improve Immunotherapy of Mesothelioma.” *Cancers* 13(13): 1–13.

Brown, Eric J., and David Baltimore. 2003. “Essential and Dispensable Roles of ATR in Cell Cycle Arrest and Genome Maintenance.” *Genes and Development* 17(5): 615–28.

Brozovic, Anamaria, Andreja Ambriović-Ristov, and Maja Osmak. 2010. “The Relationship between Cisplatin-Induced Reactive Oxygen Species, Glutathione, and BCL-2 and Resistance to Cisplatin.” *Critical Reviews in Toxicology* 40(4): 347–59.

Budzowska, Magda et al. 2015. “ Regulation of the Rev1–Pol ζ Complex during Bypass of a DNA Interstrand Cross-link .” *The EMBO Journal* 34(14): 1971–85.

Bueno, Raphael et al. 2016. “Comprehensive Genomic Analysis of Malignant Pleural Mesothelioma Identifies Recurrent Mutations, Gene Fusions and Splicing Alterations.” *Nature Genetics* 48(4): 407–16. http://dx.doi.org/10.1038/ng.3520.

Bunch, R T, and A Eastman. 1996. “Enhancement of Cisplatin-Induced Cytotoxicity by 7-Hydroxystaurosporine (UCN-01), a New G2-Checkpoint Inhibitor.” *Clin Cancer Res* 2(5): 791–97.

Bunting, Samuel F. et al. 2010. “53BP1 Inhibits Homologous Recombination in Brca1-Deficient Cells by Blocking Resection of DNA Breaks.” *Cell* 141(2): 243–54.

Byrne, By M J et al. 2020. “C i Sp La Tin a n d Ge Mc i t a Bi n e Tr e a t m e n t f o r Ma l i g n a n t M e so Th e Li o m a : A Ph a s e I I S t u Dy.” : 25–30.

Cakiroglu, Ece, and Serif Senturk. 2020. “Genomics and Functional Genomics of Malignant Pleural Mesothelioma.” *International Journal of Molecular Sciences* 21(17): 6342.

Calabrò, Luana, Giulia Rossi, and Michele Maio. 2018. “New Horizons from Immunotherapy in Malignant Pleural Mesothelioma.” *Journal of Thoracic Disease* 10(Suppl 2): S322–32.

Calcinotto, Arianna et al. 2019. “Cellular Senescence: Aging, Cancer, and Injury.” *Physiological Reviews* 99(2): 1047–78.

Caldwell, Colleen C., and Maria Spies. 2020. “Dynamic Elements of Replication

Protein A at the Crossroads of DNA Replication, Recombination, and Repair." *Critical Reviews in Biochemistry and Molecular Biology* 55(5): 482–507. https://doi.org/10.1080/10409238.2020.1813070.

Campisi, Judith. 2013. "Aging, Cellular Senescence, and Cancer." *Annual Review of Physiology* 75: 685–705.

Cantini, Luca, Raffit Hassan, Daniel H. Sterman, and Joachim G.J.V. Aerts. 2020. "Emerging Treatments for Malignant Pleural Mesothelioma: Where Are We Heading?" *Frontiers in Oncology* 10(March).

Carbone, M et al. 1994. "Simian Virus 40-like DNA Sequences in Human Pleural Mesothelioma." *Oncogene* 9(6): 1781–90.

Carbone, Michele et al. 2012. "Malignant Mesothelioma: Facts, Myths, and Hypotheses." *Journal of Cellular Physiology* 227(1): 44–58.

Carbone, M et al. 2013. "BAP1 and Cancer." *Nature Reviews Cancer* 13(3): 153–59.

Carbone, M et al. 2020. "Biological Mechanisms and Clinical Significance of BAP1 Mutations in Human Cancer." *Cancer Discovery* 10(8): 1103–20.

Carbone, Michele, Adi Gazdar, and Janet S. Butel. 2020. "SV40 and Human Mesothelioma." *Translational Lung Cancer Research* 9(Suppl 1): S47–59.

Carbone, Michele, and Haining Yang. 2012. "Molecular Pathways: Targeting Mechanisms of Asbestos and Erionite Carcinogenesis in Mesothelioma." *Clinical Cancer Research* 18(3): 598–604.

Carusillo, Antonio, and Claudio Mussolino. 2020. "DNA Damage : From Threat to Treatment." *Cells* 9(7): 1–21.

Cavone, DL. et al. 2019. "Epidemiology of Mesothelioma." *Environments* 6(7): 76.

CaymanChemical. 2022. "UCN-01." https://www.caymanchem.com/product/18130/ucn-01 (November 29, 2022).

Ceccaldi, Raphael, Beatrice Rondinelli, and Alan D. D'Andrea. 2016. "Repair Pathway Choices and Consequences at the Double-Strand Break." *Trends in Cell Biology* 26(1): 52–64. http://dx.doi.org/10.1016/j.tcb.2015.07.009.

Ceresoli, G. L. et al. 2008. "Pemetrexed plus Carboplatin in Elderly Patients with Malignant Pleural Mesothelioma: Combined Analysis of Two Phase II Trials." *British Journal of Cancer* 99(1): 51–56.

Ceresoli, G. L., and E. Bombardieri. 2019. *Mesothelioma : From Research to Clinical Practice*.

Ceresoli, Giovanni Luca et al. 2006. "Phase II Study of Pemetrexed plus Carboplatin in Malignant Pleural Mesothelioma." *Journal of Clinical Oncology* 24(9): 1443–48.

Chambers, Cecilia R., Shona Ritchie, Brooke A. Pereira, and Paul Timpson. 2021. "Overcoming the Senescence-Associated Secretory Phenotype (SASP): A Complex Mechanism of Resistance in the Treatment of Cancer." *Molecular Oncology* 15(12): 3242–55.

Chamizo, Cristina et al. 2015. "Thymidylate Synthase Expression as a Predictive Biomarker of Pemetrexed Sensitivity in Advanced Non-Small Cell Lung Cancer." *BMC Pulmonary Medicine* 15(1): 1–7. http://dx.doi.org/10.1186/s12890-015-

0132-x.

Chang, B D et al. 1999. "A Senescence-like Phenotype Distinguishes Tumor Cells That Undergo Terminal Proliferation Arrest after Exposure to Anticancer Agents." *Cancer Res* 59(15): 3761–67.

Chang, Howard H.Y., Nicholas R. Pannunzio, Noritaka Adachi, and Michael R. Lieber. 2017. "Non-Homologous DNA End Joining and Alternative Pathways to Double-Strand Break Repair." *Nature Reviews Molecular Cell Biology* 18(8): 495–506. http://dx.doi.org/10.1038/nrm.2017.48.

Chavez, Diana A, Briana H Greer, and Brandt F Eichman. 2018. "The HIRAN Domain of Helicase-like Transcription Factor Positions the DNA Translocase Motor to Drive Efficient DNA Fork Regression." *Journal of Biological Chemistry* 293(22): 8484–94.

Chen, Shang Hung, and Jang Yang Chang. 2019. "New Insights into Mechanisms of Cisplatin Resistance: From Tumor Cell to Microenvironment." *International Journal of Molecular Sciences* 20(17).

Chen, Tianen et al. 2022. "DNA Damage Response Inhibition-based Combination Therapies in Cancer Treatment: Recent Advances and Future Directions." *Aging and Cancer* 3(1): 44–67.

Chernikova, Sophia B, John C Game, and J Martin Brown. 2012. "Inhibiting Homologous Recombination for Cancer Therapy." *Cancer biology and therapy* 13(2): 61–68.

Cheung, Mitchell, and Joseph R. Testa. 2017. "BAP1, a Tumor Suppressor Gene Driving Malignant Mesothelioma." *Translational Lung Cancer Research* 6(3): 270–78.

Chew, Shan Hwu, and Shinya Toyokuni. 2015. "Malignant Mesothelioma as an Oxidative Stress-Induced Cancer: An Update." *Free Radical Biology and Medicine* 86: 166–78. http://dx.doi.org/10.1016/j.freeradbiomed.2015.05.002.

Chi, Xiying, Yue Li, and Xiaoyan Qiu. 2020. "V(D)J Recombination, Somatic Hypermutation and Class Switch Recombination of Immunoglobulins: Mechanism and Regulation." *Immunology* 160(3): 233–47.

Chipuk, Jerry E et al. 2004. "Direct Activation of Bax by P53 Mediates Mitochondrial Membrane Permeabilization and Apoptosis Published by : American Association for the Advancement of Science Stable URL : Http://Www.Jstor.Org/Stable/3836137." *American Association for the Advancement of science* 303(5660): 1010–14.

Choi, Moonju, and Choongho Lee. 2015. "Immortalization of Primary Keratinocytes and Its Application to Skin Research." *Biomolecules and Therapeutics* 23(5): 391–99.

Chu, G. J., N. van Zandwijk, and J. E. J. Rasko. 2019. "The Immune Microenvironment in Mesothelioma: Mechanisms of Resistance To Immunotherapy." *Frontiers in Oncology* 7(2).

Cicala, C., F. Pompetti, and M. Carbone. 1993. "SV40 Induces Mesotheliomas in

Hamsters.” *American Journal of Pathology* 142(5): 1524–33.
Ciccia, Alberto et al. 2007. “Identification of FAAP24 , a Fanconi Anemia Core Complex Protein That Interacts with FANCM.” : 331–43.
Ciccia, Alberto, and Stephen J. Elledge. 2010. “The DNA Damage Response: Making It Safe to Play with Knives.” *Mol Cell* 61(9 SUPPL.): 179–204.
Cigognetti, Marta et al. 2015. “BAP1 (BRCA1-Associated Protein 1) Is a Highly Specific Marker for Differentiating Mesothelioma from Reactive Mesothelial Proliferations.” *Modern Pathology* 28(8): 1043–57. http://dx.doi.org/10.1038/modpathol.2015.65.
Clauson, Cheryl, Orlando D. Schärer, and Laura Niedernhofer. 2013. “Advances in Understanding the Complex Mechanisms of DNA Inter Strand Cross-Link Repair.” *Cold Spring Harbor Perspectives in Medicine* 3(10): 1–25.
Cleary, James M., Andrew J. Aguirre, Geoffrey I. Shapiro, and Alan D. D’Andrea. 2020. “Biomarker-Guided Development of DNA Repair Inhibitors.” *Molecular Cell* 78(6): 1070–85. https://doi.org/10.1016/j.molcel.2020.04.035.
Collado, Manuel, Maria A. Blasco, and Manuel Serrano. 2007. “Cellular Senescence in Cancer and Aging.” *Cell* 130(2): 223–33.
Cooper, Max D., and Matthew N. Alder. 2006. “The Evolution of Adaptive Immune Systems.” *Cell* 124(4): 815–22.
Crickard, J Brooks et al. 2020. “Rad54 Drives ATP Hydrolysis-Dependent DNA Sequence Alignment during Homologous Recombination.” *Cell* 181(6): 1380-1394.e18. http://dx.doi.org/10.1016/j.cell.2020.04.056.
Cupit-Link, Margaret C. et al. 2017. “Biology of Premature Ageing in Survivors of Cancer.” *ESMO Open* 2(5).
Cutrone, Rochelle et al. 2005. “Some Oral Poliovirus Vaccines Were Contaminated with Infectious SV40 after 1961.” *Cancer Research* 65(22): 10273–79.
D’Arcy, Mark S. 2019. “Cell Death: A Review of the Major Forms of Apoptosis, Necrosis and Autophagy.” *Cell Biology International* 43(6): 582–92. http://dx.doi.org/10.1002/cbin.11137.
Daley, James M., and Patrick Sung. 2014. “53BP1, BRCA1, and the Choice between Recombination and End Joining at DNA Double-Strand Breaks.” *Molecular and Cellular Biology* 34(8): 1380–88.
Dart, D. Alwyn, Kate E. Adams, Ildem Akerman, and Nicholas D. Lakin. 2004. “Recruitment of the Cell Cycle Checkpoint Kinase ATR to Chromatin during S-Phase.” *Journal of Biological Chemistry* 279(16): 16433–40.
Dasari, Shaloam, and Paul Bernard Tchounwou. 2014. “Cisplatin in Cancer Therapy: Molecular Mechanisms of Action.” *European Journal of Pharmacology* 740: 364–78. http://dx.doi.org/10.1016/j.ejphar.2014.07.025.
David, Sheila S., Valerie L. O’Shea, and Sucharita Kundu. 2007. “Base-Excision Repair of Oxidative DNA Damage.” *Nature* 447(7147): 941–50.
Davidson, Ben, Pinar Firat, and Claire W.. Michael. 2018. *Serous Effusions : Etiology, Diagnosis, Prognosis and Therapy*. 2nd ed.

Davis, Anthony J., and David J. Chen. 2013. "DNA Double Strand Break Repair via Non-Homologous End-Joining." *Translational Cancer Research* 2(3): 130–43.

Dedon, Peter C., and Steven R. Tannenbaum. 2004. "Reactive Nitrogen Species in the Chemical Biology of Inflammation." *Archives of Biochemistry and Biophysics* 423(1): 12–22.

Delacroix, Sinny et al. 2007. "The Rad9-Hus1-Rad1 (9-1-1) Clamp Activates Checkpoint Signaling via TopBP1." *Genes and Development* 21(12): 1472–77.

Delgermaa, Vanya et al. 2011. "Les Décés Mondiaux Par Mésothéliome Rapportés á l'Organisation Mondiale de La Santé Entre 1994 et 2008." *Bulletin of the World Health Organization* 89(10): 716–24.

Delourme, J. et al. 2013. "Prise En Charge Diagnostique et Thérapeutique Du Mésothéliome Pleural Malin." *Revue de Pneumologie Clinique* 69(1): 26–35. http://dx.doi.org/10.1016/j.pneumo.2012.12.003.

Demaria, Marco et al. 2017. "Cellular Senescence Promotes Adverse Effects of Chemotherapy and Cancer Relapse." *Cancer Discovery* 7(2): 165–76.

Demin, Annie A. et al. 2021. "XRCC1 Prevents Toxic PARP1 Trapping during DNA Base Excision Repair." *Molecular Cell* 81(14): 3018-3030.e5. https://doi.org/10.1016/j.molcel.2021.05.009.

DeVita, Vincent T., and Edward Chu. 2008. "A History of Cancer Chemotherapy." *Cancer Research* 68(21): 8643–53.

Dhont, L., C. Mascaux, and A. Belayew. 2016. "The Helicase-like Transcription Factor (HLTF) in Cancer : Loss of Function or Oncomorphic Conversion of a Tumor Suppressor ?" *Cellular and Molecular Life Sciences*: 129–45.

Dickens, Laura S. et al. 2012. "A Death Effector Domain Chain DISC Model Reveals a Crucial Role for Caspase-8 Chain Assembly in Mediating Apoptotic Cell Death." *Molecular Cell* 47(2): 291–305.

Donaldson, Ken, Fiona A. Murphy, Rodger Duffin, and Craig A. Poland. 2010. "Asbestos, Carbon Nanotubes and the Pleural Mesothelium: A Review of the Hypothesis Regarding the Role of Long Fibre Retention in the Parietal Pleura, Inflammation and Mesothelioma." *Particle and Fibre Toxicology* 7: 1–17.

Dopp, E. et al. 1995. "Mitotic Disturbances and Micronucleus Induction in Syrian Hamster Embryo Fibroblast Cells Caused by Asbestos Fibers." *Environmental Health Perspectives* 103(3): 268–71.

Dopp, Elke, and Dietmar Schiffmann. 1998. "Analysis of Chromosomal Alterations Induced by Asbestos and Ceramic Fibers." *Toxicology letters* 97: 155–62.

Dowell, J., and S. Patel. 2016. "Modern Management of Malignant Pleural Effusions." *Lung Cancer* 23(6): 265–72.

Duan, Mingrui, Jenna Ulibarri, Ke Jian Liu, and Peng Mao. 2020. "Role of Nucleotide Excision Repair in Cisplatin Resistance." *International Journal of Molecular Sciences* 21(23): 1–13.

Dudnik, Elizabeth et al. 2021. "BAP1-Altered Malignant Pleural Mesothelioma: Outcomes With Chemotherapy, Immune Check-Point Inhibitors and Poly(ADP-

Ribose) Polymerase Inhibitors." *Frontiers in Oncology* 11(March): 1–12.
Dudnik, Elizabeth, Daniel Reinhorn, and Liran Holtzman. 2021. "Novel and Promising Systemic Treatment Approaches in Mesothelioma." *Current Treatment Options in Oncology* 22(10).
Dunkern, Torsten R, Gerhard Fritz, and Bernd Kaina. 2001. "Cisplatin-Induced Apoptosis in 43-3B and 27-1 Cells Defective in Nucleotide Excision Repair." *Mutation research/DNA repair* 486(4): 249–58.
Eddins, Michael J et al. 2006. "Mms2 – Ubc13 Covalently Bound to Ubiquitin Reveals the Structural Basis of Linkage-Specific Polyubiquitin Chain Formation." *Nature Structural and Molecular Biology* 13(10): 915–20.
Edwards, J. G. et al. 1999. "Prognostic Factors for Malignant Mesothelioma in Leicester: Validation of EORTC and CALGB Scores." *Thorax* 54(SUPPL. 3): 731–35.
Eggert, Tobias et al. 2016. "Distinct Functions of Senescence-Associated Immune Responses in Liver Tumor Surveillance and Tumor Progression." *Cancer Cell* 30(4): 533–47.
Ejegi-Memeh, Stephanie et al. 2021. "Gender and the Experiences of Living with Mesothelioma: A Thematic Analysis." *European Journal of Oncology Nursing* 52: 101966. https://doi.org/10.1016/j.ejon.2021.101966.
Elmore, Susan. 2007. "Apoptosis: A Review of Programmed Cell Death." *Toxicologic Pathology* 35(4): 495–516.
Emi, Nobuhiko, Theodore Friedmann, and Jiing-kuan Yee. 1991. "Pseudotype Formation of Murine Leukemia Virus with the G Protein of Vesicular Stomatitis Virus." *Journal of virology* 65(3): 1202–7.
Erčulj, N. et al. 2012. "DNA Repair Polymorphisms and Treatment Outcomes of Patients with Malignant Mesothelioma Treated with Gemcitabine-Platinum Combination Chemotherapy." *Journal of Thoracic Oncology* 7(10): 1609–17.
Eren and Akar, A Ruchan. 2002. "Primary Pericardial Mesothelioma." *Curr Treat Options Oncol* 3(5): 369–73.
Esposti, M. Degli. 2002. "The Roles of Bid." *Apoptosis* 7(5): 433–40.
Essers, Jeroen et al. 2005. "Nuclear Dynamics of PCNA in DNA Replication and Repair." 25(21): 9350–59.
EUROGIP. 2006. *Les Maladies Professionnelles Liées à l'amiante En Europe - Reconnaissance, Chiffres et Dispositifs Spécifiques*.
Fan, Li, Tonghui Bi, Linxiao Wang, and Wei Xiao. 2020. "DNA-Damage Tolerance through PCNA Ubiquitination and Sumoylation." *Biochem J* 477(14): 2655–77.
Fang, Ferric C. 2004. "Antimicrobial Reactive Oxygen and Nitrogen Species: Concepts and Controversies." *Nature Reviews Microbiology* 2(10): 820–32.
Faridounnia, Maryam, Gert E. Folkers, and Rolf Boelens. 2018. "Function and Interactions of ERCC1-XPF in DNA Damage Response." *Molecules* 23(12): 1–25.
Fattman, Cheryl L., Lisa M. Schaefer, and Tim D. Oury. 2003. "Extracellular

Superoxide Dismutase in Biology and Medicine." *Free Radical Biology and Medicine* 35(3): 236–56.

Fedak, Elizabeth A, Frederick R Adler, and Lisa M Abegglen. 2022. "Response Pathways." 83(4).

Filippo, Joseph San, Patrick Sung, and Hannah Klein. 2008. "Mechanism of Eukaryotic Homologous Recombination." : 229–60.

Finley, David J., and Valerie W. Rusch. 2011. "Anatomy of the Pleura." *Thoracic Surgery Clinics* 21(2): 157–63. http://dx.doi.org/10.1016/j.thorsurg.2010.12.001.

Fischer, Martin, and Gerd A. Müller. 2017. "Cell Cycle Transcription Control: DREAM/MuvB and RB-E2F Complexes." *Critical Reviews in Biochemistry and Molecular Biology* 52(6): 638–62. https://doi.org/10.1080/10409238.2017.1360836.

Flores, Raja M. et al. 2006. "Induction Chemotherapy, Extrapleural Pneumonectomy, and Postoperative High-Dose Radiotherapy for Locally Advanced Malignant Pleural Mesothelioma: A Phase II Trial." *Journal of Thoracic Oncology* 1(4): 289–95. http://dx.doi.org/10.1016/S1556-0864(15)31583-5.

Förstermann, Ulrich, and William C. Sessa. 2012. "Nitric Oxide Synthases: Regulation and Function." *European Heart Journal* 33(7): 1–13.

Frank, Arthur L., and T. K. Joshi. 2014. "The Global Spread of Asbestos." *Annals of Global Health* 80(4): 257–62. http://dx.doi.org/10.1016/j.aogh.2014.09.016.

Fred, Robert et al. 2016. "Screening of Pleural Mesotheliomas for DNA-Damage Repair Players by Digital Gene Expression Analysis Can Enhance Clinical Management of Patients Receiving Platin-Based Chemotherapy." *Journal of cancer* 7(13): 1915–25.

Frit, Philippe et al. 2014. "Alternative End-Joining Pathway(s): Bricolage at DNA Breaks." *DNA Repair* 17: 81–97. http://dx.doi.org/10.1016/j.dnarep.2014.02.007.

Fuso Nerini, Ilaria et al. 2020. "Is DNA Repair a Potential Target for Effective Therapies against Malignant Mesothelioma?" *Cancer Treatment Reviews* 90(May): 102101. https://doi.org/10.1016/j.ctrv.2020.102101.

Gabrielli, Brian, Kelly Brooks, and Sandra Pavey. 2012. "Defective Cell Cycle Checkpoints as Targets for Anti-Cancer Therapies." *Frontiers in pharmacology* 3(February): 1–6.

Galateau Salle, F. et al. 2018. "New Insights on Diagnostic Reproducibility of Biphasic Mesotheliomas: A Multi-Institutional Evaluation by the International Mesothelioma Panel From the MESOPATH Reference Center." *Journal of Thoracic Oncology* 13(8): 1189–1203. https://doi.org/10.1016/j.jtho.2018.04.023.

Gali, Himabindu et al. 2012. "Role of SUMO Modification of Human PCNA at Stalled Replication Fork." *Nucleic Acids Research* 40(13): 6049–59.

Galluzzi, L. et al. 2012. "Molecular Mechanisms of Cisplatin Resistance." *Oncogene* 31(15): 1869–83. http://dx.doi.org/10.1038/onc.2011.384.

Garcia-diaz, Angel et al. 2017. "Interferon Receptor Signaling Pathways Regulating PD-L1 and PD-L2 Expression." 19(6): 1189–1201.

Gargi, Ghosal, and Junjie Chen. 2013. “DNA Damage Tolerance: A Double-Edged Sword Guarding the Genome.” *Transl Cancer Res* 2(3): 107–29.

GCO-WHO. 2020. “Global Cancer Observatory.” *Malaysia Cancer Statistics* 593: 1–2. https://gco.iarc.fr/ (November 2, 2022).

Ghosh, Sumit. 2019. “Cisplatin: The First Metal Based Anticancer Drug.” *Bioorganic Chemistry* 88(March): 102925. https://doi.org/10.1016/j.bioorg.2019.102925.

Gibbs, Graham W., and Geoffrey Berry. 2008. “Mesothelioma and Asbestos.” *Regulatory Toxicology and Pharmacology* 52(1 SUPPL.): S223–31. http://dx.doi.org/10.1016/j.yrtph.2007.10.003.

Giglia-mari, Giuseppina, Angelika Zotter, and Wim Vermeulen. 2011. “DNA Damage Response.” : 1–19.

Globocan. 2020. “Mesothelioma.”

Gogineni, Venkateswara Rao et al. 2011. “Chk2-Mediated G2 / M Cell Cycle Arrest Maintains Radiation Resistance in Malignant Meningioma Cells.” *Cancer Letters* 313(1): 64–75. http://dx.doi.org/10.1016/j.canlet.2011.08.022.

Goldar, Samira, Mahmoud Shekari Khaniani, Sima Mansoori Derakhshan, and Behzad Baradaran. 2015. “Molecular Mechanisms of Apoptosis and Roles in Cancer Development and Treatment.” *Asian Pacific Journal of Cancer Prevention* 16(6): 2129–44.

Goldstein, Michael, and Michael B Kastan. 2015. “The DNA Damage Response : Implications for Tumor Responses to Radiation and Chemotherapy.” *Annual review of medicine* 66(1): 129–43.

Goodarzi, AA, WD Block, and SP. Lees-Miller. 2003. “The Role of ATM and ATR in DNA Damage-Induced Cell Cycle Control.” *Prog Cell Cycle Res.* 5: 393-411.

Goodman, Julie E., Marc A. Nascarella, and Peter A. Valberg. 2009. “Ionizing Radiation: A Risk Factor for Mesothelioma.” *Cancer causes & control : CCC* 20(8): 1237–54.

Goodman, Myron F, and Roger Woodgate. 2013. “Translesion DNA Polymerases.” *Cold Spring Harb Perspect Biol.*: 1–20.

de Gooijer, Cornedine J., Frank J. Borm, Arnaud Scherpereel, and Paul Baas. 2020. “Immunotherapy in Malignant Pleural Mesothelioma.” *Frontiers in Oncology* 10(February).

Gorgoulis, Vassilis et al. 2019. “Cellular Senescence: Defining a Path Forward.” *Cell* 179(4): 813–27.

Gottesman, Michael M., Tito Fojo, and Susan E. Bates. 2002. “Multidrug Resistance in Cancer: Role of ATP-Dependent Transporters.” *Nature Reviews Cancer* 2(1): 48–58.

Governa, Mario et al. 1999. “Role of Iron in Asbestos-Body-Induced Oxidant Radical Generation.” *Journal of Toxicology and Environmental Health - Part A* 58(5): 279–87.

Greimelmaier, K. et al. 2020. “Mesothelial Proliferation of the Tunica Vaginalis Testis.” *Pathologe* 41(4): 406–10.

Griess, Brandon, Eric Tom, Frederick Domann, and Melissa Teoh-Fitzgerald. 2017. "Extracellular Superoxide Dismutase and Its Role in Cancer." *Free Radical Biology and Medicine* 112(402): 464–79.

Groot, Patricia M De et al. 2018. "Diagnostic Imaging for Thoracic Surgery." *Diagnostic Imaging for Thoracic Surgery*: 189–99.

Gu, Peng et al. 2022. "Targeting the Homologous Recombination Pathway in Cancer With a Novel Class of RAD51 Inhibitors." *Frontiers in Oncology* 12(May): 1–14.

Hall, M., and S. Benafif. 2015. "An Update on PARP Inhibitors for the Treatment of Cancer." *OncoTargets and Therapy*: 519–28.

Hamaidia, M, B Staumont, R L Duysinx, and L Willems. 2016. "Improvement of Malignant Pleural Mesothelioma Immunotherapy by Epigenetic Modulators." *Curr Top Med Chem* 16(7): 777–87.

He, Guangan, Jian Kuang, Abdul R. Khokhar, and Zahid H. Siddik. 2013. "The Impact of S- and G2-Checkpoint Response on the Fidelity of G1-Arrest by Cisplatin and Its Comparison to a Non-Crossresistant Platinum(IV) Analog." *Gynecol Oncol* 122(2): 402–9.

Hedglin, Mark, and Stephen J Benkovic. 2015. "Regulation of Rad6 / Rad18 Activity During DNA Damage Tolerance." : 207–30.

Herranz, Nicolás, and Jesús Gil. 2018. "Mechanisms and Functions of Cellular Senescence." *Journal of Clinical Investigation* 128(4): 1238–46.

Hicks, J Kevin et al. 2010. "Differential Roles for DNA Polymerases Eta , Zeta , and REV1 in Lesion Bypass of Intrastrand versus Interstrand DNA Cross-Links." *Molecular and Cellular Biology* 30(5): 1217–30.

Hmeljak, Julija, Francisco Sanchez-vega, Katherine A Hoadley, and Juliann Shih. 2018. "Integrative Molecular Characterization of Malignant Pleural Mesothelioma." *Cancer Discovery*.

Hoeijmakers, Jan H.J. 2001. "Genome Maintenance Mechanisms for Preventing Cancer." *Nature* 411(6835): 366–74.

Hogg, Neil, and B. Kalyanaraman. 1999. "Nitric Oxide and Lipid Peroxidation." *Biochimica et Biophysica Acta - Bioenergetics* 1411(2–3): 378–84.

Holzer, Alison K., Gerald H. Manorek, and Stephen B. Howell. 2006. "Contribution of the Major Copper Influx Transporter CTR1 to the Cellular Accumulation of Cisplatin, Carboplatin, and Oxaliplatin." *Molecular Pharmacology* 70(4): 1390–94.

Homma, Takujiro, and Junichi Fujii. 2020. "Emerging Connections between Oxidative Stress, Defective Proteolysis, and Metabolic Diseases." *Free Radical Research* 54(11–12): 931–46. https://doi.org/10.1080/10715762.2020.1734588.

Huang, Weijun et al. 2022. "Cellular Senescence: The Good, the Bad and the Unknown." *Nature Reviews Nephrology* 18(10): 611–27.

Hunt, L T, W C Barker, and H R Chen. 1987. "A Domain Structure Common to Hemopexin, Vitronectin, Interstitial Collagenase, and a Collagenase Homolog." *Protein Seq Data Anal* 1(1): 21–26.

Husain, Aliya N. et al. 2013. “Guidelines for Pathologic Diagnosis of Malignant Mesothelioma: 2012 Update of the Consensus Statement from the International Mesothelioma Interest Group.” *Archives of Pathology and Laboratory Medicine* 137(5): 647–67.

Hylebos, Marieke, Guy Van Camp, Jan P. Van Meerbeeck, and Ken Op De Beeck. 2016. “The Genetic Landscape of Malignant Pleural Mesothelioma: Results from Massively Parallel Sequencing.” *Journal of Thoracic Oncology* 11(10): 1615–26. http://dx.doi.org/10.1016/j.jtho.2016.05.020.

IARC. 2018. “Monograph of Asbestos.” https://monographs.iarc.who.int/wp-content/uploads/2018/06/mono100C-11.pdf.

Ichim, Gabriel, and Stephen W.G. Tait. 2016. “A Fate Worse than Death: Apoptosis as an Oncogenic Process.” *Nature Reviews Cancer* 16(8): 539–48. http://dx.doi.org/10.1038/nrc.2016.58.

Inagaki, Akiko et al. 2011. “Human RAD18 Interacts with Ubiquitylated Chromatin Components and Facilitates RAD9 Recruitment to DNA Double Strand Breaks.” *PLoS ONE* 6(8).

Indovina, Paola et al. 2014. “Abrogating G2/M Checkpoint through WEE1 Inhibition in Combination with Chemotherapy as a Promising Therapeutic Approach for Mesothelioma.” *Cancer biology and therapy* 15(4): 37–41.

Ingelfinger, Julie R, David Feller-Kopman, and Richard Light. 2018. “Pleural Disease (NEJM 2018).” *N Engl J Med* 378: 740–51.

Izzi, Valerio et al. 2012. “Immunity and Malignant Mesothelioma: From Mesothelial Cell Damage to Tumor Development and Immune Response-Based Therapies.” *Cancer Letters* 322(1): 18–34. http://dx.doi.org/10.1016/j.canlet.2012.02.034.

Jackson, Stephen P., and Jiri Bartek. 2009. “The DNA-Damage Response in Human Biology and Disease.” *Nature* 461(7267): 1071–78.

Janes, Sam M, Doraid Alrifai, and Dean A Fennell. 2021. “Perspectives on the Treatment of Malignant Pleural Mesothelioma.” *N Engl J Med* 385(13): 1207–18.

Jaurand, Marie-claude, and Jocelyne Fleury-feith. 2005. “Pathogenesis of Malignant Pleural Mesothelioma.” : 2–8.

Jeggo, P. A., and M. Löbrich. 2007. “DNA Double-Strand Breaks: Their Cellular and Clinical Impact?” *Oncogene* 26(56): 7717–19.

Jensen, Cynthia G. et al. 1996. “Long Crocidolite Asbestos Fibers Cause Polyploidy by Sterically Blocking Cytokinesis.” *Carcinogenesis* 17(9): 2013–21.

Jiang, Li et al. 2012. “Iron Overload Signature in Chrysotile-Induced Malignant Mesothelioma.” *Journal of Pathology* 228(3): 366–77.

Jiricny, Josef. 2013. “Postreplicative Mismatch Repair.” *Cold Spring Harbor Perspectives in Biology* 5(4): 1–23.

Johnson, Roger D, and Maria Jasin. 2000. “Sister Chromatid Gene Conversion Is a Prominent Double-Strand Break Repair Pathway in Mammalian Cells.” 19(13).

Jones, K. R. et al. 2005. “P53-Dependent Accelerated Senescence Induced By Ionizing Radiation in Breast Tumour Cells.” *International Journal of Radiation Biology*

81(6): 445–58.
Kaarniranta, Kai et al. 2020. “Mechanisms of Mitochondrial Dysfunction and Their Impact on Age-Related Macular Degeneration.” *Progress in Retinal and Eye Research* 79: 1–46.
Kalkavan, Halime, and Douglas R. Green. 2018. “MOMP, Cell Suicide as a BCL-2 Family Business.” *Cell Death and Differentiation* 25(1): 46–55. http://dx.doi.org/10.1038/cdd.2017.179.
Kalyanaraman, Balaraman. 2013. “Teaching the Basics of Redox Biology to Medical and Graduate Students: Oxidants, Antioxidants and Disease Mechanisms.” *Redox Biology* 1(1): 244–57. http://dx.doi.org/10.1016/j.redox.2013.01.014.
Kannouche, P. L., and A. R. Lehmann. 2004. “Ubiquitination of PCNA and the Polymerase Switch in Human Cells Nd Es Sci En No t D Ist R.” (August): 1011–13.
Kent, Tatiana et al. 2015. “Mechanism of Microhomology-Mediated End-Joining Promoted by Human DNA Polymerase θ.” *Nature Structural and Molecular Biology* 22(3): 230–37. http://dx.doi.org/10.1038/nsmb.2961.
Kiraz, Yağmur, Aysun Adan, Melis Kartal Yandim, and Yusuf Baran. 2016. “Major Apoptotic Mechanisms and Genes Involved in Apoptosis.” *Tumor Biology* 37(7): 8471–86.
Klotz, Laura V. et al. 2019. “Pleurectomy/Decortication and Hyperthermic Intrathoracic Chemoperfusion Using Cisplatin and Doxorubicin for Malignant Pleural Mesothelioma.” *Journal of Thoracic Disease* 11(5): 1963–72.
Knobel, Philip A, and Thomas M Marti. 2011. “Translesion DNA Synthesis in the Context of Cancer Research.” *Cancer Cell International* 11(1): 39.
Krejci, Lumir, Stephen Van Komen, Ying Li, and Jana Villemain. 2003. “DNA Helicase Srs2 Disrupts the Rad51 Presynaptic Filament.” *Nature* 51: 305–9.
Krokan, Hans E., and Magnar Bjørås. 2013. “Base Excision Repair.” *Cold Spring Harbor Perspectives in Biology* 5(4): 1–22.
Kumar, Amit et al. 2015. “Enhanced Expression of DNA Polymerase Eta Contributes to Cisplatin Resistance of Ovarian Cancer Stem Cells.” *Proc Natl Acad Sci U S A* 112(14): 4411–16.
Kumari, Ruchi, and Parmjit Jat. 2021. “Mechanisms of Cellular Senescence: Cell Cycle Arrest and Senescence Associated Secretory Phenotype.” *Frontiers in Cell and Developmental Biology* 9(March): 1–24.
Lamarche, Brandon J., Nicole I. Orazio, and Matthew D. Weitzman. 2010. “The MRN Complex in Double-Strand Break Repair and Telomere Maintenance.” *FEBS Letters* 584(17): 3682–95. http://dx.doi.org/10.1016/j.febslet.2010.07.029.
Lapenna, Silvia, and Antonio Giordano. 2009. “Cell Cycle Kinases as Therapeutic Targets for Cancer.” *Nature Reviews Drug Discovery* 8(7): 547–66.
Lee, Bo Yun et al. 2006. “Senescence-Associated β-Galactosidase Is Lysosomal β-Galactosidase.” *Aging Cell* 5(2): 187–95.
Lee, Tae Hee, and Tae Hong Kang. 2019. “DNA Oxidation and Excision Repair

Pathways.” *International Journal of Molecular Sciences* 20(23).

Lee, Young-sam, Mark T Gregory, and Wei Yang. 2014. “Human Pol ζ Purified with Accessory Subunits Is Active in Translesion DNA Synthesis and Complements Pol η in Cisplatin Bypass.” *Proceedings of the National Academy of Sciences of the United States of America* 111(8): 2954–59.

Lehmann, Alan R et al. 2007. “Translesion Synthesis : Y-Family Polymerases and the Polymerase Switch.” 6: 891–99.

Leijen, Suzanne, Jos H Beijnen, and Jan H M Schellens. 2010. “Abrogation of the G2 Checkpoint by Inhibition of Wee-1 Kinase Results in Sensitization of P53-Deficient Tumor Cells to DNA-Damaging Agents.” *Curr Clin Pharmacol* 5(3): 186–91.

Lerner, Leticia K et al. 2018. “Predominant Role of DNA Polymerase Eta and P53-Dependent Translesion Synthesis in the Survival of Ultraviolet-Irradiated Human Cells.” *Nucleic Acids Research* 45(3): 1270–80.

Leung, Wendy, Ryan M Baxley, George-lucian Moldovan, and Anja-katrin Bielinsky. 2019. “Mechanisms of DNA Damage Tolerance : Post-Translational Regulation of PCNA.” *Genes*.

Li, Bin, Ho Lam Chan, and Pingping Chen. 2019. “Immune Checkpoint Inhibitors: Basics and Challenges.” *Curr Med Chem* 26(17): 3009–25.

Li, G. M. 2015. “DNA Mismatch Repair and the DNA Damage Response.” *DNA Repair (Amst)*: 51–53.

Li, He et al. 2020. “PARP Inhibitor Resistance : The Underlying Mechanisms and Clinical Implications.” : 1–16.

Li, Jinbao et al. 2019. “Pathways and Assays for DNA Double-Strand Break Repair by Homologous Recombination.” : 1–11.

Li, Wei et al. 2010. “Merlin/NF2 Suppresses Tumorigenesis by Inhibiting the E3 Ubiquitin Ligase CRL4DCAF1 in the Nucleus.” *Cell* 140(4): 477–90. http://dx.doi.org/10.1016/j.cell.2010.01.029.

Li, Ying-hua et al. 2012. “Inhibition of Non-Homologous End Joining Repair Impairs Pancreatic Cancer Growth and Enhances Radiation Response.” *PLoS ONE* 7(6): 1–10.

Li, Yue, Long Zhao, and Xiao Feng Li. 2021. “Hypoxia and the Tumor Microenvironment.” *Technology in Cancer Research and Treatment* 20: 1–9.

Liptay, Martin, Joana S Barbosa, and Sven Rottenberg. 2020. “Replication Fork Remodeling and Therapy Escape in DNA Damage Response-Deficient Cancers.” 10(May): 1–22.

Liu, Dekang, Guido Keijzers, and Lene Juel Rasmussen. 2017. “DNA Mismatch Repair and Its Many Roles in Eukaryotic Cells.” *Mutation Research - Reviews in Mutation Research* 773: 174–87. http://dx.doi.org/10.1016/j.mrrev.2017.07.001.

Liu, Wenjun et al. 2020. “Fanconi Anemia Pathway as a Prospective Target for Cancer Intervention.” *Cell and Bioscience* 10(1): 1–14. https://doi.org/10.1186/s13578-020-00401-7.

Liu, Zewen et al. 2018. “Role of ROS and Nutritional Antioxidants in Human Diseases.” *Frontiers in Physiology* 9(MAY): 1–14.

López-Lago, Miguel A. et al. 2009. “ Loss of the Tumor Suppressor Gene NF2 , Encoding Merlin, Constitutively Activates Integrin-Dependent MTORC1 Signaling .” *Molecular and Cellular Biology* 29(15): 4235–49.

Lovejoy, Courtney A., and David Cortez. 2009. “Common Mechanisms of PIKK Regulation.” *DNA Repair* 8(9): 1004–8.

Lu´ıs, R., C. Brito, and M Pojo. 2020. *Tumor Microenvironment: The Main Driver of Metabolic Adaptation.*

Luna, Javier et al. 2021. “GOECP/SEOR Clinical Guidelines on Radiotherapy for Malignant Pleural Mesothelioma.” *World Journal of Clinical Oncology* 12(8): 581–608.

Ma, Zhikun, Guoliang Yao, B O Zhou, and Yonggang Fan. 2012. “The Chk1 Inhibitor AZD7762 Sensitises P53 Mutant Breast Cancer Cells to Radiation in Vitro and in Vivo.” *Molecular Medicine Reports* 6(4): 897–903.

Mack, Philip C et al. 2004. “Enhancement of Radiation Cytotoxicity by UCN-01 in Non-Small Cell Lung Carcinoma Cells Enhancement of Radiation Cytotoxicity by UCN-01 in Non-Small Cell Lung Carcinoma Cells.” *Radiation research* 162(6): 623–34.

Magnani, Francesca, and Andrea Mattevi. 2019. “Structure and Mechanisms of ROS Generation by NADPH Oxidases.” *Current Opinion in Structural Biology* 59: 91–97. https://doi.org/10.1016/j.sbi.2019.03.001.

Maloisel, Laurent, Francis Fabre, and Serge Gangloff. 2008. “DNA Polymerase Is Preferentially Recruited during Homologous Recombination To Promote Heteroduplex DNA Extension .” 28(4): 1373–82.

Manfredi, James J. et al. 2005. “Evidence against a Role for SV40 in Human Mesothelioma.” *Cancer Research* 65(7): 2602–9.

Mantovani, Alberto, Paola Allavena, Antonio Sica, and Frances Balkwill. 2008. “Cancer-Related Inflammation.” *Nature* 454(7203): 436–44.

Mao, Zhiyong et al. 2009. “DNA Repair by Homologous Recombination , But Not by Nonhomologous End Joining , Is Elevated in Breast Cancer Cells 1 , 2.” *Neoplasia* 11(7): 683–91.

Maréchal, Alexandre, and Lee Zou. 2013. “DNA Damage Sensing by the ATM and ATR Kinases.” *Cold Spring Harbor Perspectives in Biology* 5(9): 1–17.

Marescal, Océane, and Iain M. Cheeseman. 2020. “Cellular Mechanisms and Regulation of Quiescence.” *Developmental Cell* 55(3): 259–71.

Marteijn, Jurgen A., Hannes Lans, Wim Vermeulen, and Jan H.J. Hoeijmakers. 2014. “Understanding Nucleotide Excision Repair and Its Roles in Cancer and Ageing.” *Nature Reviews Molecular Cell Biology* 15(7): 465–81. http://dx.doi.org/10.1038/nrm3822.

Masclef, Louis et al. 2021. “Roles and Mechanisms of BAP1 Deubiquitinase in Tumor Suppression.” *Cell Death and Differentiation* 28(2): 606–25.

http://dx.doi.org/10.1038/s41418-020-00709-4.

Mazin, Alexander V, and Stephen C Kowalczykowski. 2016. “A Novel Property of the RecA Nucleoprotein Filament : Activation of Double-Stranded DNA for Strand Exchange in Trans.” : 2005–16.

Meas, Rithy, John J. Wyrick, and Michael J. Smerdon. 2019. “Nucleosomes Regulate Base Excision Repair in Chromatin.” *Mutation Research - Reviews in Mutation Research* 780(June): 29–36. http://dx.doi.org/10.1016/j.mrrev.2017.10.002.

Van Meerbeeck, Jan P., Arnaud Scherpereel, Veerle F. Surmont, and Paul Baas. 2011. “Malignant Pleural Mesothelioma: The Standard of Care and Challenges for Future Management.” *Critical Reviews in Oncology/Hematology* 78(2): 92–111. http://dx.doi.org/10.1016/j.critrevonc.2010.04.004.

Mehta, Anuja, and James E. Haber. 2014. “Sources of DNA Double-Strand Breaks and Models of Recombinational DNA Repair.” *Cold Spring Harb Perspect Biol.*

Mei, Chao et al. 2020. “The Role of Single Strand Break Repair Pathways in Cellular Responses to Camptothecin Induced DNA Damage.” *Biomedicine and Pharmacotherapy* 125(December 2019).

Menon, Vijay, and Lawrence F. Povirk. 2017. “XLF/Cernunnos: An Important but Puzzling Participant in the Nonhomologous End Joining DNA Repair Pathway.” *DNA Repair* 58: 29–37. http://dx.doi.org/10.1016/j.dnarep.2017.08.003.

Mercer, Rachel M., Maged Hassan, and Najib M. Rahman. 2018. “The Role of Pleurodesis in Respiratory Diseases.” *Expert Review of Respiratory Medicine* 12(4): 323–34. https://doi.org/10.1080/17476348.2018.1445971.

Metro, Giulio et al. 2021. “Immune Checkpoint Inhibitors for Unresectable Malignant Pleural Mesothelioma.” *Human Vaccines and Immunotherapeutics* 17(9): 2972–80. https://doi.org/10.1080/21645515.2021.1917933.

Mikuła-Pietrasik, Justyna et al. 2020. “Mechanisms and Significance of Therapy-Induced and Spontaneous Senescence of Cancer Cells.” *Cellular and Molecular Life Sciences* 77(2): 213–29. https://doi.org/10.1007/s00018-019-03261-8.

Milisav, Irina, Samo Ribarič, and Borut Poljsak. 2018. “Antioxidant Vitamins and Ageing.” *Subcellular Biochemistry* 90: 1–23.

Mimura, Kousaku et al. 2018. “PD-L1 Expression Is Mainly Regulated by Interferon Gamma Associated with JAK-STAT Pathway in Gastric Cancer.” *Cancer Science* 109(1): 43–53.

Minnema-Luiting, Jorien, Heleen Vroman, Joachim Aerts, and Robin Cornelissen. 2018. “Heterogeneity in Immune Cell Content in Malignant Pleural Mesothelioma.” *International Journal of Molecular Sciences* 19(4).

Miozzi, Edoardo et al. 2016. “Fluoro‐edenite and Carbon Nanotubes: The Health Impact of ‘Asbestos‐like’ Fibres (Review).” *Experimental and Therapeutic Medicine* 11(1): 21–27.

Mircea, Dediu, Alexandru Aurelia, and Florentina Bratu. 2014. *Pemetrexed in Non-Small-Cell Lung Cancer*.

Moldovan, George-lucian, Boris Pfander, and Stefan Jentsch. 2007. “Review PCNA ,

the Maestro of the Replication Fork." *Cell*: 665–79.

Molinar, Linda. "Types of Mesothelioma." https://www.mesothelioma.com/mesothelioma/types/ (November 27, 2022).

Mongiardi, Maria Patrizia et al. 2021. "Cancer Response to Therapy-Induced Senescence: A Matter of Dose and Timing." *Cancers* 13(3): 1–16.

Mordes, Daniel A., Gloria G. Glick, Runxiang Zhao, and David Cortez. 2008. "TopBP1 Activates ATR through ATRIP and a PIKK Regulatory Domain." *Genes and Development* 22(11): 1478–89.

Morgan, Richard L., Barry R. De Young, Violeta R. McGaughy, and Theodore H. Niemann. 1999. "MOC-31 Aids in the Differentiation between Adenocarcinoma and Reactive Mesothelial Cells." *Cancer* 87(6): 390–94.

Mossman, Brooke T. et al. 2013. "New Insights into Understanding the Mechanisms, Pathogenesis, and Management of Malignant Mesotheliomas." *American Journal of Pathology* 182(4): 1065–77.

Mott, Frank E. 2012. "Mesothelioma: A Review." *Ochsner Journal* 12(1): 70–79.

Mouw, Kent W., and Alan D. D'Andrea. 2018. "DNA Repair Deficiency and Immunotherapy Response." *Journal of Clinical Oncology* 36(17): 710–13.

Mouw, Kent W, Goldberg Michael S, Konstantinopoulos Panagiotis A, and D'Andrea Alan D. 2018. "DNA Damage and Repair Biomarkers of Immunotherapy Response." *Cancer Discovery* 176(5): 139–48. http://europepmc.org/backend/ptpmcrender.fcgi?accid=PMC5604322&blobtype=pdf.

Muers, Martin F. et al. 2008. "Active Symptom Control with or without Chemotherapy in the Treatment of Patients with Malignant Pleural Mesothelioma (MS01): A Multicentre Randomised Trial." *The Lancet* 371(9625): 1685–94.

Mukhopadhyay, Utpal K, Adrian M Senderowicz, and Gerardo Ferbeyre. 2005. "RNA Silencing of Checkpoint Regulators Sensitizes P53 -Defective Prostate Cancer Cells to Chemotherapy While Sparing Normal Cells." *Cancer Research* 65(7): 2872–82.

Muniandy, Parameswary A et al. 2010. "DNA Interstrand Crosslink Repair in Mammalian Cells : Step by Step." *Critical Reviews in Biochemistry and Molecular Biology* 45(September 2009): 23–49.

Murakami, Hideki et al. 2011. "LATS2 Is a Tumor Suppressor Gene of Malignant Mesothelioma." *Cancer Research* 71(3): 873–84.

Murali, Rajmohan, Thomas Wiesner, and Richard A. Scolyer. 2013. "Tumours Associated with BAP1 Mutations." *Pathology* 45(2): 116–26.

Mustofa, M. K. et al. 2021. "RAD18 Mediates DNA Double-Strand Break-Induced Ubiquitination of Chromatin Protein." *Journal of biochemistry* 170(1): 33–40.

Mutsaers, Steven E. 2004. "The Mesothelial Cell." *International Journal of Biochemistry and Cell Biology* 36(1): 9–16.

Mutti, L et al. 2018. "Scientific Advances and New Frontiers in Mesothelioma Therapeutics." *J Thorac Oncol* 13(9): 1269–83.

Naderi, Soheil, Irina C Hunton, and Jean Y J Wang. 2002. “Radiation Dose-Dependent Maintenance of G(2) Arrest Requires Retinoblastoma Protein.” *Cell cycle* 1(3): 193–200.

Napoli, Francesca et al. 2021. “Pathological Characterization of Tumor Immune Microenvironment (Time) in Malignant Pleural Mesothelioma.” *Cancers* 13(11).

Naugler, Willscott E., and Michael Karin. 2008. “NF-KB and Cancer - Identifying Targets and Mechanisms.” *Current Opinion in Genetics and Development* 18(1): 19–26.

Naveed Z. Alam & Raja M. Flores. 2020. “Malignant Mesothelioma: Clinical and Imaging Findings.” In *Occupational Cancers*, https://doi.org/10.1007/978-3-030-30766-0_16.

Neelsen, Kai J, and Massimo Lopes. 2015. “Replication Fork Reversal in Eukaryotes : From Dead End to Dynamic Response.” *Nature Reviews Molecular Cell Biology* 9(February).

Niazi, Sarfaraj, Madhusudan Purohit, and Javed H. Niazi. 2018. “Role of P53 Circuitry in Tumorigenesis: A Brief Review.” *European Journal of Medicinal Chemistry* 158: 7–24. https://doi.org/10.1016/j.ejmech.2018.08.099.

Nickoloff, Jac A et al. 2017. “Drugging the Cancers Addicted to DNA Repair.” *J Natl Cancer Inst* 109: 1–13.

Nijman, Sebastian M B. 2011. “Synthetic Lethality : General Principles , Utility and Detection Using Genetic Screens in Human Cells.” *FEBS Letters* 585(1): 1–6. http://dx.doi.org/10.1016/j.febslet.2010.11.024.

Nishida, Naoyo et al. 2006. “Angiogenesis in Cancer.” *Vascular Health and Risk Management* 2(3): 213–19.

Nogueira, Augusto, Mara Fernandes, Raquel Catarino, and Rui Medeiros. 2019. “RAD52 Functions in Homologous Recombination and Its Importance on Genomic Integrity Maintenance and Cancer Therapy.” *Cancers*.

Novello, S. et al. 2016. “The Third Italian Consensus Conference for Malignant Pleural Mesothelioma: State of the Art and Recommendations.” *Critical Reviews in Oncology/Hematology* 104: 9–20. http://dx.doi.org/10.1016/j.critrevonc.2016.05.004.

On, Kin Fan et al. 2011. “Determinants of Mitotic Catastrophe on Abrogation of the G 2 DNA Damage Checkpoint by UCN-01.” *Molecular cancer therapeutics* 10(May): 784–94.

Origanti, S, S-r Cai, A Z Munir, and L S White. 2012. “Synthetic Lethality of Chk1 Inhibition Combined with P53 and / or P21 Loss during a DNA Damage Response in Normal and Tumor Cells.” *Oncogene* (July 2011): 1–12. http://dx.doi.org/10.1038/onc.2012.84.

Ou, Hui Ling et al. 2021. 15 Molecular Oncology *Cellular Senescence in Cancer: From Mechanisms to Detection*.

Ozben, Tomris. 2007. “Oxidative Stress and Apoptosis: Impact on Cancer Therapy.” *Journal of Pharmaceutical Sciences* 96(9): 2181–96.

http://dx.doi.org/10.1002/jps.20874.

Pacella, Alessandro et al. 2021. "Surface and Bulk Modifications of Amphibole Asbestos in Mimicked Gamble's Solution at Acidic PH." *Scientific Reports* 11(1): 1–11. https://doi.org/10.1038/s41598-021-93758-9.

Palovcak, Anna, Wenjun Liu, Fenghua Yuan, and Yanbin Zhang. 2018. "Stitching up Broken DNA Ends by FANCA." *Molecular and Cellular Oncology* 5(6): 1–3. https://doi.org/10.1080/23723556.2018.1518101.

Pantelidou, Constantia et al. 2020. "PARP Inhibitor Efficacy Depends on CD8+ T Cell Recruitment via Intratumoral STING Pathway Activation in BRCA-Deficient Models of Triple-Negative Breast Cancer." 9(6): 722–37.

Papouli, Efterpi et al. 2005. "Crosstalk between SUMO and Ubiquitin on PCNA Is Mediated by Recruitment of the Helicase Srs2p." *Molecular Cell* 19: 123–33.

Park, Eun Kee et al. 2011. "Global Magnitude of Reported and Unreported Mesothelioma." *Environmental Health Perspectives* 119(4): 514–18.

Pauken, Kristen E., and E. John Wherry. 2015. "Overcoming T Cell Exhaustion in Infection and Cancer." *Trends in Immunology* 36(4): 265–76. http://dx.doi.org/10.1016/j.it.2015.02.008.

Pegg, Anthony E. 2000. "Repair of O6-Alkylguanine by Alkyltransferases." *Mutation Research - Reviews in Mutation Research* 462(2–3): 83–100.

de Perrot, Marc et al. 2020. "Prognostic Influence of Tumor Microenvironment after Hypofractionated Radiation and Surgery for Mesothelioma." *Journal of Thoracic and Cardiovascular Surgery* 159(5): 2082-2091.e1. http://dx.doi.org/10.1016/j.jtcvs.2019.10.122.

Perrot, Marc de, Licun Wu, Matthew Wu, and B. C.John Cho. 2017. "Radiotherapy for the Treatment of Malignant Pleural Mesothelioma." *The Lancet Oncology* 18(9): e532–42. http://dx.doi.org/10.1016/S1470-2045(17)30459-X.

Petitprez, Florent et al. 2020. "The Tumor Microenvironment in the Response to Immune Checkpoint Blockade Therapies." *Frontiers in Immunology* 11(May): 1–11.

Petrelli, Fausto et al. 2018. "A Systematic Review and Meta-Analysis of Second-Line Therapies for Treatment of Mesothelioma." *Respiratory Medicine* 141(June): 72–80.

Peyraud, Florent, and Antoine Italiano. 2020. "Combined Parp Inhibition and Immune Checkpoint Therapy in Solid Tumors." *Cancers* 12(6): 1–28.

Pfander, Boris et al. 2005. "SUMO-Modified PCNA Recruits Srs2 to Prevent Recombination during S Phase." *Nature* 436(July): 17–22.

Piskorz, Wiktoria Monika, and Marzanna Cechowska-Pasko. 2022. "Senescence of Tumor Cells in Anticancer Therapy—Beneficial and Detrimental Effects." *International Journal of Molecular Sciences* 23(19).

Pizzino, Gabriele et al. 2017. "Oxidative Stress: Harms and Benefits for Human Health." *Oxidative Medicine and Cellular Longevity* 2017.

Playle, L C, D J Hicks, D Qualtrough, and C Paraskeva. 2002. "Abrogation of the

Radiation-Induced G2 Checkpoint by the Staurosporine Derivative UCN-01 Is Associated with Radiosensitisation in a Subset of Colorectal Tumour Cell Lines." *British Journal of Cancer* 87(3): 352–58.

Poland, Craig A. et al. 2008. "Carbon Nanotubes Introduced into the Abdominal Cavity of Mice Show Asbestos-like Pathogenicity in a Pilot Study." *Nature Nanotechnology* 3(7): 423–28.

Popat, S. et al. 2022. "Malignant Pleural Mesothelioma: ESMO Clinical Practice Guidelines for Diagnosis, Treatment and Follow-Up☆." *Annals of Oncology* 33(2): 129–42. https://doi.org/10.1016/j.annonc.2021.11.005.

Postow, Michael A., Margaret K. Callahan, and Jedd D. Wolchok. 2015. "Immune Checkpoint Blockade in Cancer Therapy." *Journal of Clinical Oncology* 33(17): 1974–82.

Prasanna, P. G. et al. 2021. "Therapy-Induced Senescence: Opportunities to Improve Anti-Cancer Therapy." *Journal of the National Cancer Institute* 119(4): 361–416.

Prazakova, Silvie, Paul S. Thomas, Alessandra Sandrini, and Deborah H. Yates. 2014. "Asbestos and the Lung in the 21st Century: An Update." *Clinical Respiratory Journal* 8(1): 1–10.

Qi, Fang et al. 2013. "Continuous Exposure to Chrysotile Asbestos Can Cause Transformation of Human Mesothelial Cells via HMGB1 and TNF-α Signaling." *American Journal of Pathology* 183(5): 1654–66. http://dx.doi.org/10.1016/j.ajpath.2013.07.029.

Quick, Quincy A., and David A. Gewirtz. 2006. "An Accelerated Senescence Response to Radiation in Wild-Type P53 Glioblastoma Multiforme Cells." *Journal of Neurosurgery* 105(1): 111–18.

Quinet, Annabel, and Delphine Lemac. 2017. "Minireview Replication Fork Reversal : Players and Guardians." *Molecular Cell*: 2015–18.

Rachael, Daffolyn, Fels Elliott, and Kirk D Jones. 2020. "Diagnosis of Mesothelioma." *Surgical Pathology* 13(1): 73–89. https://doi.org/10.1016/j.path.2019.10.001.

Rajapakse, Aleksandra et al. 2020. "Redox Regulation in the Base Excision Repair Pathway: Old and New Players as Cancer Therapeutic Targets." *Curr Med Chem* 27(12): 1901–21.

Ramamonjisoa, Nirilanto, and Ellen Ackerstaff. 2017. "Characterization of the Tumor Microenvironment and Tumor-Stroma Interaction by Non-Invasive Preclinical Imaging." *Frontiers in Oncology* 7(JAN): 28–37.

Ramazzini, Collegium. 2010. "Asbestos Is Still with Us: Repeat Call for a Universal Ban." *Occupational Medicine* 60(8): 584–85.

Reynolds, Pamela et al. 2012. "The Dynamics of Ku70/80 and DNA-PKcs at DSBs Induced by Ionizing Radiation Is Dependent on the Complexity of Damage." *Nucleic Acids Research* 40(21): 10821–31.

Rice, David et al. 2011. "Recommendations for Uniform Definitions of Surgical Techniques for Malignant Pleural Mesothelioma: A Consensus Report of the International Association for the Study of Lung Cancer International Staging

Committee and the International Mesothelioma Interest." *Journal of Thoracic Oncology* 6(8): 1304–12. http://dx.doi.org/10.1097/JTO.0b013e3182208e3f.

Ripley, Brittany M, Melissa S Gildenberg, and M Todd Washington. 2020. "Control of DNA Damage Bypass by Ubiquitylation of PCNA."

Roberson, Rachel S. et al. 2005. "Escape from Therapy-Induced Accelerated Cellular Senescence in P53-Null Lung Cancer Cells and in Human Lung Cancers." *Cancer Research* 65(7): 2795–2803.

Robinson, B. W., A. W. Musk, and R. A. Lake. 2005. "Malignant Mesothelioma." *The Lancet* 366(9483): 379–408.

Robinson, Benjamin M. 2012. "Malignant Pleural Mesothelioma: An Epidemiological Perspective." *Annals of cardiothoracic surgery* 1(4): 491–96. http://www.ncbi.nlm.nih.gov/pubmed/23977542%0Ahttp://www.pubmedcentral.nih.gov/articlerender.fcgi?artid=PMC3741803.

Rocha, Reily et al. 2018. "DNA Repair Pathways and Cisplatin Resistance : An Intimate Relationship." *Clinics* (8): 1–10.

Rodgers, Kasey, and Mitch Mcvey. 2016. "Error-Prone Repair of DNA Double-Strand Breaks." *Journal of Cellular Physiology* 231(1): 15–24.

Røe, Dimitri Oluf et al. 2010. "Lung Cancer Malignant Pleural Mesothelioma : Genome-Wide Expression Patterns Reflecting General Resistance Mechanisms and a Proposal of Novel Targets." *Lung Cancer* 67(1): 57–68.

Røe, Oluf Dimitri, and Giulia Maria Stella. 2015. "Malignant Pleural Mesothelioma: History, Controversy and Future of a Manmade Epidemic." *European Respiratory Review* 24(135): 115–31. http://dx.doi.org/10.1183/09059180.00007014.

Rollins, Kristan D., and Celeste Lindley. 2005. "Pemetrexed: A Multitargeted Antifolate." *Clinical Therapeutics* 27(9): 1343–82.

Roos, Wynand P., and Bernd Kaina. 2013. "DNA Damage-Induced Cell Death: From Specific DNA Lesions to the DNA Damage Response and Apoptosis." *Cancer Letters* 332(2): 237–48. http://dx.doi.org/10.1016/j.canlet.2012.01.007.

Rossi, Matthew J, Sarah F Didomenico, Mikir Patel, and Alexander V Mazin. 2021. "RAD52 : Paradigm of Synthetic Lethality and New Developments." 12(November): 1–16.

Rothkamm, Kai et al. 2003. "Pathways of DNA Double-Strand Break Repair during the Mammalian Cell Cycle Pathways of DNA Double-Strand Break Repair during the Mammalian Cell Cycle." *Cellular Biology* 23(16): 5706–15.

Roushdy-Hammady, Iman et al. 2001. "Genetic-Susceptibility Factor and Malignant Mesothelioma in the Cappadocian Region of Turkey." *Lancet* 357(9254): 444–45.

Rowshanravan, Behzad, Neil Halliday, and David M Sansom. 2018. "Europe PMC Funders Group CTLA-4 : A Moving Target in Immunotherapy." *Blood* 131(1): 58–67.

Ryan, Daniel P, and Tom Owen-hughes. 2011. "Snf2-Family Proteins : Chromatin Remodellers for Any Occasion." *Current Opinion in Chemical Biology* 15(5): 649–56. http://dx.doi.org/10.1016/j.cbpa.2011.07.022.

Saha, Priyanka et al. 2020. “DNA Polymerase Eta : A Potential Pharmacological Target for Cancer Therapy.” *Journal of Cellular Physiology* 236(6): 4106–20.

Saha, Santu et al. 2022. “Determining the Potential of DNA Damage Response (DDR) Inhibitors in Cervical Cancer Therapy.” *Cancers* 14(17): 4288.

Salaroglio, Iris Chiara et al. 2022. “SKP2 Drives the Sensitivity to Neddylation Inhibitors and Cisplatin in Malignant Pleural Mesothelioma.” *Journal of Experimental & Clinical Cancer Research* 23(41): 75. https://doi.org/10.1186/s13046-022-02284-7.

Saleh, Tareq et al. 2020. “Therapy-Induced Senescence: An ‘Old’ Friend Becomes the Enemy.” *Cancers* 12(4): 1–38.

Sanoff, Hanna K. et al. 2014. “Effect of Cytotoxic Chemotherapy on Markers of Molecular Age in Patients with Breast Cancer.” *Journal of the National Cancer Institute* 106(4): 2–9.

Santivasi, Wil L., and Fen Xia. 2014. “Ionizing Radiation-Induced DNA Damage, Response, and Repair.” *Antioxidants and Redox Signaling* 21(2): 251–59.

Santoro, Armando et al. 2008. “Pemetrexed plus Cisplatin or Pemetrexed plus Carboplatin for Chemonaïve Patients with Malignant Pleural Mesothelioma: Results of the International Expanded Access Program.” *Journal of Thoracic Oncology* 3(7): 756–63. http://dx.doi.org/10.1097/JTO.0b013e31817c73d6.

Sarmah, Amrit, and Ram Kinkar Roy. 2013. “Understanding the Preferential Binding Interaction of Aqua-Cisplatins with Nucleobase Guanine over Adenine: A Density Functional Reactivity Theory Based Approach.” *RSC Advances* 3(8): 2822–30.

Sartori, Alessandro A et al. 2007. “Human CtIP Promotes DNA End Resection.” 450(November).

Sato, Hiro et al. 2017. “DNA Double-Strand Break Repair Pathway Regulates PD-L1 Expression in Cancer Cells.” *Nature Communications* 8(1). http://dx.doi.org/10.1038/s41467-017-01883-9.

Scherpereel, Arnaud et al. 2020. “ERS/ESTS/EACTS/ESTRO Guidelines for the Management of Malignant Pleural Mesothelioma.” *European Respiratory Journal* 55(6). http://dx.doi.org/10.1183/13993003.00953-2019.

Schinwald, Anja et al. 2012. “The Threshold Length for Fiber-Induced Acute Pleural Inflammation: Shedding Light on the Early Events in Asbestos-Induced Mesothelioma.” *Toxicological Sciences* 128(2): 461–70.

Schug, Z. T. et al. 2011. “BID Is Cleaved by Caspase-8 within a Native Complex on the Mitochondrial Membrane.” *Cell Death and Differentiation* 18(3): 538–48. http://dx.doi.org/10.1038/cdd.2010.135.

Sekido, Yoshitaka. 2013. “Molecular Pathogenesis of Malignant Mesothelioma.” *Carcinogenesis* 34(7): 1413–19.

Seluanov, Andrei, Zhiyong Mao, and Vera Gorbunova. 2010. “Analysis of DNA Double-Strand Break (DSB) Repair in Mammalian Cells.” *Journal of Visualized Experiments* (43): 3–9.

Seong, C. et al. 2009. “Regulation of Rad51 Recombinase Presynaptic Filament

Assembly via Interactions with the Rad52 Mediator and The." *Journal of Biological Chemistry* 284(36): 24363–71.

Sfeir, Agnel, and Lorraine S. Symington. 2015. "Microhomology-Mediated End Joining: A Back-up Survival Mechanism or Dedicated Pathway?" *Trends in Biochemical Sciences* 40(11): 701–14. http://dx.doi.org/10.1016/j.tibs.2015.08.006.

Shachar, Sigal et al. 2009. "Two-Polymerase Mechanisms Dictate Error-Free and Error-Prone Translesion DNA Synthesis in Mammals." *The EMBO journal* 28(4): 383–93.

Shaheen, Montaser, Christopher Allen, Jac A Nickoloff, and Robert Hromas. 2011. "Review Article Synthetic Lethality : Exploiting the Addiction of Cancer to DNA Repair." *BLOOD* 117(23): 6074–82. http://dx.doi.org/10.1182/blood-2011-01-313734.

Shamas-Din, Aisha, Hetal Brahmbhatt, Brian Leber, and David W. Andrews. 2011. "BH3-Only Proteins: Orchestrators of Apoptosis." *Biochimica et Biophysica Acta - Molecular Cell Research* 1813(4): 508–20. http://dx.doi.org/10.1016/j.bbamcr.2010.11.024.

Shi, Li, Ting-yan et al. 2013. "DNA Polymerase f as a Potential Biomarker of Chemoradiation Resistance and Poor Prognosis for Cervical Cancer." *Medical Oncology* 30(2).

Shmulevich, Riva, and Valery Krizhanovsky. 2021. 34 Antioxidants and Redox Signaling *Cell Senescence, DNA Damage, and Metabolism.*

Shukla, Arti et al. 2003. "Multiple Roles of Oxidants in the Pathogenesis of Asbestos-Induced Diseases." *Free Radical Biology and Medicine* 34(9): 1117–29.

Siddik, Zahid H. 2003. "Cisplatin: Mode of Cytotoxic Action and Molecular Basis of Resistance." *Oncogene* 22(47 REV. ISS. 6): 7265–79.

Sinn, Katharina, Berta Mosleh, and M. Alireza Hoda. 2021. "Malignant Pleural Mesothelioma: Recent Developments." *Current Opinion in Oncology* 33(1): 80–86.

Šmahel, Michal. 2017. "PD-1/PD-L1 Blockade Therapy for Tumors with Downregulated MHC Class I Expression." *International Journal of Molecular Sciences* 18(6): 1–14.

Smith, Hannah L., Harriet Southgate, Deborah A. Tweddle, and Nicola J. Curtin. 2020. "DNA Damage Checkpoint Kinases in Cancer." *Expert Reviews in Molecular Medicine* 22.

Smith, Joanne, Lye Mun Tho, Naihan Xu, and David A. Gillespie. 2010. 108 Advances in Cancer Research *The ATM-Chk2 and ATR-Chk1 Pathways in DNA Damage Signaling and Cancer*. 1st ed. Elsevier Inc. http://dx.doi.org/10.1016/B978-0-12-380888-2.00003-0.

Somers, Angela N. A. et al. 1991. "Effects of Amosite Asbestos Fibers on the Filaments Present in the Cytoskeleton of Primary Human Mesothelial Cells." In *Mechanisms in Fibre Carcinogenesis*, , 481–490.

Spivak, Graciela. 2015. “Nucleotide Excision Repair in Humans.” *DNA Repair* 36: 13–18. http://dx.doi.org/10.1016/j.dnarep.2015.09.003.

Stayner, Leslie, Laura S Welch, and Richard Lemen. 2013. “The Worldwide Pandemic of Asbestos-Related Diseases.” 34(1): 205–16.

Stojic, Lovorka, Richard Brun, and Josef Jiricny. 2004. “Mismatch Repair and DNA Damage Signalling.” *DNA Repair* 3(8–9): 1091–1101.

Strange, Chad D et al. 2021. “Imaging of Malignant Pleural Mesothelioma: Pearls and Pitfalls.” *Semin Ultrasound CT MR* 42(6): 542–51.

Stucci, Stefania et al. 2017. “Immune-Related Adverse Events during Anticancer Immunotherapy: Pathogenesis and Management.” *Oncology Letters* 14(5): 5671–80.

Su, Ting, Michael Z. Ludwig, Jiajie Xu, and Richard G. Fehon. 2017. “Kibra and Merlin Activate the Hippo Pathway Spatially Distinct from and Independent of Expanded.” *Developmental Cell* 40(5): 478-490.e3. http://dx.doi.org/10.1016/j.devcel.2017.02.004.

Sugiura, Hisatoshi, and Masakazu Ichinose. 2011. “Nitrative Stress in Inflammatory Lung Diseases.” *Nitric Oxide - Biology and Chemistry* 25(2): 138–44. http://dx.doi.org/10.1016/j.niox.2011.03.079.

Sullivan, Kelly D., Matthew D. Galbraith, Zdenek Andrysik, and Joaquin M. Espinosa. 2018. “Mechanisms of Transcriptional Regulation by P53.” *Cell Death and Differentiation* 25(1): 133–43. http://dx.doi.org/10.1038/cdd.2017.174.

Sun, Huan H., Allen Vaynblat, and Harvey I. Pass. 2017. “Diagnosis and Prognosis-Review of Biomarkers for Mesothelioma.” *Annals of Translational Medicine* 5(11): 1–8.

Sun, Jiahua et al. 2022. “Analysis of the Mechanism of RAD18 in Glioma.” *Neuroimmunomodulation*: 1–11.

Sung, Jung Suk, and Bruce Demple. 2006. “Roles of Base Excision Repair Subpathways in Correcting Oxidized Abasic Sites in DNA.” *FEBS Journal* 273(8): 1620–29.

Sung, Patrick, and Hannah Klein. 2006. “Mechanism of Homologous Recombination : Mediators and Helicases Take on Regulatory Functions.” 7: 739–50.

Sung, Patrick, Lumir Krejci, Stephen Van Komen, and Michael G Sehorn. 2004. “Recombination Mediators *.” *Journal of Biological Chemistry*.

Sutherland, Betsy M., Paula V. Bennett, Olga Sidorkina, and Jacques Laval. 2000. “Clustered DNA Damages Induced in Isolated DNA and in Human Cells by Low Doses of Ionizing Radiation.” *Proceedings of the National Academy of Sciences of the United States of America* 97(1): 103–8.

Suzui, Masumi et al. 2016. “Multiwalled Carbon Nanotubes Intratracheally Instilled into the Rat Lung Induce Development of Pleural Malignant Mesothelioma and Lung Tumors.” *Cancer Science* 107(7): 924–35.

Suzuki, Motofumi, Tohru Yamamori, and Tomoki Bo. 2017. “MK-8776 , a Novel Chk1 Inhibitor , Exhibits an Improved Radiosensitizing Effect Compared to UCN-01 by Exacerbating.” *Translational Oncology* 10(4): 491–500.

http://dx.doi.org/10.1016/j.tranon.2017.04.002.
Symington, Lorraine S., and Jean Gautier. 2011. "Double-Strand Break End Resection and Repair Pathway Choice." *Annual Review of Genetics* 45: 247–71.
Takahashi, Tetsuya et al. 2007. "Aprataxin, Causative Gene Product for EAOH/AOA1, Repairs DNA Single-Strand Breaks with Damaged 3′-Phosphate and 3′-Phosphoglycolate Ends." *Nucleic Acids Research* 35(11): 3797–3809.
Tatfi, Moussab, Olivier Hermine, and Felipe Suarez. 2019. "Epstein-Barr Virus (EBV)-Related Lymphoproliferative Disorders in Ataxia Telangiectasia: Does ATM Regulate EBV Life Cycle?" *Frontiers in Immunology* 10(JAN): 1–9.
TCIChemical. 2022. "Pemetrexed." https://www.tcichemicals.com/FR/fr/p/P2288 (November 29, 2022).
Thanan, Raynoo et al. 2014. "Oxidative Stress and Its Significant Roles in Neurodegenerative Diseases and Cancer." *International Journal of Molecular Sciences* 16(1): 193–217.
Van Thiel, Eric, Rabab Gaafar, and Jan P. Van Meerbeeck. 2011. "European Guidelines for the Management of Malignant Pleural Mesothelioma." *Journal of Advanced Research* 2(4): 281–88.
Tiwari, V., and David M. Wilson. 2019. "DNA Damage and Associated DNA Repair Defects in Disease and Premature Aging." *American Journal of Human Genetics* 105(2): 237–57. https://doi.org/10.1016/j.ajhg.2019.06.005.
Tomczyk, Przemysław, Ewelina Synowiec, Daniel Wysokiński, and Katarzyna Woźniak. 2016. "Eukaryotic TLS Polymerases." *Postepy Hig Med Dosw (Online)*: 522–33.
Toumpanakis, Dimitrios, and Stamatios E. Theocharis. 2011. "DNA Repair Systems in Malignant Mesothelioma." *Cancer Letters* 312(2): 143–49. http://dx.doi.org/10.1016/j.canlet.2011.08.021.
Toyokawa, Gouji et al. 2014. "Gemcitabine and Vinorelbine as Second-Line or beyond Treatment in Patients with Malignant Pleural Mesothelioma Pretreated with Platinum plus Pemetrexed Chemotherapy." *International Journal of Clinical Oncology* 19(4): 601–6.
Toyokuni, Shinya. 2002. "Iron and Carcinogenesis: From Fenton Reaction to Target Genes." *Redox Report* 7(4): 189–97.
Toyokuni, Shinya. 2014. "Iron Overload as a Major Targetable Pathogenesis of Asbestos-Induced Mesothelial Carcinogenesis." *Redox Report* 19(1): 1–7.
Tsao, Anne S., Ignacio Wistuba, Jack A. Roth, and Hedy Lee Kindler. 2009. "Malignant Pleural Mesothelioma." *Journal of Clinical Oncology* 27(12): 2081–90.
Ummat, Ajay et al. 2012. "Structural Basis for Cisplatin DNA Damage Tolerance by Human Polymerase η during Cancer Chemotherapy." *Nat Struct Mol Biol* 19(6): 628–32.
Urso, Loredana et al. 2019. "Metabolic Rewiring and Redox Alterations in Malignant Pleural Mesothelioma." *British Journal of Cancer* (August): 1–10. http://dx.doi.org/10.1038/s41416-019-0661-9.

Vainio, Harri et al. 2016. “Helsinki Criteria Update 2014: Asbestos Continues to Be a Challenge for Disease Prevention and Attribution.” *Epidemiologia e Prevenzione* 40(1): 15–19.

Vaisman, Alexandra, Roger Woodgate, Alexandra Vaisman, and Roger Woodgate. 2017. “Translesion DNA Polymerases in Eukaryotes : What Makes Them Tick ? Translesion DNA Polymerases in Eukaryotes : What Makes Them Tick ?” *Critical Reviews in Biochemistry and Molecular Biology* 52(3): 274–303. http://dx.doi.org/10.1080/10409238.2017.1291576.

Valko, M. et al. 2006. “Free Radicals, Metals and Antioxidants in Oxidative Stress-Induced Cancer.” *Chemico-Biological Interactions* 160(1): 1–40.

Vikas, Praveen, Nicholas Borcherding, Adithya Chennamadhavuni, and Rohan Garje. 2020. “Therapeutic Potential of Combining PARP Inhibitor and Immunotherapy in Solid Tumors.” *Frontiers in Oncology* 10(April): 1–10.

Vivo, C et al. 2003. “Cell Cycle Checkpoint Status in Human Malignant Mesothelioma Cell Lines : Response to Gamma Radiation.” *British Journal of Cancer* 88(3): 388–95.

Vogelzang, Nicholas J. et al. 2003. “Phase III Study of Pemetrexed in Combination with Cisplatin versus Cisplatin Alone in Patients with Malignant Pleural Mesothelioma.” *Journal of Clinical Oncology* 21(14): 2636–44.

Wadowski and De Rienzo, Bueno. 2020. “The Molecular Basis of Malignant Pleural Mesothelioma.” *Thorac Surg Clin* 30(4): 383–93.

Wagner, J.C., J.W. Skidmore, R.J. Hill, and D.M. Griffiths. 1990. “Erionite Exposure and Mesotheliomas in Rats.” *Br J Cancer* 51(5): 727–30.

Wang, Boshi, Jaskaren Kohli, and Marco Demaria. 2020. “Senescent Cells in Cancer Therapy: Friends or Foes?” *Trends in Cancer* 6(10): 838–57. https://doi.org/10.1016/j.trecan.2020.05.004.

Wang, Huibo et al. 2009. “For Synergistic Therapy.” *Neuro-Oncology* 11(6): 790–802.

Wang, Huichen et al. 2003. “Biochemical Evidence for Ku-Independent Backup Pathways of NHEJ.” *Nucleic Acids Research* 31(18): 5377–88.

Wang, Minli et al. 2006. “PARP-1 and Ku Compete for Repair of DNA Double Strand Breaks by Distinct NHEJ Pathways.” *Nucleic Acids Research* 34(21): 6170–82.

Wang, Ying, Robyn Branicky, Alycia Noë, and Siegfried Hekimi. 2018. “Superoxide Dismutases: Dual Roles in Controlling ROS Damage and Regulating ROS Signaling.” *Journal of Cell Biology* 217(6): 1915–28.

Weber, Anika Maria, and Anderson Joseph Ryan. 2015. “ATM and ATR as Therapeutic Targets in Cancer.” *Pharmacology and Therapeutics* 149: 124–38. http://dx.doi.org/10.1016/j.pharmthera.2014.12.001.

Wherry, E. John. 2011. “T Cell Exhaustion.” *Nature Immunology* 12(6): 492–99. http://dx.doi.org/10.1038/ni.2035.

Won, John K., and Samuel F. Bakhoum. 2020. “The Cytosolic DNA-Sensing CGAS–Sting Pathway in Cancer.” *Cancer Discovery* 10(1): 26–39.

Wright, William Douglass, Shanaya Shital Shah, and Wolf-dietrich Heyer. 2018.

"Homologous Recombination and the Repair of DNA Double-Strand Breaks." 293: 10524–35.

Wu, Bing et al. 2019. "High Expression of RAD18 in Glioma Induces Radiotherapy Resistance via Down-Regulating P53 Expression." *Biomedicine & Pharmacotherapy* 112(August 2018): 108555. https://doi.org/10.1016/j.biopha.2019.01.016.

Wu, Danli, and Patricia Yotnda. 2011. "Production and Detection of Reactive Oxygen Species (ROS) in Cancers." *Journal of Visualized Experiments* 2(57): 1–5.

Wu, Fang, Xinjian Lin, Tsuyoshi Okuda, and Stephen B Howell. 2004. "DNA Polymerase Regulates Cisplatin Cytotoxicity , Mutagenicity , and The Rate of Development of Cisplatin Resistance." *Cancer Research* 64(21): 8029–35.

Wu, Leonard et al. 2000. "The Bloom ' s Syndrome Gene Product Interacts with Topoisomerase III." 275(13): 9636–44.

Xu, Xuebo, Yueyang Lai, and Zi Chun Hua. 2019. "Apoptosis and Apoptotic Body: Disease Message and Therapeutic Target Potentials." *Bioscience Reports* 39(1): 1–17.

Xu, Yixi, and Dongyi Xu. 2020. "Repair Pathway Choice for Double-Strand Breaks." *Essays Biochem* 64(5): 765–77.

Yalcin, Nilay Gamze, Cliff K.C. Choong, and Norman Eizenberg. 2013. "Anatomy and Pathophysiology of the Pleura and Pleural Space." *Thoracic Surgery Clinics* 23(1): 1–10. http://dx.doi.org/10.1016/j.thorsurg.2012.10.008.

Yan, Xueqi, and Ming Chen. 2019. "RAD18 May Function as a Predictor of Response to Preoperative Concurrent Chemoradiotherapy in Patients with Locally Advanced Rectal Cancer through Caspase - 9 - Caspase - 3 - Dependent Apoptotic Pathway." *Cancer Medicine* (April): 3094–3104.

Yang, Haining, Joseph R. Testa, and Michele Carbone. 2008. "Mesothelioma Epidemiology, Carcinogenesis, and Pathogenesis." *Current Treatment Options in Oncology* 9(2–3): 147–57.

Yang, Junbao, Weilong Ding, Xiangyu Wang, and Yongsheng Xiang. 2021. "Knockdown of DNA Polymerase ζ Relieved the Chemoresistance of Glioma via Inhibiting the PI3K / AKT Signaling Pathway Inhibiting the PI3K / AKT Signaling Pathway." *Bioengineered* 12(1): 3924–33. https://doi.org/10.1080/21655979.2021.1944027.

Yang, Li et al. 2015. "REV3L , a Promising Target in Regulating the Chemosensitivity of Cervical Cancer Cells." *PLoS ONE* 10(3): 1–18.

Yang, Tsung Ying et al. 2013. "Effect of Folic Acid and Vitamin B 12 on Pemetrexed Antifolate Chemotherapy in Nutrient Lung Cancer Cells." *BioMed Research International* 2013.

Yang, Wei, and Yang Gao. 2018. "Translesion and Repair DNA Polymerases : Diverse Structure and Mechanism." *Annual review of biochemistry* 87(1): 239–61.

Yang, Yang et al. 2017. "DNA Repair Factor RAD18 and DNA Polymerase Pol κ Confer Tolerance of Oncogenic DNA Replication Stress." *The journal of cell*

biology 216(10): 3097–3115.

Yao, Yixin, and Wei Dai. 2014. "Genomic Instability and Cancer." *J Carcinog Mutagen* 23(1): 1–7.

Yap, Timothy A., Joachim G. Aerts, Sanjay Popat, and Dean A. Fennell. 2017. "Novel Insights into Mesothelioma Biology and Implications for Therapy." *Nature Reviews Cancer* 17(8): 475–88. http://dx.doi.org/10.1038/nrc.2017.42.

Yi, Chengqi, and Chuan He. 2013. "DNA Repair by Reversal of DNA Damage." *Cold Spring Harbor Perspectives in Biology* 5(1).

Youle, Richard J., and Andreas Strasser. 2008. "The BCL-2 Protein Family: Opposing Activities That Mediate Cell Death." *Nature Reviews Molecular Cell Biology* 9(1): 47–59.

Zalcman, Gérard et al. 2016. "Bevacizumab for Newly Diagnosed Pleural Mesothelioma in the Mesothelioma Avastin Cisplatin Pemetrexed Study (MAPS): A Randomised, Controlled, Open-Label, Phase 3 Trial." *The Lancet* 387(10026): 1405–14.

Zander, Linda, and Mats Bemark. 2004. "Immortalized Mouse Cell Lines That Lack a Functional Rev3 Gene Are Hypersensitive to UV Irradiation and Cisplatin Treatment." *DNA Repair* 3(7): 743–52.

Zanellato, Ilaria et al. 2011. "In Vitro Anti-Mesothelioma Activity of Cisplatin – Gemcitabine Combinations : Evidence for Sequence-Dependent e V Ects." *Cancer Chemotherapy and Pharmacology* 67(2): 265–73.

Zauderer, Marjorie G et al. 2014. "Vinorelbine and Gemcitabine as Second- or Third-Line Therapy for Malignant Pleural Mesothelioma." *Lung Cancer* 84(3): 271–274.

Zellweger, Ralph et al. 2015. "Rad51-Mediated Replication Fork Reversal Is a Global Response to Genotoxic Treatments in Human Cells." *The journal of cell biology* 208(5): 563–79.

Zhang, Junran. 2013. "The Role of BRCA1 in Homologous Recombination Repair in Response to Replication Stress : Significance in Tumorigenesis and Cancer Therapy." 1: 1–14.

Zhao, H et al. 2001. "Gamma-Radiation-Induced G2 Delay, Apoptosis, and P53 Response as Potential Susceptibility Markers for Lung Cancer." *Cancer Res* 61(21): 7819–24.

Zhao, Shengyuan, Serkalem Tadesse, and Dawit Kidane. 2021. "Significance of Base Excision Repair to Human Health." *Int Rev Cell Mol Biol* 364: 163–93.

Zolondick, Alicia A. et al. 2021. "Asbestos-Induced Chronic Inflammation in Malignant Pleural Mesothelioma and Related Therapeutic Approaches—a Narrative Review." *Precision Cancer Medicine* (4): 1–15.

Zou, Shitao et al. 2018. "RAD18 Promotes the Migration and Invasion of Esophageal Squamous Cell Cancer via the JNK-MMPs Pathway." *Cancer Letters* 417: 65–74.

8

Appendices

1. Details regarding viral vectors

Table 5. Description of the viral vectors used for transduction of ZL34 cells.

Viral vectors	Plasmid name	Company	#catalog	Target sequence	Resistance gene
VV-19.0293 sh698 hRAD18 3469	sh698 hRAD18 3469	Merck/Sigma	TRCN0000003469	GAACCAAGAAACAAGCGTAAT	Puromycin
VV-19.0294 sh699 hRAD18 3468	sh699 hRAD18 3468	Merck/Sigma	TRCN0000003468	TGCTTCGAGTATTTCAACATT	Puromycin
VV-19.0295 sh712 anti-Luc (puroR)	sh712 anti-Luc	Merck/Sigma	SHC007	CGCTGAGTACTTCGAAATGTC	Puromycin

VV-19.0296 sh113 pLKO.1-puro-CMV-TagRFP	sh113 pLKO.1-puro-CMV-TagRFP	Merck/Sigma	SHC012	TACAACAGCCACAACGTCTAT	Puromycin
VV-19.0297 pLV shRNA hHLTF #1 (Neo)	GVV_656 pLV shRNA hHLTF #1 (Neo)	VectorBuilder	VB170410-1092zgh	GCTGTGTCTGAGGTATAAATA	Neomycin
VV-19.0298 pLV shRNA hHLTF #4 (Neo)	GVV_658 pLV shRNA hHLTF #4 (Neo)	VectorBuilder	VB170410-1096mww	GCAGGTGGAGTTGGTTTGAAT	Neomycin
VV-19.0299 pLV shRNA NT (Neo)	GVV_659 pLV shRNA NT (Neo)	VectorBuilder	VB170410-1097dbn	CCTAAGGTTAAGTCGCCCTCG	Neomycin
VV-20.0040 pLV U6 shRNA NT PGK GFP-T2A-Neo	GVV_591 pLV U6 shRNA NT PGK GFP-T2A-Neo	VectorBuilder	VB170111-1074rzg	cctaaggttaagtcgccctcg	Neomycin

2. Genes studied in bioinformatics analysis

Table 6. List of the genes and their related proteins analyzed for bioinformatics analysis. A brief description of their functions is mentioned (GeneCard). The mutational and transcriptional profile of these genes were studied.

Genes	Proteins	Functions
APEX1	APE1	"Apurinic/apyrimidinic endodeoxyribonuclease in the DNA BER pathway"
ATM	ATM	"Serine/threonine protein kinase which activates checkpoint signaling upon DSBs"
ATR	ATR	"Serine/threonine protein kinase which activates checkpoint signaling upon ionizing radiation, ultraviolet light, or DNA replication stalling"
ATRIP	ATRIP	"Complex with ATR to bind ssDNA"
BAP1	BAP1	"Deubiquitinating enzyme that acts as a regulator of cell growth; mediates deubiquitination of histone H2A"
BLM	BLM	"ATP-dependent DNA helicase that unwinds single- and double-stranded DNA in a 3'-5' direction; participates in DNA replication and repair"
BRCA1	BRCA1	"E3 ubiquitin-protein ligase that contributes to HR repair and acts as a transcriptional activator"
BRCA2	BRCA2	"Binds RAD51 and potentiates recombinational DNA repair by promoting assembly of RAD51 onto ssDNA"
CHEK1	CHK1	"Serine/threonine-protein kinase which is required for checkpoint-mediated cell cycle arrest and activation of DNA repair"
CHEK2	CHK2	"Serine/threonine-protein kinase which is required for checkpoint-mediated cell cycle arrest, activation of DNA repair and apoptosis in response to the presence of DNA DSBs"
DCLRE1C	Artemis	"Nuclease involved in DNA NHEJ; required for DSB repair and V(D)J recombination"
DNA2	DNA2	"ATPase and endonuclease activities involved in in Okazaki fragments processing and DSB repair"
ERCC1	ERCC1	"Endonuclease making 5'-incision during the NER and the repair of interstrand cross-links; required for homology-directed repair of DNA DSBs"
ERCC4	XPF	"Catalytic component of ERCC1 during NER and interstrand cross-link repair"
ERCC5	XPG	"Single-stranded structure-specific DNA endonuclease involved in DNA NER"

ETAA1	ETAA1	"Replication stress response protein that accumulates at DNA damage sites and promotes replication fork progression and integrity"
EXO1	EXO1	"Functions in DNA MMR to excise mismatch-containing DNA tracts directed by strand breaks located either 5' or 3' to the mismatch"
FEN1	FEN1	"Structure-specific nuclease with 5'-flap endonuclease and 5'-3' exonuclease activities involved in DNA replication and repair"
HLTF	HLTF	"Possesses both helicase and E3 ubiquitin ligase activities for 'Lys-63'-linked polyubiquitination of chromatin-bound PCNA for error-free postreplication repair"
HUS1	HUS1	"Component of the 9-1-1 cell-cycle checkpoint response complex that acts as a sliding clamp platform on DNA in long-patch BER"
HUS1B	HUS1B	"Paralog of HUS1"
LIG1	DNA ligase 1	"ATP-dependent DNA ligase acting in DNA replication, recombination, and the BER process"
LIG3	DNA ligase 3	"Functions as heterodimer with DNA repair protein XRCC1; involved in NER, BER and Alt-EJ pathway"
LIG4	DNA ligase 4	"Catalyzes the NHEJ ligation step of the broken DNA during DSB repair by resealing the DNA breaks after the gap-filling is completed"
MDC1	MDC1	"Required for checkpoint mediated cell cycle arrest in response to DNA damage within both the S phase and G2/M phases of the cell cycle; scaffold for the recruitment of DNA repair and signal transduction proteins to discrete foci of DNA damage marked by 'Ser-139' phosphorylation of histone H2AX"
MGMT	MGMT	"Involved in the cellular defense against the biological effects of O6-methylguanine in DNA; repairs the methylated nucleobase in DNA by transferring the methyl group to a cysteine residue in the enzyme"
MLH1	MutL	"Heterodimerizes with PMS2 to form MutLα, a component of the post-replicative DNA MMR system; its nuclease activity introduces SSBs near the mismatch"
MRE11	MRE11	"Component of the MRN complex, which plays a central role in DSB repair, DNA recombination"
MSH2	MSH2	"Component of the post-replicative DNA MMR system; binds to DNA mismatches thereby initiating DNA repair"
MSH6	MSH6	"Component of the post-replicative DNA MMR system; heterodimerizes with MSH2 to form MutSα,

		which binds to DNA mismatches thereby initiating DNA repair"
MUS81	MUS81	"Endonuclease with substrate preference for branched DNA structures with a 5'-end at the branch nick; processes stalled or collapsed replication forks"
NBN	NBS1	"Component of the MRN complex which plays a critical role in the cellular response to DNA damage and the maintenance of chromosome integrity"
NHEJ1	XLF	"DNA repair protein involved in DNA NHEJ; promotes the ligation of various mismatched and non-cohesive ends"
OGG1	8-oxoguanine DNA glycosylase	"DNA repair enzyme that incises DNA at 8-oxoG residues"
PARP1	PARP-1	"Mediates ADP-ribosylation of proteins; promotes Alt-EJ repair by mediating poly-ADP-ribosylation"
PAXIP1	PTIP	"Participates in NHEJ repair and in preventing HR; is activated through ATM-dependent 53BP1 phosphorylation"
PCNA	PCNA	"Homotrimer increasing the processivity of leading strand synthesis during DNA replication; is ubiquitinated in response to DNA damage"
POLA	DNA Polymerase α	"Catalytic subunit of the DNA polymerase α complex; plays an essential role in the initiation of DNA synthesis"
POLB	DNA Polymerase β	"Repair polymerase that plays a key role in BER"
POLD1	DNA Polymerase δ 1, catalytic subunit	"Plays a crucial role in high fidelity genome replication, including in lagging strand synthesis, and repair. Exhibits both DNA polymerase and 3'- to 5'-exonuclease activities"
POLE	DNA Polymerase ε, catalytic subunit	"Required during synthesis of the leading DNA strands at the replication fork, binds at/or near replication origins and moves along DNA with the replication fork; has 3'-5' proofreading exonuclease activity that corrects errors arising during DNA replication ; involved in DNA synthesis during DNA repair; along with DNA polymerase POLD1 and DNA polymerase POLK, has a role in NER repair synthesis following ultraviolet irradiation"
POLH	DNA Polymerase η	"DNA polymerase specifically involved in TLS"
POLI	DNA Polymerase ι	"DNA polymerase specifically involved in TLS"
POLK	DNA Polymerase κ	"DNA polymerase specifically involved in TLS"

POLL	DNA Polymerase λ	"DNA polymerase involved in BER responsible for repair of lesions that give rise to abasic sites in DNA; also contributes to DNA DSB repair by NHEJ and HR"
POLM	DNA Polymerase μ	"Gap-filling polymerase involved in repair of DNA DSBs by NHEJ"
POLN	DNA Polymerase ν	"The least accurate of the DNA polymerase A family; error-prone DNA polymerase that preferentially misincorporates dT regardless of template sequence"
POLQ	DNA Polymerase θ	"DNA polymerase that promotes microhomology-mediated end-joining"
PRKDC	DNA-PKcs	"Serine/threonine-protein kinase that acts as a molecular sensor for DNA damage ; involved in DNA NHEJ repair"
RAD1	RAD1	"Component of the 9-1-1 cell-cycle checkpoint response complex that plays a major role in DNA repair"
RAD17	RAD17	"Essential for sustained cell growth, maintenance of chromosomal stability, and ATR-dependent checkpoint activation upon DNA damage; participates in the recruitment of the 9-1-1 complex and in CHEK1 activation"
RAD18	RAD18	"E3 ubiquitin-protein ligase involved in DDT pathways; associates to the E2 ubiquitin conjugating enzyme RAD6 to form the RAD6-RAD18 ubiquitin ligase complex involved in mono-ubiquitination of DNA-associated PCNA on 'Lys-164'"
RAD50	RAD50	"Component of the MRN complex; required to bind DNA ends and hold them in close proximity which could facilitate searches for short or long regions of sequence homology in the recombining DNA templates, and may also stimulate the activity of DNA ligases and/or restrict the nuclease activity of MRE11 to prevent nucleolytic degradation past a given point"
RAD51	RAD51	"Plays an important role in homologous strand exchange, a key step in DNA repair through HR"
RAD51B	RAD51B	"Paralog of RAD51; promotes the assembly of presynaptic RAD51 nucleoprotein filaments"
RAD51C	RAD51C	"Paralog of RAD51; acts at different stages of the BRCA1-BRCA2-dependent HR pathway"
RAD51D	RAD51D	"Paralog of Rad51; acts at different stages of the BRCA1-BRCA2-dependent HR pathway"
RAD52	RAD52	"Involved in DSBs repair; plays a central role in genetic recombination and DNA repair by promoting the annealing of complementary ssDNA and by stimulation of the RAD51 recombinase"

RAD54L	RAD54	"Involved in HR; acts as a molecular motor during the homology search and guides RAD51 ssDNA along a donor dsDNA thereby changing the homology search from the diffusion-based mechanism to a motor-guided mechanism; plays an essential role in RAD51-mediated synaptic complex formation which consists of three strands encased in a protein filament formed once homology is recognized. Once DNA strand exchange occurred, dissociates RAD51 from nucleoprotein filaments formed on dsDNA"
RAD9A	RAD9A	"3' to 5' exonuclease activity ; component of the 9-1-1 cell-cycle checkpoint response complex which acts then as a sliding clamp platform on DNA for several proteins involved in long-patch BER"
RAD9B	RAD9B	"3' to 5' exonuclease activity ; component of the 9-1-1 cell-cycle checkpoint response complex which acts then as a sliding clamp platform on DNA for several proteins involved in long-patch BER"
RBBP8	CtIP	"Endonuclease that cooperates with the MRN complex in DNA-end resection, the first step of DSB repair through the HR pathway; key determinant of DSB repair pathway choice, as it commits cells to HR by preventing c-NHEJ"
RECQL	RECQ1	"DNA helicase playing a role in DNA repair ; exhibits a magnesium-dependent ATP-dependent DNA-helicase activity that unwinds single- and double-stranded DNA in a 3'-5' direction"
REV1	Rev1 DNA Directed Polymerase	"Deoxycytidyl transferase involved in DNA repair. Transfers a dCMP residue from dCTP to the 3'-end of a DNA primer in a template-dependent reaction. May assist in the first step in the bypass of abasic lesions by the insertion of a nucleotide opposite the lesion"
REV3L	REV3 Like, DNA Directed Polymerase ζ catalytic subunit	"Catalytic subunit of the DNA polymerase zeta complex, an error-prone polymerase specialized in TLS; lacks an intrinsic 3'-5' exonuclease activity and thus has no proofreading function"
RIF1	RIF1	"Key regulator of TP53BP1 that plays a key role in the repair of DSBs; promotes NHEJ-mediated repair; interacts with ATM-phosphorylated TP53BP1"
RPA1	RPA 1	"Part of the heterotrimeric replication protein A complex that binds and stabilizes ssDNA intermediates that form during DNA replication or upon DNA stress thus preventing their reannealing and in parallel, recruits and activates different proteins and complexes

		involved in DNA replication and the cellular response to DNA damage"
RPA2	RPA2	"Part of the heterotrimeric replication protein A complex that binds and stabilizes ssDNA intermediates that form during DNA replication or upon DNA stress thus preventing their reannealing and in parallel, recruits and activates different proteins and complexes involved in DNA replication and the cellular response to DNA damage"
RPA3	RPA3	"Part of the heterotrimeric replication protein A complex that binds and stabilizes ssDNA intermediates that form during DNA replication or upon DNA stress thus preventing their reannealing and in parallel, recruits and activates different proteins and complexes involved in DNA replication and the cellular response to DNA damage"
SHPRH	SHPRH	"E3 ubiquitin-protein ligase involved in DNA repair; upon genotoxic stress, accepts ubiquitin from the MMS2-UBC13 E2 complex and transfers it to 'Lys-164' of PCNA which had been mono-ubiquitinated by RAD6-RAD18, promoting the formation of non-canonical poly-ubiquitin chains linked through 'Lys-63'"
SMARCAL1	SMARCAL1	"ATP-dependent annealing helicase that binds selectively to fork DNA relative to ssDNA or dsDNA and catalyzes the rewinding of the stably unwound DNA"
TOP3A	TOP3α	"Releases the supercoiling and torsional tension of DNA introduced during the DNA replication and transcription by transiently cleaving and rejoining one strand of the DNA duplex"
TOPBP1	TOPBP1	"Induces a large increase in the kinase activity of ATR; plays a role in the rescue of stalled replication forks and checkpoint control"
TP53	p53	"Involved in cell cycle regulation as a trans-activator that acts to negatively regulate cell division by controlling a set of genes required for this process"
TP53BP1	53BP1	"Plays a key role in the repair of DSBs in response to DNA damage by promoting NHEJ-mediated repair of DSBs and specifically counteracting the function of the HR repair protein BRCA1"
UBE2B	RAD6	"Accepts ubiquitin from the E1 complex and catalyzes its covalent attachment to other proteins"
UBE2N	UBC13	"Plays a role in the error-free DNA repair pathway and contributes to the survival of cells after DNA damage; acts together with the E3 ligases, HLTF and SHPRH,

		in the 'Lys-63'-linked poly-ubiquitination of PCNA upon genotoxic stress, which is required for DNA repair"
UBE2V2	MMS2	"MMS-UBC13 heterodimer catalyzes the synthesis of non-canonical 'Lys-63'-linked polyubiquitin chains"
WRN	WRN	"Multifunctional enzyme that has both magnesium and ATP-dependent DNA-helicase activity and 3'->5' exonuclease activity towards dsDNA with a 5'-overhang; binds preferentially to DNA substrates containing alternate secondary structures, such as replication forks and Holliday junctions; plays an important role in the dissociation of joint DNA molecules that can arise as products of HR, at stalled replication forks or during DNA repair; alleviates stalling of DNA polymerases at the site of DNA lesions"
XRCC1	XRCC1	"Scaffold protein involved in DNA SSBs repair by mediating the assembly of DNA break repair protein complexes; negatively regulates ADP-ribosyltransferase activity of PARP1 during BER in order to prevent excessive PARP1 activity"
XRCC2	XRCC2	"Involved in the HR pathway thought to repair chromosomal fragmentation, translocations and deletions; part of the RAD51 paralog protein complex CX3 which acts in the BRCA1-BRCA2-dependent HR pathway"
XRCC3	XRCC3	"Involved in the HR pathway thought to repair chromosomal fragmentation, translocations and deletions; part of the RAD51 paralog protein complex CX3 which acts in the BRCA1-BRCA2-dependent HR pathway; the complex binds predominantly to the intersection of the four duplex arms of the HJ and to junctions of replication forks ; involved in HJ resolution and thus in processing HR intermediates late in the DNA repair process"
XRCC4	XRCC4	"DNA NHEJ core factor ; associates with NHEJ1/XLF to form alternating helical filaments that bridge DNA and act like a bandage, holding together the broken DNA until it is repaired"
XRCC5	Ku80	"ssDNA-dependent ATP-dependent helicase that plays a key role in DNA NHEJ by recruiting DNA-PK to DNA"
XRCC6	Ku70	"ssDNA-dependent ATP-dependent helicase that plays a key role in DNA NHEJ by recruiting DNA-PK to DNA"

ZRANB3	ZRANB3	"DNA annealing helicase and endonuclease required to maintain genome stability at stalled or collapsed replication forks by facilitating fork restart and limiting inappropriate recombination that could occur during template switching events"

3. Transcriptional analysis of DDR and DDT genes

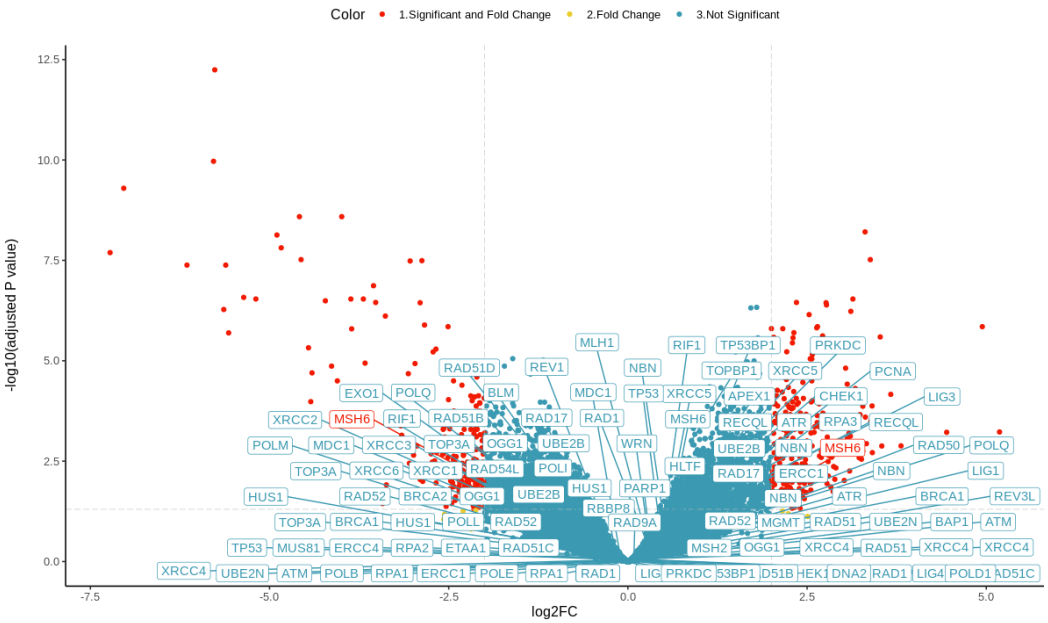

Figure 37. MSH6 is upregulated and downregulated in MPM patients. Volcano plot demonstrating differential gene expression of the DDR and DDT genes listed in Appendix 2, from microarray data collected from GEO with MPM tumor specimens (n=40) and normal pleura specimens (n=5). X-axis displays logFC set at 2 while y-axis represents –log10(adjusted p-value) with a threshold set at 0.05. Significant genes are shown in red.

4. Reporter plasmids for HR and NHEJ quantitative measurement

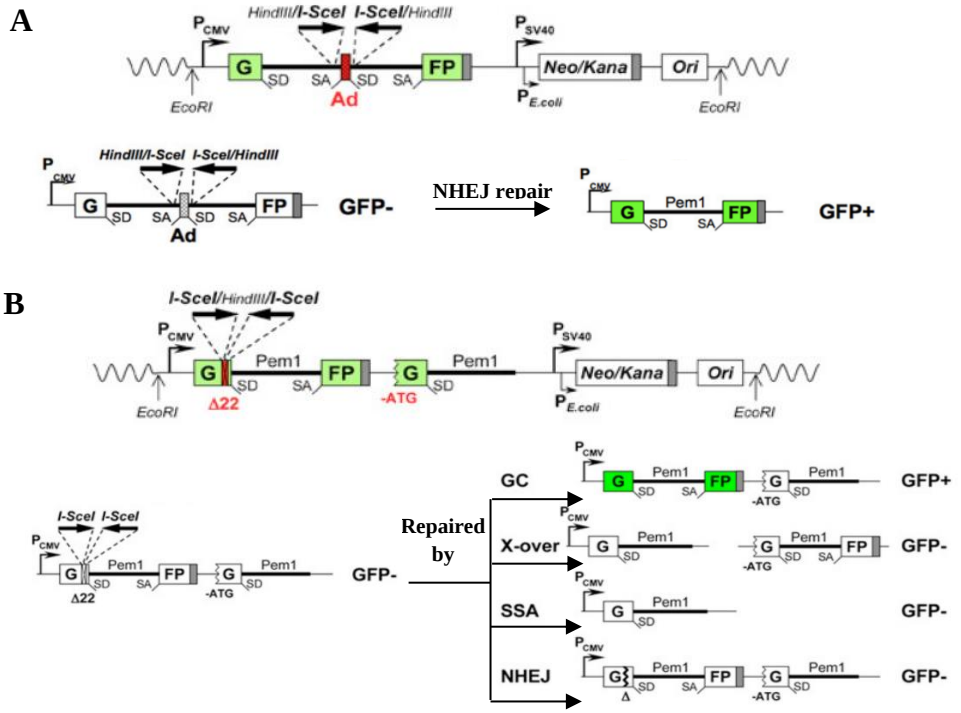

Figure 38. Reporter constructs to quantitatively measure efficiency of DSBs repair pathways. (A) NHEJ repair efficiency was evaluated using a reporter plasmid expressing the GFP gene including a 3 kb intron from the Pem1 gene which contains an adenoviral exon (Ad2) flanked by inverted nonpalindromic I-SceI recognition sequences. Endonuclease cleavage through digestion removes Ad2 and generates incompatible DNA ends that can subsequently be repaired through NHEJ pathway, thus restoring GFP gene expression. **(B)** HR repair efficiency was also quantified using a similar GFP-Pem1 reporter plasmid containing in its first intron a 22 bp deletion ensuring no repair through NHEJ and displaying inverted I-SceI restriction sites I-SceI/HindIII/I-SceI whose digestion produces incompatible ends. In addition, HR construct further includes a second copy of the GFP-Pem1 first intron and exon, although lacking the promoter and the first ATG codon. Upon induction of DSBs by I-SceI digestion, HR by gene conversion (GC) exclusively restores functional GFP expression. Indeed, other DSB repair mechanisms such as crossing-over (X-over), single-strand annealing (SSA) and NHEJ generate repair products with an inactive GFP gene. X-over repair product is indicated for intramolecular recombination. Extramolecular recombination will generate the same product but located on one chromosome. Genes expressing active GFP protein are indicated in green. SD: splice donor; SA: splice acceptor; shaded rectangles: polyadenylation sites; Neo/Kana: single open reading frame controlled by two promoters: SV40 conferring neomycin resistance in mammalian cells, and β-lactamase conferring kanamycin resistance in *Escherichia coli*; Ori: *E. coli* origin of replication. Adapted from Seluanov *et al* (Seluanov, Mao, and Gorbunova 2010).

5. Molecular structure of drugs

Table 7. Chemical structure of drugs used in experiments conducted in this thesis. (CaymanChemical 2022)(Abcam 2022a)(TCIChemical 2022)(Abcam 2022b)

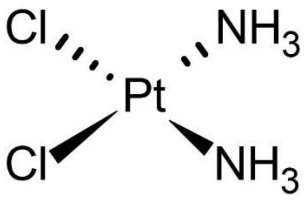

Cisplatin

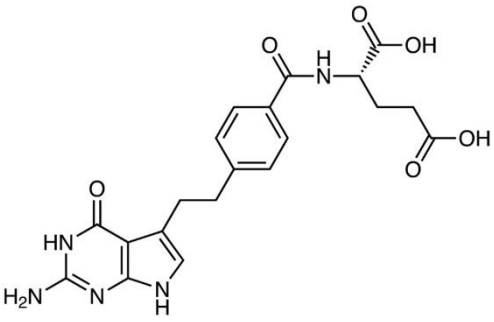

Pemetrexed

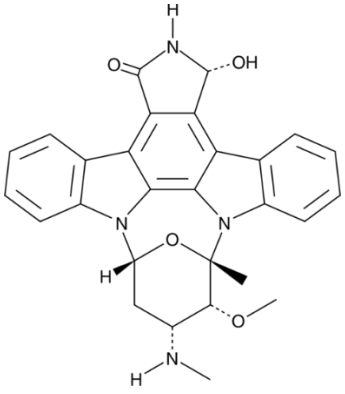

UCN-01

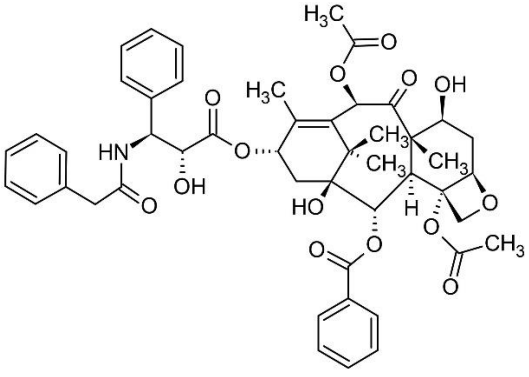

Taxol